शैक्षणिक प्रतिवेदन
Academic Report
2020-21

होमी भाभा राष्ट्रीय संस्थान
HOMI BHABHA NATIONAL INSTITUTE

परमाणु ऊर्जा विभाग की सहायता प्राप्त संस्था
और यूजीसी अधिनियम 1956 की धारा 3 के तहत विश्वविद्यालय माना जाता है
(A Deemed to be University u/s 3 of UGC Act 1956 and a Grant-in-Aid
Institute of the Department of Atomic Energy, Govt. of India)

Location of HBNI Central Office, Constituent Institutions & Off Campus Centre

Academic Report
2020-21

Contents

Section-1 Overview

Introduction.....1-3
Composition of the Bodies of the Institute.....4-9
List of Faculty members.....10-23
HBNI at a Glance.....24-26

Section-II Theses at a Glance

Chemical Sciences.....28-50
Engineering Sciences.....51-66
Life Sciences.....67-90
Mathematical Sciences.....91-94
Medical & Health Sciences.....95-95
Physical Sciences.....96-128

Section-III List of students who have completed Ph.D. during April 1, 2020- July 31, 2021.....130-150

Section-IV List of students who have completed M.Tech. and M.Sc. (Engg.) during April 1, 2020- July 31, 2021.....152-155

Section-V List of students who have completed D.M., M.Ch. and M.D. during April 1, 2020- July 31, 2021.....157-164

From the Vice Chancellor's Desk

I take great pleasure in presenting the academic report of HBNI for the year 2020-21. In June 2020, HBNI completed 15 years of existence. Over the last 15 years, HBNI has established itself as one of the best research universities in the country, encouraging research in various facets of nuclear science and technology including mathematics, and providing valuable human resources to the country in a variety of domains, including superspecialities in medicine. Till July 31, 2021, HBNI has awarded 1881 Ph.D., 558 M.D., and 193 M.Ch. and 168 D.M. degrees.

In the National Institute Ranking Framework (NIRF) exercise conducted by Ministry of Human Resource and Development, HBNI was placed in the 14th position among the Indian Universities in the year 2020 and has been accredited by NAAC for the second cycle in March 2021 with A^{+} grading. Based on high-quality publications in Nature Group of Journals, the Nature Index 2021 placed HBNI in the second position among all institutions in India, and in the first position with regard to publications in physical sciences.

From March 2020 the deadly Covid-19 pandemic descended on the country and seriously impacted the regular functioning of Central Office and all CIs/OCC. However, HBNI responded to the crisis in a remarkable manner and took several measures to ensure that all the academic processes are able to proceed smoothly by adapting to online mode for submission and approval of the required documents causing minimum inconvenience to the stakeholders. HBNI also started conducting a series of webinars and unique courses of high value online over WebEx platform during the year. The webinars and courses are also made available on YouTube channel of HBNI, **HBNI Webinar** for free access by students/faculty all over the country. Despite the pandemic the research and development activities at different CIs/OCC of HBNI kept up a good pace with time and HBNI awarded 234 Ph.D., 26 M.Tech, 85 M.D, 26 D.M and 25 M.Ch degrees during August 2020-July 2021.

The high quality of the Ph.D. programmes taken by HBNI students is obvious through a perusal of the summary of the theses included in this report. The mission of HBNI, research infrastructure and knowledge base available in its different constituent institutions and off-campus centre provides unique opportunities to its students to choose the challenging problems not only in the field related to nuclear science and engineering but also in other thrust areas of science and technology and encourage inter-disciplinary research. HBNI also conducts various value-added courses for its students, particularly for post graduate medical students which help the students to develop the skills in their chosen field of study.

HBNI made forays into newer territories pertinent to post-graduate and Ph.D. programmes during the year. Six new academic programs were introduced during the year, three of them at NISER, Bhubaneswar: Ph.D. (Earth & Planetary Sciences), Ph.D. (Humanities & Social Sciences), Ph.D. (Computer Science) and M.Sc. (Medical & Radiological Physics), M.Sc.

(Public Health and Epidemiology) and M.Sc. (Occupational Therapy in Oncology). Other important initiatives during the year included the formation of a Research Scholars' Forum to encourage and support academic links and collaboration among the research scholars of CIs/OCC of HBNI, obtain their feedback and suggestions for new programs and processes, and provide a forum for enhancing their communication skills.

HBNI students and faculty members have continued to make a mark nationally and internationally through high-quality publications from high quality research work which has been recognised by peers and society in the form of several awards and fellowships conferred on faculty members and students.

I take this opportunity to extend my gratitude to Shri K. N. Vyas, Chairman, Council of Management, HBNI for his valuable support and guidance in all endeavours of HBNI. Thanks are due to Prof. R. B. Grover, Emeritus Professor, HBNI who has provided advice and guidance to the HBNI team in several important matters. Thanks, are also due to the members of Council of Management, Academic Council and the planning and Monitoring board of HBNI. I would also like to place on record my thanks to Board of studies members, Deans (Academic), Deans (Student Affairs), nodal officers at our CIs/OCC and HBNI colleagues for their dedicated efforts and contribution in making HBNI an Institute of great repute nationally and internationally.

I am confident that HBNI will continue to work towards fulfilling its mission and vision, i.e., to design and offer academic programmess, integrating basic research with technology development to meet national needs in various domains and scale new heights in the days to come.

(P. R. Vasudeva Rao)

Section I
(OVERVIEW)

Introduction

The Homi Bhabha National Institute (HBNI) brings together the academic and research programmes conducted by the following eleven premier institutions of DAE, as its Constituent Institutions (CIs)/ Off Campus Centre (OCC):

1. Bhabha Atomic Research Centre (BARC), Mumbai
2. Indira Gandhi Centre for Atomic Research (IGCAR), Kalpakkam
3. Raja Ramanna Centre for Advanced Technology (RRCAT), Indore
4. Variable Energy Cyclotron Centre (VECC), Kolkata
5. Saha Institute of Nuclear Physics (SINP), Kolkata
6. Institute for Plasma Research (IPR), Gandhinagar
7. Institute of Physics (IoP), Bhubaneswar
8. Harish-Chandra Research Institute (HRI), Allahabad
9. Institute of Mathematical Sciences (IMSc), Chennai
10. Tata Memorial Centre (TMC), Mumbai
11. National Institute of Science Education and Research (NISER), Bhubaneswar

Academic Programmes of the Institute

The HBNI offers a range of academic programmes in Chemical Sciences, Engineering Sciences, Medical & Health sciences, Life sciences, Mathematical Sciences and Physical Sciences. It also has a program in Applied Systems Analysis. All institutions, except NISER, conduct programmes at post-graduate level. NISER admits Higher Secondary passed students for its five years Integrated M.Sc. program.

- **Disciplines in which HBNI Offers Ph.D. and Integrated Ph.D.**:
  - ✓ Physical Sciences
  - ✓ Chemical Sciences
  - ✓ Mathematical Sciences
  - ✓ Life Sciences
  - ✓ Engineering Sciences
  - ✓ Medical & Health Sciences
  - ✓ Applied Systems Analysis

Most of the Ph.D. programmes are multi-disciplinary in nature having guides and co-guides from different branches of science and engineering.

- **M.Tech**. in Engineering Sciences and **M.Phil**. in Physical Sciences and Chemical Sciences are also offered. These programmes consist of one year of course work and

one year of project work. The course work is offered at all the campuses of BARC Training School and IPR Training School. Project work is offered at BARC, IGCAR, RRCAT, VECC, IPR and units of DAE. Those who are not able to pursue or are not interested in pursuing a project/research work have the option to get a post graduate diploma in lieu of M.Tech. or M.Phil. degree. BARC training school also offers post graduate diploma in Life Sciences after one year of course work.

- **M.Sc. (Engg)** program emphasizes on research project work extending upto one and a half years after one year of course work. This program is offered at BARC, IGCAR, VECC, RRCAT and IPR.

- **Integrated M.Sc.** of five-year duration in Physical Sciences, Chemical Sciences, Mathematics and Life Sciences is offered at NISER. M.Sc. in Physical Sciences of two-year duration is offered at HRI.

Super Specialty Courses in Medical & Health Sciences offered at TMC are listed below:

- **Doctor of Medicine (D.M.)** in Medical Oncology, Pediatric Oncology, Gastroenterology, Critical Care, Oncopathology and Interventional Radiology

- **Master of Chirurgiae (M.Ch.)** in Surgical Oncology, Gynecological Oncology, Plastic Surgery & Reconstructive Surgery, Head & Neck Oncology

Two years Certified Fellowship Programmes in Medical & Health Sciences offered at TMC are listed below:

Post- MD fellowship program is offered with specialization in Orthopedic Oncology, Breast Oncology, Thoracic Oncology, Uro Oncology, Interventional Oncology, Surgical Pathology, Haemato Pathology, Dental & Prosthetic Surgery, Preventive Oncology, Infectious Diseases & HIV Medicine, Gastrointestinal Oncology, Pulmonary Oncology, Molecular Haemato Oncology, Oral Oncology with Reconstructive Surgery

Post Graduate Courses in Medical & Health Sciences at TMC include:

- **MD** (Pathology, Anesthesia, Radio-diagnosis, Radiation Oncology, Microbiology, Nuclear Medicine, Palliative Medicine, Immuno-Hematology & Transfusion Medicine and in Nuclear Medicine).

- **M.Sc. (**Nursing**), M.Sc. (**Clinical research), **M.Sc**. (Public Health in Epidemiology) and **M.Sc**. (Occupational Therapy in Oncology) programmes are offered at TMC.

- **M.Sc. (Nuclear Medicine and Molecular Imaging Technology)** is offered at TMC & Radiation Medicine Centre of BARC.

- **M.Sc. (Hospital Radiophamacy**) is offered at Radiation Medicine Centre of BARC.

Post Graduate Courses in Medical & Health Sciences at RMC-BARC:

- **M.D. (Nuclear Medicine)**
- **M.Sc. (Nuclear Medicine and Molecular Imaging Technology)**

PG Diploma at TMC:

- **Fusion Imaging Technology (PGDFIT)**

PG Diploma Courses at BARC:

- **Diploma in Radiological Physics (DipRP)**
- **Diploma in Medical Radio Isotope Techniques (DMRIT)**
- **Diploma in Nuclear Science and Engineering (DipNSE)**

Management of HBNI

The **Council of Management** chaired by Secretary, DAE is the apex body for the management of HBNI. **Academic Council** chaired by Vice Chancellor, HBNI manages the academic issues and functions on the advice of the **Board of Studies** which has been constituted for each major discipline and has representatives from all CIs and OCC as well as experts from other reputed Indian institutes.

To manage the affairs of the HBNI, each CI has one or more **Deans-Academic**. **Standing Committee of Deans chaired by VC, HBNI** and comprising of Dean, HBNI, Associate Deans at HBNI, Deans (Academic) from all the institutions, ensures harmony in the processes. CIs have also established a robust framework of admission by **Standing Academic Committee**.

The Council of Management is the prime body for the management of the Institute.

Council of Management (CoM)
(As on August 1, 2021)

Shri K. N. Vyas, Secretary DAE & Chairman, AEC	**Chairman**
Prof. P. R. Vasudeva Rao, Vice Chancellor	Member
Shri Talleen Kumar, Member (Finance), AEC	Member
Prof. A. K. Mohanty, Director, BARC	Member
Prof. A. K. Bhaduri, Director, IGCAR	Member
Prof. R. A. Badwe, Director, TMC	Member
Prof. Sudhakar Panda, Director, NISER	Member
Prof. Surendra Prasad, Former Chairman NBA & Former Director, IIT Delhi	Member
Prof. Mustansir Barma, Professor Emeritus, TIFR Centre For Inter-Disciplinary Sciences, Hyderabad	Member
Shri S. S. Sandhu, IAS, Additional Secretary, Department of Higher Education, MHRD, New Delhi	Member
Prof. P. D. Naik, Dean, HBNI	Member
Dr. B. Chandrasekar, Registrar, HBNI	Secretary

Academic Council
(As on August 1, 2021)

Prof. P. R. Vasudeva Rao, Vice Chancellor	**Chairperson**
Prof. A. K. Mohanty, Director, BARC	Member
Prof. A. K. Bhaduri, Director, IGCAR	Member
Prof. R. A. Badwe, Director, TMC	Member
Prof. Sudhakar Panda, Director, NISER	Member
Prof. S. M. Yusuf, Director, IoP	Member
Shri D. Das, Director, RRCAT	Member
Dr. Sumit Som, Director, VECC	Member
Prof. Shashank Chaturvedi, Director, IPR	Member
Prof. Gautam Bhattacharyya, Director, SINP	Member
Prof. Pinaki Majumdar, Director, HRI	Member
Prof. V. Arvind/Prof. V. Ravindran, Director, IMSc	Member
Prof. Indranil Manna, IIT Kharagpur	Member
Prof. Kannan N. Iyer, IIT Bombay	Member
Prof. E. D. Jemmis, IISc, Bangalore	Member
Prof. Shishir Deshpande, Director, ITER-IPR	Member
Prof. B. Venkatraman, IGCAR	Member
Prof. P. K. Pujari/Prof. Vivekanand Kain, BARC	Member
Prof. P. D. Naik, Dean, HBNI	Member
Prof. R. B. Grover, Convenor, BoS (Applied Systems Analysis)	Member
Prof. S. M. Yusuf, Convenor, BoS (Physical Sciences)	Member
Prof. A. P. Tiwari, Convenor, BoS (Engineering Sciences)	Member
Prof. S. V. Chiplunkar/Prof. Prasanna Venkatraman, Convenor, BoS (Life Sciences)	Member
Prof. Meena Mahajan, Convenor, BoS (Mathematical Sciences)	Member
Prof. S. D. Banavali, Convenor, BoS (Medical & Health Sciences)	Member
Prof. S. Kannan, Convenor, BoS (Chemical Sciences)	Member
Prof. Bedangadas Mohanty, Convenor, BoS (Integrated Masters Programme)	Member
Dr. B. Chandrasekar, Registrar, HBNI	Secretary

Advisory Committee	
Secretary, DAE and Chairman, AEC	**Chairman**
Vice Chancellor	Member
Director, BARC	Member
Director, IGCAR	Member
Director, RRCAT	Member
Director, VECC	Member
Director, IPR	Member
Director, SINP	Member
Director, TMC	Member
Director, IMSc	Member
Director, TIFR	Member
Director, NISER	Member
Director, HRI	Member
Director, IOP	Member
Dean, HBNI	Member-Secretary

Officers of the Institute

Academic		Administrative	
Prof. P. R. Vasudeva Rao	Vice Chancellor	Dr. B. Chandrasekar	Registrar
Prof. P. D. Naik	Dean	Shri B. V. Balaji	Deputy Registrar
Prof. B. K. Dutta	Institute Chair Professor	Shri J. K. Makwana	Administrative Officer-III
Prof. B. S. Tomar	Institute Chair Professor	Smt. Bharati Suwarna	Assistant Registrar
Prof. D. K. Maity	Associate Dean	Shri Shailash Jakhotia	Finance Officer
Prof. A. K. Dureja	Associate Dean		
Prof. G. Ravi Kumar	Associate Dean		

Board of Studies of HBNI

(As on August 1, 2021)

❖ **BoS (Chemical Sciences)**
1. Prof. S. Kannan, BARC - Convener
2. Prof. A. K. Tyagi, BARC - Co-Convener
3. Prof. A. Dutta, IIT, Bombay
4. Prof. A. Srinivasan, NISER
5. Prof. D. K. Maity, HBNI
6. Prof. N. Sivaraman, IGCAR
7. Prof. P. K. Mohapatra, BARC
8. Prof. H. S. Biswal, NISER
9. Prof. Deepa Khushalani, TIFR
10. Prof. Avinash Kumbhar, SPPU
Balancing Members:
1. Prof. K. S. Bindra, RRCAT
2. Prof. S. Santoshkumar, BARC
❖ **BoS (Engineering Sciences)**
1. Prof. A. P. Tiwari, BARC-Convener
2. Prof. Shaju K. Albert, Director, MMG, IGCAR- Co-Convener
3. Prof. Archana Sharma, BARC
4. Prof. A. K. Bhattacharjee, BARC
5. Prof. A. K. Nayak, BARC
6. Prof. J. Chattopadhyay, BARC
7. Prof. C. P. Paul, RRCAT
8. Prof. Paramita Mukherjee, VECC
9. Prof. S. K. Pathak, IPR
10. Prof. V. Kain, BARC
Balancing Members:
1. Prof. Jane Alam, VECC
2. Prof. A. K. Dureja, HBNI
❖ **BoS (Medical & Health Sciences)**
1. Prof. S. D. Banavali, TMC – Convener
2. Prof. Sandeep Basu, RMC-Co-Convener
3. Prof. Sudeep Gupta, Director ACTREC, TMC
4. Dr. Nithya Gogte, KEM Hospital, Mumbai
5. Dr. Ashutoshnath Agarwal, PGIMER, Chandigarh
6. Dr. Manisha Pawar, TMH
7. Prof. Siddhartha Laskar, TMC
8. Dr. Ajay Puri, TMC
9. Dr. J. P. Agarwal, TMC
10. Dr. Suyash Kulkarni, TMC
Balancing Members:
1. Dr. Rajesh Kinhikar, TMC
2. Prof. A. K. Dureja, HBNI
❖ **BoS (Life Sciences)**
1. Prof. Prasanna Venataraman, Dy. Director, ACTREC - Convener
2. Prof. Abhijit Chakrabarty, Sr. Professor, SINP - Co-Convener
3. Prof. Praful Singru, SBS, NISER
4. Prof. Rahul Siddharthan, IMSc
5. Prof. Rajiv Sarin, ACTREC
6. Prof. Harapriya Mohaptra, NISER
7. Prof. S. Santoshkumar, BARC
8. Prof. S. Gautam, BARC
9. Prof. H. S. Mishra, BARC
10. Prof. Sharmila Bapat, NCCS, Pune
Balancing Members:
1. Prof. D. K. Maity, HBNI
2. Prof. Hema Rajaram, BARC
❖ **BoS (Mathematical Sciences)**
1. Prof. Meena Mahajan, IMSc - Convener
2. Prof. D. Surya Ramana, HRI Co-Convener
3. Prof. B. Sury, ISI, Bangaluru
4. Prof. C. S. Rajan, TIFR, Mumbai
5. Prof. Jugal K. Verma, IIT Bombay
6. Prof. K. N. Raghavan, IMSc
7. Prof. K. V. Subrahmanyam, CMI-Chennai
8. Prof. Mahuya Datta, ISI-Kolkata
9. Prof. Brundaban Sahu, NISER
Balancing Members:
1. Prof. Sudhir Jain, BARC
2. Prof. A. K. Dureja, HBNI
❖ **BoS (Physical Sciences)**
1. Prof. S. M. Yusuf, BARC-Convener
2. Prof. Jane Alam, VECC-Co-Convener

3. Prof. Anushuman Maharana, HRI
4. Prof. Sandip Kumar Dhara, IGCAR
5. Prof. D. Indumathi, IMSc
6. Prof. Shikha Varma, IoP
7. Prof. Sudip Sengupta, IPR
8. Prof. B. Mohanty, NISER
9. Prof. K. S. Bindra, RRCAT
10. Prof. Kumar Sankar Gupta, SINP
Balancing Members:
1. Prof. Saibal Basu, HBNI
2. Prof. A. K. Tyagi, BARC
❖ **BoS (Applied Systems Analysis)**
1. Prof. R. B. Grover, HBNI-Convener
2. Prof. Pranay Swain, NISER Co-Convener
3. Prof. Karuna Jain, IIT Bombay
4. Prof. G. Ravikumar, BARC
5. Prof. Surinder Jaswal, TISS
6. Prof. S. Kannan, BARC
7. Prof. B Raja Shekhar, Pro-Vice Chancellor, University of Hyderabad
Balancing Members:

1. Prof. A. K. Dureja, Associate Dean, HBNI
❖ **BoS (Integrated Masters Programme)**
1. Prof. Bedangadas Mohanty, NISER - Convener
2. Prof. Pranay Swain, NISER – Co-Convener
3. Chair, School of Life Sciences, NISER (Ex-Officio)
4. Chair, School of Chemical Sciences, NISER (Ex-Officio)
5. Chair, School of Mathematics, NISER (Ex-Officio)
6. Chair, School of Physical Sciences, NISER (Ex-Officio)
7. Chair, School of Undergraduate Studies Committee, NISER (Ex-Officio)
8. Prof. Anirban Basu, HRI
9. Prof. B. R. Sekhar, IoP
10. Prof. Sujit Roy, IIT Bhubaneswar
Balancing Members:
1. Prof. B. S. Tomar, HBNI
2. Prof. Meena Mahajan
3. Prof. Partha Saha

Deans Academic at Constituent Institutions (CIs)/Off-Campus Centre (OCC)

(As on August 1, 2021)

S. No.	Name of the CI/Off-campus centre	Discipline	Name of the Dean Academic
1	Bhabha Atomic Research Centre	Life Sciences	Prof. Hema Rajaram
		Chemical Sciences	Prof. Tapan Kumar Ghanty
		Physical & Mathematical Sciences	Prof. Dinesh Udupa
		Engineering Sciences Stream-I	Prof. Raghavendra Tewari
		Engineering Sciences Stream-II	Prof. S. Mukhopadhyay
		Health Sciences	Prof. Sandip Basu
2	Indira Gandhi Centre for Atomic Research	Chemical Sciences	Prof. C. V. S. B. Rao
		Physical Sciences	Prof. Awadesh Mani
		Engineering Sciences	Prof. Anish Kumar
3	Raja Ramanna Centre for Advanced Technology	All Disciplines	Prof. Arup Banerjee
4	Variable Energy Cyclotron Centre	Physical Sciences	Prof. Parnika Das
		Engineering Sciences	Prof. Sarbajit Pal
5	Saha Institute of Nuclear Physics	Chemical & Life Sciences	Prof. Partha Saha
		Physical Sciences	Prof. Prakash Mathews
6	Institute for Plasma Research	All Disciplines	Prof. Sudip Sengupta
7	Institute of Physics	Physical Sciences	Prof. Pankaj Agrawal
8	Institute of Mathematical Sciences	Mathematical Sciences	Prof. Vijay Kodiyalam
		Physical Sciences	Prof. Satyavani Vemparala
		Life Sciences	Prof. Sitabhra Sinha
9	Harish-Chandra Research Institute	All Disciplines	Prof. Prasenjit Sen
10	Tata Memorial Centre	All Disciplines	Prof. Shripad Banavali
11	National Institute of Science Education and Research	All Disciplines	Prof. Pranay Swain

List of Faculty Members
(As on August 1, 2021)

HBNI

1. Prof. P. R. Vasudeva Rao
2. Prof. Prakash Dattatray Naik
3. Prof. Ravi Bhushan Grover
4. Prof. Jyeshtharaj Bhalchandra Joshi
5. Prof. Bijan Kumar Dutta
6. Prof. Sunil Kumar Ghosh
7. Prof. Dilip Kumar Maity
8. Prof. Adarsh Kumar Dureja

BARC

❖ Chemical Sciences

9. Prof. A. K. Tyagi
10. Prof. Alok Kumar Ray
11. Prof. Arya Ashok Kumar
12. Prof. Awadhesh Kumar
13. Prof. Chetan Prakash Kaushik
14. Prof. Lalit Varshney
15. Prof. Pradeep Kumar Pujari
16. Prof. Prasanta Kumar Mohapatra
17. Prof. S. Kannan
18. Prof. Smruti Dash
19. Prof. Tapan Kumar Ghanty
20. Prof. A. K. Tripathi
21. Prof. A. L. Rufus
22. Prof. A. C. Bhasikuttan
23. Prof. A. C. Sahayam
24. Prof. Ashok Kumar Pandey
25. Prof. Chiranjib Majumder
26. Prof. Ghasi Ram Dey
27. Prof. Hari Prasad Upadhyaya
28. Prof. P. A. Hassan
29. Prof. Hirendra Nath Ghosh
30. Prof. K. Dash
31. Prof. M. P. Srinivasan
32. Prof. Niharendu Choudhury
33. Prof. Patra Chandra Nath
34. Prof. R. Mishra
35. Prof. R. J. Kshirsagar
36. Prof. Raghunath Acharya
37. Prof. Rajesh V. Pai
38. Prof. Rakesh Kumar Singhal
39. Prof. Renu Agarwal
40. Prof. S. K. Jha
41. Prof. S. N. Achary
42. Prof. Sangita D Kumar
43. Prof. Sanjiv Kumar
44. Prof. Soumyakanti Adhikari
45. Prof. Sreenivas T.
46. Prof. Subir Kumar Ghosh
47. Prof. Sudarsan V.
48. Prof. Sukhendu Nath
49. Prof. Suresh C. Parida
50. Prof. Tusar Bandyopadhyay
51. Prof. Y K Bhardwaj
52. Dr. A Jahur Mondal
53. Dr. Adya Prasad Mishra
54. Dr. Ajay K. Singh
55. Dr. Anil Kumar Pabby
56. Dr. Anshu Singhal
57. Dr. Anupkumar B.
58. Dr. Aparna Banerjee
59. Dr. Aruna Korde
60. Dr. Arunasis Bhattacharyya
61. Dr. Ashis Kumar Satpati
62. Dr. Asim Kumar Ghosh
63. Dr. Dayamoy Banerjee
64. Dr. Dhandeep Dutta
65. Dr. Dhurva Kumar Singh
66. Dr. Dimple Dutta
67. Dr. Drishty Satpati
68. Dr. Faby Sunny
69. Dr. Hemant Shivram Sodaye
70. Dr. Jayshree Ramkumar
71. Dr. Jyotirmayee Mohanty
72. Dr. Kallola Kumar Swain
73. Dr. Kumar Abhinav Dubey
74. Dr. M. C. Rath
75. Dr. M. S. Murali
76. Dr. Madhava B Mallia

77. Dr. Madhumita Goswami
78. Dr. Mainak Roy
79. Dr. Manidipa Basu
80. Dr. Manoj Kumbhakar
81. Dr. Mrinal R. Pai
82. Dr. Musharaf Ali S. K.
83. Dr. N. N. Meeravli
84. Dr. Naina Raje
85. Dr. Nandita Maiti
86. Dr. Neetika Rawat
87. Dr. P. S. Ramanjaneyulu
88. Dr. P. Mathi
89. Dr. Pradeep Kumar
90. Dr. Pramod Sharma
91. Dr. R. Ganguly
92. Dr. Rahul Tripathi
93. Dr. Ravi Joshi
94. Dr. Ritu M Srivastava
95. Dr. S. Jayakumar
96. Dr. Salil Varma
97. Dr. Sandeep Nigam
98. Dr. Sandip Dey
99. Dr. Sanjukta A Kumar
100. Dr. Shilpa N Sawant
101. Dr. Suchismita Mishra
102. Dr. Sudarshan Kathi
103. Dr. Sumit Kumar
104. Dr. Suparna Sodaye
105. Dr. Tapas Das
106. Dr. Tirumalesh Keesari
107. Dr. Usha Pandey
108. Dr. Vandana Pulhani
109. Dr. Vinita Grover Gupta
110. Dr. Virendra Kumar
111. Dr. Aishwarya Soumitra Kar
112. Dr. Ajish Kumar K. S.
113. Dr. Amit Kunwar
114. Dr. Ankita Rao
115. Dr. Arijit Sengupta
116. Dr. Arnab Sarkar
117. Dr. Arup Kumar Pathak
118. Dr. Atanu Barik
119. Dr. Atindra Banerjee
120. Dr. Balaji Prasad Mandal
121. Dr. Beena G. Singh
122. Dr. Chhavi Agarwal
123. Dr. Dibakar Goswami
124. Dr. Gunjan Verma
125. Dr. J. Selvakumar
126. Dr. K. C. Barick
127. Dr. K. R. S. Chandrakumar
128. Dr. Kaustava Bhattacharyya
129. Dr. Kedarnath G
130. Dr. Mahesh Sundararajan
131. Dr. Malaya Kumar Nayak
132. Dr. Manjulata Saha
133. Dr. Manoj Mohapatra
134. Dr. Manoj Kumar Sharma
135. Dr. Mhejabeen Sayed
136. Dr. N. R. Singh
137. Dr. Pankaj Kumar Patro
138. Dr. Prabhat Kumar Singh
139. Dr. Prasad Padmakar Phadnis
140. Dr. Priya Maheshwari
141. Dr. Raghunath Chowdhury
142. Dr. Ritesh Ruhela
143. Dr. Rubel Chakravarty
144. Dr. Ruma Gupta
145. Dr. Sajeev Y.
146. Dr. Sandeep Kumar Sharma
147. Dr. Sangita D Lenka
148. Dr. Sanhita Chaudhury
149. Dr. Sanjay Kumar
150. Dr. Santosh Kumar Gupta
151. Dr. Saurav Kumar Gupta
152. Dr. Seemita Banerjee
153. Dr. Seraj Ahmad Ansari
154. Dr. Sharmishta Dutta Choudhury
155. Dr. Sipra Choudhury
156. Dr. Soumyaditya Mula
157. Dr. Sumana Sengupta

❖ **Engineering Sciences**

158. Prof. Akhilanand Pati Tiwari
159. Prof. Anup Kumar Bhattacharjee
160. Prof. Archana Sharma
161. Prof. Arun Kumar Nayak

162. Prof. D. N. Badodkar
163. Prof. Deb Mukhopadhyay
164. Prof. Gopal Joshi
165. Prof. Gopalakrishnan Sugilal
166. Prof. Jayanta Chattaopadhyay
167. Prof. N. K. Maheshwari
168. Prof. Prabhakar V Varde
169. Prof. Raghvendra Tewari
170. Prof. Ram Nivas Singh
171. Prof. Siddaratha Mukhopadhyay
172. Prof. Soumitra Kar
173. Prof. Vivekanand Kain
174. Prof. Sujay Bhattacharya
175. Prof. A. Vinod Kumar
176. Prof. Alok Awasthi
177. Prof. Amit Sinha
178. Prof. Aniruddha Biswas
179. Prof. Anita Vinay Topkar
180. Prof. Biswaranjan Dikshit
181. Prof. D. Mandal
182. Prof. D. C. Kar
183. Prof. Deep Prakash
184. Prof. Dinesh Kumar Chandraker
185. Prof. Gopika Vinod
186. Prof. Joydipta Banerjee
187. Prof. Jung Bahadur Singh
188. Prof. Kapilesh Bhargava
180. Prof. Arun Kumar Nayak
190. Prof. Kulwant Singh
191. Porf. M. K. Samal
192. Prof. Namita Maiti
193. Prof. R. K. Bajpai
194. Prof. Rajeev Kapoor
195. Prof. S. R. Shimijith
196. Prof. Sulekha Mukhopadhyay
197. Prof. Supratik Roychowdhury
198. Prof. T. A. Dwarakanath
199. Prof. Tarasankar Mahata
200. Prof. Tessy Vincent
201. Prof. V. H. Patankar
202. Prof. Yogita Parulekar
203. Dr. Abhijeet Mohan Vaidya
204. Dr. Anindya Chakravarty
205. Dr. Arijit Laik
206. Dr. Betty C. A.
207. Dr. C. B. Basak
208. Dr. Chiradeep C Gupta
209. Dr. Debanik Roy
210. Dr. Imran Ali Khan
211. Dr. K. K. Singh
212. Dr. Kamal Singh
213. Dr. Kinshuk Dasgupta
214. Dr. Maha Nand Jha
215. Dr. Noble Jacob
216. Dr. Pranesh Sengupta
217. Dr. Praveen Kumar
218. Dr. Ramkrishna Das
219. Dr. Ranjan Kumar
220. Dr. Rishi Verma
221. Dr. Sanjib Majumdar
222. Dr. Sudipta Chakraborty
223. Dr. Suman Neogy
224. Dr. Suneel Kumar Gupta
225. Dr. T. Sree Rama Chandra Murthy
226. Dr. Onkar Suresh Gokhale
226. Dr. Sangita Pal
228. Dr. Surender Kumar Sharma
229. Dr. Vishwanadh Bathula

❖ **Medical & Health Sciences**

230. Prof. A. J. Khandekar
231. Prof. A. R. Kulkarni
232. Prof. Anita Gadgil
233. Prof. Gaurav Malhotra
234. Prof. N. N. More
235. Prof. R. V. Jadhav
236. Prof. Sandip Basu
237. Dr. Ashwini Kalshetty
238. Dr. J. G. Kalbhande
239. Dr. Priyanka Verma
240. Dr. Satish C Mishra
241. Dr. Sunil Dutta Sharma
242. Dr. Sunita Nitin Sonavane
243. Dr. Yogesh K Shejul
244. Dr. Ashwini Kalshetty
245. Dr. Priyanka Verma

246. Dr. Sunita Nitin Sonavane

❖ **Life Sciences**

247. Prof. V. P. Venugopalan
248. Prof. B. N. Pandey
249. Prof. Birajalaxmi Das
250. Prof. Briija Sankar Patro
251. Prof. Hari S. Misra
252. Prof. Hema Rajaram
253. Prof. Prasad S Variyar
254. Prof. Prasun Kumar Mukherjee
255. Prof. Sandur Santosh Kumar
256. Prof. Sanjay J Jambhulkar
257. Prof. Satyendra Gautam
258. Prof. Savita Kulkarni
259. Prof. T R Ganapathi
260. Prof. Toleti Subba Rao
261. Prof. Y. V. Nancharaiah
262. Dr. Ajay Saini
263. Dr. Anand D Ballal
264. Dr. Anand M Badigannavar
265. Dr. Anu Ghosh
266. Dr. Archana Mukherjee
267. Dr. Archana Joshi Saha
268. Dr. B. K. Das
269. Dr. Bhakti Basu
270. Dr. Bhavani S Shankar
271. Dr. Deepak Sharma
272. Dr. Gagan Deep Gupta
273. Dr. J. Souframanien
274. Dr. Joy G. Manjaya
275. Dr. Mahesh Subramanian
276. Dr. Nagesh Bhat
277. Dr. R. Shashidhar
278. Dr. Rajesh Kumar
279. Dr. Ramesh Hire
280. Dr. Rath Devashish
281. Dr. Ravindra D Makde
282. Dr. S. N. Jamdar
283. Dr. S. P. Chawla
284. Dr. Sheetal Uppal
285. Dr. Vishwas M Kulkarni
286. Dr. Amit Das
287. Dr. Amit Kumar
288. Dr. Aruna Jyothi Kora
289. Dr. Ashish Kumar Srivastava
290. Dr. Bhaskar Sanyal
291. Dr. Bibhuti Bhusan Mishra
292. Dr. Celin Acharya
293. Dr. Dharmendra Kumar Maurya
294. Dr. Himanshi N Mishra
295. Dr. Hiren Joshi
296. Dr. Jitendra Kumar
297. Dr. Manisha Banerjee
298. Dr. P Sriyutha Murthy
299. Dr. Rachna Agarwal
300. Dr. Rahul Checkar
301. Dr. Rajani Kant Chittela
302. Dr. S. T. Mehetre
303. Dr. Sachin Nandkumar Hajare
304. Dr. Shraddha Singh
305. Dr. Sonia Chadha
306. Dr. Subhash Chandra Bihani
307. Dr. Sudhir Singh
308. Dr. Sudhir Kumar Gupta
309. Dr. Suvendu Mondal
310. Dr. Swathi Kota
311. Dr. Vandan Nagar
312. Dr. Yogrndra Singh Rajpurohit

❖ **Physical Sciences**

313. Prof. Ajit Kumar Mohanty
314. Prof. Dinesh Kumar Aswal
315. Prof. G Ravikumar
316. Prof. Kannan Umasankari
317. Prof. S. M. Yusuf
318. Prof. Sanjay C. Gadkari
319. Prof. Srinivas Krishnagopal
320. Prof. Vinay Bhaskar Chandratre
321. Prof. A. K. Debnath
322. Prof. A. K. Gupta
323. Prof. Abhas Kumar Mitra
324. Prof. Aditi Ray
325. Prof. Ahmed Zafar
326. Prof. Alka B. Garg
327. Prof. Amitabh Das
328. Prof. Aniruddha Kumar
329. Prof. Anurag Gupta

330. Prof. Aradhana Shrivastava
331. Prof. B. K. Sapra
332. Prof. B. N. Rajasekhar
333. Prof. Bency V. John
334. Prof. D. M. Gaitonde
335. Prof. Debabrata Biswas
336. Prof. Debasis Sen
337. Prof. Dibyendu Bhattacharyya
338. Prof. Dinesh Venkatesh Udupa
339. Prof. Dipanwita Dutta
340. Prof. Divakar K. Rao
341. Prof. Hemant Govind Salunke
342. Prof. J. Padma Nilaya
343. Prof. K. K. Yadav
344. Prof. Keshaw D. Joshi
345. Prof. Lalit Mohan Pant
346. Prof. Lavanya M Ramaniah
347. Prof. M. V. Suryanarayana
348. Prof. Mala N. Rao
349. Prof. Mukesh Kumar
350. Prof. Mukund Shrinivas Kulkarni
351. Prof. N. Padma
352. Prof. Nandini Garg
353. Prof. Prashant Shukla
354. Prof. Ranjan Mittal
355. Prof. Rekha Rao
356. Prof. S. G. Nakhate
357. Prof. Satyaranjan Santra
358. Prof. Shambhu Nath Jha
359. Prof. Srikumar Ghorui
360. Prof. Subhankur Mitra
361. Prof. Subir Bhattachryya
362. Prof. Subir Ranjan Jain
363. Prof. T. Palani Selvam
364. Prof. U. P. Sastry
365. Dr. V. K. Aswal
366. Dr. A. K. Rajarajan
367. Dr. Ajay Singh
368. Dr. Ajay Kumar Mishra
369. Dr. Amitava Roy
370. Dr. Anil Kumar Chauhan
371. Dr. Aparna Shastri
372. Dr. Asawari D. Rath
373. Dr. Ashok Kumar Bakshi
374. Dr. Bhushan Dhabekar
375. Dr. Bidyut Jyoti Roy
376. Dr. Brahmananda Chakraborty
377. Dr. Chitra Murli
378. Dr. D. R. Mishra
379. Dr. Debarati Bhattacharya
380. Dr. G. Sridhar
381. Dr. Himanshu Kumar Poswal
382. Dr. Keka R. Chakraborty
383. Dr. Kripamay Mahata
384. Dr. Manoj Kumar Warrier
385. Dr. Mayank Shukla
386. Dr. Paritosh Modak
387. Dr. Partha Sarathi Sarkar
388. Dr. Prakash Chandra Rout
389. Dr. Pratap Baburao Wagh
390. Dr. Priyamvada M Dighe
391. Dr. Ramesh Chandra Das
392. Dr. Renju George Thomas
393. Dr. S. Anand
394. Dr. Sanjay Kumar Sahu
395. Dr. Sanjay V Thakare
396. Dr. Santanu Bera
397. Dr. Shashwati Sen Yeram
398. Dr. Soumen Bhattacharyya
399. Dr. Sukanta Karmakar
400. Dr. Surendra Singh
401. Dr. Swapan Das
402. Dr. Swarupananda Pradhan
403. Dr. T. Jayasekharan
404. Dr. V. Jha
405. Dr. Vinod Singh Rawat
406. Dr. Yogesh Kashyap
407. Dr. Rohit Shukla
408. Dr. Amit Kumar
409. Dr. Amit Verma
410. Dr. Amit Srivastava
411. Dr. Anil Jain
412. Dr. Apu Sarkar
413. Dr. B. Sunder Sahayanathan
414. Dr. Babita Tiwari
415. Dr. C. D. Sijoy

416. Dr. C. L. Prajapat
417. Dr. Debjani Karmakar
418. Dr. Goutam Dev Mukherjee
419. Dr. H. Kumawat
420. Dr. Himal Bhatt
421. Dr. Jitendra Bahadur
422. Dr. Kiran R. M.
423. Dr. Manmeet Kaur
424. Dr. Mohit Tyagi
425. Dr. Pramod Bhatt
426. Dr. Purushottam Jha
427. Dr. Rosaline Mishra
428. Dr. S. P. Tripathy
429. Dr. Sanjay Kumar Mishra
430. Dr. Shankar Prasad Koiry
431. Dr. Shivanand Chaurasia
432. Dr. Shovit Bhattacharya
433. Dr. Sunita Kedia
434. Dr. Veerendra Kumar Sharma
435. Dr. Venkata RamanaIkkurthi
436. Dr. Vibha Saxena
437. Dr. Vinayak Mishra
438. Dr. Yogesh K. Gupta

IGCAR

❖ Chemical Sciences

439. Prof. A. Suresh
440. Prof. K. Ananthasivan
441. Prof. K. A. Venkatesan
442. Prof. M. Joseph
443. Prof. N. Sivaraman
444. Prof. R. V. Subbarao
445. Prof. R. Kumar
446. Prof. Rajesh Ganesan
447. Prof. V. Jayaraman
448. Dr. C. V. S. Brahmmananda Rao
449. Dr. K. Sundararajan
450. Dr. K. I. Gnanasekar
451. Dr. Sublime Ningshen
452. Dr. A. Sree Rama Murthy
453. Dr. Arindam Das
454. Dr. Ashish Jain
455. Dr. B. Anandkumar
456. Dr. Chowdari Jagadeeswara Rao
457. Dr. Durairaj Ponraju
458. Dr. Hrudananda Jena
459. Dr. N. Ramanathan
460. Dr. Pavan Kumar Narayanam
461. Dr. R. Kumaresan
462. Dr. R. Venkata Krishnan
463. Dr. Satendra Kumar

❖ Engineering Sciences

464. Prof. Arun Kumar Bhaduri
465. Prof. B. P. C. Rao
466. Prof. Shaju K Albert
467. Prof. A. John Arul
468. Prof. Aniruddha Moitra
469. Prof. Anish Kumar
470. Prof. M. Vasudevan
471. Prof. V. Karthik
472. Dr. A. Nagesha
473. Dr. A. Jasmin Sudha
474. Dr. C. Sudha
475. Dr. Chitta Ranjan Das
476. Dr. Mahadevan S
477. Dr. P Mangarjuna Rao
478. Dr. R Mythili
479. Dr. V. S. Srinivasan
480. Dr. Vani Shankar
481. Dr. A. Ravi Shankar
482. Dr. Diptimayee Samantaray
483. Dr. G .V. Prasad Reddy

❖ Physical Sciences

484. Prof. B. Venkataraman
485. Prof. G. Amarendra
486. Prof. Ramchandran Divakar
487. Prof. Awadhesh Mani
488. Prof. G. Raghavan
489. Prof. John Philip
490. Prof. K. Devan
491. Prof. N. Subramanian
492. Prof. N. V. Chandra Shekar
493. Prof. R. Govindaraj
494. Prof. R. Rajaraman
495. Prof. Sandip Kumar Dhara
496. Prof. T. R. Ravindran
497. Dr. Arup Dasgupta

498. Dr. B. Sundaravel
499. Dr. C. Venkata Srinivas
500. Dr. G. Mangamma
501. Dr. K. Gireesan
502. Dr. Nithya Ravindran
503. Dr. Parthasarathi Gangopadhyay
504. Dr. R. Krishnan
505. Dr. R. Ramaseshan
506. Dr. R. Venkatesan
507. Dr. S. Ganesamoorthy
508. Dr. S. Tripura Sundari
509. Dr. Sharat Chandra
510. Dr. Tom Mathews
511. Dr. V. Sivasubramanian
512. Dr. V. Subramanian
513. Dr. Arun K. Prasad
514. Dr. Barid Baran Lahiri
515. Dr. Deepak Kumar Baisnab
516. Dr. Edward Prabu Amaladass
517. Dr. K. Ganesan
518. Dr. K. Prabhakar
519. Dr. N. R. Sanjay Kumar
520. Dr. O. Annalakshmi
521. Dr. Rajendra Ganpat Joshi
522. Dr. Ramanathaswamy Pandian
523. Dr. Ravi Chinnappan
524. Dr. S. Abhaya
525. Dr. S. Amrithapandian
526. Dr. S. C. Vanithkumari
527. Dr. Vinod K.

RRCAT

❖ Chemical Sciences

528. Dr. Dipankar Nanda

❖ Engineering Sciences

529. Dr. Christ Prakash Paul
530. Dr. Prabhat Kumar Gupta
531. Dr. Rahul Shukla

❖ Life Sciences

532. Prof. Alok Dube

❖ Physical Sciences

533. Prof. Kushvinder Singh Bindra
534. Prof. Alka A. Ingale
535. Prof. Anand Moorti
536. Prof. Aparna Chakrabarti
537. Prof. J. A. Chakera
538. Prof. Mohammed Hussein Modi
539. Prof. Mukesh Joshi
540. Prof. Om Prakash
541. Prof. Satya Ram Mishra
542. Prof. Shovan K Majumder
543. Prof. Sudhir Kumar Dixit
544. Prof. Tapas Ganguli
545. Prof. Tarun Kumar Sharma
546. Prof. Vidya Sagar Tiwari
547. Prof. Vinit Kumar
548. Dr. Arvind Kumar Srivastava
549. Dr. Avinsh K Sharma
550. Dr. Chandrachur Mukherjee
551. Dr. Gurvinderjit Singh
552. Dr. Haranath Ghosh
553. Dr. Indranil Bhaumik
554. Dr. J. Jayabalan
555. Dr. Manoj Kumar Tiwari
556. Dr. M. K. Chattopadhyay
557. Dr. P. K. Mukhopadhyay
558. Dr. Pankaj Misra
559. Dr. Rajeev Bhatt
560. Dr. Raktim Dasgupta
561. Dr. Shreyashkar Dev Singh
562. Dr. Srinibas Satapathy
563. Dr. Sunil Verma
564. Dr. Surya Mohan Gupta
565. Dr. Vibhuti Bhushan Tiwari
566. Dr. Vijay Kumar Dixit
567. Dr. Yogesh Kumar
568. Dr. Archana Sagdeo
569. Dr. C. Kamal
570. Dr. Chandra Pal Singh
571. Dr. Himanshu Singhal
572. Dr. Maheswar Nayak
573. Dr. Manoj Kumar Singh
574. Dr. Pooja Gupta
575. Dr. Sanyasi Rao Bobbili
576. Dr. Shankar Lal
577. Dr. Soma Banik
578. Dr. Suparna Pal

579. Dr. T. Sathyanaryana Annam
580. Dr. Uday Chakravarty
581. Dr. Vishnu Kumar Sharma

VECC

❖ Engineering Sciences

582. Prof. P. Y. Nabhiraj
583. Prof. Paramita Mukherjee
584. Prof. Sarbajit Pal
585. Dr. Sandip Pal
586. Dr. Tapatee Kundu Roy

❖ Physical Sciences

587. Prof. Jane Alam
588. Prof. Arup Bandyopadhyay
589. Prof. Chandana Bhattacharaya
590. Prof. Parnika Das
591. Prof. Rashid Md. Haroon
592. Prof. Sourav Sarkar
593. Prof. Subhasis Chattopadhyay
594. Dr. Gargi Chaudhri
595. Dr. Gayathri N. Banerjee
596. Dr. Gopal Mukherjee
597. Dr. Kaushik Banerjee
598. Dr. Nitin Kumar Das
599. Dr. Sanyal Dirtha
600. Dr. Sarmishtha Bhattacharyya
601. Dr. Tumpa Bhattacharjee
602. Dr. Vaishali Naik
603. Dr. Ajay Kumar Himanshu
604. Dr. Anand Kumar Dubey
605. Dr. Animesh Goswami
606. Dr. Ayan Ray
607. Dr. Debasis Bhowmick
608. Dr. Deepak Pandit
609. Dr. Partha Pratim Bhaduri
610. Dr. Prasanta Karmakar
611. Dr. Pratap Roy
612. Dr. Rupa Chatterjee
613. Dr. Sadhukhan Jhilam
614. Dr. Samir Kundu
615. Dr. Shashi C. Srivastava
616. Dr. Supriya Mukhopadhyay
617. Dr. Tapan Kumar Rana
618. Dr. Tilak Kumar Ghosh
619. Dr. Zubayer Ahammed

SINP

❖ Chemical Sciences

620. Porf. Susanta Lahiri
621. Dr. Dulal Senapati
622. Dr. Montu K Hazra
623. Dr. Padmaja Prasad Mishra

❖ Life Sciences

624. Prof. Abhijit Chakrabarti
625. Dr. Debashis Mukhopadhyay
626. Dr. Gautam Garai
627. Dr. Partha Saha
628. Dr. Rahul Banerjee
629. Dr. Sampa Biswas
630. Dr. Udayaditya Sen
631. Dr. Chandrima Das
632. Dr. H. Raghuraman
633. Dr. Kaushik Sengupta
634. Dr. Oishee Chakrabati
635. Dr. Sangram Bagh
636. Dr. Soumen Kanti Manna
637. Dr. Subhabrata Majumder
638. Dr. Subhendu Roy

❖ Physical Sciences

639. Prof. Gautam Bhattacharyya
640. Prof. Satyajit Saha
641. Prof. Abhik Basu
642. Porf. Ambar Ghosal
643. Prof. Bijay Kumar Agrawal
644. Prof. Bireswar Basu Mallick
645. Prof. Chandan Mazumder
646. Prof. Debasish Majumdar
647. Prof. Harvendra Singh
648. Prof. Indranil Das
649. Prof. Kumar Sankar Gupta
650. Prof. Mustafa Munshi Golam
651. Prof. Mylavarapu Sita Janki
652. Prof. Nikhil Chakrabarti
653. Prof. P. M. G. Namissan
654. Prof. Prabhat Kumar Mandal
655. Prof. Pradip Kumar Roy
656. Prof. Prakash Mathews
657. Prof. Satyajit Hazra

658. Prof. Sukalyan Chattaopadhyay
659. Prof. Supratik Mukhopadhyay
660. Prof. Tapas Kuamr Chini
661. Prof. Ushasi Datta
662. Dr. Amit Ghosh
663. Dr. Anjali Mukherjee
664. Dr. Arunava Mukherjee
665. Dr. Chandi Charan Dey
666. Dr. Chinmay Basu
667. Dr. Krishnakumar S R Menon
668. Dr. Maitreyee Nandy
669. Dr. Manoj K. Sharan
670. Dr. Nayana Majumdar
671. Dr. Sandip Sarkar
672. Dr. Satyaki Bhattacharya
673. Dr. Subir Sarkar
674. Dr. Suchandra Dutta
675. Dr. Supratic Chakraborty
676. Dr. Arnab Kundu
677. Dr. Arti Garg
678. Dr. Biswajit Karmakar
679. Dr. Biswarup Satpati
680. Dr. Debasish Banerjee
681. Dr. Debasish Das
682. Dr. Kalpataru Pradhan
683. Dr. Koushik Dutta
684. Dr. Mala Das
685. Dr. M.K. Mukhopadhyay
686. Dr. Pratik Majumdar
687. Dr. Sankar De
688. Dr. Tinku Sinha

IPR

❖ Chemical Sciences

689. Prof. Sudhir Kumar Nema

❖ Engineering Sciences

690. Prof. Shashank Chaturvedi
691. Prof. Surya kumar Pathak
692. Dr. Alphonsa Joseph
693. Dr. Nirav I. Jamnapara
694. Dr. Paritosh Chaudhuri
695. Dr. Rajesh Kumar
696. Dr. Suryakant B. Gutpa
697. Dr. Vipulkumar L. Tanna

❖ Physical Sciences

698. Prof. Abhijit Sen
699. Prof. Shishir P. Deshpande
700. Prof. Prabal Kumar Chattapadhyay
701. Prof. Subrata Pradhan
702. Prof. Subroto Mukherjee
703. Prof. Sudip Sengupta
704. Prof. Vinay Kumar
705. Dr. Anitha V. P.
706. Dr. Asim Kumar Chattopadhyay
707. Dr. Debasis Chandra
708. Dr. Ganesh Rajaraman
709. Dr. Hem Chandra Joshi
710. Dr. Hiteshkumar B Pandya
711. Dr. Jana Mukti Ranjan
712. Dr. Joydeep Ghosh
713. Dr. Lalit Mohan Awasthi
714. Dr. Mainak Bandopadhyay
715. Dr. Mrityunjay Kundu
716. Dr. Mukesh Ranjan
717. Dr. Nirmal Kumar Bisai
718. Dr. Pramod Kumar Sharma
719. Dr. Raju Daniel
720. Dr. Saikia Bipul
721. Dr. Samir Khirwadkar
722. Dr. Sanjeev Kumar Sharma
723. Dr. Sanjeev Kumar Varshney
724. Dr. Ziauddh Khan
725. Dr. C. Balasubramanian
726. Dr. Devendra Sharma
727. Dr. Gourab Bansal
728. Dr. N Ramasubramanian
729. Dr. Pintu Bandyopadhyay
730. Dr. Ravi G.
731. Dr. Sarveshwar Sharma
732. Dr. Shantanu Kumar Karkari
733. Dr. Smruti R. Mohanty
734. Dr. Subhash V.

IOP

❖ Physical Sciences

735. Prof. Karuna Kar Nanda
736. Prof. Biju Raja Sekhar

737. Prof. Parlapalli Venkata Satyam
738. Prof. Pradip Kumar Sahu
739. Prof. Shikha Varma
740. Prof. Som Tapobrata
741. Prof. Sudipta Mukherji
742. Prof. Suresh Kumar Patra
743. Dr. Sanjib Kumar Agarwalla
744. Dr. Arjit Saha
745. Dr. Aruna Kumar Nayak
746. Dr. Debasish Chaudhuri
747. Dr. Debottam Das
748. Dr. Dinesh Topwal
749. Dr. Goutam Tripathy
750. Dr. Kirtiman Ghosh
751. Dr. Manimala Mitra
752. Dr. Samal Debakanta
753. Dr. Saptarshi Mandal
754. Dr. Satyaprakash Sahoo
755. Dr. Shamik Banerjee

HRI

❖ Mathematical Sciences

756. Prof. Kalyan Chakraborty
757. Prof. Manoj kumar
758. Prof. P. K. Ratnakumar
759. Prof. Punita Batra
760. N. Raghavendra
761. Prof. R. Thangadurai
762. Prof. Surya D Ramana
763. Dr. N Raghavendra
764. Dr. Gyan Prakash
765. Dr. Hemangi Madhusudan Shah
766. Dr. Umeshkumar V. Dubey

❖ Physical Sciences

767. Prof. Pinaki Majumdar
768. Prof. Aditi Sen De
769. Prof. Arun Kumar Pati
770. Prof. Asesh Krishna Datta
771. Prof. Dileep Prabhakar Jatkar
772. Prof. Prasenjit Sen
773. Prof. Ujiwal Sen
774. Dr. Anirban Basu
775. Dr. Anshuman Maharana
776. Dr. Santosh Kumar Rai
777. Dr. T. P. Pareek
778. Dr. Tapas kumar Das
779. Dr. Tathagata Ghosh

IMSc

❖ Life Sciences

780. Prof. Gautam I. Menon
781. Dr. Rahul Siddharthan
782. Dr. Areejit Samal

❖ Mathematical Sciences

783. Prof. K. N. Raghavan
784. Prof. Amritanshu Prasad
785. Prof. C. R. Subramanian
786. Prof. Jaya N. Iyer
787. Prof. Meena Bhaskar Mahajan
788. Prof. Saket Saurabh
789. Prof. Sankaran Viswanath
790. Prof. Sanoli Gun
791. Prof. Srinivas Kotyada
792. Prof. Venkatesh Raman
793. Prof. Vijay Kodiyalam
794. Dr. Anilesh Mohari
795. Dr. Anirban Mukhopadhyay
796. Dr. Pralay Chatterjee
797. Dr. Vikram Sharma
798. Dr. Anup Biswanath Dixit
799. Dr. Indrava Roy
800. Dr. Prakash Saivsan
801. Dr. S. Sundar
802. Dr. Sushmita Gupta
803. Dr. Sushmita Venugopal

❖ Physical Sciences

804. Prof. V. Ravindran
805. Prof. Indumathi D.
806. Prof. Nita Sinha
807. Prof. Raghib Hassan Syed
808. Prof. Rajesh R.
809. Prof. Satyavani Vemparala
810. Prof. Sibasish Ghosh
811. Prof. Sitabhra Sinha
812. Dr. Gopalakrishna Sharihari
813. Dr. Manjari Bagchi
814. Dr. Mukul S. Laad
815. Dr. Partha Mukhopadhyay

816. Dr. Pinaki Chaudhuri
817. Dr. Ronojoy Adhikari
818. Dr. Sanatan Digal
819. Dr. Sujay K. Ashok
820. Dr. V. S. Nemani
821. Dr. Ajit Coimbatore Balram
822. Dr. Chandrashekar C. M.
823. Dr. Dhiraj Kumar Hazra
824. Dr. Ganesh Ramchadran
825. Dr. Roji Pius
826. Dr. Sayantan Sharma

NISER

❖ Applied Systems Analysis

827. Dr. Amarendra Das
828. Dr. Amarjeet Nayak
829. Dr. Debashis Pattanaik
830. Dr. Joe Varghese Yeldho
831. Dr. Pranaya Kumar Swain
832. Dr. Rooplekha Khuntia

❖ Chemical Sciences

833. Prof. Alagar Srinivasan
834. Dr. Bhargava B. L.
835. Dr. Chandra Shekhar Purohit
836. Dr. Chidambaram Gunanathan
837. Dr. Himansu Sekhar Biswal
838. Dr. Jogendra Nath Behera
839. Dr. Moloy Sarkar
840. Dr. Nagendra Kumar Sharma
841. Dr. Nembenna Sharanappa
842. Dr. P. C. Ravikumar
843. Dr. Prasenjit Mal
844. Dr. Sanjib Mal
845. Dr. Saravanan Peruncheralathan;
846. Dr. Subhadip Ghosh
847. Dr. Sudip Barman
848. Dr. Upakarasamy Lourderaj
849. Dr. Venkatasubbaiah Krishnan
850. Dr. Arindam Ghosh
851. Dr. Bidraha Bagh
852. Dr. Bishnu Prasad Biswal
853. Dr. Dipak Samanta

❖ Life Sciences

854. Dr. Chandan Goswami
855. Dr. Debasmita Pankaj Alone
856. Dr. Harapriya Mohapatra
857. Dr. K. Chandrasekhar Panigrahi
858. Dr. Manjusha Dixit
859. Dr. Palok Aich
860. Dr. Pankaj Vidyadhar Alone
861. Dr. Praful S. Singru
862. Dr. Subhasis Chattopadhyay
863. Dr. Anirudhha Datta Roy
864. Dr. K. Venkatsai Badireenath
865. Dr. Mohammed Saleem
866. Dr. Renjith Mathew
867. Dr. Rudresh Acharya
868. Dr. Srinivasan Ramanujam
869. Dr. Tirumala Kumar Chowdary

❖ Mathematical Sciences

870. Dr. Anil Kumar Karn
871. Dr. Binod kumar Sahoo
872. Dr. Brundaban Sahu
873. Dr. Anisur Rahaman Molla
874. Dr. Anupam Pal Chowdhary
875. Dr. Arita Banik
876. Dr. Deepak Kumar Dalai
877. Dr. Chitrabhanu Chaudhury
878. Dr. Dinesh Kumar Keshari
879. Dr. Kamal Lochan Patra
880. Dr. Kaushik Majumder
881. Dr. Krishanu Dan
882. Dr. Manas Ranjan Sahoo
883. Dr. Manoj Mishra
884. Dr. Meher Jaban
885. Dr. Nabin Kumar Jana
886. Dr. Panchugopal Bikram
887. Dr. Ramesh Manna
888. Dr. Rishiraj Bhattacharyya
889. Dr. Ritwik Mukherjee
890. Dr. Roy Sutanu
891. Dr. Sanjay Parui
892. Dr. Senthil Kumar K.
893. Dr. Subhankar Mishra

❖ Physical Sciences

894. Prof. Sudhakar Panda
895. Prof. Bedangadas Mohanty

896. Dr. Ashok Kumar Mohapatra
897. Dr. Colin Benjamin
898. Dr. Prasanjit Samal
899. Dr. Pratap Kumar Sahoo
900. Dr. Ritwik Das
901. Dr. Sanjay Kumar Swain
902. Dr. Subhankar Bedanta
903. Dr. A.V. Anil Kumar
904. Dr. Abdur Rahman
905. Dr. Ajaya Kumar Nayak
906. Dr. Amaresh Kumar Jaiswal
907. Dr. Anamitra Mukherjee
908. Dr. Ashis Kumar Nady
909. Dr. Chethan N. Gowdigere
910. Dr. Guneshwar Thangjam
911. Dr. Jaya Khanna
912. Dr. Joydeep Bhattacharjee
913. Dr. Kartikeswar Senapati
914. Dr. Kush Saha
915. Dr. Liton Majumdar
916. Dr. Najmal Haque
917. Dr. Nishikanta Khandai
918. Dr. Prathikrit Bhattacharya
919. Dr. Prolay Kumar Mal
920. Dr. Sayantani Bhattacharyya
921. Dr. Subhasish Basak
922. Dr. Sumedha
923. Dr. V. Ravi Chandra
924. Dr. Victory Roy
925. Dr. Yogesh Kumar Srivastava

❖ **Engineering Sciences**

926. Dr. Anup Kumar Bhattacharya
927. Dr. Sabyasachi Karati

TMC

❖ **Health Sciences**

928. Prof. Rajendra Achyut Badwe
929. Prof. Ajay Puri
930. Prof. Aliasgar V Moiyadi
931. Prof. Asmita Maheswari
932. Prof. Ashwini Narsingrao
933. Prof. Atul Prabhakar Kulkarni
934. Prof. Avanish Parmesh Saklani
935. Prof. Bharat Rekhi
936. Prof. Conjeevaram S. Parmesh
937. Prof. Devendra Arvind Chaukar
938. Prof. Gulia Seema
939. Prof. Jai Prakash Agarwal
940. Prof. Jigeeshu Vasishtha Divatia
941. Prof. Kedar Kamalakar Deodhar
942. Prof. Laskar Sarbani Ghosh
943. Prof. Manisha Nandkumar Pawar
944. Prof. Manju Sengar
945. Prof. Mukta Ravindra Ramdwar
946. Prof. Nita Sukumar Nair
947. Prof. Pankaj Chaturvedi
948. Prof. P. Ganesan Subramanian
949. Prof. Prabhakar Kumar
950. Prof. Prachi Sunil Patil
951. Prof. Prakash Shetty
952. Prof. Prathamesh Pai Srinivas
953. Prof. Rajesh Prabhakar Dikshit
954. Prof. Rakesh Jalali
955. Prof. Reena Zarir
956. Prof. Sajid Shafique Quresh
957. Prof. Saneeta Bhikaji Desai
958. Prof. Sanjay Biswas
959. Prof. Sarin Rajiv
960. Prof. Shailesh Vinayak Shrikhande
961. Prof. Sharmila Anil Pimple
962. Prof. Sheila Anil Myatra
963. Prof. Shripad Dinanath Banavali
964. Prof. Shylasree Thumkur Surappa
965. Prof. Sridhar Epari
966. Prof. Sudeep Gupta
967. Prof. Sumeet Gujral
968. Prof. Sumitra Ganesh Bakshi
969. Prof. S. B. Rajadhyaksha
970. Prof.Tanuja Manjanath Shet
971. Prof. Tejpal Gupta
972. Prof. Umesh M. Mahantshetty
973. Prof. Vani Parmar
974. Prof. Venkatesh Rangarajan
975. Prof. Vijaya Prakash Patil
976. Dr. Abhishek Mahajan
977. Dr. Amit Prakashchandra Joshi

978. Dr. Amol Trymbakrao Kothekar
979. Dr. Anant Ramaswamy
980. Dr. Anuja Dhananjay Deshmukh
981. Dr. Aparna Sanjay Chatterjee
982. Dr. Archi Ramesh Agrawal
983. Dr. Bhausaheb Pandurang Bagal
984. Dr. Deepa Ravindranathan Nair
985. Dr. Dushyant Jaiswal
986. Dr. Ganesh Kailas Bakshi
987. Dr. Gaurav Narula
988. Dr. Gauravi Ashish Mishra
989. Dr. George Karimundackal
990. Dr. Girish Chinnaswamy
991. Dr. Goda Jayant Sastri
992. Dr. Gouri Himalaya Pantvaidya
993. Dr. Gulia Ashish
994. Dr. Jaya Ghosh
995. Dr. Jayita Kedar Deodhar
996. Dr. Jeson Ranjan Doctor
997. Dr. Jyoti Bajpai
998. Dr. Kinjalka Ghosh
999. Dr. Madhavi Dattatarya Desai
1000. Dr. Madhavi G. Shetmahajan
1001. Dr. Mahendra Pal
1002. Dr. Mahesh Goel
1003. Dr. Malini Premkumar Joshi
1004. Dr. Munita Meenu Bal
1005. Dr. Murthy Vedang
1006. Dr. Naveen Sulakshan Salins
1007. Dr. Navin Khattry
1008. Dr. Nayana Shekar Amin
1009. Dr. Nilendu C. Purandare
1010. Dr. Nitin Sudhakar Shetty
1011. Dr. Priti Dhansukhbhai Desai
1012. Dr. Priya Ranganathan
1013. Dr. Raghu Sudarshan Thota
1014. Dr. Rajesh Ashok Kinhikar
1015. Dr. S. Ramkiran
1016. Dr. Sabita Shambhul Jiwnani
1017. Dr. Santosh Menon
1018. Dr. Seema Ashish Kembhavi
1019. Dr. Shashank Ojha
1020. Dr. Shashikant CU Patne

1021. Dr. Sheela Prashant Sawant
1022. Dr. Shilpushp Bhosale
1023. Dr. Sharddha Patkar
1024. Dr. Siddhartha Sankar Laskar
1025. Dr. Sneha Shah
1026. Dr. Sohan Lal Solanki
1027. Dr. Supriya Jayant Sastri
1028. Dr. Suyesh S. Kulkarni
1029. Dr. Swapnil Rane
1030. Dr. Tushar Shailesh Vora
1031. Dr. Vandana Agarwal
1032. Dr. Vanita Maria Noronha
1033. Dr. Vikarm Anil Chaudhari
1034. Dr. Vinay Kant Shankhdhar
1035. Dr. Abhishek Chatterjee
1036. Dr. Akanksha Chichra
1037. Dr. Anisha A. Navkudar
1038. Dr. Anuprita Dilip Daddi
1039. Dr. Aparna Katdare
1040. Dr. Asawari Jingonda Patil
1041. Dr. Ashwin Luis Desouza
1042. Dr. Ashwini D. Rane
1043. Dr. Pankaj Chaturvedi
1044. Dr. Atanu Bhattacharjee
1045. Dr. Avinash Rameshrao Pagdhune
1046. Dr. Basant L. Malpani
1047. Dr. Bandira Cheriyalinkal Parambil
1048. Dr. Bhakti Dushyant Trivedi
1049. Dr. Dhanlaxmi L Shetty
1050. Dr. Gauri Raman Gangakhedar
1051. Dr. Gauri Rohan Deshpande
1052. Dr. Hasmukh Kantilal Jain
1053. Dr. Janu Amit Kumar
1054. Dr. Jifmi Jose Manjali
1055. Dr. Lingaraj Nayak
1056. Dr. Maya Prasad
1057. Dr. Neha Mittal
1058. Dr. Nehal Rishi Khanna
1059. Dr. Nikhil Vijay Patkar
1060. Dr. Nilesh Pandurang Sable
1061. Dr. Nivedita Chakrabarty
1062. Dr. Omshree Shetty
1063. Dr. Dhanlaxmi L. Shetty

1064. Dr. Palak Bhavesh Popat
1065. Dr. Prathiban K Velayutham
1066. Dr. Poonam K Panjwani
1067. Dr. Prabhat Bhargava
1068. Dr. Prakash Gagan
1069. Dr. Prashant Ramesh Tembhare
1070. Dr. Pratik Chandrani
1071. Dr. Rahul Krishnatry
1072. Dr. Rajiv Kumar
1073. Dr. Reshma Ambulkar
1074. Dr. Ritu Raj Upreti
1075. Dr. Sandeep Vivek Gurav
1076. Dr. Sangeeta Kakoti
1077. Dr. Santam Chakraborty
1078. Dr. Shaesta Adulaziz Mehta
1079. Dr. Shalaka Prakash Joshi
1080. Dr. Shiva Kumar Thiagarajan
1081. Dr. Shrikant C. Raut
1082. Dr. Shewetabh Sinha
1083. Dr. Sudhir Vasudevan Nair R
1084. Dr. Sudivay Prashant Sharma
1085. Dr. Sujata Lall
1086. Dr. Swapnil Parab Yeshwant
1087. Dr. Tabassum A. Wadasadawala
1088. Dr. Uma Bhaskar Dangi
1089. Dr. Vijay Maruti Patil
1090. Dr. Vikas Sureshchand Ostwal
1091. Dr. Vivek Gajana Bhat

❖ **Life Sciences**

1092. Prof. Arvind D Ingle
1093. Prof. Sorab Nariman Dalal
1094. Dr. Abhijt De
1095. Dr. Amit Dutta
1096. Dr. Ashok Varma
1097. Dr. Chilakapati Murali Krishna
1098. Dr. Joyti Anand Kode
1099. Dr. Kakoli Bose
1100. Dr. Manoj Balkrishna Mahimkar
1101. Dr. Pritha Ray
1102. Dr. Rukmini Balkrishna Govekar
1103. Dr. Sanjay Gupta
1104. Dr. Tanuja Rajendra Teni
1105. Dr. Venkatraman Prasanna
1106. Dr. Vikram Suryaprakash Gota
1107. Dr. Dibyendu Bhattacharyya
1108. Dr. Khizer Hasan Syed
1109. Dr. Nandini Verma
1110. Dr. Rohan Jayant Khadilkar
1111. Dr. Sanjeev Waghmare
1112. Dr. Sejal Patwardhan
1113. Dr. Sharath Chandra Arandkar
1114. Dr. Shilpee Dutt
1115. Dr. Sonam Mehrotra

HBNI at a Glance

During the last academic year (August 1, 2020-July 31, 2021), HBNI has awarded 234 Ph.D. degrees. The total number of Ph.D. degrees awarded by HBNI till July 31, 2021 stands at 1881. HBNI also awarded 25 M. Tech., 5 M.Sc. (Engg.) 49 M.Sc. in various science disciplines, 136 post graduate & super specialty medical degrees with specializations in Oncology, 24 diplomas in radiological physics (DipRP), 4 post graduate diplomas in Medical Radioisotope Technology (DMRIT), and 10 post graduate diplomas in Fusion Imaging Technology (PGDFIT) during this period. 755 students have been admitted to different academic programmes during 2020-21, out of which 187 students are for Ph.D. program.

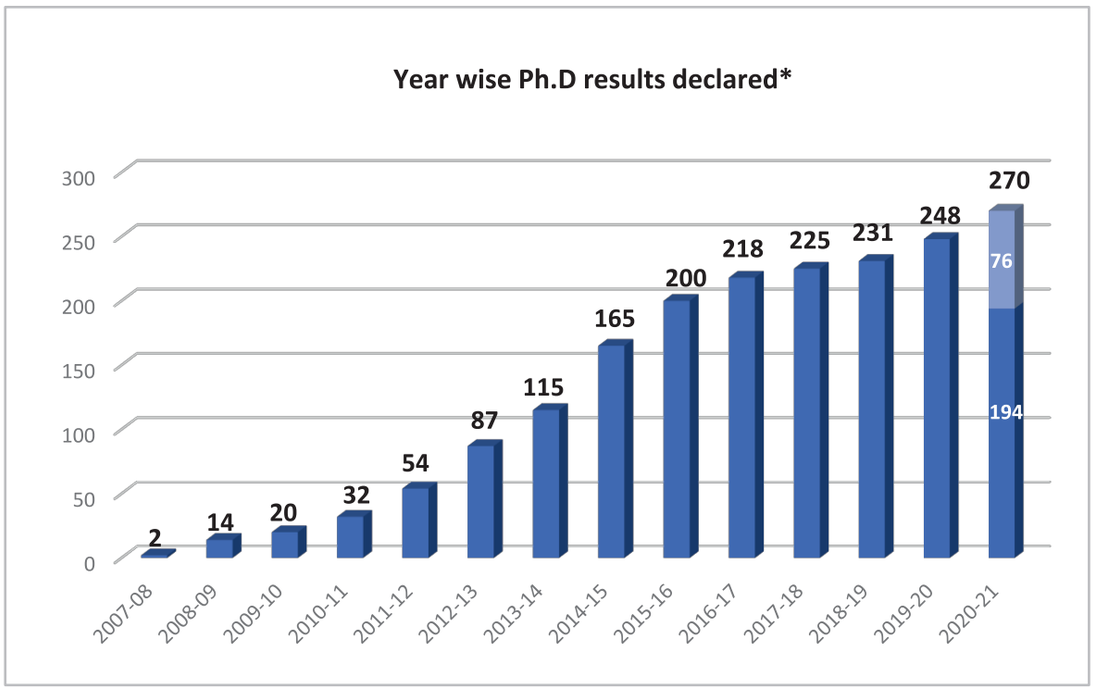

***The data from 2007-08 to 2019-20 is for the period April 1 of preceding year to March 31 of the ending year. The data for 2020-21 is for the period April 1, 2020 to July 31, 2021. Dark blue area (194) gives the data from April 1, 2020 to March 31, 2021, light blue area (76) gives the data from April 1, 2021 to July 31, 2021**

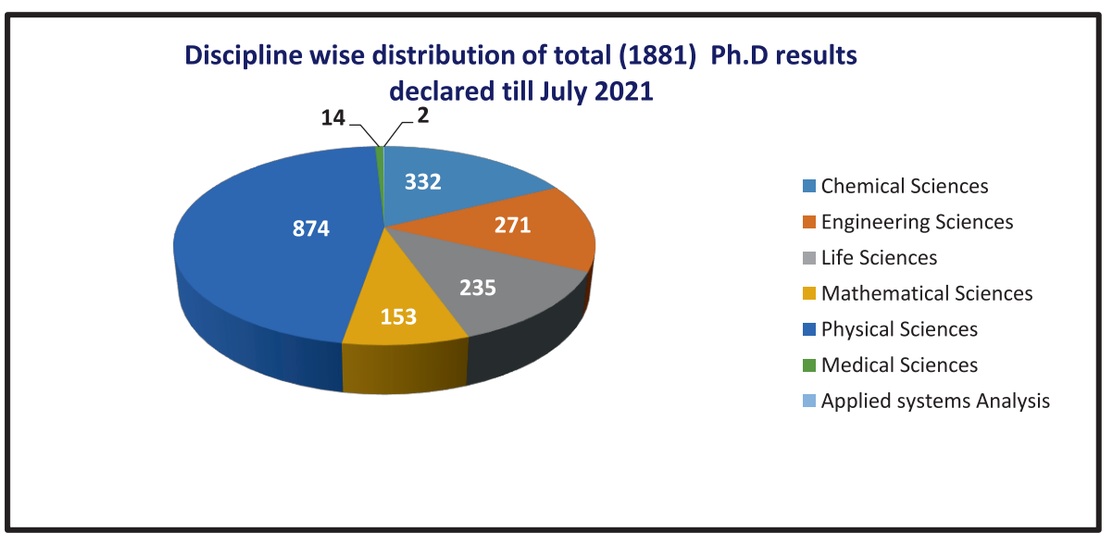

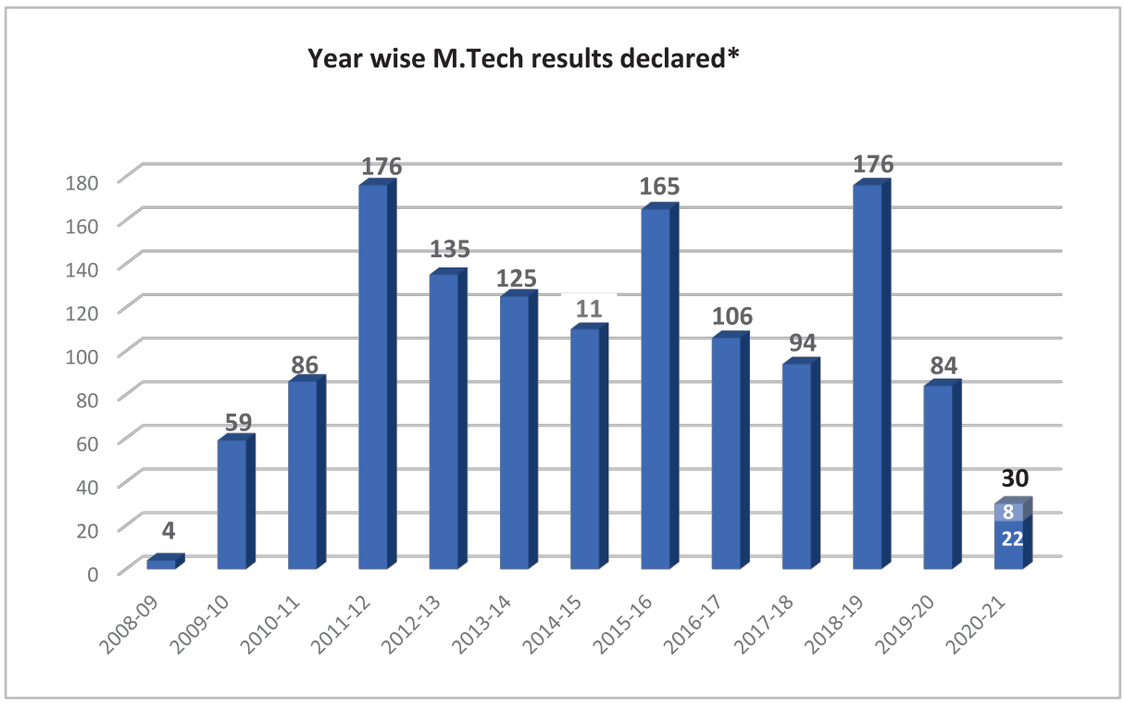

*The data from 2008-09 to 2019-20 is for the period April 1 of the preceding year to March 31 of the ending year. The data for 2020-21 is for the period April 1, 2020 to July 31, 2021. Dark blue area (22) gives the data from April 1, 2020 to March 31, 2021, light blue area (8) gives the data from April 1, 2021 to July 31, 2021

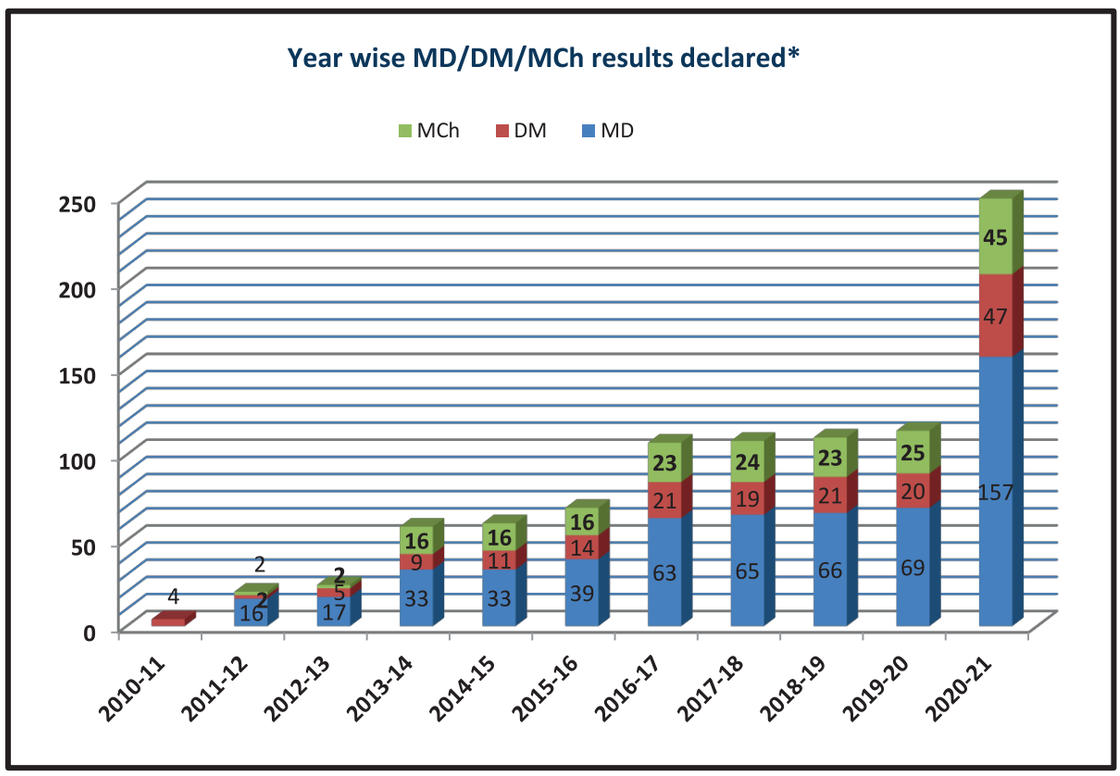

*The data from 2010-11 to 2019-20 is for the period April 1 of preceding year to March 31 of the ending year. The data for 2020-21 is for the period April 1, 2020 to July 31, 2021.

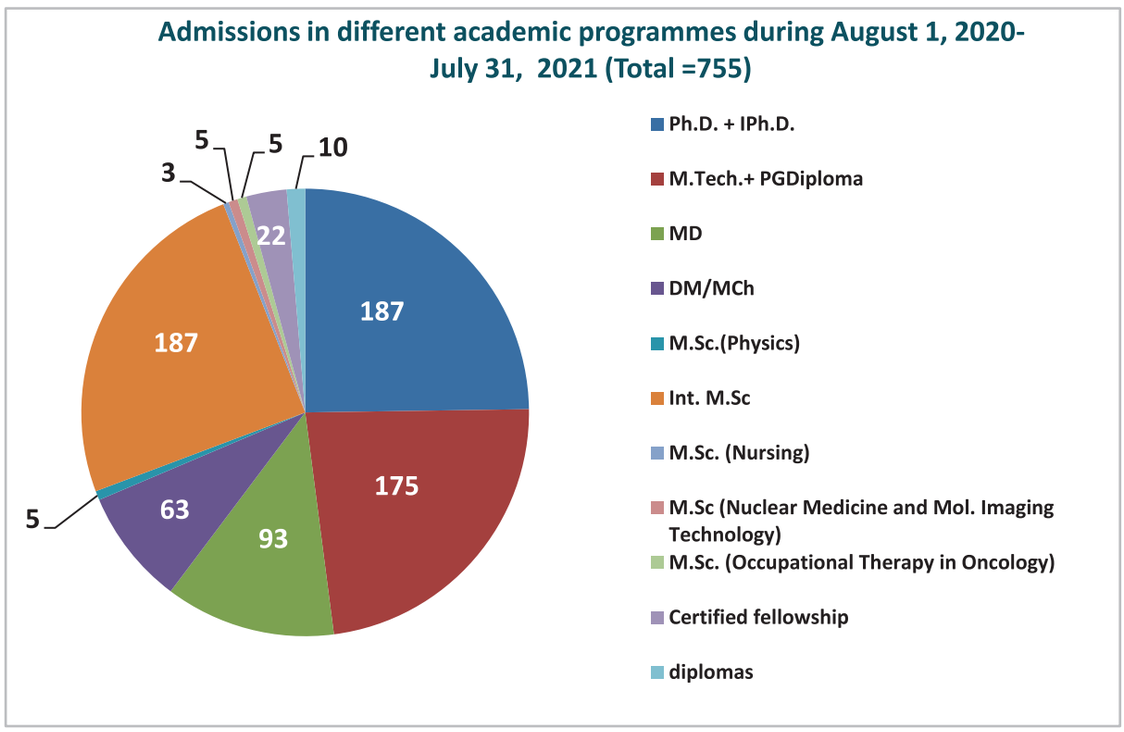

Number of students admitted to the different academic programmes of CIs/OCC during August 1, 2020 –July 31, 2021

Academic Program	BARC	IGCAR	RRCAT	VECC	SINP	IPR	TMC	IoP	IMSc	HRI	NISER	Total
Ph.D. + Integrated Ph.D.	56	….	12	6	13	11	11	7	13	18	40	187
M.Tech + PG Diploma	132	30	13	….	….	….	….	….	….	….	….	175
MD	1	….	….	….	….	….	92	….	….	….	….	93
DM/MCh	….	….	….	….	….	….	63	….	….	….	….	63
M.Sc. Physics	….	….	….	….	….	….	….	….	….	5	….	5
Integrated M.Sc.	….	….	….	….	….	….	….	….	….		187	187
M.Sc. (Nursing)	….	….	….	….	….	….	3	….	….	….	….	3
M.Sc (Nuclear Medicine and Molecular Imaging Technology)	….	….	….	….	….	….	5	….	….	….	….	5
M.Sc. (Occupational Therapy in Oncology)	….	….	….	….	….	….	5	….	….	….	….	5
Certified fellowship	….	….	….	….	….	….	22	….	….	….	….	22
Diplomas	….	….	….	….	….	….	10	….	….	….	….	10
Total	189	30	25	6	13	11	211	7	13	23	227	**755**

Section II
(Theses at a Glance)

1. Chemical Sciences

During the period of report, HBNI awarded 34 Ph.D. degrees in Chemical Sciences in a variety of research areas such as catalysis, environmental chemistry, actinide separation & speciation, materials chemistry, nanoscience, nuclear chemistry, radiopharmaceuticals and molecular modelling towards selective metal ion extractions. The summary of some of the theses is given below.

1.1 Bhabha Atomic Research Centre, Mumbai

1.1.1 Synthesis, mechanistic study and interaction of metal nanoparticles with biologically important molecules

The thesis reports the research work carried out on synthesis, characterization and uses of metal nanoparticles (NPs) in different applications. Stable AuNPs have been prepared in this study following decarboxylation of tryptophan. The AuNPs accumulate preferentially at the cell membrane. An *in-vitro* MTT assay using these AuNPs for glioma cell line (U-87MG) shows a decrease in the survival in the presence of gamma radiation, suggesting the possible radio-sensitization of these NPs. Plasmonic gold and silver NP (AuNP and AgNP) loaded alginate films have also been developed for surface enhanced Raman scattering (SERS) based sensing, demonstrating the detection of cresyl violet, and rhodamine 6G at nM concentrations. These films show the potentials for dosimetric uses also, as investigated in the presence of X-ray and ^{125}I sources, whereby they work as radiosensitizers due to surface plasmon property of the NPs, enhancing the exposed radiation dose, monitored by using commercial EBT3 radiochromic film. It is seen that AgNPs and AgCl/Ag NP dimmers (NPDs) can be used for SERS based detection of sildenafil citrate in the nM concentration range. Similarly, SERS based detection and conformational studies have also been carried out for 2,5-Dimercapto-1,3,4-thiadiazole (DMTD) and thioflavin T (ThT) molecules, using both gold and silver NPs.

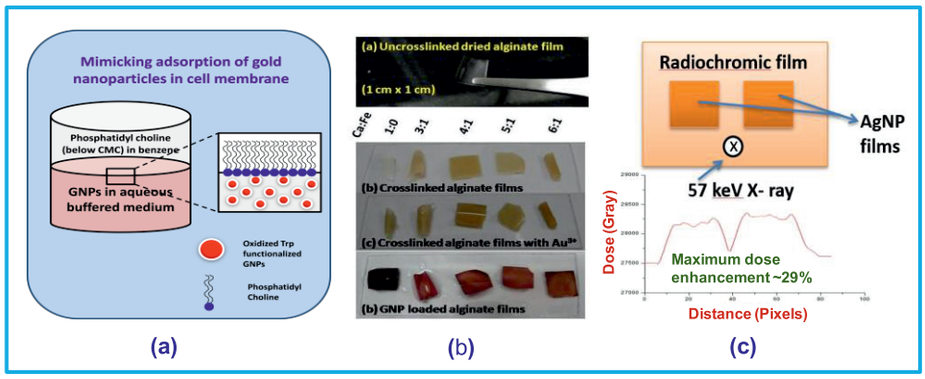

Schematic presentation of (a) preferential accumulation of GNPs at the interface and cell membrane (b) plasmonic nanoparticles loaded film and (c) dose enhancement by AgNP based radiosensitizer films.

1.1.2 Radiochemical separation and purification of molybdenum-99 for medical and industrial applications

The development of a novel method for the production of medical grade ^{99}Mo with high specific activity following ^{235}U(n,f)^{99}Mo reaction through thermal neutron irradiation of U-Al alloy, labelling fatty acids with ^{99}Mo radioisotope, and bio-evaluating their uses for single-photon emission-computed tomographic (SPECT) myocardial imaging have been the objectives of the present thesis. Development of a ^{99}Mo based industrial radiotracer has also been other aim of the present thesis. A new separation method has been developed for high specific activity ^{99}Mo, which is then used to produce ^{99m}Tc isotope using ^{99}Mo^{99m}Tc based column generator. The ^{99m}Tc isotope is subsequently used to prepare ^{99m}Tc-labelled fatty acids for their applications in the SPECT based myocardial imaging. In the present thesis, a coordination complex of ^{99}Mo with α-benzoinoxime (ABO) ligand has also been developed in organic phase which is successfully used in the identification of leaky heat-exchangers in a petroleum refinery. Schematics of the preparations of ^{99m}Tc-labelled fatty acid samples are shown in the schematic.

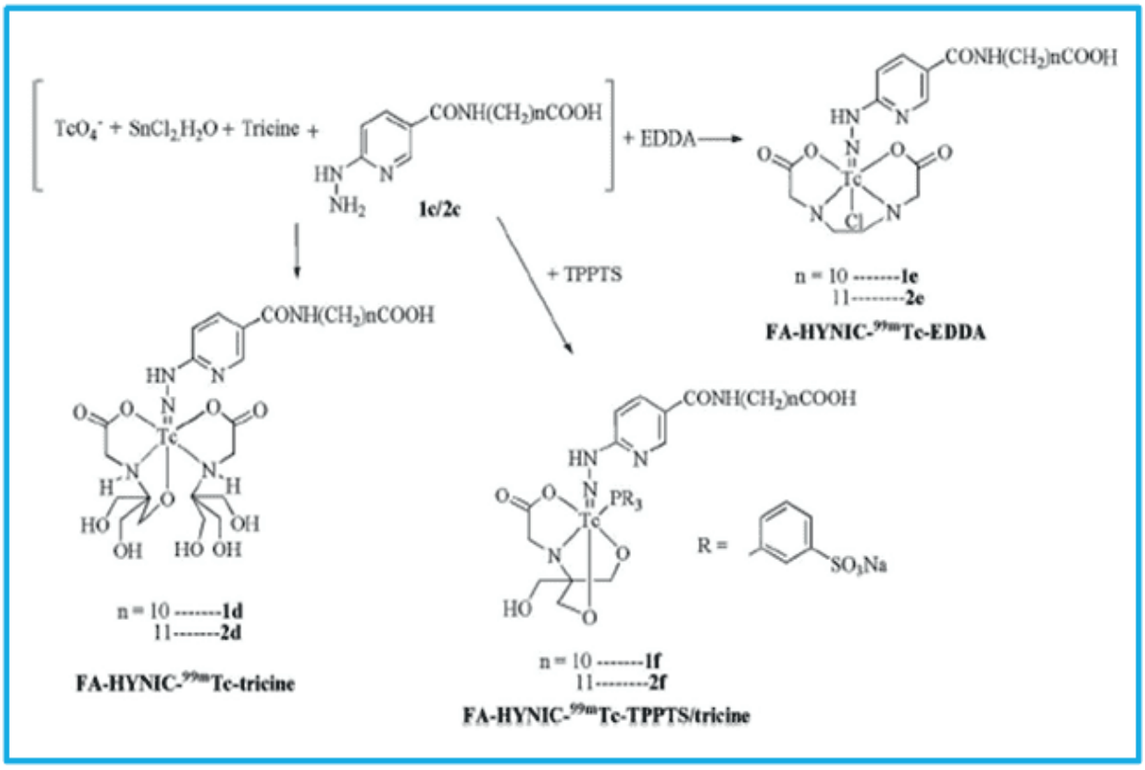

Schematic diagram showing the preparation of the ^{99m}Tc-labelled fatty acids for medical applications. Fatty acids (FA) having 11C and 12C chains conjugated with hydrazinopyridine-3-carboxylic acid (HYNIC) is used in this study.

1.1.3 Kinetic studies of gas phase reactions of volatile organic compounds (VOCs) relevant in atmospheric chemistry

Understanding the atmospheric implications of some selective volatile organic compounds (VOCs) investigated through their gas phase reactions with tropospheric oxidants like OH, Cl and O_3, and also identifying their reaction products have been the main theme of the present thesis. VOCs with varying structural features like degree of unsaturation, presence of hetero atoms, functional groups, and ring strains, have been investigated. Cyclic hydrocarbon-based VOCs like cyclooctane, cis-cyclooctene and 1,5-cyclooctadiene have been studied to unravel the effect of unsaturation. The 1-chlorocyclopentene has been investigated to understand the effect of chlorine substitution on its reactivity as compared to unsubstituted analogue. Cyclic ester and cyclic ether-based VOCs like gamma-valerolactone, alpha-methyl gamma-butyrolactone, and epichlorohydrin have been investigated to understand the role of ring oxygen on the reactivity of these molecules. Estimated rate coefficients (k_{Cl}, k_{OH}, and k_{O3}) and reaction product analysis suggest the major degradation channel of the studied VOCs is their reaction with OH, though reaction with Cl also becomes important especially at the marine boundary layer. It is inferred that the impact of the studied VOCs on the atmosphere would mostly be local in nature, however, for ethers, especially, the impact can extend up to the regional level at least. Major aspects of atmospheric implications of VOCs as investigated in the thesis are schematically shown below.

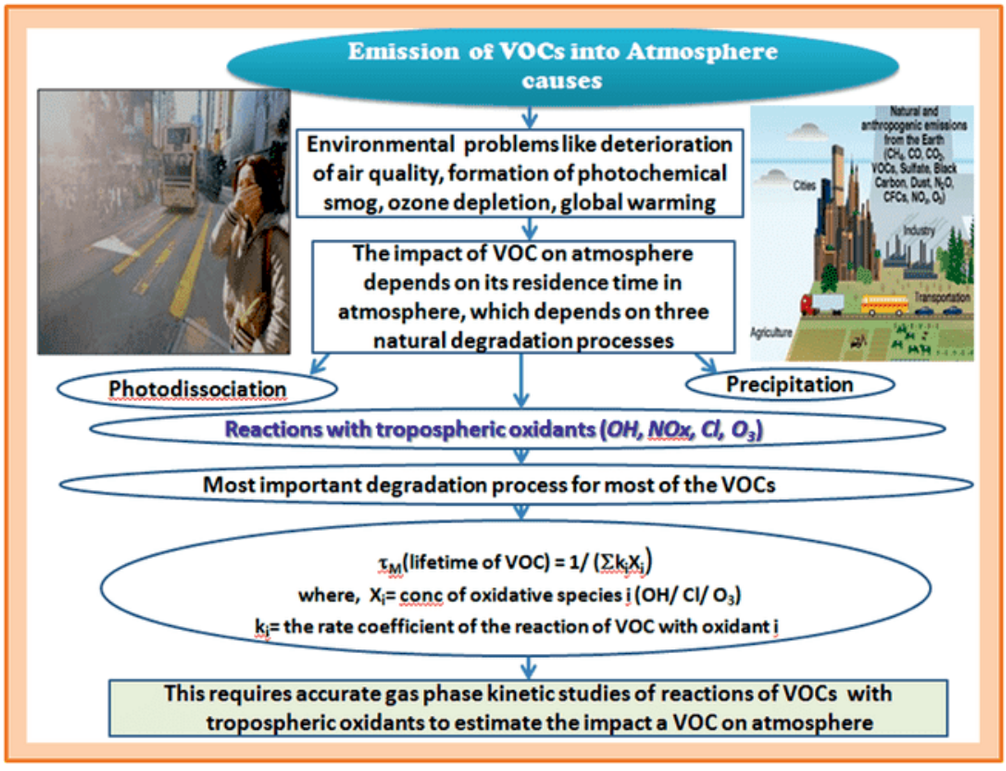

Schematic presentation of various implications of the VOCs emission into atmosphere.

1.1.4 Thermodynamic investigations of phosphate-based crystalline ceramic matrices for HLW immobilization

Understanding thermodynamic stability and leaching of different phosphate-based ceramic materials for their uses as the glass matrices for radioactive wastes disposals is the major aim of the thesis. Thermodynamic parameters such as heat capacity enthalpy of dissolution and standard molar enthalpy of formation have been estimated to judge the suitability of the studied materials. The values for enthalpy of formation are found to be the most negative for $LaPO_4$ and $(La_{0.7}Sr_{0.15}Th_{0.15})PO_4$ among the rare-earth phosphates (monazites) and monazite-cheralite solid solutions, respectively. The leach rate for metal ions from $(La_{0.7}Sr_{0.15}Th_{0.15})PO_4$ is $<10^{-10}$ $g{\cdot}cm^{-2}{\cdot}d^{-1}$, much lower than the borosilicate glasses (10^{-4} $g{\cdot}cm^{-2}{\cdot}d^{-1}$) used presently in the radioactive wastes disposals. The materials studied are quite stable in ground water in the pH range 2-9, suggesting quite small release of actinide ions from these materials. The ternary phase diagram and E_H-pH diagram of a typical Th-P-O system have also been investigated in the present thesis. It is inferred that $(La_{0.7}Sr_{0.15}Th_{0.15})PO_4$ is very suitable material for immobilization of fission products like divalent Sr^{2+}, trivalent actinides (Am^{3+}, Cm^{3+}) and tetravalent actinides (Pu^{4+}, Np^{4+}). Representative results of the present study are shown in the following figure.

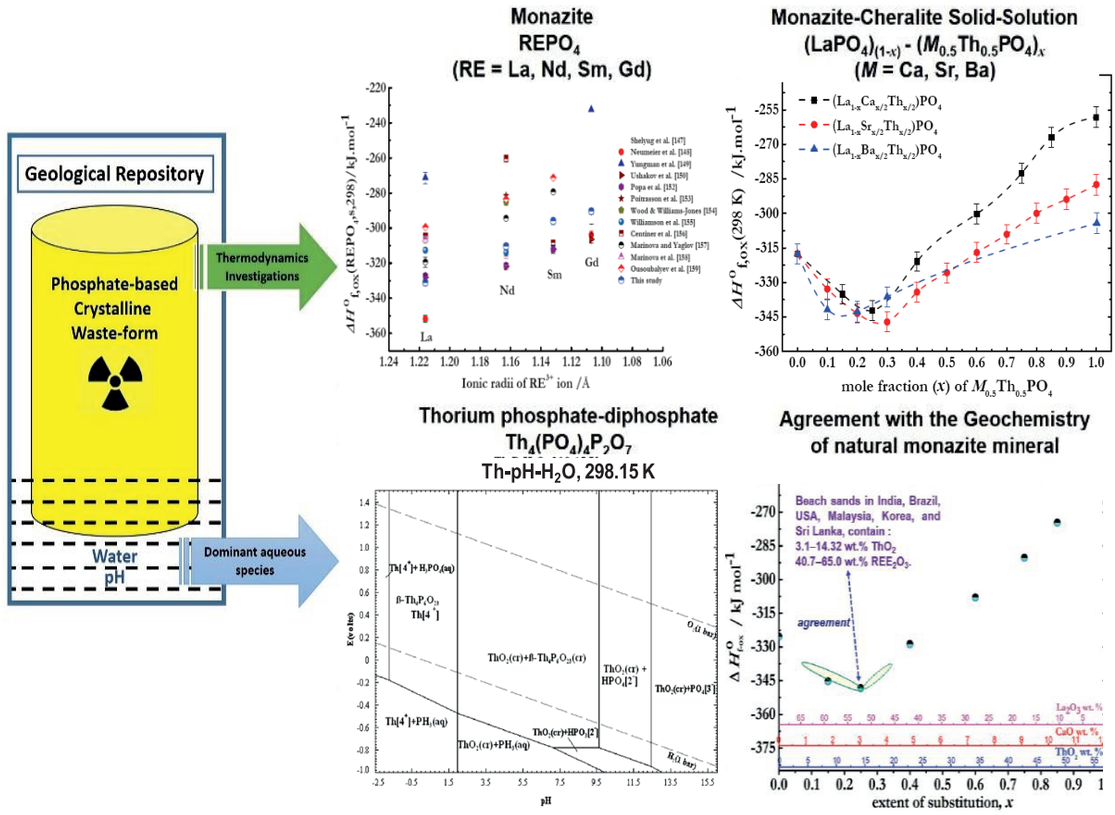

Thermodynamic parameters of the phosphate based ceramic materials investigated as possible alternatives to borosilicate glasses for radioactive waste disposals.

1.1.5 Preparation, characterization and thermophysical investigations on thorium based nuclear fuels and related systems

The thesis deals with the studies on thermophysical property of two thorium-based materials, namely, thorium-based metallic alloys and nano-crystalline thoria-based ceramics, having potential uses as the fuels in three-stage Indian nuclear power program. Though thorium-based metallic alloys are excellent fuels for both thermal and fast neutrons, data on their thermophysical properties are very limited. Preparations, characterizations and high temperature thermophysical properties evaluations for Th-U binary alloys (Th-10U and Th-20U) and Th-U-Zr ternary alloys (90Th-7U-3Zr and 90Th-3U-7Zr) have been carried out in the present thesis. It is revealed that these alloys have phase dispersion microstructures that consist of uranium-rich phases uniformly dispersed into thorium-rich matrices, suitable for both thermal and fast neutron irradiation. Thermophysical properties of the nano-crystalline thoria-based ceramics (ThO_2), prepared through combustions of citrate-Th(IV)-nitrate complex in solution and glycine-Th(IV)-nitrate complex in gel, have also been studied in the present thesis. While the material prepared from glycine-Th(IV)-nitrate show de-sintering behaviour, the material prepared from citrate-Th (IV)-nitrate does not show any de-sintering behaviour, suggesting the useful of the latter material for nuclear fuel pellet preparations. Some of the thorium-based materials, their microstructures and their thermal conductivity results are shown below.

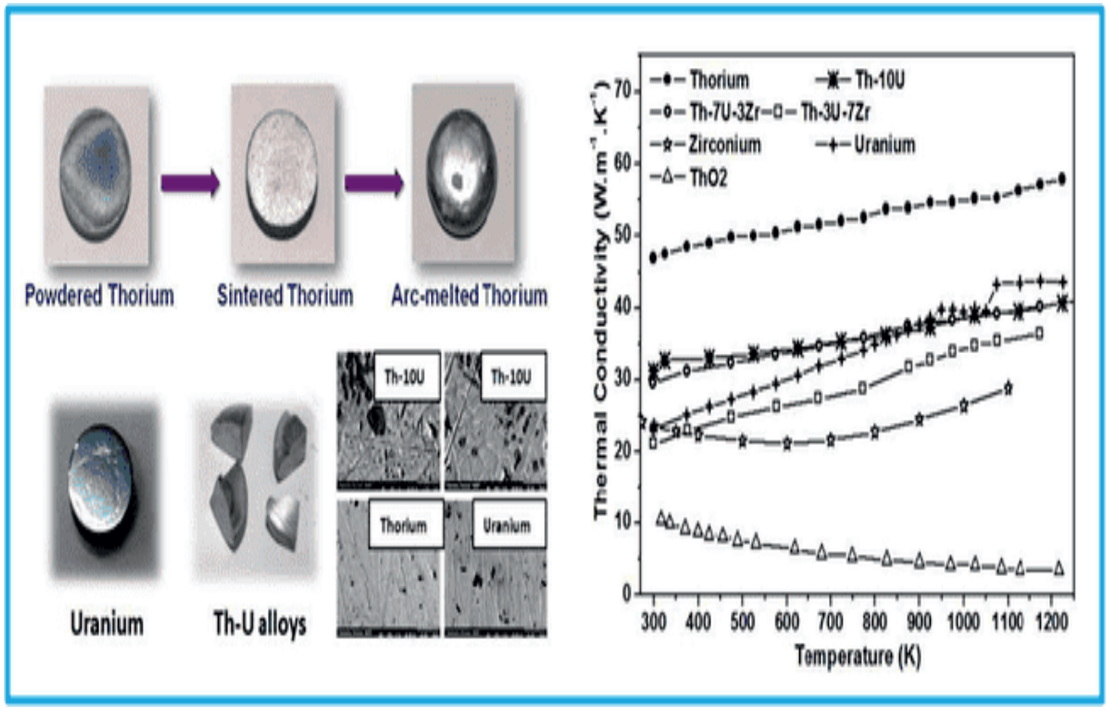

The pictures of some thorium-based materials, the back scattered electron (BSE) microscopy images and the thermal conductivity results of the materials investigated.

1.1.6 Isotope and hydrochemical investigation on uranium in groundwater of south west Punjab and central Rajasthan

The role of geology, hydrogeology, geochemistry and aquifer dynamics on the uranium contamination of groundwater at two geologically different alluvial formations, one in Punjab and other in Rajasthan, have been investigated in the present thesis. For the alluvial formation in Punjab, the range of uranium concentration in different groundwater samples is found to be 1-610 µg/L, while that for alluvial formation in Rajasthan is found to be 0.5-177 µg/L. Importantly, the permissible uranium concentration limit in groundwater from WHO is < 30 µg/L. In Punjab area, through the analysis of the environmental isotopes, it is realized that ground water recharge in the shallow zones occurs from three sources, namely, precipitation, canal water, and irrigation return flow, while that in the deeper zones occurs mainly through regional groundwater flows. In Rajasthan area, for both alluvial formation and hard rock formation, ground water recharge occurs mainly from precipitation and irrigation return flow. Following $^{234}U/^{238}U$ activity ratios, the oxidative dissolution is inferred as the main mechanism for uranium mobilization in shallow zones in Punjab, attributed to the presence of excessive nitrate ions due to extensive agricultural activity. In the deeper zone, mixing of the regional water flows with uranium contaminated shallow groundwater is the main reason for uranium concentration present. For the alluvial and hard rock formations in Rajasthan, both alpha recoil and oxidative leaching are realized as the main processes for high uranium contamination present in groundwater. Proposed models for uranium release in the alluvial formations in Punjab and the alluvial and hard rock formation in Rajasthan are schematically shown below.

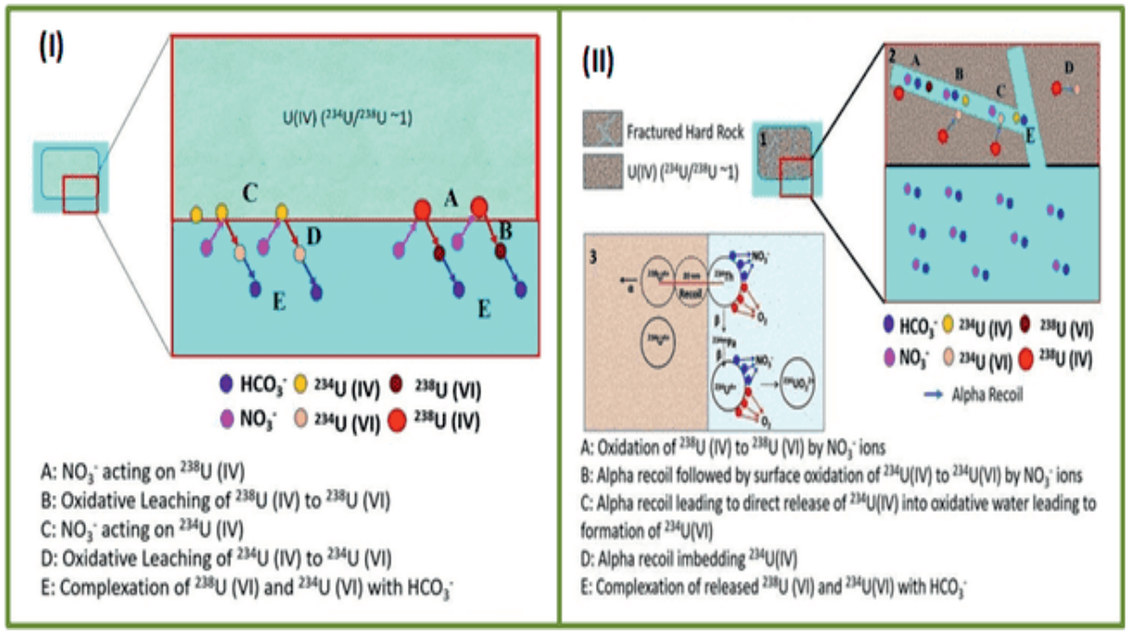

Conceptual model of uranium release in (i) alluvial formation in Punjab and (ii) hard rock formation in Rajasthan.

1.1.7 Experimental detection of actinides in human body and computational investigations of their decorporation mechanism

The aim of the thesis was to develop direct monitoring methodology for quick estimation of radioactive actinide contaminants like Th, U, Pu, Am, and Cm, in biological samples, to assess the total contamination levels, exposureby the concerned contaminants and to find ways for decorporation of these contaminants before their deposition in various organs. Knowing that in the body the actinides are mainly transported by the serum glycoproteins transferrin (sTf), which is basically an iron carrier, detailed binding interactions of the concerned actinide ions with sTf protein have been investigated in the present thesis. The tetravalent Pu(IV), Th(IV) ions bind more strongly with sTf than trivalent Cm(III) ion., The efficacy of two chelating molecules, hydroxypyridinone (HOPO) and catecholamide (CAM), as the potential agents for decorporation of actinide ions from sTf binding sites has also been investigated in this thesis. It is especially found that CAM has the potential to detach Pu(IV) from sTf binding site. The thesis also highlights the *in-vivo* detection of actinide contaminations as shown in he schematic diagram below and focuses on the multi-scale modelling of actinide biochemistry, having relevance to the discovery of potential chelating agents for actinide decorporation.

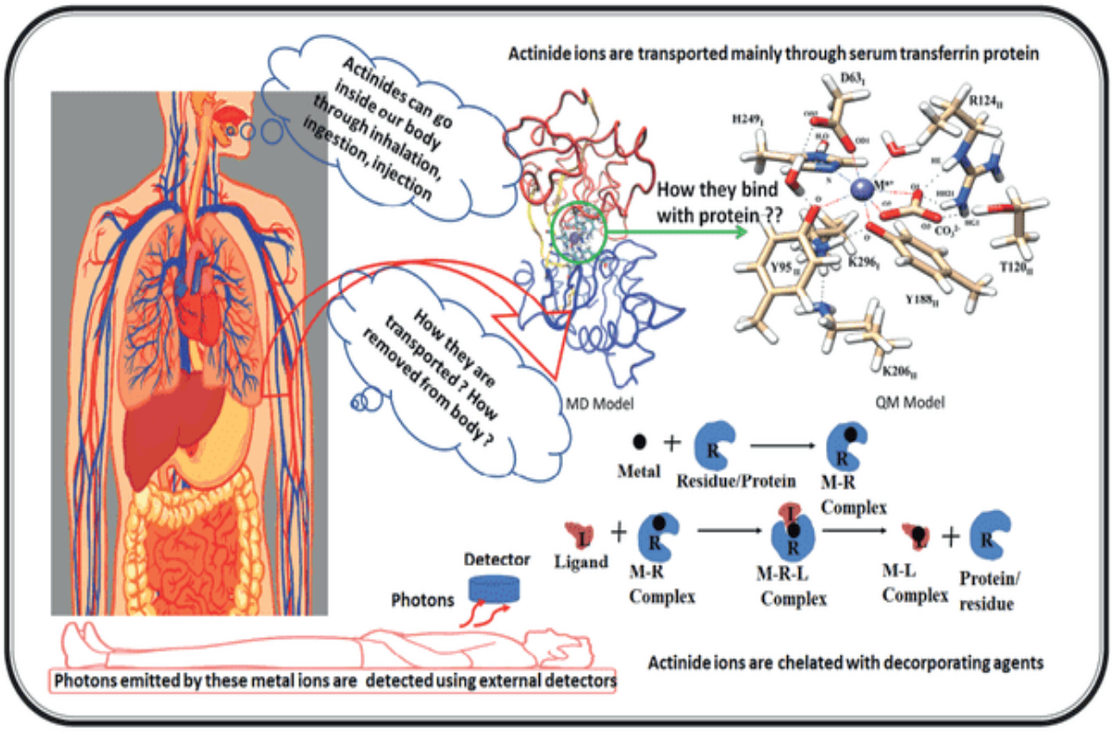

Schematic diagram showing entry routes for actinide contamination, their transport into human body, their in-vivo detection and metal ion bounding into a protein site.

1.1.8 Studies on uptake of arsenic by metal oxides

The thesis investigates the arsenic uptake by indigenously synthesized iron and manganese oxide sorbents, having relevance to arsenic removal from contaminated ground water. Sorption studies have been carried out in batch equilibration mode using ^{76}As ions as the radiotracer. Results from electrochemical studies suggest that while both As(III) and As(V) are taken up as such by magnetite (Fe_2O_3), the uptake by hematite (Fe_2O_3) and goethite [FeO(OH)] involves a partial conversion of As(III) to As(V). While As(V) uptake by MnO_2 occurs without any redox process, the As(III) uptake is, however, involves its oxidation to As(V). These results are also substantiated by X-ray photoelectron spectroscopy studies. Comparing the results involving iron and manganese oxides, the MnO_2 is found to be more promising for arsenic sorption. Accordingly, a sonochemical permanganate reduction method has been devised to prepare MnO_2 nanoparticle coated XAD-4 resins and applied successfully to quantitatively remove arsenic from contaminated groundwater samples collected from North 24 Parganas, West Bengal, India. A schematic of the ground water contamination by arsenic and different ailments associated with the arsenic poisoning is given below.

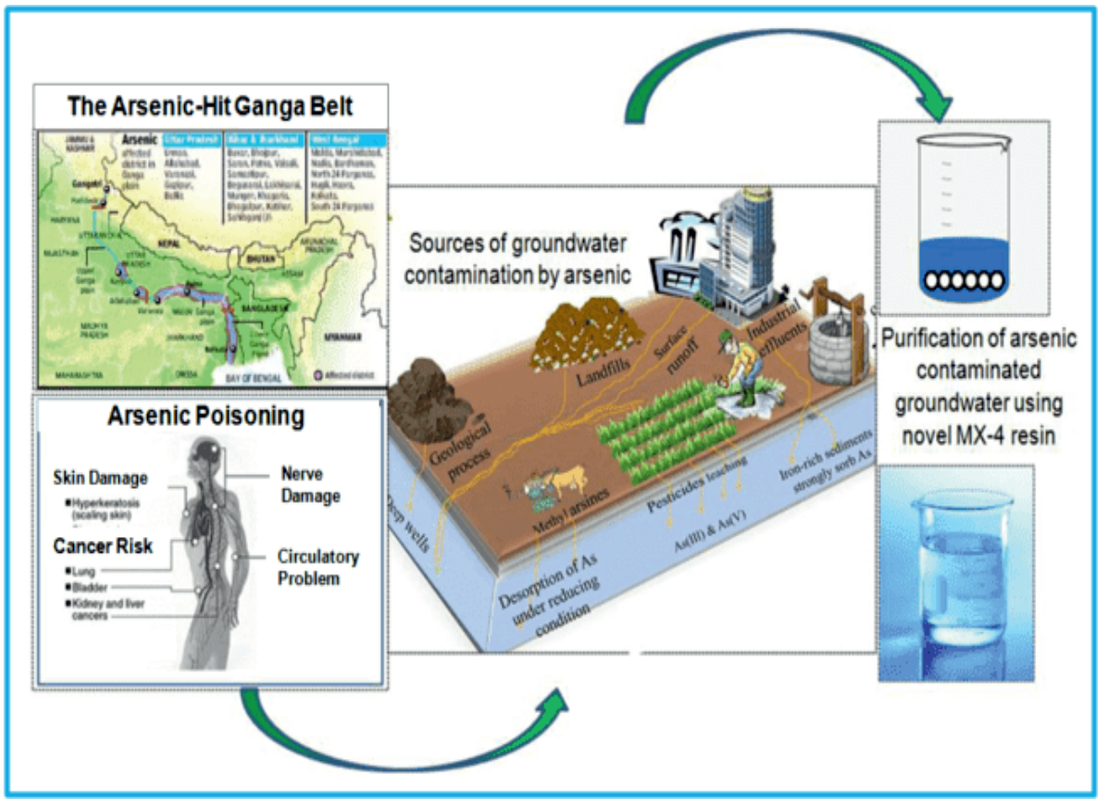

Schematic of ground water contamination by arsenic and the effects of arsenic poising in human body.

1.1.9 Synthesis and evaluation of specific extractants for separation processes in back-end of fuel cycle

Development of selective solvents and efficient separation processes for the recovery of important radionuclides from high level liquid wastes generated during the reprocessing of spent nuclear fuels are the aims of the thesis. Ligands like N,N,N´,N´-tetra-isobutyl pyridine di-glycolamide (PDGA), N,N,N´,N´-tetra(2ethylhexyl) di-glycolamide (TEHDGA) & N,N-bis(2-ethylhexyl)glycolamide (BEHGA) have been synthesised, characterized, and tested in this thesis for separation of various radionuclides from simulated waste solutions. The ligand PDGA shows higher selectivity for tetravalent plutonium over minor actinides as well as alkali and alkaline earth metal ions on using nitrobenzene (NB) and ionic liquid (IL) as the diluents. The ligand TEHDGA extracts both minor actinides, lanthanides & Sr(II) ions from nitric acid medium on using isodecyl alcohol (IDA)-dodecane mixture as the diluent. Further, from the loaded organic phase, Sr is selectively stripped using 18-crown-6 as the complexing agent, resulting in the separation of Sr from the trivalent elements. TEHDGA is also found to be useful in extracting Tc ions from the solutions having low nitric acid concentration. With dodecane as the diluent, the ligand BEHGA shows better extraction for Am, lanthanides, Zr and Mo at higher acidities, with negligible extraction for Sr. In the present thesis an innovative process has been developed for the recovery of ^{106}Ru from actual waste solution, which has been used subsequently to prepare brachytherapy sources (plaque sources) useful for eye cancer treatment. A schematic presentation of the separation of metal ions by the ligands and the thumbnail view of the ^{106}Ru plaque prepared is shown below.

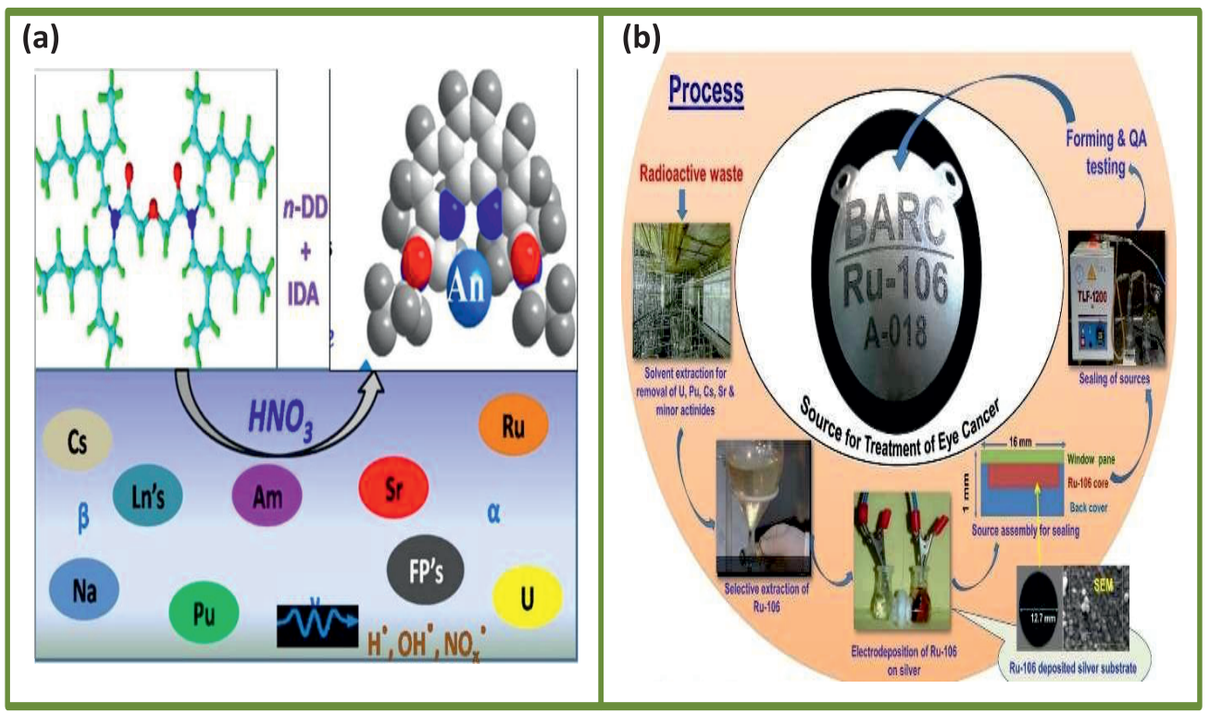

Schematic presentation of the separation of metal ions using ligands (a) and the thumbnail view of the processes associated with the production of ^{106}Ru plaque from the pronuclear waste solution (b).

1.1.10 Studies on the development of technology for the production, separation and purification of iodine-131 for formulation of therapeutic radiopharmaceuticals

The thesis describes the research carried out on the development of a robust dry distillation method for production, separation and purification of radioactive ^{131}I isotope in pilot-scale from the irradiated tellurium dioxide target. Successful large-scale production and supply of ^{131}I with multi-curie activity on regular basis for medical uses have been achieved. For high dose therapeutic capsule preparations, a column chromatography-based post processing concentration enhancement methodology for ^{131}I has also been developed. The applications of ^{131}I produced by the developed method have also been demonstrated through improved drug formulations, methodology and technology, for clinical dose preparations involving ^{131}I-Lipiodol system, for the treatment of thyroid cancer and hepatocellular carcinoma. The protocol used for the production, separation and purification of radioactive ^{131}I, and the utilization of the isotope in the therapeutic applications are schematically shown below.

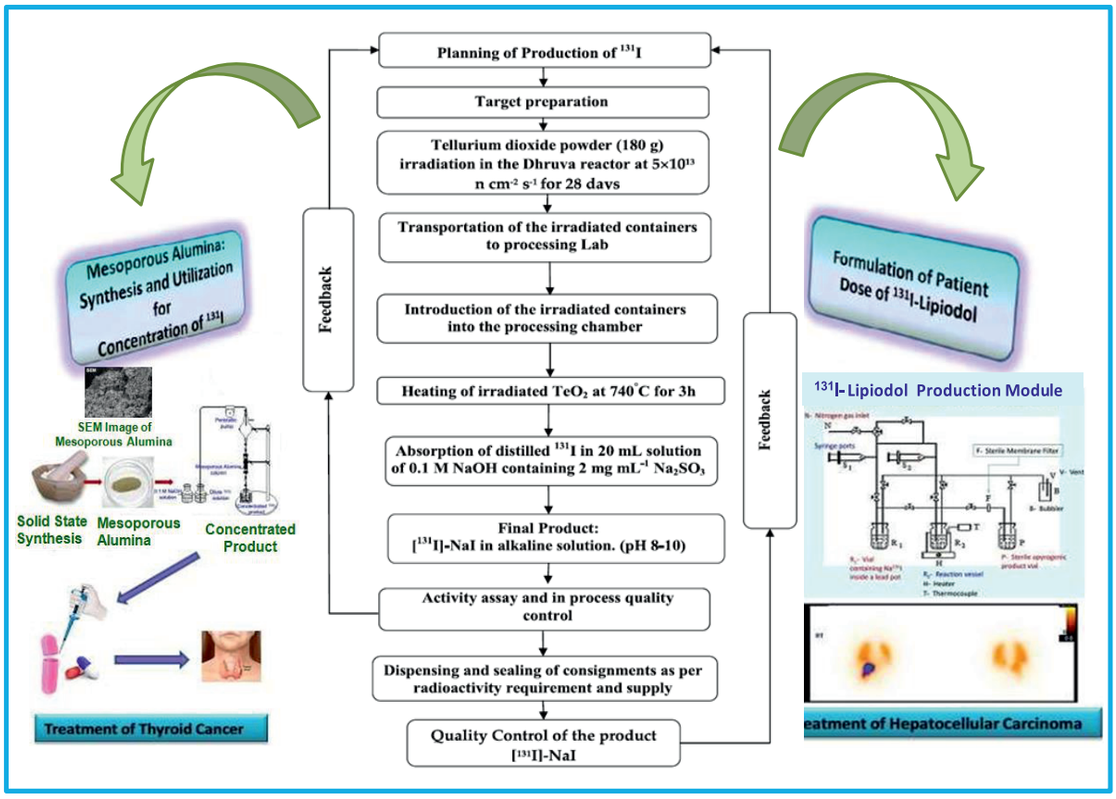

Flow sheet of protocol for radiochemical processing of ^{131}I and the schematics for its uses in the treatment of thyroid cancer and hepatocellular carcinoma.

1.1.11 Interfacial modification of manomaterials for biomedical applications

The research work carried out on the development of materials for drug delivery and cancer therapeutic applications have been described in the thesis. Using self-assembly of organic molecules at the interface of inorganic nanoparticles, various surface functionalized superparamagnetic Fe_3O_4 particles have been developed for possible applications in cancer therapy. Biocompatible additives such as sugar alcohols, vitamins and proteins have been used as the passivating agents for these Fe_3O_4 based magnetic nano-carriers. The uniqueness of present drug delivery carriers lie on the fact that the chemotherapeutic drug is covalently conjugated with the nanoparticles involving carbamate and hydrazone linkages, resulting their slow and sustained release at the tumour sites. The developed materials show substantial cellular internalization with significant toxicity towards cancer cells. They can also be used for hyperthermia-based cancer therapeutic applications. The present thesis also demonstrates a method to immobilize micelles in supercooled matrices at ambient temperature. Thus, frozen micelles in a supercooled sugar-urea melt have been identified unambiguously following X-ray scattering, neutron scattering and HR-TEM studies. This matrix has also been used to solubilize lipids to produce surface charge tuned liposomes, having potential for drug delivery applications. The schematic shown below presents the cellular internalization and drug release of the developed functionalized nanocarriers.

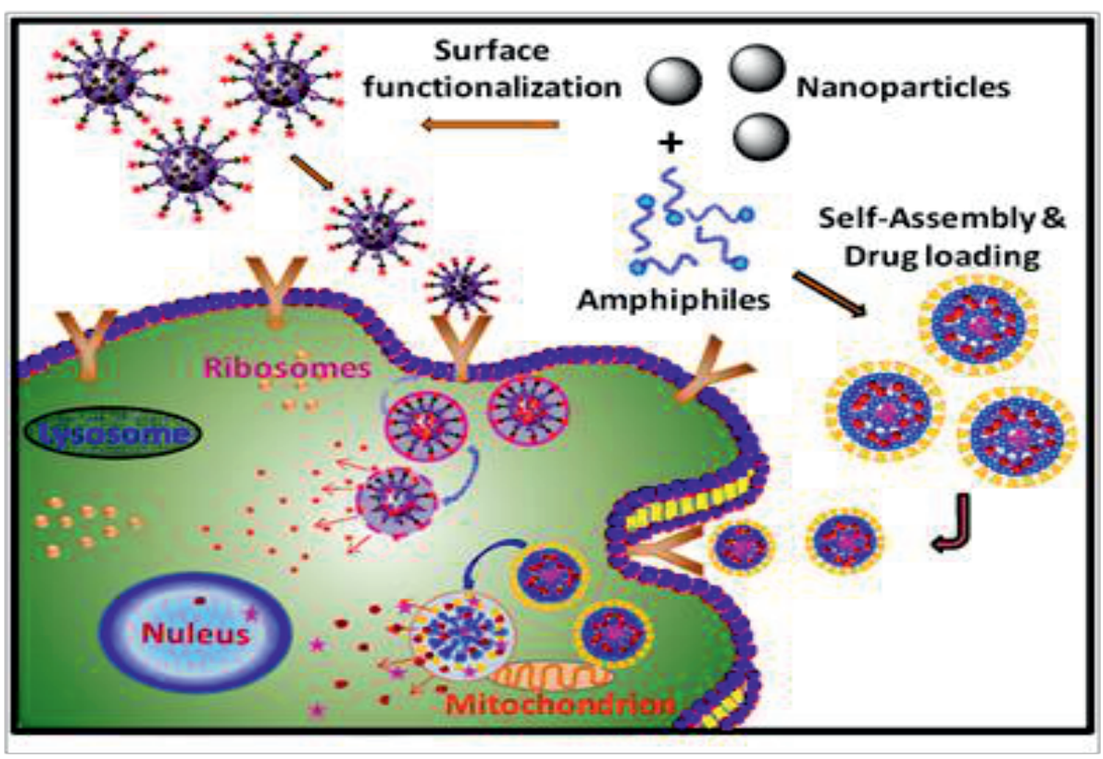

Schematic presentation of the cellular internalization and drug release of functionalized nanocarriers developed.

1.1.12 Investigation of physico-chemical properties of fast reactor metallic fuels

Investigations on the phase stability, transformations, microstructures and thermo-physical properties of potential metallic fuel systems, namely, the binary alloys U-Zr, U-Nb, and U-Mo, and the ternary alloys U–Zr–Nb and U–Zr–Mo, recognised as the promising candidates for fast breeder reactors (FBRs), have been reported in the thesis. In these materials, the total alloying content (Zr, Nb and Mo) is kept limited to 6 wt% only, as the metallic fuels with relatively lower Zr wt% are known to give higher breeder ratio. Significant variations in the crystal structures, lattice parameters, and microstructures have been observed depending upon the compositions and heat treatments used. The furnace-cooled alloys are found to be far from their equilibrium phase compositions. The water quenching also leads to various non-equilibrium phases, due to diffusionless martensitic transformations. The step cooling of the alloys under near equilibrium condition leads to the formation of various equilibrium phases. While the replacement of Zr in the U–6Zr alloy by Nb increases the solidus temperature, the replacement of Zr by Mo decreases the solidus temperatures. The replacement of Zr by equivalent amount of Nb or Mo leads to a decrease in the molar heat capacity, adding an advantage of storing less amount of energy into the fuel. Such replacements also decrease the overall thermal expansion. Fuel-cladding compatibility has also been investigated using T91 steel cladding and is found to be satisfactory at the reactor operating temperature, though on exceeding eutectic liquefaction temperature the fuel-cladding compatibility fails.

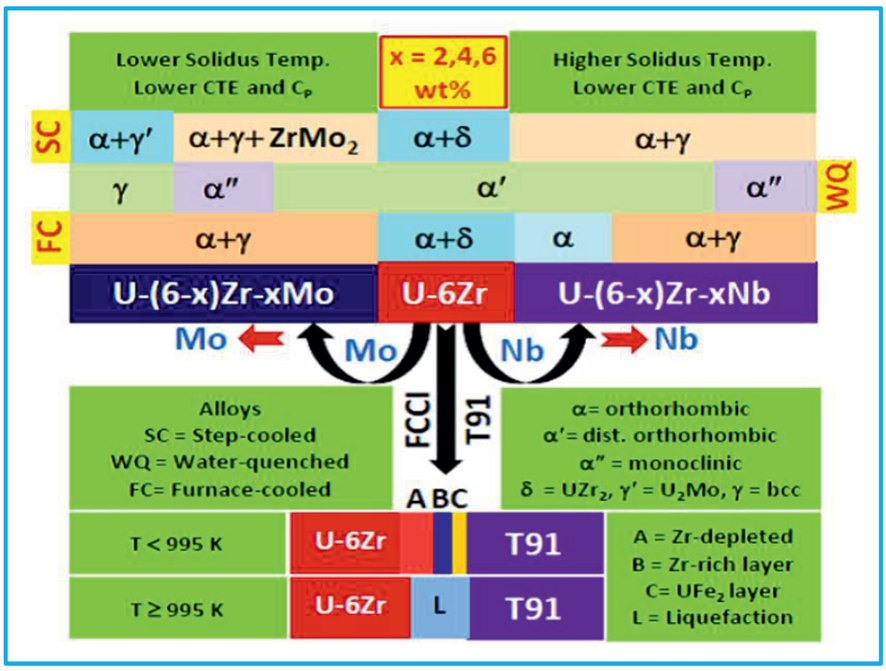

***C**onceptual presentation of the phase relations, thermo-physical properties and fuel-cladding interactions of binary and ternary metallic fuel systems.*

1.1.13 Investigation of bi-metallic oxide composites for electrochemical and photoelectrochemical splitting of Water

The thesis presents the research work carried out on the development of cathode and anode materials for the electrochemical and photoelectrochemical generation of hydrogen and oxygen through water splitting. Three-dimensional graphene (3D-G) materials have been synthesized by green and cost-effective manner and used for the preparation of various noble and non-noble metal based composite cathode materials for electrocatalytic splitting of water. It is seen that the Pt/3D-G composite has a better cathode material for catalytic hydrogen evolution reaction (HER) than Pt/C composite. Similarly, molybdenum disulphide/graphene oxide (MoS_2/GO) composite shows better HER catalytic activity compared to MoS_2/reduced graphene oxide (MoS_2/rGO) composite. it is also revealed that MoS_2 in metallic 1T phase provides more HER activity than the semiconducting 2H phase. Both pristine $BiVO_4$, and modified $BiVO_4$ (through Mo doping and cobalt borate and SnO_2 incorporation) have also been investigated in the thesis to understand their catalytic activity as anode materials. The cobalt borate modified $BiVO_4$ gives improved photoelectrochemical (PEC) efficiency. The effects of photocharging and gamma irradiation on the anode materials have also found to be effective in improving the PEC efficiency.

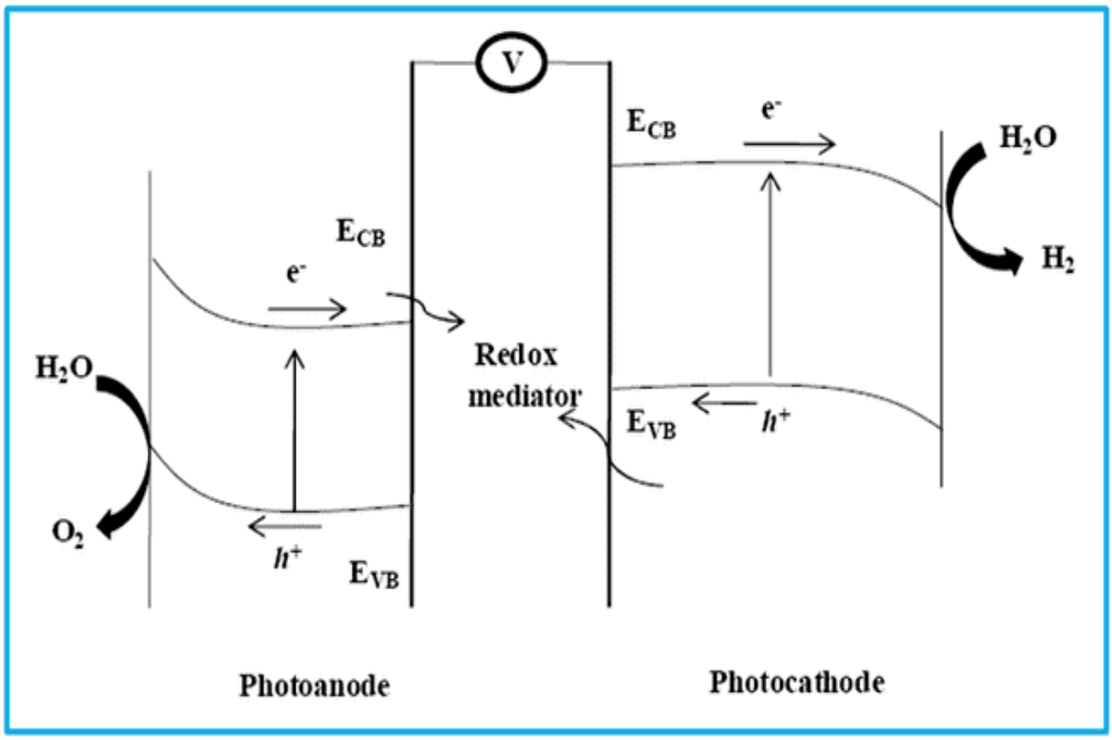

Conceptual presentation of the function of an electrotytic cell used for photoelectrochemical splitting of water.

1.1.14 Chemical durability assessment of glasses for immobilisation of high level radioactive waste

The thesis presents the development of modified borosilicate GM11 (using Al_2O_3 and CaO as additives) and GM44 (using BaO as the additive) glasses for immobilisation of uranium rich and thorium rich waste solutions. These glasses have been characterised for their homogeneity, thermal stability and chemical durability. Observed results are compared with those of an international standard glass (ISG), as well as with those of a natural analogue, namely the basalt rock sample, collected from natural hot spring region in Vajreshwari, Maharashtra. Surface alteration of these glasses after leaching with ground water under hydrothermal condition indicate the formation of crystalline zeolite phase, appearing as precipitates on the surface. Surface alterations of these glasses under high temperature and pressure autoclave leaching with ground water are somewhat similar to those found in basalt rock samples. It is inferred that after millions of years of continuous leaching, zeolite phases would form over these glasses like the basalt rocks, and these phases being very stable, they will substantially retard the leaching of these glasses at the longer time. SEM images of the studied glasses before and after leaching experiments are shown below.

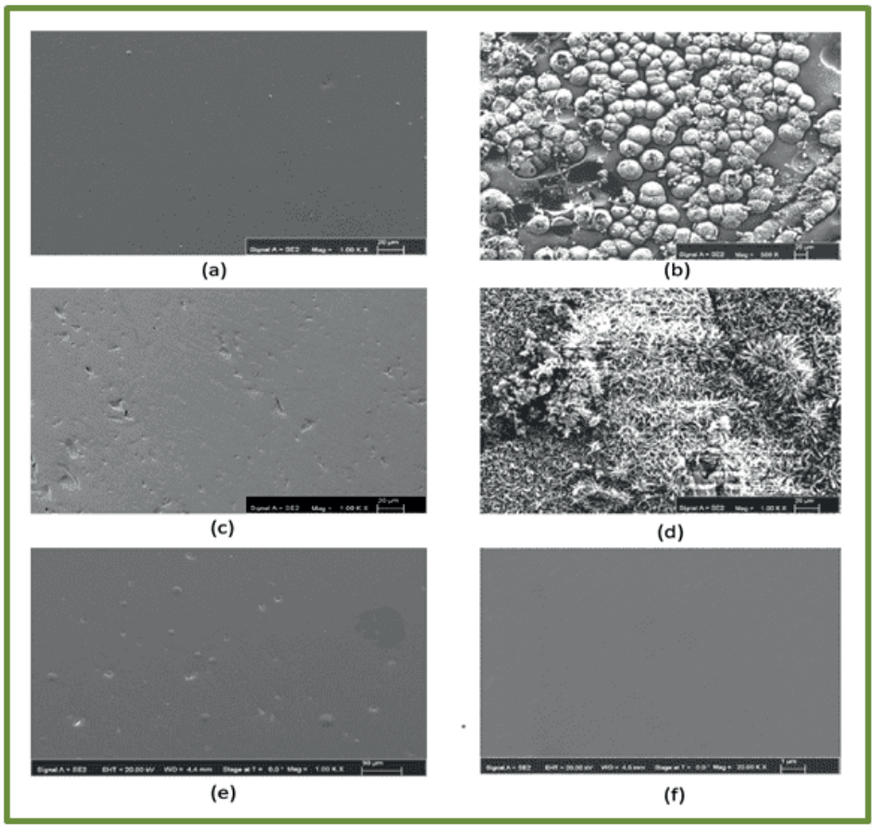

SEM images obtained before (left) and after (right) leaching of the GM11 (a, b), GM44 (c, d), and ISG (e, f) glass samples.

1.2 Indira Gandhi Centre for Atomic Research, Kalpakkam

1.2.1 Solvent extraction of some trivalent lanthanides and actinides in alkyldiglycolamides and the aggregation and spectroscopic investigations on the extracted phase

The research work carried out on the solvent extraction of trivalent actinides [Am(III) and Cm(III)] from high-level liquid waste (HLLW) using diglycolamide (DGA) ligand in n-paraffin solvents has been reported in the present thesis. During solvent extraction from high-level liquid waste (HLLW) using DGA in a n-paraffin solution there is often undesirable segregating of solvent into two phases, one as diluent rich phase, and other as metal-solvate rich phase (third phase), hindering the efficiency of the extraction process. In the present thesis, the effect of the alkyl chain lengths, present either as a substituent of the DGA ligand or in the n-paraffin solvent, towards the formation third phase has been investigated thoroughly using dynamic light scattering, ATR-FTIR and MD simulation studies. The role of phase modifiers like TBP, DHOA, long chain alcohols, HDEHP, PC88A, and CYANEX-272, in controlling the above third phase formation has also been investigated. It is revealed that the aggregate size in the third phase can be brought down significantly by increasing the alkyl chain length of DGA and by adding significant quantity of the phase modifiers. Development of a single-cycle separation method for minor actinides from HLLW using various neutral and acidic ligands has also been investigated. Results show that the solvents containing acidic extractants with lower pK_a values are more suitable for selective separation of trivalent actinides from HLLW. The two cycle and single cycle extraction processes of lanthanides and actinides from HLLW are schematically shown below.

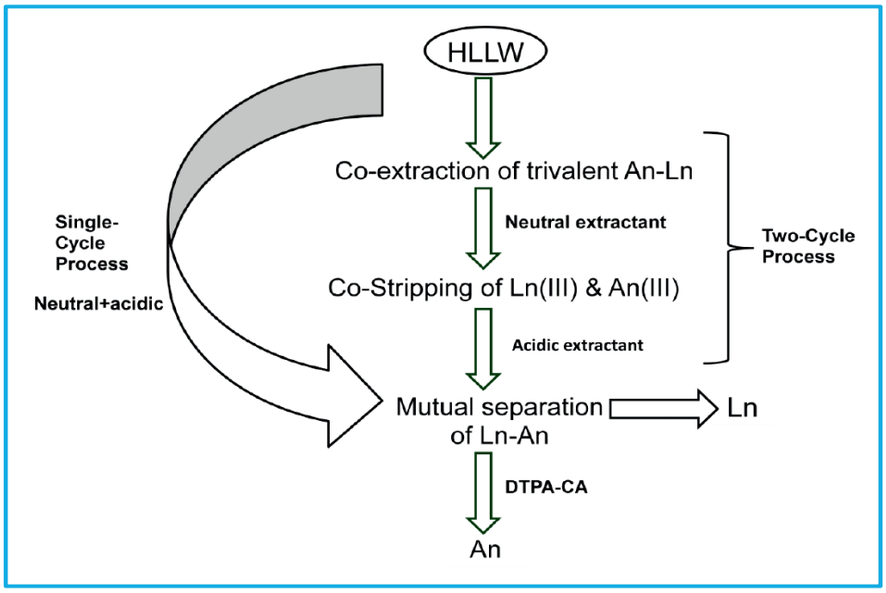

Schematic representation of two cycle and single cycle extraction processes of lanthanide (Ln(III)) and actinide (An(III)) ions from HLLW.

1.2.2 Some Studies on the electrochemical behavior of actinides and fission products in room temperature ionic liquids for nuclear fuel cycle applications

The thesis reports research work carried out on the electrochemical behaviour of uranium and fission products in room temperature ionic liquid (RTIL) containing organic ligands, aiming at the recovery of these metals by electrodeposition. The oxidative dissolution of U_3O_8 in the presence of small amount of nitric acid in RTIL medium has been studied and the electrochemical behaviour of UO_2^{2+} has been investigated in the presence and absence of fission products like Pd^{2+}, Eu^{3+} and Ru^{3+}. It is seen that the solubility of UO_2^{2+} is improved by employing the dicyanamide anion based ILs, e.g. [C_4mIm][DCA] and [C_4mPy][DCA]. The coordination environment of uranium in these IL media has been investigated using FTIR, Raman and UV-vis spectroscopy. To understand the uses of ILs in the metallic fuel (U-Pu-Zr ternary alloy) reprocessing applications, anodic dissolutions of U and Zr metals has been performed and the electrochemical behaviour of Zr(IV) and U(IV) has been investigated in C_4mpyNTf$_2$ IL medium. Further, rare earth containing neutral ligand ionic liquids (NLIL), like [Ln(DHOA)$_3$][(NTf2)$_3$], have also been prepared by dissolving Ln(NTf$_2$)$_3$ salt (Ln = Eu, Nd, Dy) in dihexyloctanamide (DHOA) and the electrochemical behaviour of Ln^{3+} ions in these RTILs has been investigated using cyclic voltammetry method. Resonance structures of the dicyanamide anion ligand and structures of different dicyanamide based RTILs investigated in the study.

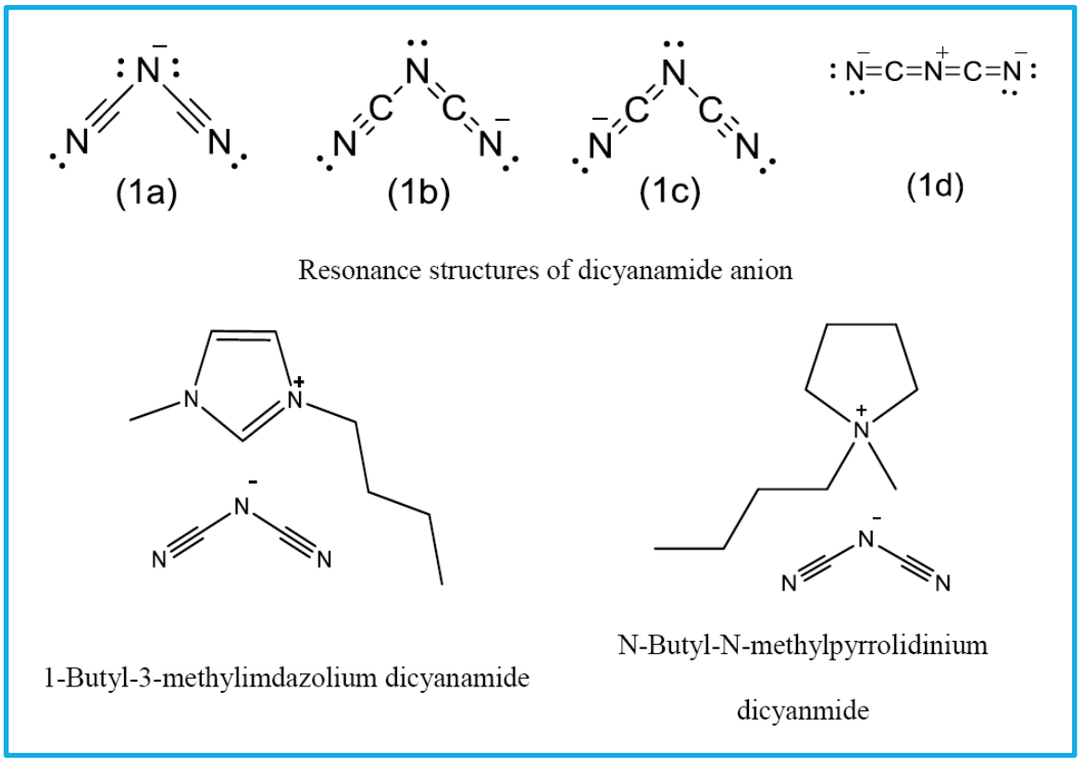

Resonance structures of dicyanamide anion and structures of the dicyanamide based RTILs investigated in the study.

1.2.3 Lanthanide and transition metal ions activated advanced phosphors for optical and radiation dosimetry applications

In the thesis, phosphor materials prepared by doping of suitable metal ions into the alkaline earth borophosphate ($MBPO_5$, M = Ca, Sr, Ba; doped with Ce^{3+} and Gd^{3+}), barium cerate ($BaCeO_3$; doped with Eu^{3+}) and lithium aluminate ($LiAl_5O_8$; doped with Fe^{3+}, Cr^{3+} and Eu^{3+}) hosts have been investigated for their uses as LEDs, phototherapeutics and radiation dosimeters. While $SrBPO_5:Ce^{3+}$ phosphor is found to be suitable for medium wavelength UV (UV-B) LED devices, the $BaCeO_3:Eu^{3+}$ phosphor is found to be a potential candidate for red and white LEDs. The $BaCeO_3:Eu^{3+}$ and $MBPO_5:Gd^{3+}$ phosphors are also suitable for phototherapeutic and radiation dosimetry applications. Photoluminescence of the lithium aluminate-based phosphors with 0.5 mol% Eu^{3+}, 100 ppm $Cr3^{+}$, and 500 ppm $Fe3^{+}$ exhibit intense deep red-NIR emission with 100% colour purity and improved colour coordinates than that of the national television system committee (NTSC) recommendations, suggesting the potentials of these materials in solid-state lighting (SSL), lasers, and biomedical applications. The diagram below shows the typical crystal structures and chromaticity diagrams of three different phosphor systems investigated in the thesis.

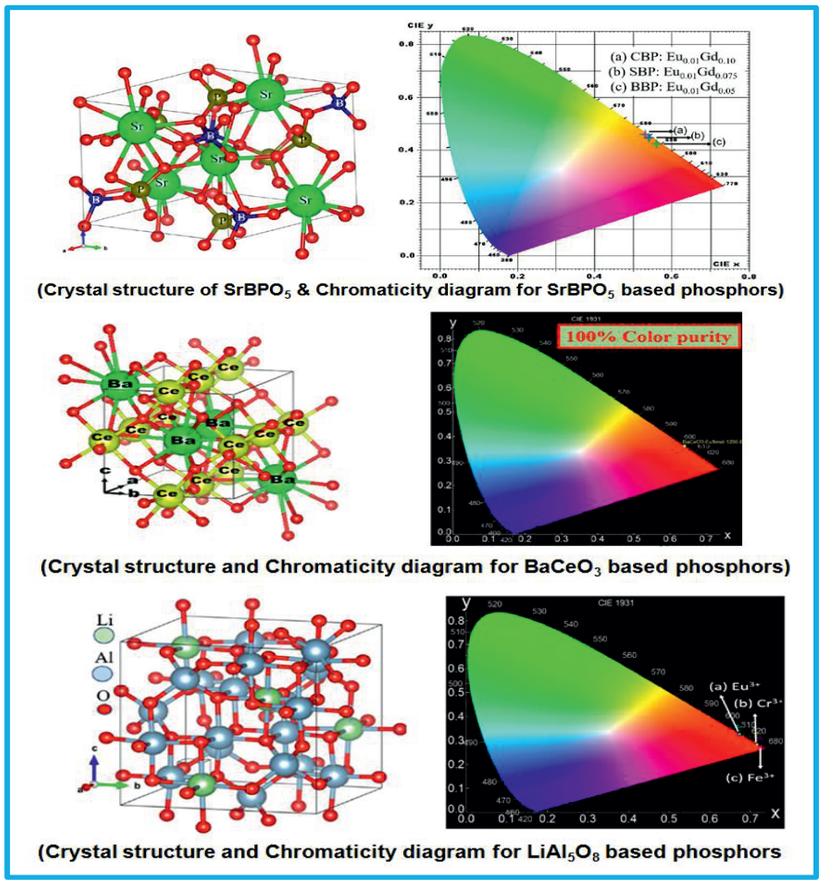

Crystal structures and chromaticity diagrams of different phosphor systems

1.3 Raja Ramanna Centre for Advanced Technology, Indore

1.3.1 Second harmonic (SH) spectroscopic studies on the effect of amphiphilic molecules-induced adsorption and transport characteristics of an organic cation across a POPG lipid bilayer

Interactions of amphiphiles like pluronics, polyene antibiotic Amphotericin B (AmB), and bile salts, with lipid bilayer of palmitoyloleoylphosphatidylglycerol (POPG) liposome and the consequent changes in the adsorption and transport characteristics of cationic organic dye LDS-698 (LDS^+) across the bilayer, as investigated by second harmonic (SH) spectroscopic technique, have been reported in the present thesis. For pluronics, the transport of LDS^+ across lipid bilayer is modulated largely depending on the PPO block length of the polymers, attributed to the preferential insertion of hydrophobic PPO block into the bilayer, affecting the bilayer packing. With AmB polyene, both in the absence and presence of ergosterol (Ergo) or cholesterol (Chol), it is interestingly seen that at lower AmB/Liposome (A/L) values, the rate of LDS^+ transport across bilayer is gradually decreased as a function A/L ratio, whereas at the significantly higher A/L values, the rate gets saturated to a final value. It is suggested that at higher A/L values, the AmB gets aggregated within the bilayer and thereby enhances the bilayer permeability, irrespective of its composition. The pH dependent studies involving bile salt-POPG liposome system indicate that the bile acids in the neutral form can alter the POPG membrane properties more significantly as compared to their ionic form. Schematics of the incorporation of the amphiphiles into lipid bilayers, and the representative results obtained in the present thesis are shown below.

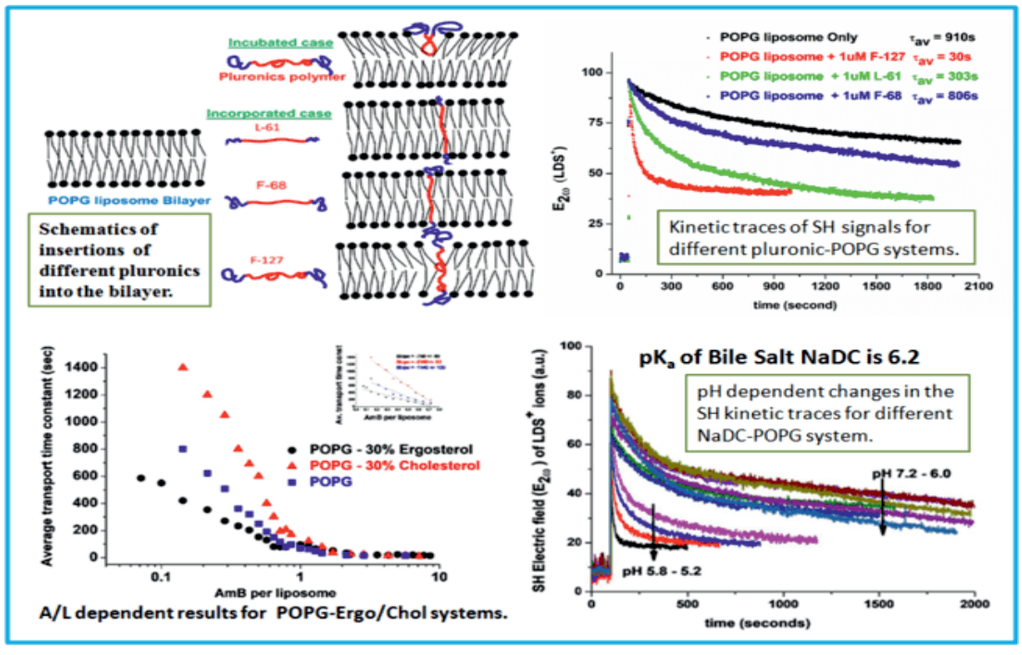

Schematic of insertions of amphiphiles into the lipid bilayers, and the representative results obtained with different systems investigated.

1.4 Saha Institute of Nuclear Physics, Kolkata

1.4.1 Crystal engineering to fabricate Au, Ag, & Au-Ag alloy nanoparticles: Application in technology, pathology & theranostics

The thesis presents the synthesis, characterization and uses of Au, Ag, and Au-Ag alloy nanoparticles (NPs) for sensing of human metabolites and trace metal ions. The electrochemical methods like differential pulse voltammetry (DPV), square wave voltammetry (SWV), linear sweep voltammetry (LSV) and electrochemical impedance spectroscopy (EIS) have been used in different studies. The prepared bud-to-blossom shaped Au NPs are useful in sensing Vitamin C through DPV measurement. Similarly, prism shaped bimetallic hollow Au-Ag NPs are useful in detecting uric acid using both DPV and SWV measurements. The thesis also reports the morphological changes of the prism shaped Ag NPs upon interaction with As^{3+} ion, enabling the sensing of arsenic through colorimetric and spectrometric methods. The grain-boundary enriched flower-like Au NSs are seen to support electrocatalytic hydrogen evolution, as investigated through LSV method. Porous bimetallic Au-Ag nanorods as synthesized in this work are useful for electrocatalytic sensing of various human metabolites and trace metal ions. A DNA-aptamer based Au-Ag nanobioconjugate for sensing of DENV-2 virus using EIS method is also reported in this thesis. Representative results of the present study are schematically shown below.

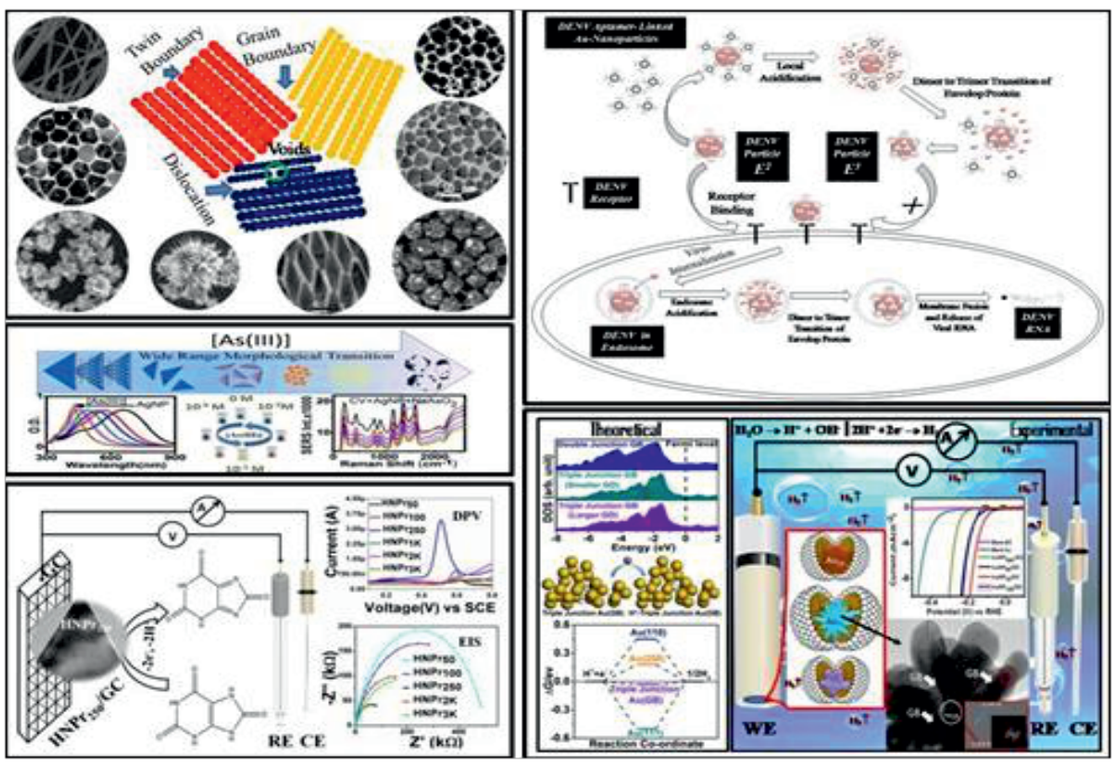

Representative images and results obtained on using different nanostructure materials investigated

1.5 National Institute of Science Education and Research, Bhubaneswar

1.5.1 Sustainable strategies for carbon-sulfur bond formation reactions in organic synthesis

The thesis describes the synthetic methods developed for the preparation C-S bonds using sustainable reagent conditions. Thus, iodine triggered oxysulfonylation of olefins have been achieved via aerial dioxygen activation strategy. Similarly, Markovnikov selective or anti-Markovnikov selective Thiol-Ene and Thiol-Yne click reactions have also been realized by exploiting the role of S–H···π non-covalent interactions under neat conditions. Additionally, cascaded C-S and S-O bond formation reactions leading to the construction of aryl sulfinylarene and sulfoxide arene adducts are also achieved by using appropriate amount of phenyliodine(III) diacetate (PIDA) into thiophenol. A unique reaction route for Knoevenagel condensation has also been revealed leading to the formation of α,β-unsaturated diphenylacrylonitrile derivative from benzyl cyanide and benzyl mercaptan, via C-S bond cleavage under basic condition. Additionally, in situ C-X (X = Cl, F) bond functionalizations have also been achieved leading to the formation of halo substituted diphenylacrylonitriles. The schematic representations of various C-S bond formation reactions investigated in the thesis are shown below.

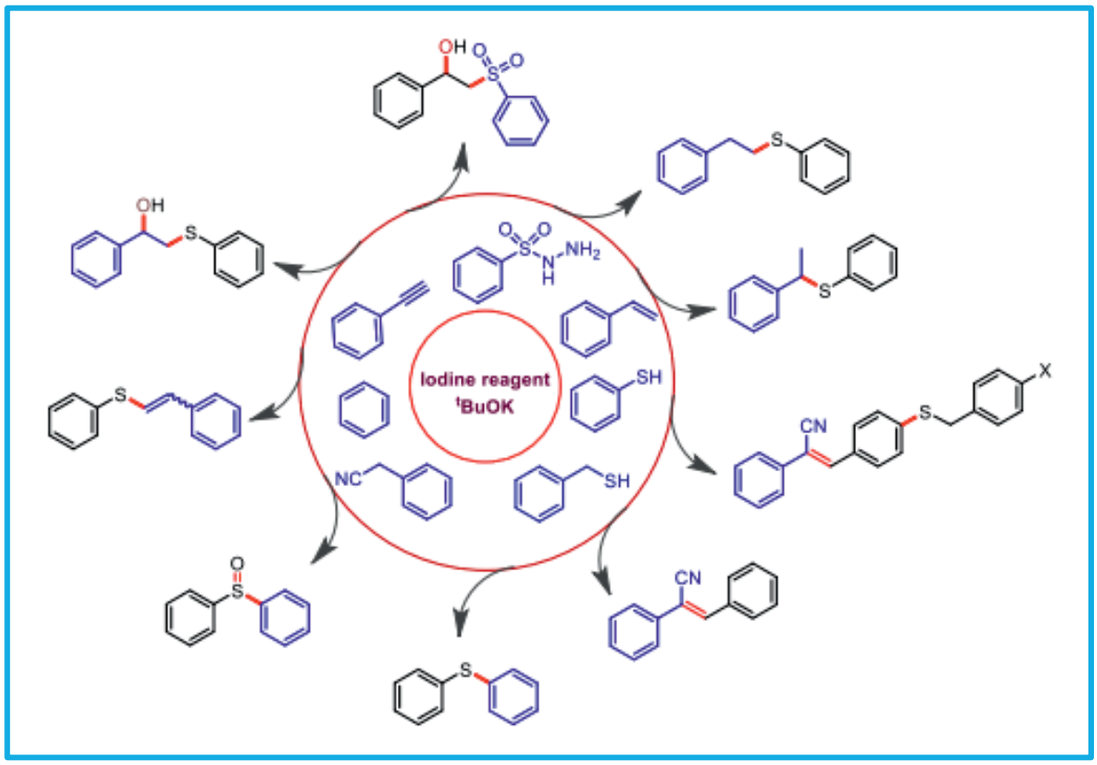

Sustainable reagents promote the formation of various C-S bond

1.5.2 Catalysis based on ruthenium pincer complexes

Research work carried out on the uses of Ru-Macho [Ru(II) pincer complexes] catalysts in different organic synthesis have been presented and discussed in the present thesis. Various primary alcohol mediated α-alkylations of arylmethyl nitriles, catalyzed by Ru-Macho, have been reported, where metal-ligand cooperation facilitates the alkylation reaction. The Ru(II) pincer catalyzed olefination of nitrile compounds using secondary alcohols have also been reported in the thesis to produce various α-vinyl nitriles. The thesis also describes a new kind of catalytic reaction whereby varieties of cyclic, acyclic, symmetrical, and unsymmetrical secondary alcohols are selectively coupled with aromatic benzylic secondary alcohols to produce β-disubstituted ketones. H_2 and H_2O are the only byproducts from these reactions, making the processes atom economical and environment friendly. The Ru(II)-catalyzed synthesis of N,N-disubstituted acylhydrazides through alkylation of acylhydrazide by primary and secondary alcohols, and the highly selective Markovnikov hydrogenation of terminal epoxides to produce secondary alcohols, are also the important synthesis protocols reported in the present thesis. Various Ru(II)-catalyzed reactions studied in this thesis are schematically shown below.

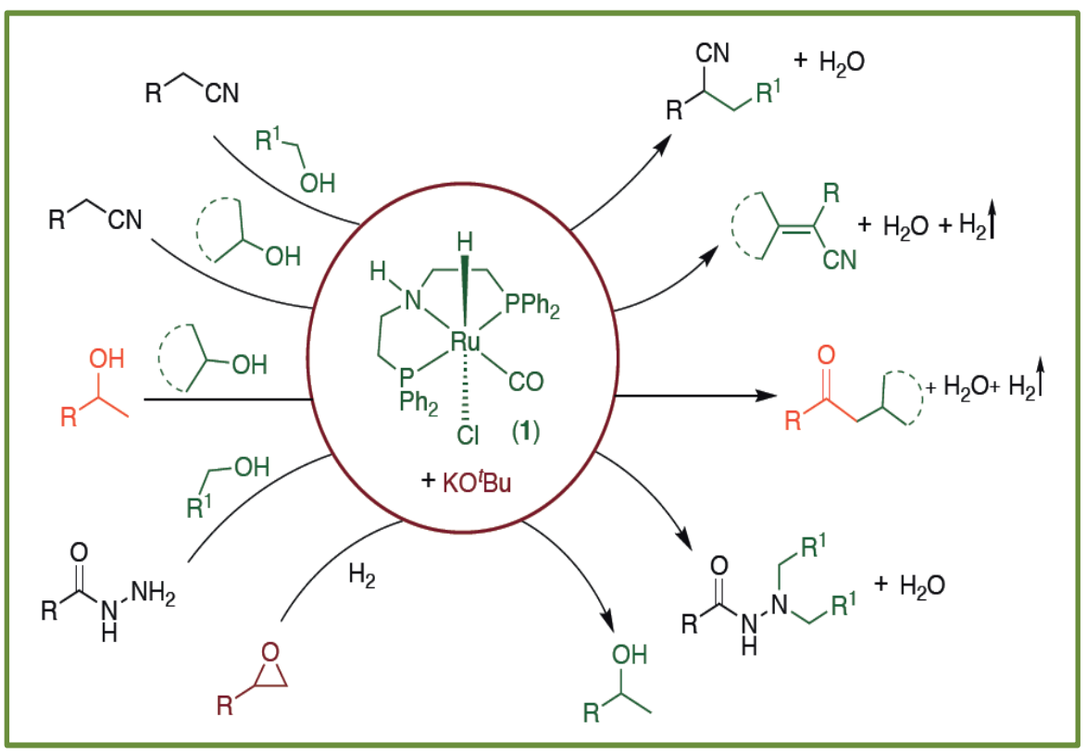

Schematic presentation of the various Ru-Macho catalyst reactions

1.5.3 Contracted and expanded carbaporphyrinoids: Syntheses, conformation, and coordination chemistry

The thesis describes the synthesis of contracted and expanded porphyrinoids which have wide ranging applications in coordination chemistry. While augmentation and decrease of an atom in the inner porphyrin core can lead to the formation of expanded and contracted porphyrinoids, respectively, replacement of one or more pyrrole units in the porphyrin motif by polycyclic aromatic moieties, especially, can lead to the formation of modified porphyrinoid compounds, distinctly referred as the carbaporphyrinoid systems. The thesis reports the synthesis of different contracted carbaporphyrinoids, obtained through the incorporation of biphenyl and substituted biphenyl units into the porphyrin core. Coordination chemistry of these momolecules with metal ions like Cu(III), Pd(II), Au(III), Rh(I), Rh(III), etc. have also been investigated thoroughly. Synthesis of expanded carbaporphyrinoids formed by the incorporation of bis-(*m,p*)-biphenyl units into porphyrin core (hexaphyrin systems), and their structural and isomerisation behaviours have also been discussed in the thesis. The last part of the thesis also reports the synthesis, spectral characteristics and structural aspects of expanded carbaporphyrinoids that involve bis-(*p-p*)-biphenyl units incorporated into the porphyrin core (octaphyrin systems). Obtained octaphyrin systems have also been exploited for its structural diversity following their protonation and coordination with bis-Rh ions. The typical porphyrin analogues investigated in the thesis are shown in the schematic diagram below.

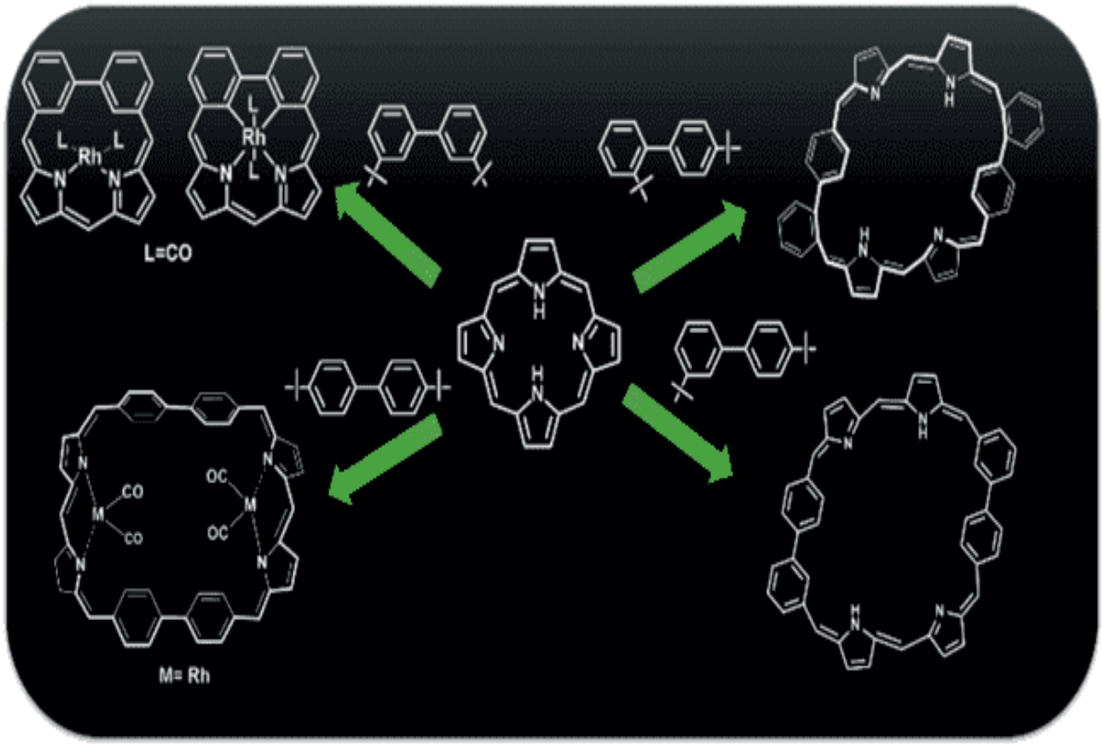

Representative contracted and expanded porphyrin analogues

1.5.4 Expanded porphyrins: Ideal models to probe conformational topology, Möbius and Hückel Aromaticity

The thesis presents the synthesis of a varieties of core-modified expanded porphyrins, like homoporphyrins, hexaphyrins, heptaphyrins, octaphyrins and decaphyrins, and investigates the properties of these porphyrin-based systems, namely their conformational structures, Hückel-Möbius aromatic switch-over mechanisms, electronic structures, optical, electrochemical, photochemical and excited state behaviours, and so on. The, 1,2-diphenyl-1,2-dithienyl ethene embedded 30π and 28π core-modified hexaphyrins synthesised show protonation triggered Hückel-Möbius aromatic transformation. The synthesis, characterization and properties of dithienothiophene fused 30π heptaphyrin and 34π octaphyrin systems have also been reported in the thesis. These systems show interesting flipping for the fused groups, which is unprecedented in the literature. In a part of the study, some 34π aromatic core-modified octaphyrins have been synthesised which are found to crystallize with two different structural isomers within a single unit cell, a unique feature not reported before in the literature. Syntheses, structural analysis and properties of more complex core-modified 48π and 42π decaphyrins have also been reported in the present thesis. Representative examples of expanded porphyrin analogues investigated in the present thesis are shown below.

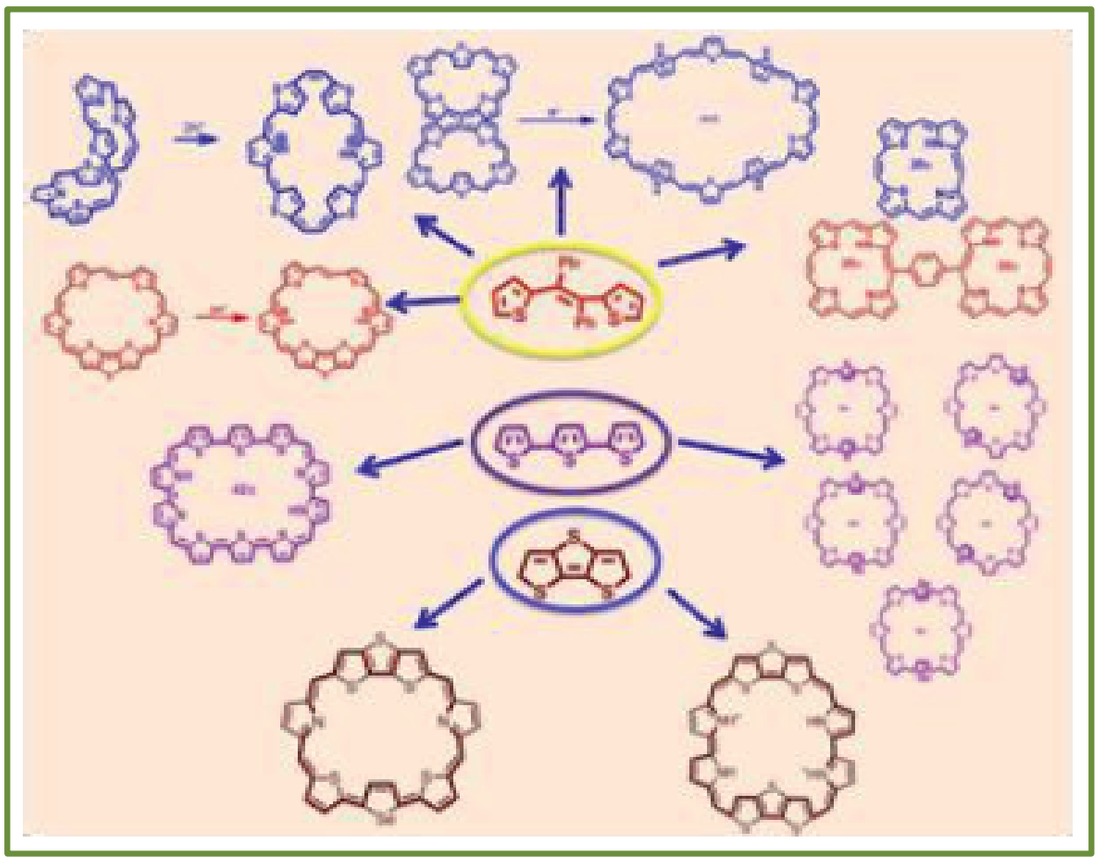

Representative examples of the expanded porphyrin systems investigated in the thesis.

2. Engineering Sciences

During the period of report, HBNI awarded 42 Ph.D. degrees in Engineering Sciences. The summary of some of the theses is given below.

2.1 Bhabha Atomic Research Centre, Mumbai

2.1.1 Multipass optical cavity based technique for trace level detection of heavy water

A system based on OA-ICOS technique has been designed and developed for the detection of heavy water leaks in PHWRs.The concept of cavity gain variation with per pass absorbance in the cell has been introduced and it is shown to be an important factor for obtaining linear calibration curve for wide concentration range. The measurement of heavy water concentration in water samples and in air samples has been demonstrated through [HDO] measurements. The suitability of the system for heavy water leaks in PHWRs has been verified by measurements on samples from DRUVA reactor and comparison with measurements obtained by conventional techniques. Minimum detectable [HDO] of 45 ppbv and the sensitivity of 113 ppbv of HDO fraction in air is achieved, which is sufficient for the detection of minor leakages in PHWRs. A signal processing algorithm has been developed to improve the measurement accuracy.

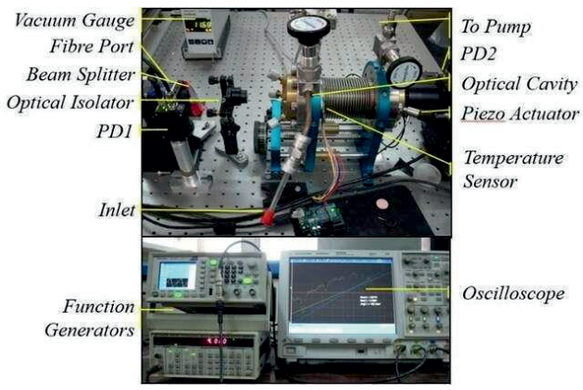

Photograph of the developed system

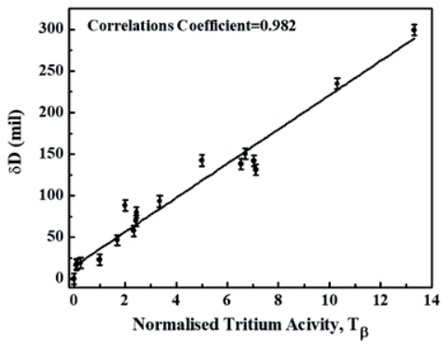

Correlation between measured change in deutrium concentration by the developed system and tritium activity by LSC

2.1.2 Design of an efficient venturi-scrubber for retention of radionuclides during severe accident of a nuclear reactor

Under extreme conditions in a nuclear reactor, primary containment pressure may rise beyond design pressure and therefore, it must be depressurized to maintain containment integrity. In addition, the radioactive materials released during accident progression in the containment atmosphere must be retained to have negligible impact beyond the boundary. Filtered Containment Venting System (FCVS) is installed to carry out these functions. The design of FCVS employs a manifold of venturi scrubbers and a demister pad upstream thus providing two stages of filtration. There are several scientific issues associated with the design of the venturi scrubber such as (a) The hydrodynamic behaviour of venturi scrubber is complex due to the interaction of the different phases present and it plays an important role in deciding the scrubbing behaviour and retention of radionuclides. (b) Lack of test data creates major issues in understanding the fundamentals in the scrubbing behavior especially the influence of operating parameters and geometry (c) Flow phenomena inside the venturi scrubber is multidimensional and CFD model needs to be developed to treat the complex flow physics inside the venturi scrubber and (d) Performance of venturi scrubber for actual reactor application is not known since it is influenced by large number of operating and geometric parameters.The above issues have been addressed in the present work through experiments and CFD simulations. Detailed study of the hydrodynamics and scrubbing behaviour of FCVS is demonstrated for an advanced Indian nuclear reactor through experiments in a scaled facility (having a single venturi scrubber of 1:1 geometry) (shown in Figure 1). For relatively high-pressure conditions, pressure drop reveals an increase with the gas flow rate similar to single phase flow and forced feed scrubbers. The scrubbing efficiency increased with gas flow rate. The effect of submergence depth on iodine retention is prominent at low gas flow rates while at high gas flow rates the values of iodine retention converge to similar values. The overall decontamination factor of iodine vapors indicate that the target scrubbing efficiency is achieved. The multi-phase interaction in the venturi scrubber is modelled through a CFD model benchmarked against the results in literature. The model is subsequently applied to predict the hydrodynamics and scrubbing behaviour observed for the experiments conducted in the present study. The performance of the FCVS is predicted under reactor prototypic conditions.

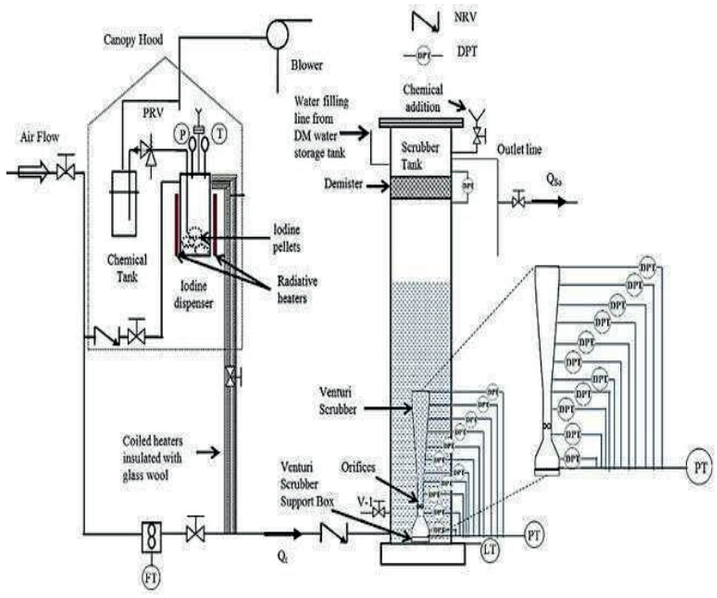

Schematic of experimental facility for FCVS

2.1.3 Development of vanadium alloys for advanced energy systems

The thesis discusses the development of V-Ti-Ta alloys as structural materials for fusion reactors with the purpose of widening the working temperature window of the material. In this work, thermodynamic phase stability, evolution of microstructure during recrystallization, mechanical properties evaluation, oxidation and wear resistance have been investigated for a series of V-4Ti-xTa alloys. In doing so, the relevant temperature domains over which these alloys are expected to operate, have been considered.

This study has shown that the presence of Ta in V-Ti-Ta alloys decreases partial free energies of V and Ti, which, in turn, stabilizes the matrix phase of the alloys at high temperatures. Microstructural and phase investigations have revealed higher stability of precipitates, where the role of Ta in enhancing the stability of the precipitates is rationalized by thermodynamic estimations. It has been shown that substitutional solid strengthening effect of Ta increases the yield strength (370 MPa) of the alloy. Hence, the synergistic effects of Ta addition by solid solution strengthening and by enhancing high temperature precipitate phase stability in V-Ti-Ta alloys would increase the working temperature window of fusion reactor. V-4Ti-7Ta alloy exhibited superior oxidation resistance (50 % lower specific weight gain in comparison to unalloyed V), which was attributed to the reduced thermodynamic activity of V in the alloy. Higher activation energy for the onset of oxidation and lower diffusivity of oxygen ions (70 % lower compared to V) were the two major governing factors for improved oxidation performance of V-Ti-Ta alloys. Superior wear performance of V-Ti-Ta alloys were attributed to the formation of mixed tribo-layer encompassing elements like Ti, Ta, Fe in solid solution with vanadium oxides.

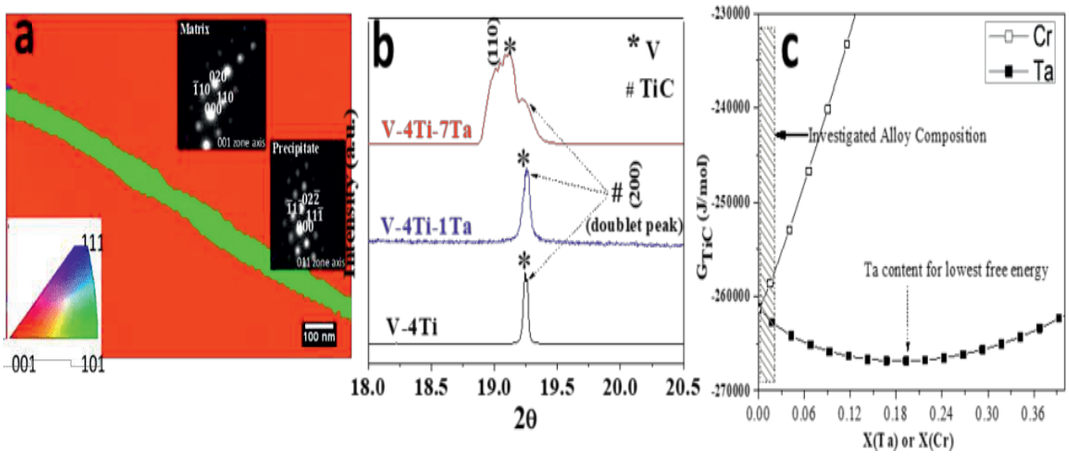

(a) Image of the precipitate obtained under transmission electron microscope using precession electron diffraction technique (PED). (b) XRD patterns of the three alloys exhibiting a shift in the (200) peak of the precipitate phase upon increasing Ta. (c) Free energy change of TiC phase with respect to the addition of Ta or Cr.

2.1.4 Development of macrocyclic extractants for selective separation of cesium, strontium and technetium from radioactive waste solutions

High Level Liquid Waste (HLLW) generated during reprocessing of spent fuel by PUREX (Plutonium Uranium Reductive EXtraction) process retains majority of radio-toxicity of the original spent fuel. ^{137}Cs ($t_{1/2}$ = 30.1 y) and ^{90}Sr ($t_{1/2}$ = 28.9 y) are major heat emitting nuclides contributing largely on heat and radiation load of HLLW. ^{99}Tc, a beta emitting radionuclide ($t_{1/2}$ = $2.11x10^5$ y) present in alkaline low-level waste (LLW) as $NaTcO_4$. Separation of these elements is necessary for safe waste management and also for their uses in societal applications.

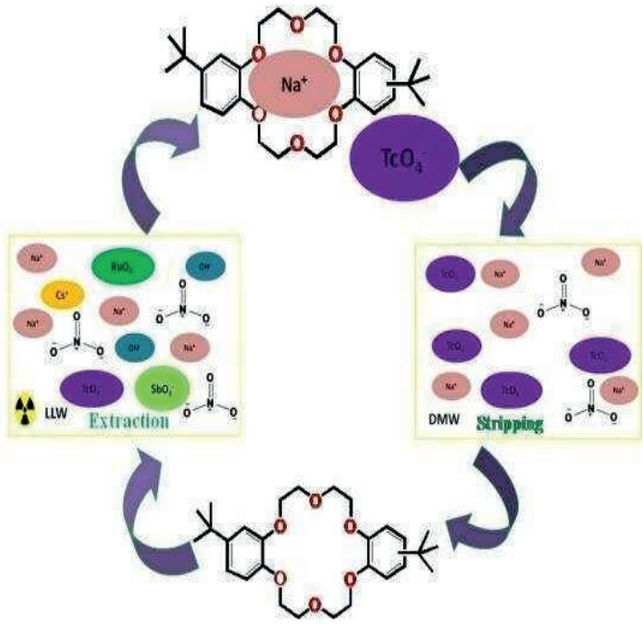

Pictorial representation of extraction and stripping of $Na^+TcO_4^-$ from LLW

The study carried out is focused on development of macrocyclicextractants of the class calix-crown-6 and crown ethers for selective separation of Cs, Sr and Tc from high salt content radioactive waste solutions. The extractants developed are 1,3-dioctyloxycalix[4]arenecrown-6 (CC6)and1,3-bis(2-ethylhexyloxy)calix[4] arene-crown-6 (branched calix-crown-6) for selective separation of Cs^+ from HLLW, 4,4´(5´)-[di-*tert*-butyldicyclohexano]-18-crown-6 (DtBuCH18C6) for selective separation of Sr^{2+} from HLLW and 4,4´(5´)-[di-*tert*-butyldibenzo]-18-crown-6 (DtBuDB18C6) for selective separation of $Na^+TcO_4^-$ from LLW and are dissolved in a new diluents system, a mixture of isodecyl alcohol and *n*-dodecane for extraction studies. ^{137}Cs removal from HLLW was more than 99.5% with impurity level <1 mg/L in 4 stage counter-current continuous extraction with 0.03 M CC6 +30% isodecyl alcohol/*n*-dodecane. The extraction mechanism determined for Cs^+ and Sr^{2+} displays solvation and $Na^+TcO_4^-$ as ion-pair association. The combining ratio of extractant to metal ion is 1:1 in all the cases. The figure shown above depicts pictorial representation of extraction of $Na^+TcO_4^-$ from LLW using 0.2 M DtBuDB18C6 +50% IDA/*n*-dodecane and stripping of $Na^+TcO_4^-$ from loaded solvent with DM water. Radiolytic and hydrolytic degradation studies have indicated high stability of solvents. Degradation mechanism and recycling of degraded solvent has also been established.

2.1.5 Design, analysis and performance evaluation of fiberoptic pressure sensors based on Fabry-Perot interferometer

In the present research work, fiber optic pressure sensors working on the principle of a Fabry-Perot Interferometer (FPI) and having MEMS based design are studied. The effects of the trapped gas in sealed microcavity sensors have been investigated. An analytical model is developed and phenomenon of "suppression of span" in the sealed microcavity pressure sensors is brought out, especially for low pressure range sensors.

The suppression is stronger for sealed cavities of small lengths and higher trapped gas pressures. The analytical model is validated through numerical simulations. Pressure sensors of 1 bar range and different cavity lengths have been designed, fabricated and tested. A technique is developed for noncontact measurement and characterization of cavity lengths and deflection shape of diaphragm using "angle-cut" multimode optical fiber.

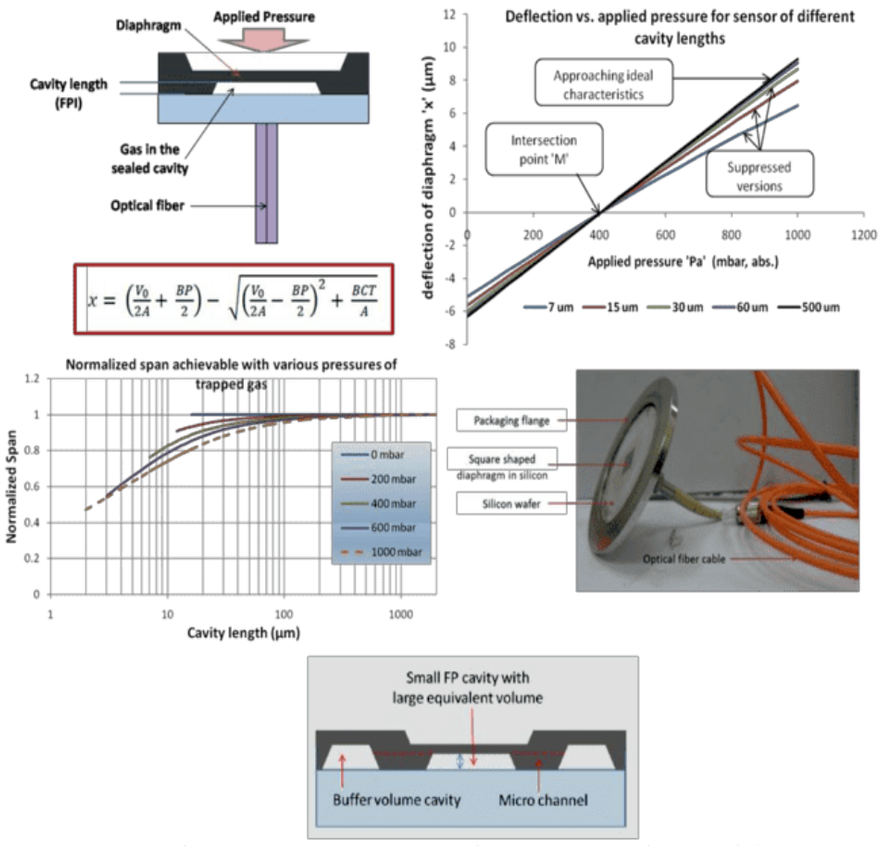

The FPIbased pressure sensor with trapped gas in the sealed cavity, deflection characteristics of diaphragm, achievable spans, packaged sensor and concept of buffer cavity

The study concludes that large cavity lengths are beneficial to reduce the effects of trapped gas. However, by optical design small cavity length Fabry-Perot sensors are preferred. In order to accommodate these two contradictory requirements, inclusion of a "buffer cavity" is suggested. This cavity would be coupled to the main (Fabry-Perot) cavity and would provide extra volume to circumvent the problem of suppression of span. The efficacy of the buffer cavity is validated through numerical simulations.

2.1.6 Robot-based autonomous neuro-registration and neuronavigation for neurosurgery

The thesis discusses the development of methods, algorithm and image processing techniques to conduct robot assisted minimally invasive neurosurgical procedures. The thesis develops systematic methods for patient data preparation. The robot-based neurosurgery involves the mapping of medical image space and real patient space called neuro-registration. The neuro-registration relates the physical robot space to the medical image space (virtual space) by measuring the corresponding reference points in both the spaces. The thesis formulates a rule, which eliminates error prone process of correspondence.

The thesis presents the autonomous, highly accurate, and faster robot-based frameless stereotactic neurosurgery as shown in figure. The primary objective is to eliminate human errors and enhance the accuracy and reliability of robot-based neurosurgery. To serve the objectives, the design of the algorithms operating in real-time and methods robust to the varied ambiance of the operation theatre for conducting successful autonomous neuro-registration is implemented. Further, the line of sight problem associated with the frameless stereotactic neurosurgery is eliminated and quick neuro-registration and time-optimal neurosurgical procedures are achieved.

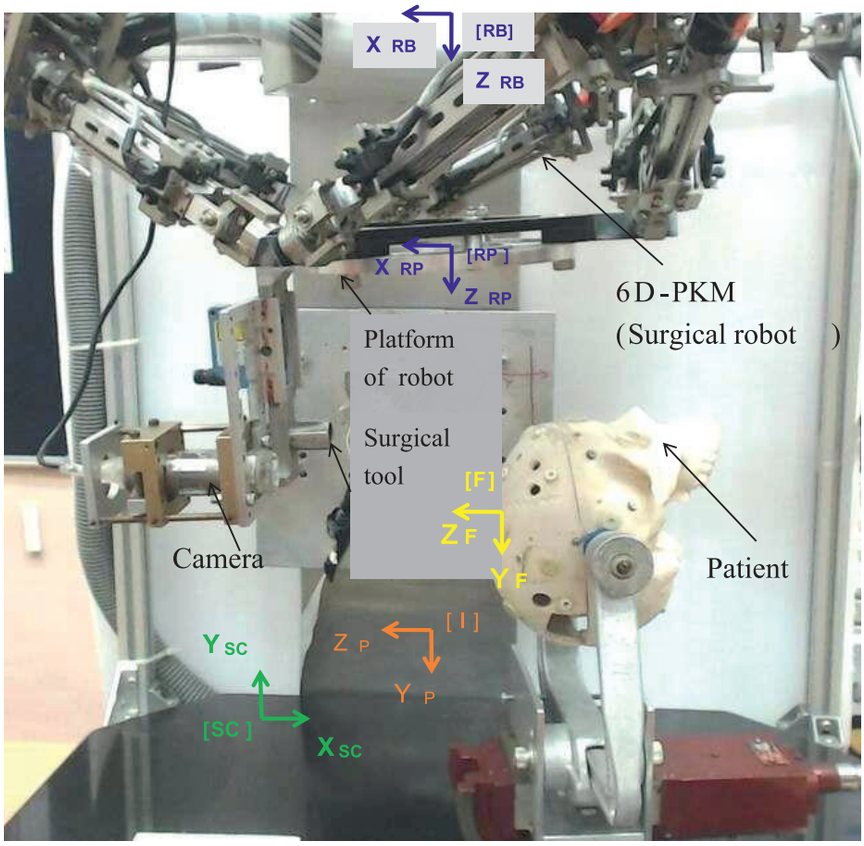

Surgical robot with tool and camera, skull phantom placed in HFS pose

2.1.7 Development and characterization of radiation resistant nanocomposite polymeric membranes

The polymeric membranes have inherent limitations of low radiation stability, as the backbone is susceptible to radiation induced damages. In order to develop radiation resistant property of polymeric membranes, for the first time the research was oriented towards development of mixed-matrix membranes with enhanced radiation resistance attributes. These membranes can have sustainable application in radioactive effluent treatment. Attempts were made to exploit the unique properties of nanodiamond (ND) and cerium oxide (ceria) nanoparticles for protection of polysulfone (Psf) membrane matrix from consequences of radiation induced damage and attack of free radicals generated in water during membrane operation. The following investigations were carried out in the thesis.

The study helped in understanding the role and influence of nanomaterials (ND and ceria) towards enhancing the life of polymeric membrane matrix in radiation environment. Mixed-matrix membranes showed up to 10 times enhanced life-span in γ-radiation environment as compared to the control polymeric membrane, without compromise in its structural, mechanical, and chemical properties, as well as membrane performance (throughput and selectivity). The study has been a unique one, wherein the potential role of two nanomaterials was established in the gamma radiation environment.

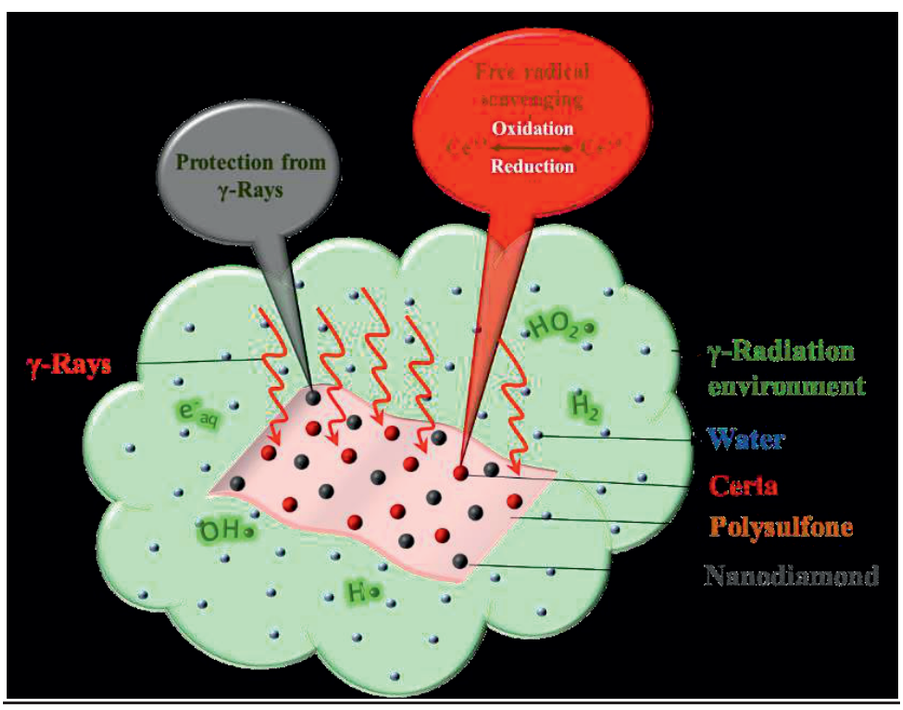

Schematic representation of mixed matrix membrane and the role of nanomaterials (nanodiamond and ceria) for the protection of mixed matrix membrane in γ-radiation environment.

2.1.8 Phase extraction of optical interferometric signals based on improved time-frequency method with application to high strain rate measurement

Optical interferometry-based non-contact type measurements play a key role in determination of free surface velocity of target material under high strain rate experiments. Michelson interferometer in velocity as well as displacement mode configuration is widely used. It is important to extract the phase or IF of the fringe signal as the information of velocity is hidden in phase or instantaneous frequency (IF). In time domain approach, multiple fringes are required to extract phase and noise sensitive numerical differentiation is necessary for getting the IF of the fringe signal. Although computationally less expensive, the accuracy of this method may get affected significantly by various measurement imperfections like, nonlinearity, amplitude and phase angle error. On the other hand, in frequency domain approach single fringe may be sufficient to extract IF and numerical differentiation could be avoided.

In the thesis, phase extraction based on quadrature phase shifting method, reassigned Continuous Wavelet Transform (CWT) method and Smoothed Pseudo Wigner-Ville Distribution (SPWVD) method have been described and developed. In phase shifting method amplitude and phase angle error have been corrected by efficient ellipse fitting method by combining algebraic as well as geometric technique. In CWT, time-bandwidth product of Morlet wavelet is optimized as 0.6 and simultaneous reassignment technique is applied for accurate IF extraction. SPWVD method is proposed for extracting IF of highly non-stationary polynomial frequency modulated fringe signal. Cohen class signal representation is followed and time and frequency resolutions are independently optimized using Gaussian separable kernel. Reassignment technique is further applied for sharpening of the spectrogram with these optimized kernels that improves accuracy in IF significantly. Finally, some of these developed phase extraction algorithms are applied to free surface velocity measurement under high strain rate experiments and different dynamic mechanical properties such as Spall Strength, Hugonoit Elastic limit (HEL), Strain Rate at HEL etc. of AL2024T4 target material are derived from extracted velocity profile.

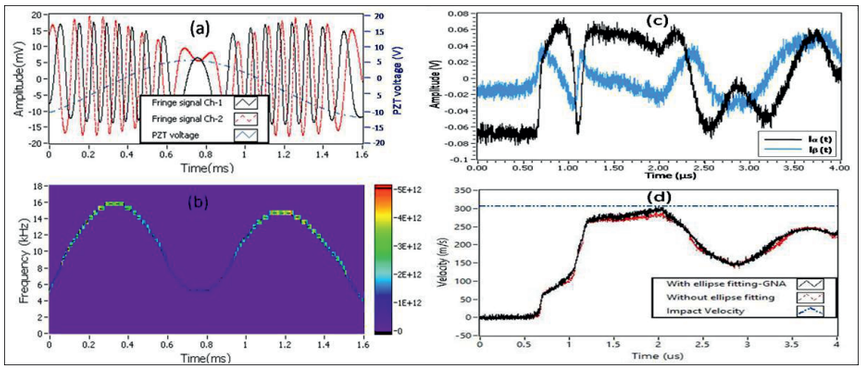

(a) Measured quadrature fringe signal with PZT supply voltage (b) Corresponding Reassigned CWT spectrogram (f0t=0.6) obtained from Ch-1 fringe signal. (c) VISAR Fringe signals obtained in plate impact experiment using Gas Gun facility and (d) Corresponding free surface velocity profile by phase shifting method

2.1.9 Liquid-liquid two-phase flow and mass transfer in microchannels

The thesis reports experiments on extraction of U(VI) and HNO3 from nitric acid solution inmicrochannels by using 30% (v/v) TBP in dodecane as the organic phase The research work is carried out to understand liquid-liquid two-phase flow hydrodynamics andvarious aspects of solvent extraction in microchannels using liquid-liquid systems relevant tosolvent extraction in nuclear fuel cycle. There are several advantages of carrying out solvent extraction in microchannels. In microchannels, the size of the dispersed phase is restricted leading to high specific interfacial area and high overall volumetric mass transfer coefficients. The quality of dispersion can be precisely controlled, which helps in fast settling thereby reducing the size of phase disengagement section. Scale-up of solvent extraction in microchannel is relatively easier as throughput is increased by numbering-up approach. However, the liquiq-liquid two-phase hydrodynamics in a microchannel is very complex as different flow patterns are possible. The specific interfacial area and overall volumetric mass transfer coefficient in a microchannel depends on the type of the flow pattern. The flow pattern affects liquid-liquid phase separation also. Therefore, mass transfer and phase separation is significantly affected by the prevailing hydrodynamics. The experimental work carried out in this thesis aimed at understanding hydrodynamics, mass transfer and phase separation for solvent extraction in microchannels. Generalized flow regime maps for liquid-liquid two-phase fow in Y-junction microchanenls are obtained. The methodology to identify an optimum configuration for solvent extraction in microchannel at a desired throughput for a given liquid-liquid system is proposed. A novel monoblock distributor having in-built microfluidic junctions for realizing higher throughputs using numbering-up approach is conceptualized and tested. Intensification of phase separation of a liquid-liquid dispersion generated at a microfluidic junction is explored by using an in-line phase separator housing a metallic mesh (Figure). Finally, a complete intensified process of recovery of uranium from lean streams comprising of extraction, and direct precipitation from loaded organic is demonstrated by using microchannels.

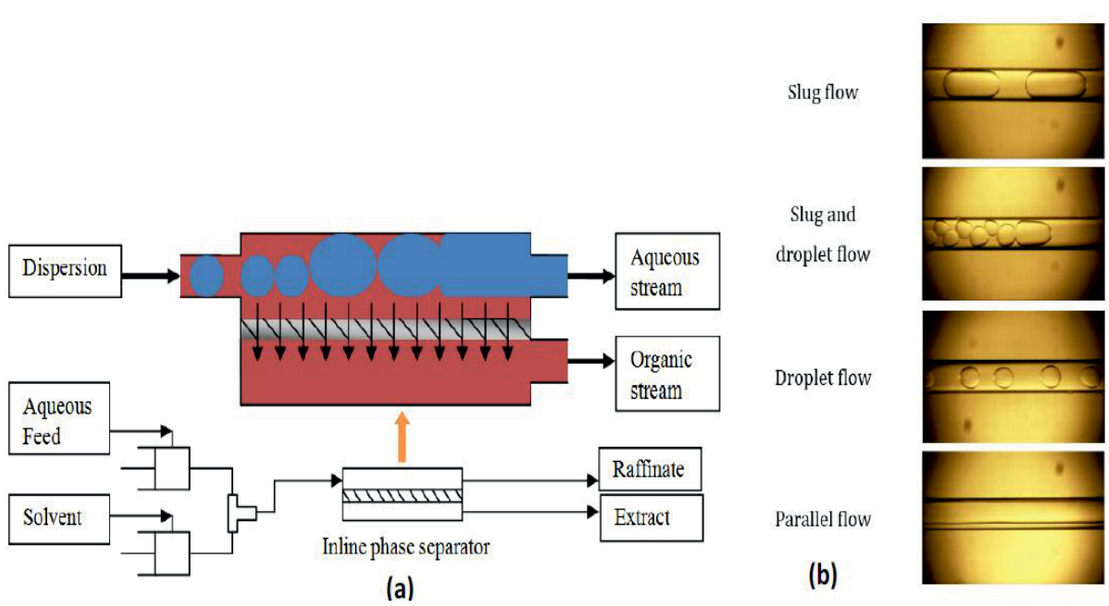

(a) In-line phase separator housing a metallic mesh (b) Different flow patterns in Y-junction microchannels.

2.2 Indira Gandhi Centre for Atomic Research, Kalpakkam

2.2.1 Study of nano-dispersoid characteristics in oxide dispersoid strengthened alloys

The thesis presents a mechanistic study of microstructural evolution of the oxide dispersoids during the synthesis of the oxide dispersoid strengthened (ODS) alloys. It is customary to use small quantities of Y_2O_3 and Ti along with pre-alloyed steel powder to synthesize the ODS steel for future fast breeder reactor (FBR) core structural material application. The mechanical properties of this steel derived from the uniform distribution of the dispersoids in the metal matrix. Ti is added to Y_2O_3 to form finer Y-Ti-O complex oxide, however the structure and chemistry of this oxide dispersoid is barely under control during the complex powder processing route. In this thesis, a detailed structural characterisation of the dispersoid at different stages of mechanical milling and subsequent annealing has been studied on a model concentrated alloy of Fe-15Y_2O_3-x Ti (x = 0 – 15 wt. %). The study on concentrated alloys helps in ease of structural characterization and gaining basic understanding about evolution of dispersoid in ODS steel and also to optimize the Ti and Y_2O_3 content in the steel to form finer $Y_2Ti_2O_7$ type dispersoid. It observed that nanocrystalline Y_2O_3 becomes amorphous upon milling, but the Y_2O_3 is not fragmented to Y and O. Upon annealing at 1273K, the structure and stoichiometry of the evolved Y-Ti-O complex oxide dispersoid was governed by Y_2O_3 and Ti content in the alloy. The Y_2O_3 to Ti ratio of 1:1 resulted in formation of $Y_{1.6}Ti_{1.8}Fe_{0.4}O_{6.6}$ oxide (structure ~ $Y_2Ti_2O_7$) and finer (2-25 nm) in size. With optimized Y_2O_3 and Ti content (1:1 wt. % ratio) two varieties of 9Cr ODS steels were fabricated and their microstructure and nano-mechanical properties were evaluated and compared with the 9Cr ODS F/M steel extruded rod and clad tube, fabricated in collaborations with ARCI and NFC, Hyderabad.

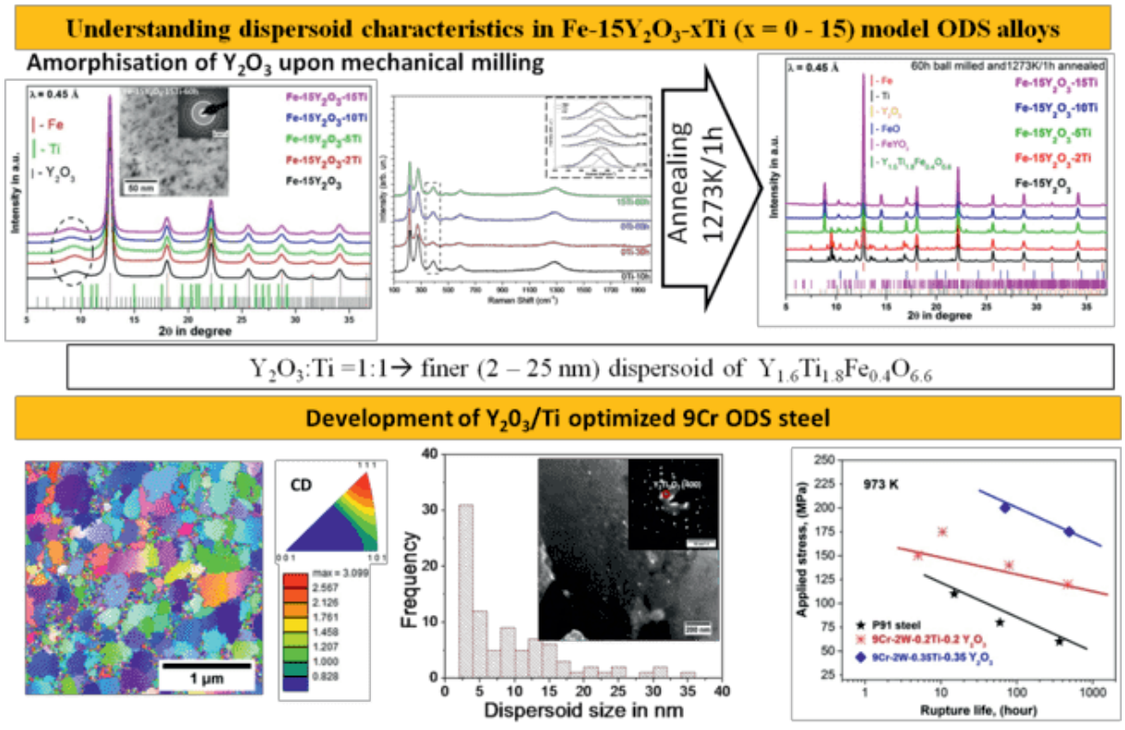

2.2.2 Studies on deep excavation behaviour in engineered backfilling adjacent to nuclear safety related structures

The research work carried out in the thesis is aimed at (a) identifying a suitable constitutive model to predict the behaviour of deep excavation in multilayered & engineered backfill (b) evaluating the stiffness of soil using field instrumentation data and (c) evaluating the efficacy of engineered backfill in limiting the settlements during future excavation. Numerical analysis carried out for deep excavation in engineered backfill soil adjacent to criticalstructures using field calibrated stiffness highlighted the requirement of higher order constitutive model, viz., HS model for prediction of deep excavation behaviour. The study also indicated that while the available empirical formulations for predicting deep excavation behaviour are adequate to define maximum settlements in primary zone, a site-specific analysis accounting in-situ stiffness & dewatering effects is warranted for evaluating secondary zone of settlements. Additional measures like strutting and ground improvement are required to limit the settlement in secondary zone. The results highlighted the inadequacy of present retaining wall assisted deep excavation to limit the settlement and displacements during future excavation.

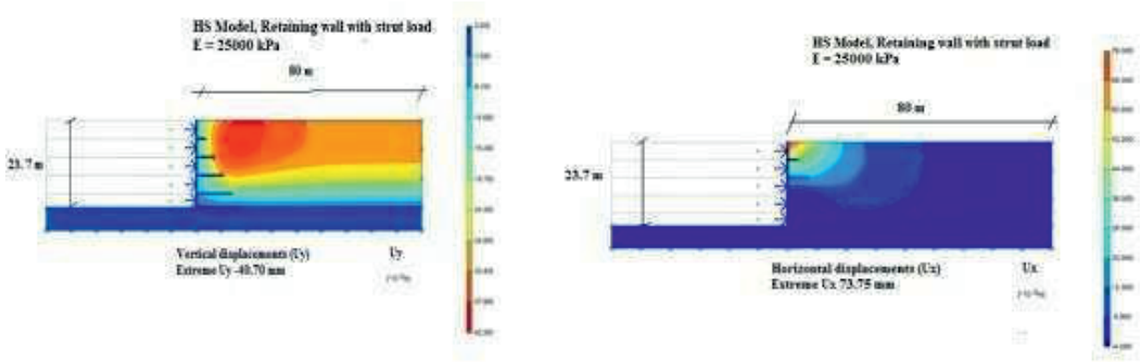

Displacement profile of the improved system at the end of excavation

2.2.3 Study of radiation effects in SRAM based FPGAs for NPP I&C system design

The aim of the present dissertation was to study the radiation effects in SRAM based FPGAs targeted for NPP I & C system design. As there is no history of data available for commercial grade SRAM based FPGAs used in nuclear applications this study has its significant importance. This study has given focus to cumulative absorbed dose effects due to gamma radiation. As gamma radiation can cause TID effects as well as SEUs in the MOS based devices, an experimental study has been conducted to measure the tolerance level of the system in such environment. Based on the radiation experiments carried out using Gamma-chamber 5000, it is observed that the device under test (Spartan 6 FPGA) is functionally tolerant up to a radiation dose level of 322 krad, suggesting that if the system is implemented with SEU mitigation techniques, the device can withstand up to 322 krad of accumulated dose without any failure. The major parameter changes have been measured during irradiation. The power supply current variation due to absorbed dose is illustrated in the figure. For further improvement in efficiency, appropriate shielding can be provided. The efficiency of shielding has been Based on the computational modelling of shielding box and TLD based dose rate measurement in the

Gamma chamber, it is found that the duration of functional time of the device under test can be extended almost two times by using shielding. A detailed investigation in to various SEU mitigation techniques has been carried out and their efficiencies are quantified based on area overhead, complexity of implementation. Also, a Golay code-based error recovery mechanism has been proposed which can detect and correct up to 3 errors in a block of 24 bits, the state diagram is given in fig.2. SRAM based FPGAs provides a diversity in safety related applications and if deploy inside the RCB it can avoid the extra penetrations

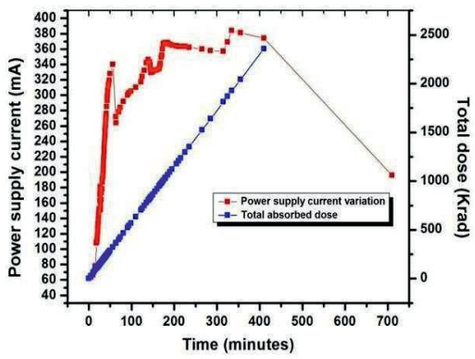

Power supply current variation due to total determined using the 2D transport code DORT and IGC- radiation absorbed dose-DUTS3 cross-section data set.

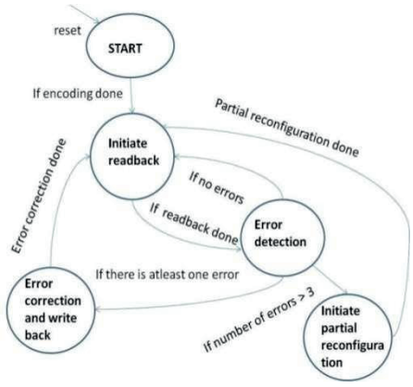

Control logic state diagram of error recovery mechanism for taking out the cables.

2.2.4 Synthesis and modification of graphene nanowalls using plasma immersion ion implantation and deposition facility

Graphene nanowalls (GNWs/VGNs) are demonstrated as excellent electrode material for several electrochemical energy conversion/storage devices. Nitrogen incorporation into GNWs offers large potential for improving the performance. The study describes the synthesis and nitrogen modification of GNWs (N-GNWS) in a custom-made plasma immersion ion implantation and deposition (PIII&D) facility. The utility of GNWs is fundamentally related to its morphology and electronic structure. Hence, GNWs of tunable morphology is synthesized, and the morphological and electronic properties are studied using FESEM, Raman and FTIR spectroscopy, TEM and EELS. Presence of bridging methylene induces secondary growth which further release enormous surface area and large number of edges. Plasma ion implantation is a high throughput technique for surface modification. Implantation generates additional defects and changes the surface chemistry. Electrochemical studies of N-GNWs showed >100 times increase in charge storage and increase in discharge time for 1 kV energy and 2 min. (~4.5 at %) nitrogen implantation. The supercapacitance of N-GNWs is attributed to super hydrophilic nature, minimal damage to graphene backbone and increase in quantum capacitance of the surfaces. The study demonstrates synthesis of N-GNWs suitable for application in advanced devices.

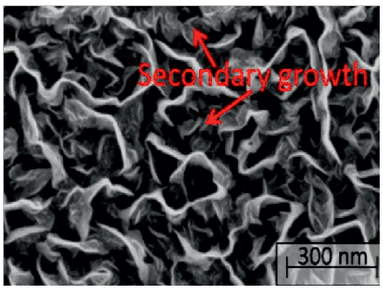

SEM image of GNWs showing secondary growth

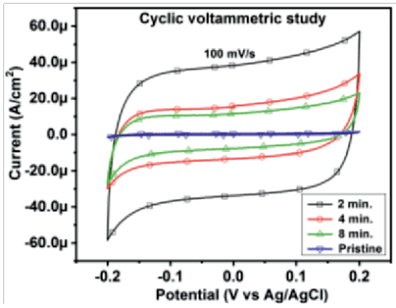

C V showing multifold increase in charge storage in N-CGWs

2.2.5 Design and development of wireless acoustic emission sensor system for structural health monitoring applications

The thesis highlights the first of its kind design and development of wireless acoustic emission sensor system (AE-SS), based on programmable system on chip (PSoC) technology. A combination of hardware and software co-design approaches has been implemented in PSoC towards achieving the objective. In order to design and develop the wireless AE sensor system, several novel design steps, challenges and issues were addressed.

The developed wireless AE sensor system has been successfully validated and applied for structural health monitoring on concrete. The developed wireless system offers unique advantages of its compactness in size (85 mm x 56 mm), low power consumption capability (50 mA), battery operated, portability, reduced wiring complexity, and reduced cost and remote operational capability. This system can be effectively utilized for condition monitoring of structures and components such as NPP containments, bridges, tanks, and components in petrochemical industries where corrosion is a potential issue, with utmost

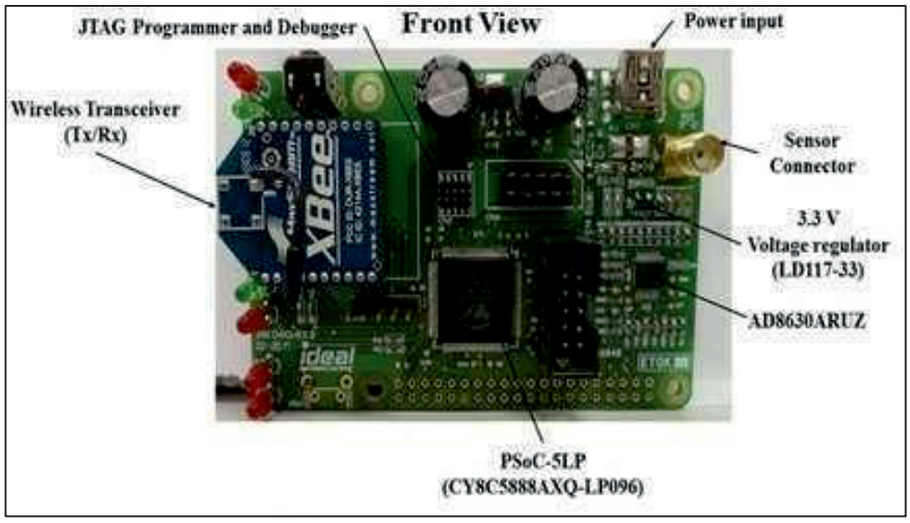

Developed wireless sensor

2.2.6 A Study on deformation mechanism in perfect and twinned Cu nanowires by atomistic simulations

Metallic nanowires exhibit mechanical properties different from their bulkcounterparts due to high surface area to volume ratio and low defect density. Hence, it is necessary to characterize and understand the deformation of nanowires. With rapidprogress of computational capability and availability of reliable inter-atomic potentials, molecular dynamics (MD) approach has become an important simulation tool toexamine the deformation behaviour. In the present thesis, deformation and dislocationmechanism of single crystalline and twinned nanopillars has been studied using MDsimulations. The simulation results indicated that:

- In single-crystalline Cu nanowires with different orientations, the yield stress exhibits tension-compression asymmetry. Also, deformation behaviour varies significantly with compression and tension. Under compression, orientations close to<100> corner of a standard stereographic triangle orientations deformed by twin, while remaining orientations deformed by full dislocation slip. On the other hand, all orientations deformed by twinning mechanism under tension.
- For <100> Cu nanowires, Young's modulus and yield strength values decreased rapidly in small size nanowires followed by gradual decrease approaching towards saturation at larger size. Yielding in all nanowires occurs through the nucleation of 1/6<112> Shockley partial dislocations. The plastic deformation in small size nanowires occurred mainly by slip of partial dislocations at all strains, while in largesize nanowires, slip of partial dislocations at low strains followed by slip of extended dislocation at high strains were observed.
- In large size nanowires, the leading partial annihilation at the surface gives rise to the nucleation of a new trailing partial dislocation, while in small size nanowires, it gives rise to multiple reflections from the nanowire surface.
- Yield stress increases with decreasing twin boundary spacing in twinned nanopillars.
- In polycrystalline Cu, yield stress follows inverse Hall–Petch relation with grain size.

2.3 Raja Ramanna Centre for Advanced Technology, Indore

2.3.1 Experimental studies and parametric investigations on laser directed energy deposition based additive manufacturing of hastelloy-X thin walls and bulk structures

Laser Additive Manufacturing (LAM) is one of the advanced manufacturing technologies witnessing a rising demand in aerospace and power sector to build high-performance components subjected to extreme duty conditions. Hastelloy-X (Hast-X) is one of the nickel-based superalloys suitable for high-temperature applications due to the appropriate blend of high-temperature strength, toughness and resistance to degradation in a corrosive or oxidizing environment. Laser Directed Energy Deposition (LDED) based LAM has potential for building Hast-X components used in aerospace and power sector. The present thesis is focused on the engagement of the versatile LDED to build defect free Hast-X thin-wall and bulk structures, and comprehensively investigate their behavior at different process and service conditions experimentally.

The research work carried out in the thesis comprehends and contributes to the existing understanding on the LDED of Hast-X structures from single tracks to multiple overlapped multi-layer tracks under different process conditions yielding thin walls and bulk structures in terms of processing, geometry, microstructural and mechanical characteristics. The quality of deposition (cracking, continuity, surface quality and porosity) and properties (geometric, microstructural and mechanical) can be tailored by varying the process parameters. A simple analytical technique has been developed for the faster predictions of track geometry at various processing parameters and a finite element based numerical tool is deployed to get the process insight. The obtained theoretical results find good match with the experimental results. The investigated mechanical properties of LDED built Hast-X structures are found to be higher than conventionally build Hast-X structures. The microstructures are found to be non-homogenous with finer grain size. It is found that in-situ treatment, i.e. Sequential Layer by Layer Remelting (SLLR) can improve the density and surface finish of the built components and ex-situ treatments such as solution treatment can aid to achieve homogenization and properties close to conventional components. One of the potential applications of Hast-X is the development of Printed Circuit Heat Exchanger (PCHE), generally used in advanced power sectors. A protoype PCHE is build as shown in Figure 1 using LDED by deploying straight walls, overhang walls and bulk structures to demonstrate the process capabilty. The acquired know-how from the above comprehensive studies in single tracks, wall structures and bulk structures is used for building the PCHE.

Photographic view of LDED built Printed Circuit Heat Exchanger of size 200 mm x 200 mm x 170 mm.

2.4 Institute of Plasma Research, Gandhinagar

2.4.1 Nuclear activation studies in fusion Systems: New methods and algorithms

The thesis presents various methods and algorithms developed to simulate neutron interaction with the material and evaluate the nuclear response of the material in spatially and temporally varying neutron fields. Low activation materials are pre-requisite for fusion reactor development. No tools were available in the literature to directly evaluate the best material composition based on nuclear responses of the material. Hence, composition optimization scheme for materials, based on various radiological responses and experiencing a spatial and temporal variation of the neutron spectrum is developed.

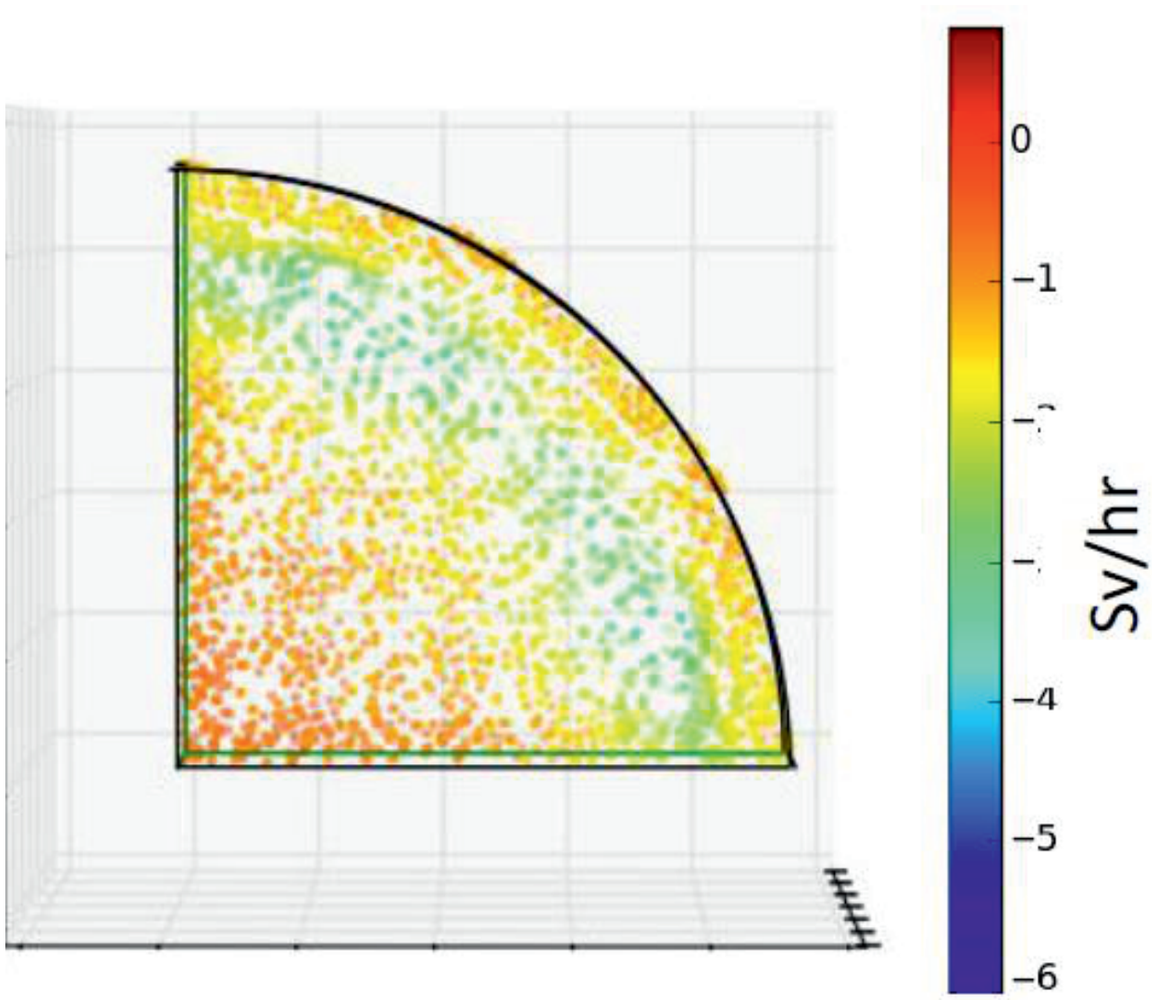

Total contact dose rate in log scale at 2085 mesh locations in stainless steel plate

3. Life Sciences

During the period of the report, HBNI awarded 34 Ph.D. degrees in Life Sciences. Some of the theses are summarized below.

3.1 Tata Memorial Centre Mumbai

3.1.1 A study on understanding the modulation in MAPK/ERK and PI3KCA/Akt signaling during acquirement of drug resistance

Majority of epithelial ovarian cancer (EOC) cases relapse with chemoresistance disease within a short time. **The thesis reports** that increased autophagy anda lysosomal degradation process foster initiation of resistance. Targeting ERK1/2 signalling impeded autophagy and sensitized cells at the onset of resistance. Repurposing metformin, a common anti-diabetic drug, is demonstrated to delay resistance development by targeting the cancer-stem-cell population. Further utilizing Bioluminescence-Resonance-Energy-Transfer (BRET) based ERK and AKT sensor, a molecular platform for evaluation of therapeutic efficacy of common non-platinum agents against resistant EOC is proposed. Altogether the work proposes stage-specific interventions to deter the development of platinum-taxol resistance in ovarian cancer.

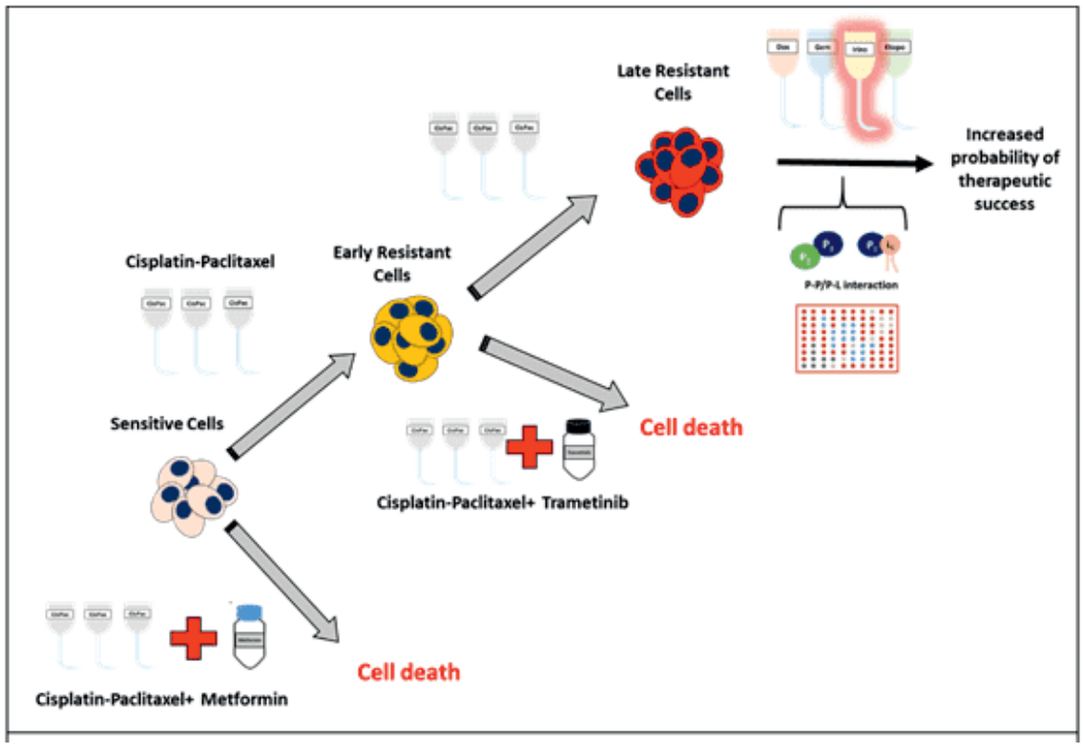

A stage specific therapeutic intervention approach to deter platinum-taxol resistance in cancer cells

3.1.2 Identifying mechanisms that regulate human sodium iodide symporter (NIS) gene expression in breast cancer

The thesis presents a thorough investigation on sodium iodide symporter (NIS) gene expression in breast cancer. NIS protein present in thyroid cell forms the basis of targeted radio-iodine therapy procedure in thyroid cancer clinic. However, though NIS expression was recorded in breast cancer tissues, due to its gene function disparities in breast cancer tissue, radio-iodine application was difficult. The thesis addressed key molecular defects involved by performing in depth molecular and subcellular localization analysis in breast cancer cells, and animal model and demonstrated definite way out for the breast cancer clinic.

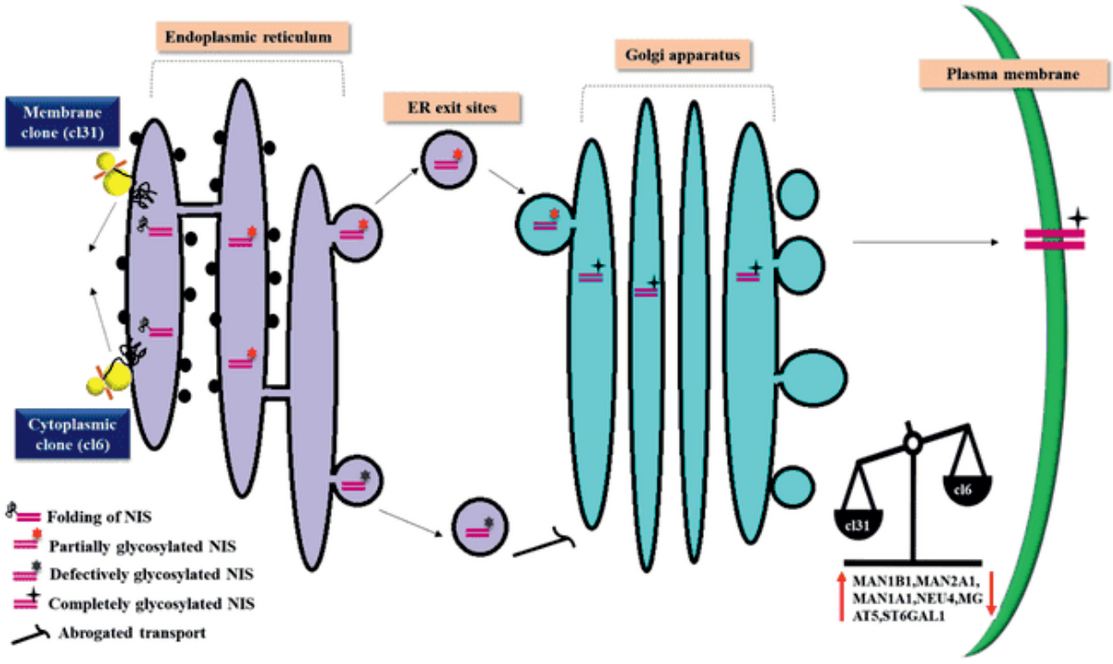

Diagrammatic representation of differential NIS protein trafficking across cytoplasmic and membrane over-expressing cell population

3.1.3 Molecular imaging of STAT3 signaling *in vivo*

Breast cancer is a global disease with highest incidence. This thesis covers discovery of a new biology for challenging a specific subtype of breast cancer, where the protein target, STAT3, undergoes certain modifications causing poor disease outcome in patients. In an effort to understand this problem, a major part of the thesis focused on designing a molecular imaging sensor and used that sensor for identification of novel drug compounds with high specificity for STAT3 target. Some of the drugs identified showed specific curative measure of the disease.

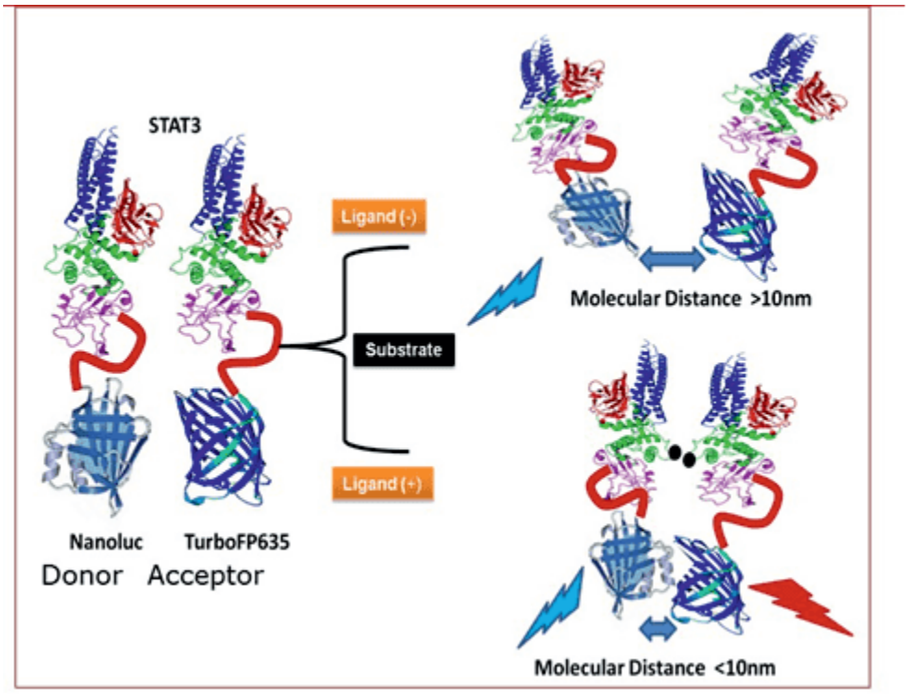

Phospho-BRET sensor for STAT3 activation

3.1.4 Creation of novel photochangable fluorescent protein through directed evolution

Microscopy has revolutionized biological science, and fluorescence super-resolution microscopy enables scientists to see inside of biological cells in the highest resolution. mEos3.2 is a necessary probe for such super-resolution microscopy on chemically fixed cells that are dead. However, it is not bright enough for such super-resolution microscopy of living cells. Therefore, mEosBrite, a brighter variant of mEos3.2 was developed. The study showed that mEosBrite could improve brightness in live super-resolution microscopy.

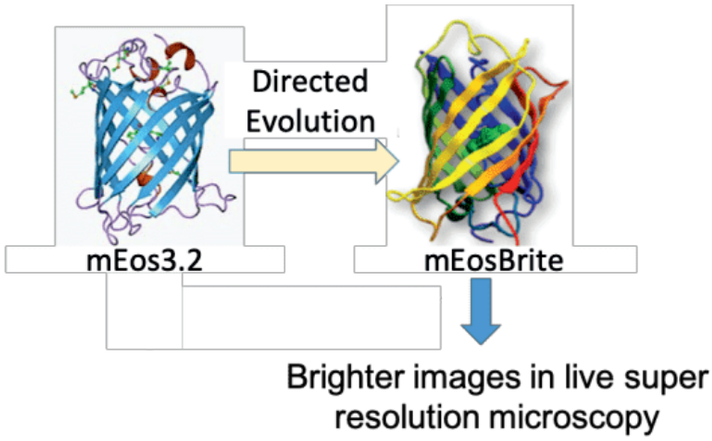

mEosBrite improves brightness in live super-resolution microscopy

3.1.5 Molecular mechanism underlying the effect of miRNA expression on medulloblastoma cell behavior

Medulloblastoma, a highly malignant brain tumour in children, consists of four different types. Both WNT and Group 3 tumour types express an oncogene called MYC that is known to make cancers aggressive. WNT cases, however, have excellent survival rate of over 90%. A small RNA called miR-193a is expressed in the WNT tumour type. When miR-193a was expressed in the cells of Group 3 tumour type, there was reduction in their growth and their capacity to form tumours. MiR-193a was found to target MAX, thereby reduced the activity of MYC. MiR-193a, therefore, is useful for the treatment of MYC overexpressing aggressive cancers. Another small RNA called miR-204 was found to make the tumours less aggressive by reducing the activity of lysosomal degradation pathway that is required for degradation of damaged components in the tumour cells and therefore also has therapeutic potential.

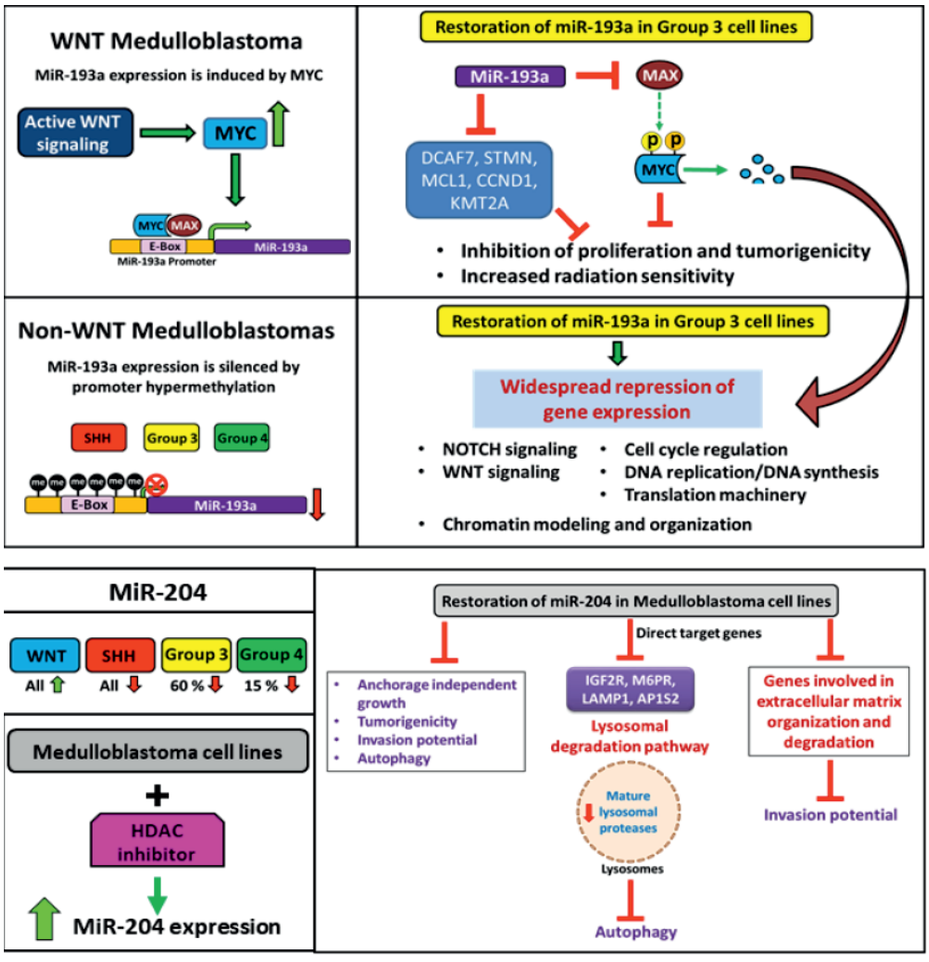

Role of miR-193 and miR-204 in medulloblastoma biology

3.1.6 Role of IGF1R in ovarian cancer metastasis

Recurrent metastatic epithelial ovarian cancer (EOC) is associated with treatment limitations and has no cure. Herein, we studied the role of insulin like growth factor 1 receptor (IGF1R) signaling in the organ-specific metastasis of EOC cells developing chemoresistance. Distant spread of EOC cells with enhanced lung homing was augmented by chemoresistance, particularly in the extreme stage. While α6 integrin-IGF1R dual signaling governed the initial metastatic events in these cells, secretion of S100A4 by these cells activated lung fibroblasts, the inhibition of which abrogated their lung-metastasis. Altogether, IGF1R-α6 integrin-S100A4 network was identified as a critical determinant for organ-specific metastasis of chemoresistant EOC cells.

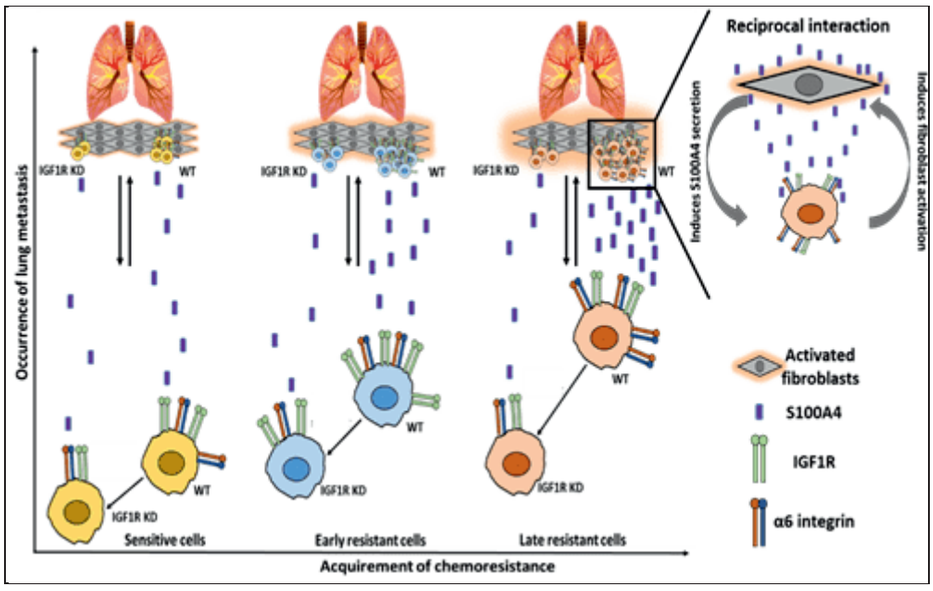

IGF1R-α6 integrin-S100A4 network governs the metastatic organotropism of chemoresistant epithelial ovarian cancer

3.1.7 Investigating the role of IGF-1R signalling in development and maintenance of chemoresistance in ovarian carcinoma

Deregulated Insulin like growth factor receptor-1 (IGF-1R) controls proliferation, drug-resistance, survival of tumor cells. Targeting IGF1R in tumors using antibodies/inhibitors was unsuccessful due to overlapping Insulin signaling. In the study, RUNX1 was identified as an IGF1R regulator and it was shown that the interaction between RUNX1 and FOXO3a and their binding to IGF1R regulatory regions controls the dynamic modulation of IGF1R at different stages of resistance. The study revealed that IGF1R regulates cancer stem cell phenotype and inhibition of RUNX1 led to sensitization of tumors to platinum-taxol *in vivo*. The study thus validated a new therapeutic strategy of controlling IGF1R at transcriptional level to prevent chemoresistance.

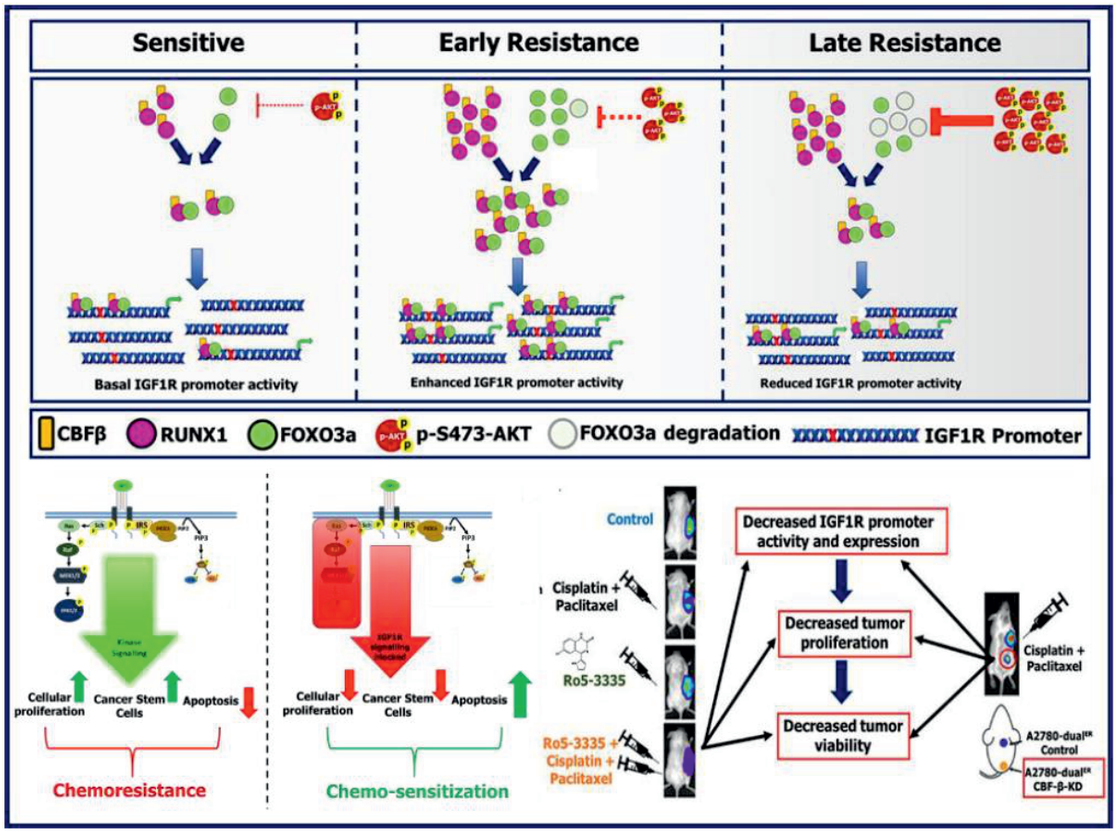

Dynamic model of IGF1R promoter modulation by RUNX1/FOXO3a/AKT and IGF1R/MAPK/ERK signalling mediated chemoresistance during acquirement of chemoresistance development in EOC cells.

3.1.8 Histone H3 modifications and their role in DNA damage response

The DNA, which is the master regulator of the cell, is securely located inside the nucleus. Interestingly, only few proteins have the privilege to enter the nuclear domain and even fewer have direct access to the DNA. The negatively charged DNA has five positively charged histone proteins associated with it (H1, H2A, H2B, H3 and H4) that help in its compaction. The thesis focuses on understanding the role of histone post translational modifications, especially histone phosphorylation and acetylation during cell cycle phase specific DNA damage response. One of the most interesting findings of the research work was that one of the ways by which breast cancer tumor becomes radio-resistant is by removing acetylation from histones. Therefore, through usage of drugs that decrease the activity of HDACs (called an HDAC inhibitor -Sodium Valproate), thers is a possibility that the persistence of acetylation on histones will decrease DNA-histone affinity and make DNA more accessible to damage by reactive oxygen radicals. The thesis proposes that checking the activity of HDACs in a tumor before beginning radiotherapy may help us to decide the candidates who might benefit from this treatment. This is due to epigenetic heterogeneity that persists within a population, even within different organs of the same body. Hence, a clinician should understand which patients should be given HDAC inhibitor therapy by understanding the intra-tumoral epigenetic environment. This could reduce the chances of relapse or poor response.

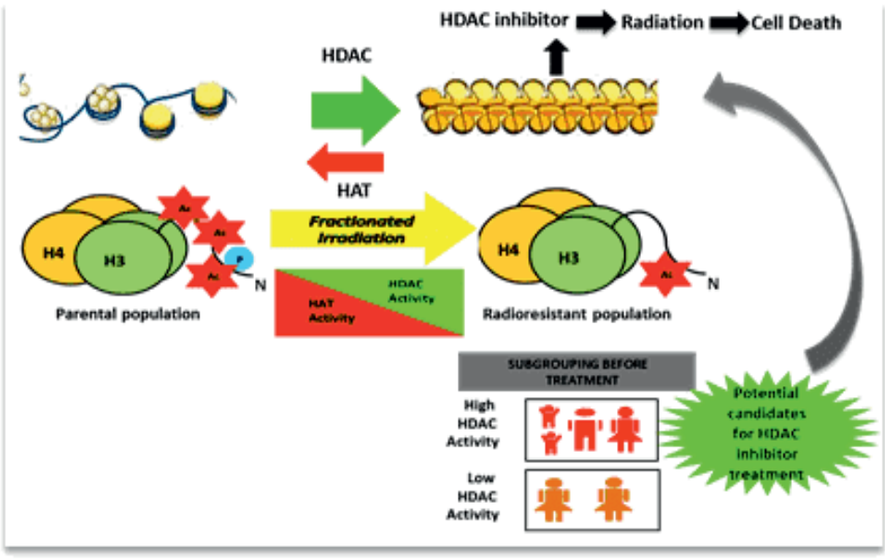

Mechanism of checking the activity of HDACs in a tumor before radiotherapy

3.1.9 Assessing the role of activins / inhibins in human oral cancers

Oral (mouth) cancer is very common in India. It spreads rapidly to neck and other organs leading to death of patients. Despite many years of research, the doctors are unable to treat higher stage oral cancers. In the study, it was found that excessive Activin A and p63 proteins in oral cancer patients and these patients survived for lesser time. It was proved that Activin A and p63 proteins are responsible for oral cancer spread and stopping their actions with the help of Vactosertib, a drug against Activins, will help save oral cancer patients from the spread of cancer and improve their life expectancy.

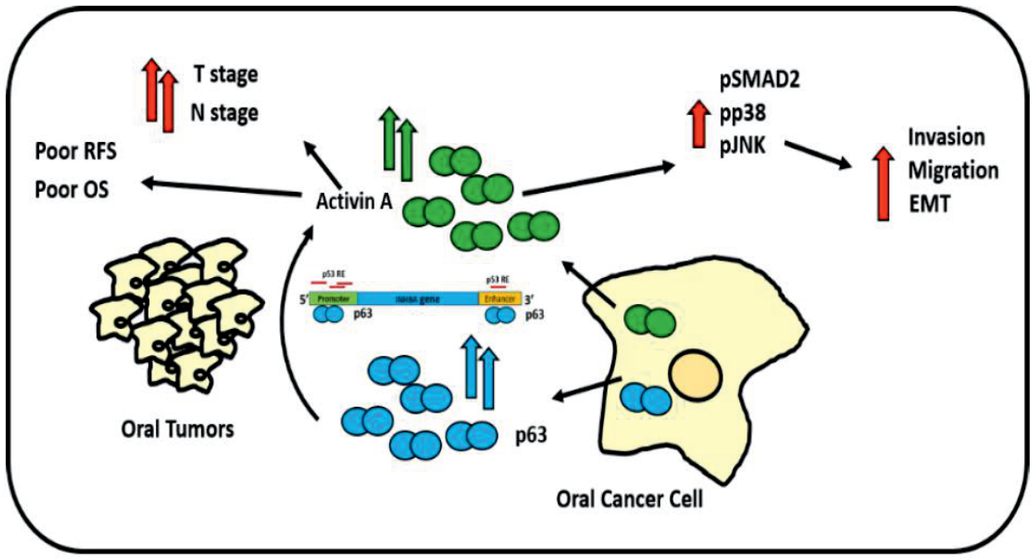

Role of Activin A signalling in oral cancers

3.1.10 Role of miR-204 and miR-592 in medulloblastoma pathogenesis

Medulloblastoma is a highly malignant brain tumour in children. Although ~70% children survive beyond 5 years, they suffer from long-term side effects due to the aggressive treatment. Among the four types of medulloblastomas, Group 3 and Group 4 tumour types are similar with respect to many genetic alterations but differ in their survival rates. MiR-204, a small RNA is expressed in almost all Group 4 tumours but only in about 50% of Group 3 tumours. The Group 3 tumors that do not express miR-204, were found to be the most aggressive tumor type. Thus, only this subset requires aggressive treatment, other Group 3, Group 4 tumors may be treated with less aggressive treatment in future. MiR-204, when expressed in the Group 3 tumor cells reduced their growth and malignant potential indicating its therapeutic potential. MiR-592, a small RNA expressed only in Group 4 tumors when expressed in Group 3 cells, gave them Group 4 characteristics showing how Group 3 tumors can be made less aggressive.

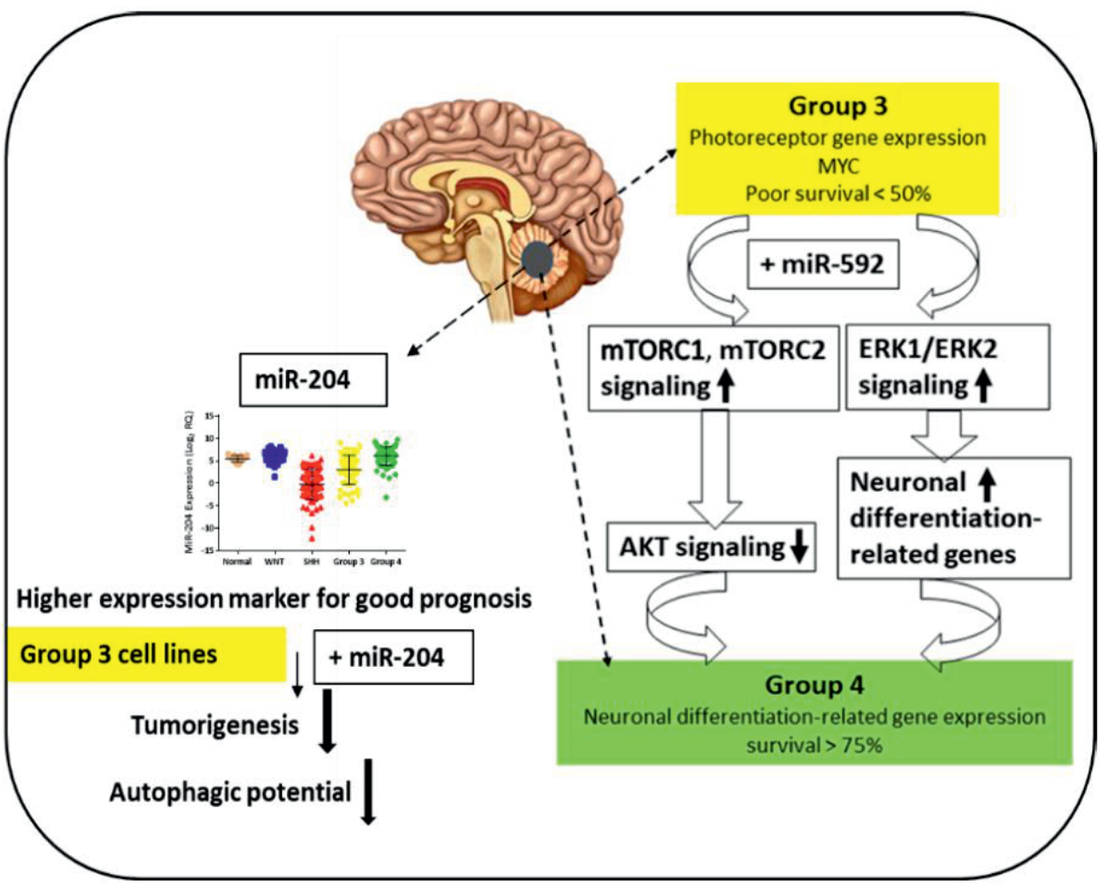

Role of miR-204 and mi592 in the disease pathogenesis of medulloblastoma

3.1.11 Fine specificity of domain-motif interaction and the role of structure: a case study with proteasomal chaperones

Just like all living being communicate, proteins inside our body communicate with other proteins, DNA etc (molecules). This is essential for a cell alive to remain alive, function well and repair any damage that occurs and make sure no foreign body such as a virus gets inside. Similar to the differences in the language, signal or style that is different to different species or communities, molecules communicate in a coded language. Because proteins undergo modifications or change during diseases, some of these specific codes will change either in the context or will be used more often to help the cancer cell multiply, resist treatment and spread from one place to another. Using tools and techniques in the field of biochemistry, biophysics and structural biology, one such important code involved in the survival pathways of cancer cells was identified. Having deciphered the purpose of the code, an alternate code to manipulate the message was also created. Identification of chemicals that act along this communication channel and kill the cancer cells that survive chemo or radiation treatment could be a futuristic plan.

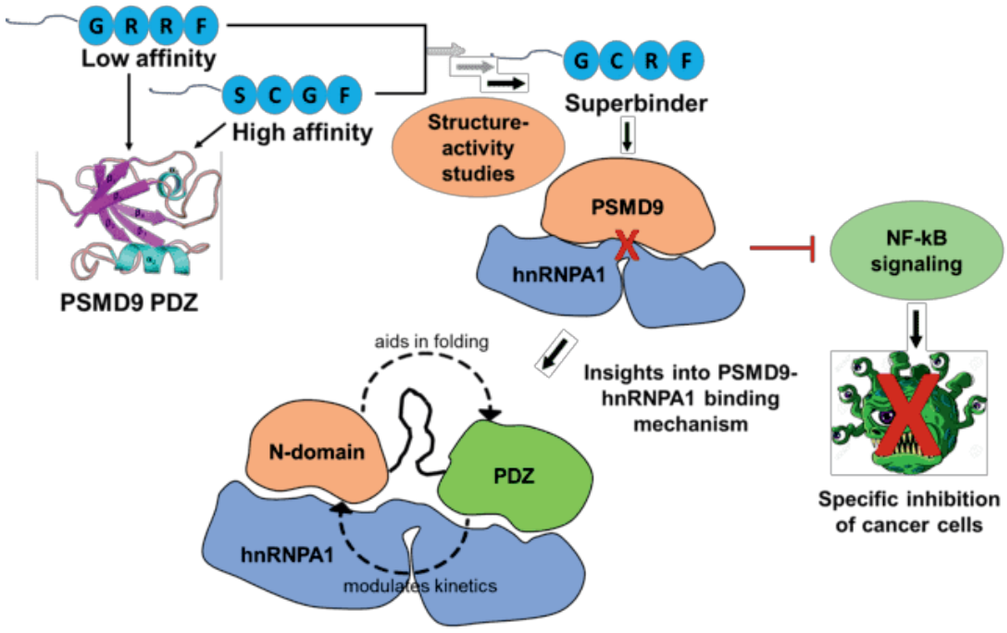

Identification of superbinder peptide and differential role of domains of PSMD9 in binding to growth hormone and hnRNPA1

3.1.12 Proteomic profiling of leukemic cells in Philadelphia chromosome positive leukemia

Chronic myeloid leukemia is blood cancer caused by an erroneously formed fusion gene BCR-ABL1. It encodes an enzyme which is constitutively active and its inhibition by imatinib successfully controls the disease in the initial chronic phase. However, imatinib is ineffective in 80% patients in the terminal blast crisis and in 40% among them despite inhibition of the Bcr-Abl activity by imatinib. This indicates the need for a therapeutic target besides Bcr-Abl1. Towards this, a large-scale study of proteins was

undertaken and it was found that the inhibition of p38-MAPK activity can overcome imatinib resistance in blast crisis, thereby providing a novel therapeutic strategy.

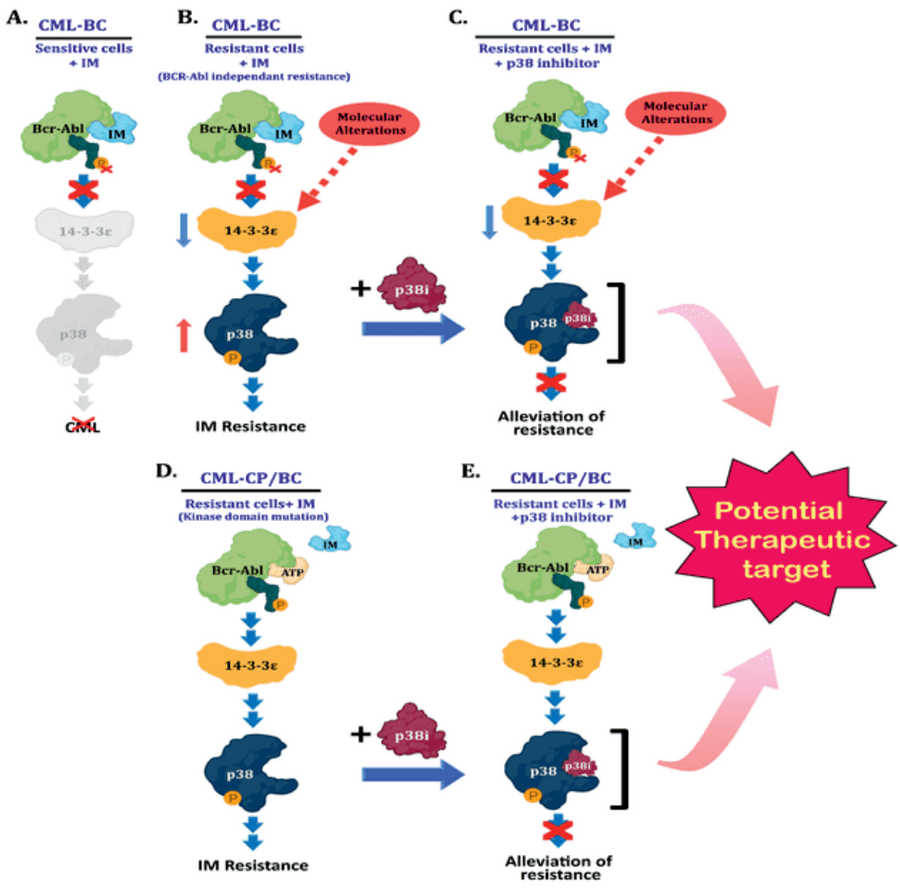

Modulation of downstream components of Bcr-Abl pathway i.e., downregulation of 14-3-3ε and increased phosphorylation of p38-MAPK, in a Bcr-Abl independent manner, contributes to development of IM-resistant phenotype. (B) Inhibition of Ser/Thr kinase activity of p38 sensitizes the cells to IM, thereby signifying its potential as therapeutic target to overcome to IM-resistance

3.1.13 Defining the molecular signaling mechanism in epidermal stem cell regulation and cancer

Adult stem cells (SCs) reside in every tissue, which play an important role in maintaining the tissue either through normal homeostatis (wear & tear process) or repair during injury throughout the life. For instance, in skin, multi-potent hair follicle stem cells (HFSCs) reside that are involved in normal process of hair regeneration and wound repair upon injury in skin. The process and maintenance of stem cells is controlled by several molecular mechanisms and one of them is developmental signalling such as Wnt signalling. However, perturbations in the signalling pathways within epidermal SCs have been reported in the development of basal and squamous cell carcinomas (BCC and SCC). Secreted frizzled related protein 1 (*Sfrp1*) regulates the Wnt pathway, which is upregulated in the HFSCs; however, its role in the epidermal SC regulation, tumor initiation and cancer stem cells regulation is unknown.

In this study, the Sfrp1 knockout mice was used and it was shown that Sfrp1 loss resulted in decreased HFSC population, faster hair cycle and delayed wound repair. Remarkably, the decreased HFSCs population was restored by the age of PD49 (postnatal day 49) in Sfrp1 knockoutmice as compared to WT. Thus, loss of Sfrp1 showed down-regulation of Wnt β-Catenin signaling activity mediated through BMP/AKT/GSK3β-mediatedsignaling present within HFSCs population.

Further, the research work showed that loss of Sfrp1 resulted in increased tumor initiation in murine skin induced cell carcinoma (SCC). Secondly, the cancer stem cells population that reside or present in the tumor, which are responsible for tumor recurrence after the cancer treatment showed enhanced aggressiveness of the tumorigenecity in skin squamous cell carcinoma (SCC) thereby suggesting that SCC becomes aggressive with the loss of Sfrp1. Further, loss of Sfrp1 showed higher expressionof genes involved in proliferation, tumor aggression, Epithelial-to-mesenchymal transition, and stemness. The major findings of the study were that when there is a loss of Sfrp1, it results in increased gene expression of Sox2 in mice skin squamous cell carcinoma (SCC). Further, the data obtained from mice SCC was validated in the multiple human epithelial cancers such as skin cutaneous SCC, Head & neck and breast cancers, which showed low gene expression of Sfrp1 that was observed in mice SCC. Most importantly, low level of Sfrp1 protein level co-related with overall poor survival of patients in head& neck, breast and skin melanoma, which may have clinical significance in future.

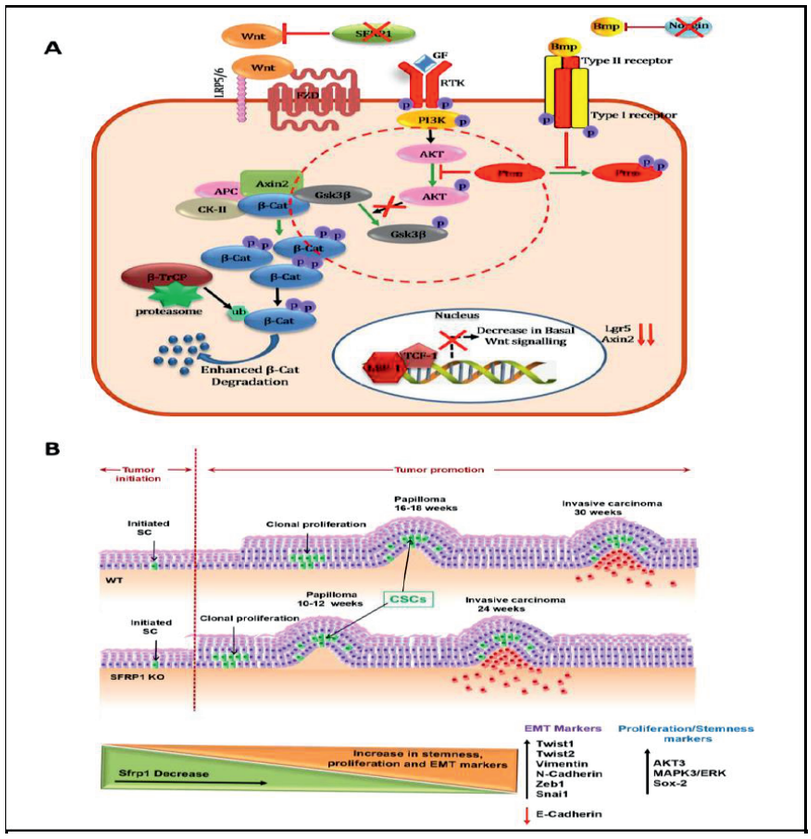

BMP/AKT/GSK3β signalling inhibits aberrant activation of Wnt signalling in HFSCs in the absence of Sfrp1 (A); Diagrammatic representation of accelerated skin tumor initiation and CSC regulation due to loss of Sfrp1

3.1.14 Elucidating the role of Clusterin in human oral cancers

In an attempt to understand the molecular changes driving the oral tumorigenesis, the study undertaken demonstrated the decreased levels of Clusterin in oral tumor samples compared to their adjacent normal tissues. Oral cancer patients with decreased levels of Clusterin showed poor overall survival and its downregulation in oral cancer cell lines showed increased cell proliferation and ribosome biosynthesis suggesting its tumor suppressor like role in oral cancers. The study for the first time demonstrated the presence of Clusterin in the nucleolus of oral cancer cells and its role in nuclear shape maintenance. Computational analysis ofclusterin structure predicted the binding of it with other nucleolar proteins thereby suggesting its chaperone like role in their stabilization.

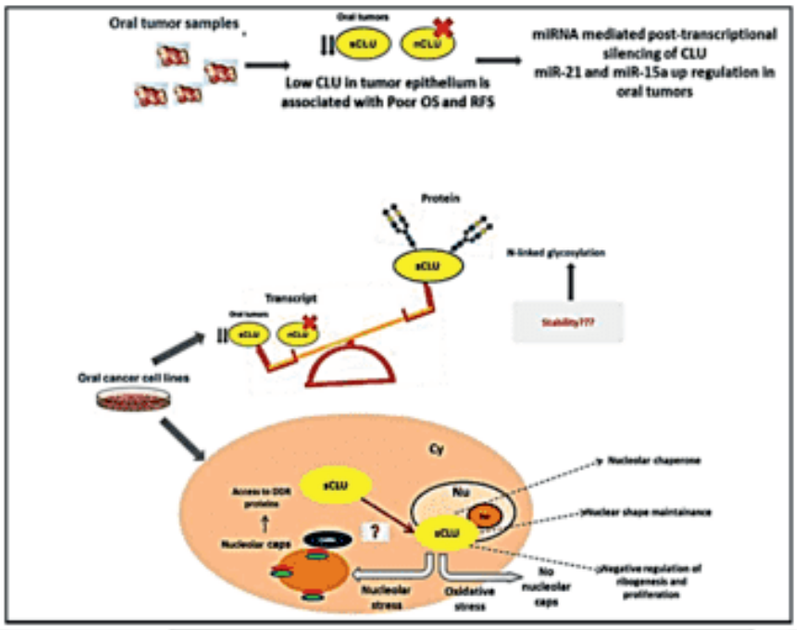

Role of CLU in humal oral cancers

3.1.15 Genome-wide approaches to characterize novel genetic elements causing cancer

The thesis presents an integrated genomic characterization of cervical cancer to discover clinically relevant actionable gene targets. Recurrent genomic alterations were observed in *PIK3CA*, *ERBB2*, *FGFR2*, and *ARID1A* with an overexpression of the components of the MMPs, AKT, and ERBB pathway. The functional characterization revealed a complex role of ERBB signaling in cervical cancers. A genetic perturbation experiment by performing shRNA-mediated knockdown of *ERBB1* or *2* revealed a non-essential role of these kinases in C33A cervical cancer cells, known to overexpress *ERBB2*. However, as a surprise finding, the C33A cells were found to be sensitive to the ERBB pharmacological inhibitor *in-vitro* and *in-vivo* mouse xenograft assays, suggesting a cooperative role of the ERBB family members through hetero-dimerization. These findings have potential therapeutic implications in the treatment and management of the disease. In a complementary functional genomics approach, a pooled kinomeRNAi screen, targeting all human kinases, was performed in AW13516 cancer cell lines. The output data of the RNAi screen was integrated with gene

expression and copy number data using a computational tool, DepRanker developed in the lab. *AURKB* and *TK1* were predicted as essential genes in promoting proliferation and survival in the AW13516 cells.

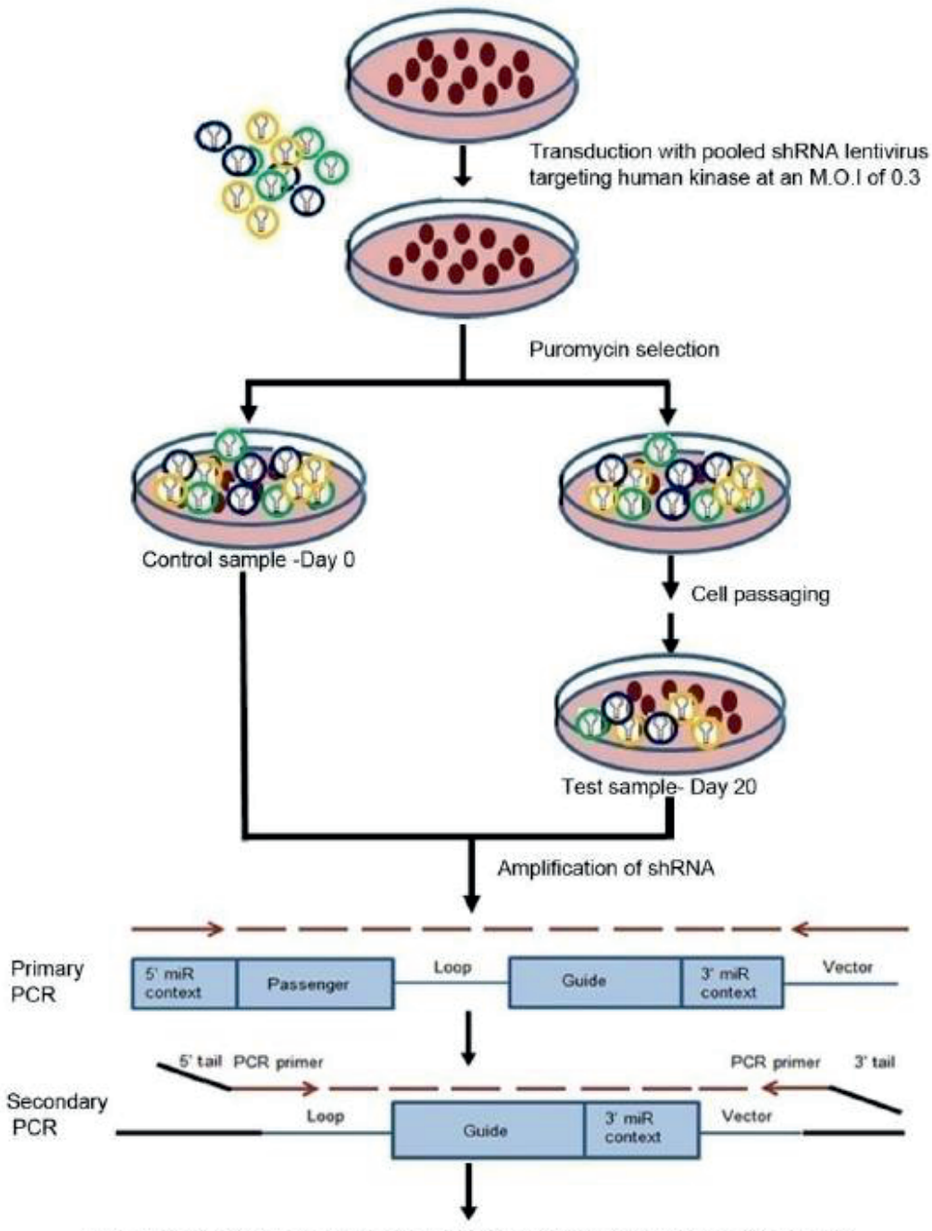

Schematic representation of pooled shRNA screen in AW13516 cells

3.2 Bhabha Atomic research Centre, Mumbai

3.2.1 Functional analysis of three genes downregulated in a non-conidiating mutant of *Trichoderma virens*

Towards understanding the conidiation process in the fungus, *Trichodermavirens*, three genes were identified usingSSH (suppression subtractive hybridization) library where a non-conidiating mutant strain was subtracted from the conidiating wild type strain. These three proteins are orthologs of translationally controlled tumour protein (Tcp1), Proline-, glycine-, tyrosine-rich protein (Pgy1) and Ecm33. Through the generation of independent knockout mutants (*Δtcp1, Δpgy1* and *Δecm33*), their role in conidiation, mycoparasitism, antibiosis, secondary metabolite biosynthesis, cell wall integrity, hydrophobicity and stress responses were studied. All these independent mutants showed slower radial growth rate on PDA compared to wild type (WT) and Δ*tcp1* mutants also showed significant decrease in dry weight compared to WT. Stress tolerance response analysis of WT and mutants confirmed that, Δ*tcp1* mutant had sensitivity to salt while highest sensitivity to SDS and Congo red was noticed in Δ*ecm33* mutant. Study of Δ*ecm33* mutant also confirmed the role of *ecm33* gene in cell wall integrity and hydrophobicity. Confrontation assay confirmed the roles of *pgy1* and *ecm33* genes in the mycoparasitic activity against the plant pathogens *Rhizoctoniasolani*, *Sclerotiumrolfsii* and *P. aphanidermatum* while *Δtcp1* mutants retained the mycoparasitic activity against *P. aphanidermatum*. The *pgy1* and *ecm33* genes are also involved in viridin biosynthesis while all the three genes are involved in volatile compounds biosynthesis.

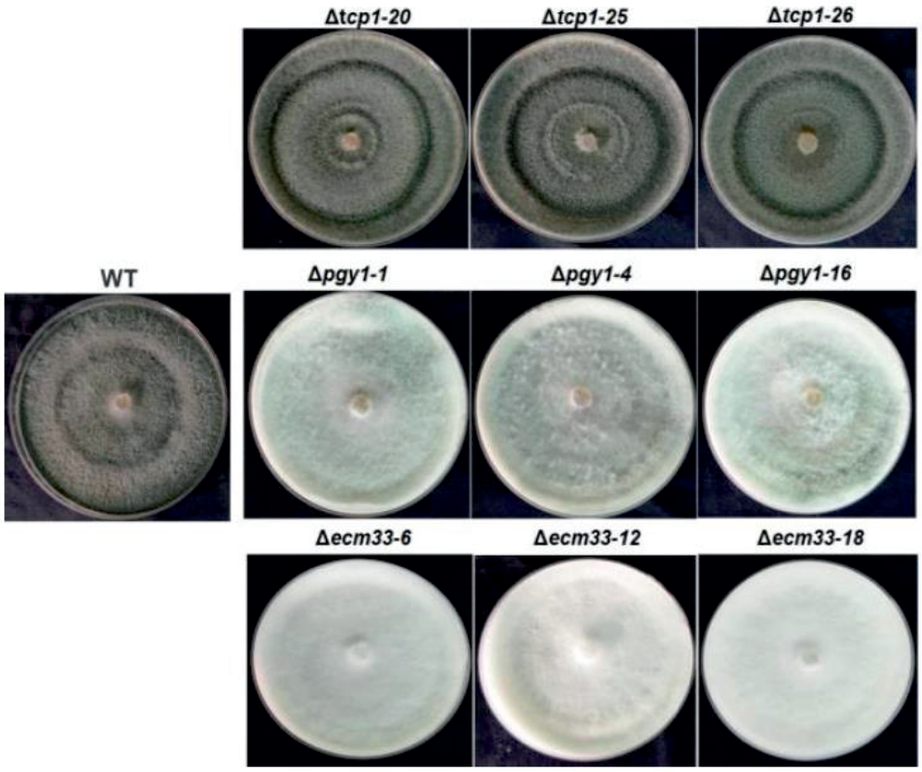

Morphology of WT, Δtcp1, Δpgy1 and Δecm33 mutants on PDA after 7 days of incubation.

3.2.2 Investigation of molecular mechanisms of underlying antibacterial potential of Allylarene and stilbene class of phytochemicals

The emergence of antibiotic resistant bacteria at an alarming rate is of great concern to human well being. In view of the alarming rate at which our existing treatments become unviable, it is imperative to find newer molecules and strategies to combat bacterial infections. With this objective, two classes of phytochemicals allylarenes and stilbenes were evaluated. Hydroxychavicol was identified from a number of allylarenes to be the best antibacterial molecule and its molecular basis, kinetics of target damage was elucidated. This information is helpful in identifying a strategy to sensitize gram negative bacteria to large molecular weight antibiotics.

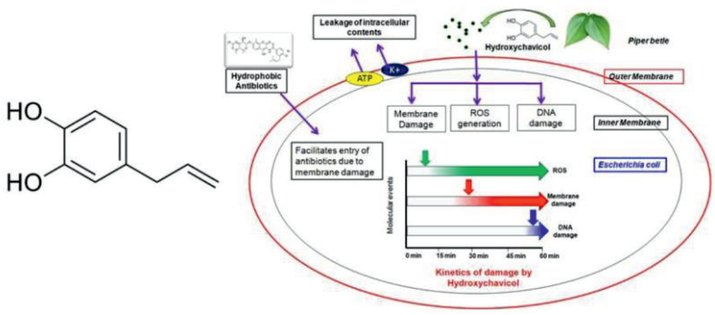

Graphical representation of HC antibacterial mechanism in E. coli.

Structure- function relationship study in stilbenes revealed, not only the antibacterial activity of stilbenes varied with different substitutions, the predominant mechanism of action also changes. The best stilbene, Dimer stilbene (DS) identified in the study exhibited positive co-operativity with kanamycin and eradicated *S. aureus*infection in a mouse model.

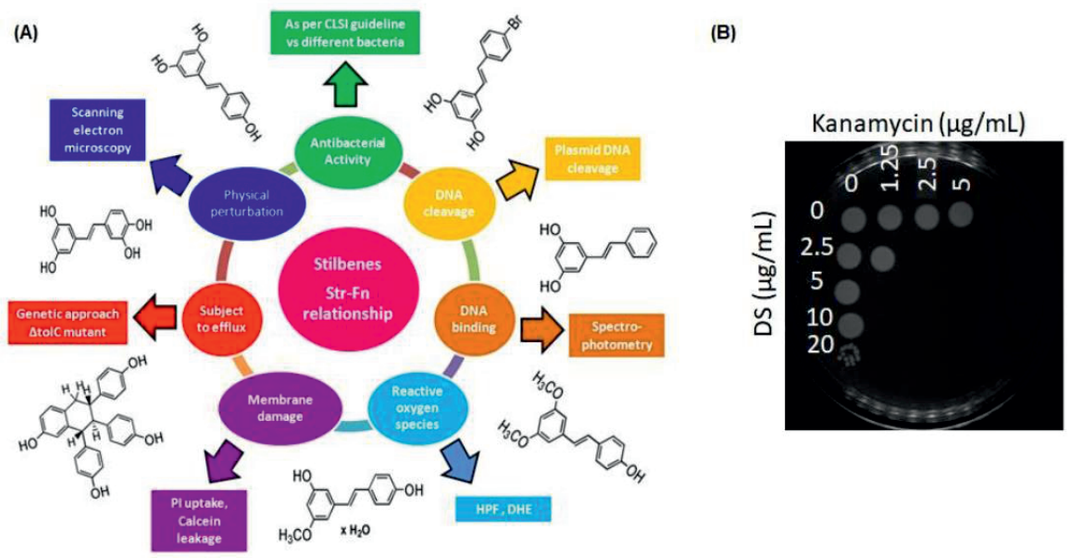

(A) Structure antibacterial activity relationship in stilbenes. (B) DS exhibits co-operativity with kanamycin

3.2.3 Physiological and structural characterization of a manganese catalase (KatB) from the filamentous, heterocystous, N_2-fixing Cyanobacterium *Anabaena* PCC 7120

The *katB* gene of *Anabaena* PCC7120, which encodes a Mn-catalase KatB, is not only induced by osmotic stress, but also plays a major role in cellular adaptation to salinity and oxidative stress. Promoter analysis revealed that the gene is expressed only in the vegetative cells and not in heterocysts, which is the seat of nitrogen-fixation. Biochemical analysis of the KatB protein revealed that it is a thermostable, robust Mn-catalase that functions in alkaline pH and in high ionic strength. Its crystal structure showed the protein to be a compact hexamer with four-helix bundle type architecture and active site that is distinctly different from other Mn-catalases. The N-terminal region of KatBwas found to be involved in oligomerization and in particular, the second residue (a non-active site residue) is essential for inter-subunit interactions and for the formation of the proper hydrophobic pocket that held the active site together. Due to its effective catalase activity, it can be used for commercial purpose and to this effect the protein was overexpressed and isolated from *Anabaena*, as the activity of KatB protein isolated from *Anabaena* was higher than that isolated from *E. coli*.

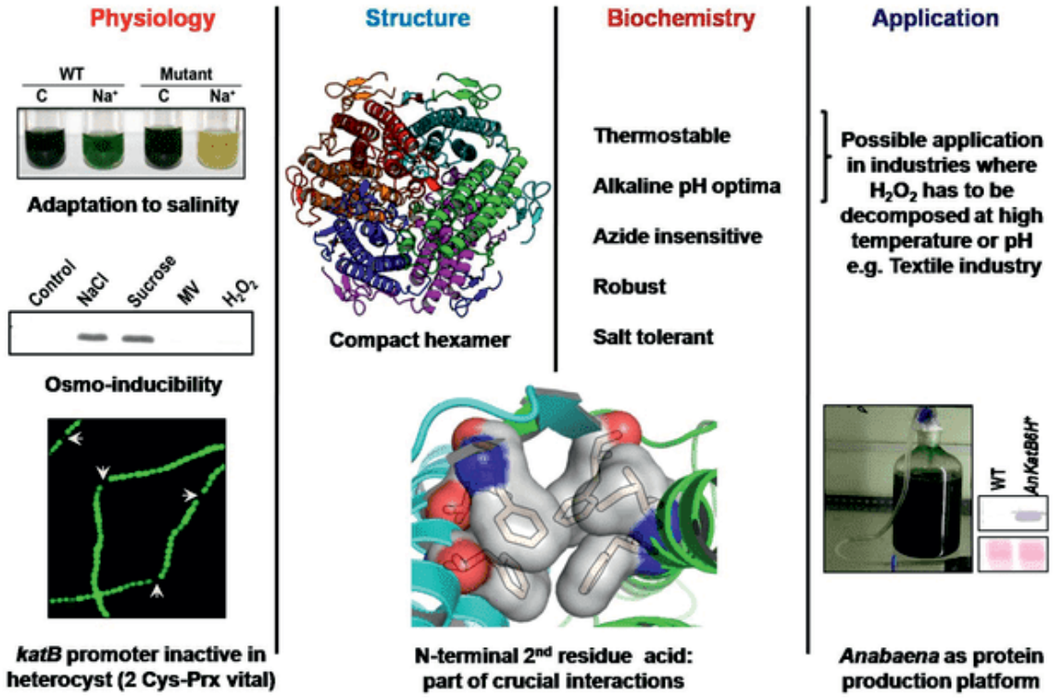

An overview on AnabaenaKatB: Physiologicaland biochemical implications

3.2.4 Biological evaluation and mechanistic insights of targeted nano-formulation for combinatorial cancer therapy

The growing burden of Cancer in India as well as worldwide, warrants development of improved cancer treatment strategies. Although, nanotechnology has been increasingly contributing towards cancer theranostic applications, most of the clinical or pre-clinical nano-formulations are passively targeted to tumor and lack deeper mechanistic insights. The thesis discusses the synthesis and rationale design of two types of nano-formulations, viz., MN-OA and T-LMD and their characterization

by different bio-physical techniques. The mechanism of enhanced tumor cell killing by MN-OA in combination with magnetic hyperthermia therapy and gamma radiation has been elucidated. Modulation of intracellular HSP90 by MN-OA and down-regulation of its client proteins was identified as one of the major mechanisms of thermal and radio-sensitization by MN-OA. For tumor targeted delivery of MN-OA and doxorubicin, T-LMD was synthesized and its tumor targeting efficacy was demonstrated in cancer cells and fibrosarcomatumor model. T-LMD showed enhanced uptake in human glioblastoma cells by cRGD induced receptor mediated endocytosis. Moreover, in fibrosarcomatumor model as well, T-LMD showed ~ 7-fold higher accumulation at tumor site as compared to the non-targeted formulation. Additionally, T-LMD showed significantly higher anti-cancer efficacy than commercial formulation of doxorubicin, LippodTM. Furthermore, T-LMD showed significant combinatorial chemo-, radio- and magnetic hyperthermia therapy efficacy in murine fibrosarcomatumor model. Toxicity analysis by determination of whole blood, serum and histopathological parameters suggested in-significant toxicity of T-LMD in healthy as well as fibrosarcomatumor bearing BALB/c mice as compared to control. Furthermore, T-LMD showed in-significant cardio-toxicity as confirmed by serum levels of CK-MB (early cardiac damage marker) and haematoxylin and eosin staining of heart tissue section. The results demonstrate the potential of T-LMD for further clinical translation as a tumor targeted nano-formulation for combinatorial cancer therapy applications.

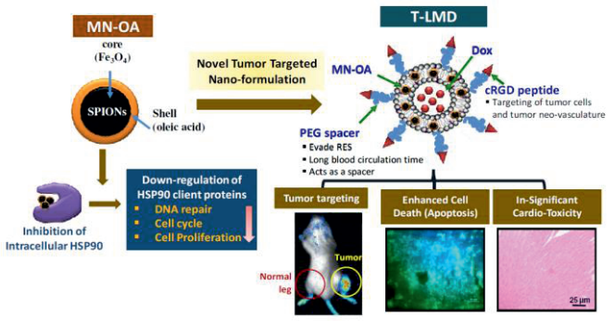

Design and Biological attributes of two types of nanoparticles: MN-OA and T-LMD

3.2.5 Cellular and molecular basis of thorium-induced cytotoxicity and carcinogenesis

Thorium utilization in nuclear industry has increased drastically which in turn enhanced the risk of its exposure to occupational workers/public. Thus, understanding the mechanism of thorium toxicity and carcinogenesis in humans using both *in-vitro* and *in-vivo* model is essential. A simple inexpensive colorimetric method for thorium estimation in biological samples was first standardised. Studies under in vitro model showed that thorium is mainly intracellularized using Ca^{2+}ion channels present on plasma membrane and is deposited mainly on cytoskeletal proteins. Thorium bio-distribution studies on mice showed liver, spleen and skeleton to be the major target organs of thorium deposition where thorium deposits mainly around blood vessels. Histopathological evaluation indicated hepatocyte hypertrophy in liver, megacytokaryosis in spleen and deposition of an amorphous proteinaceous material in liver and spleen. Papillary adenoma was also observed in lungs. Evaluation of serum biochemical changes suggested an increase in glucose, ALT and ALP concentration. Elevated levels of inflammatory and proliferative cytokine and chemokine were also observed. Long term thorium exposure under both in vitro and in vivo conditions causes alterations in the expressions of various

genes involved in various pathways of cell survival (TGF-β, MAPK, PI3k, RAS and cell cycle/apoptosis), cell fate (transcriptional regulation) and genomic maintenance (DNA damage control). However, further experiments need to be performed to establish these pathways as key pathways involved in thorium induced hepatocarcenogenesis.

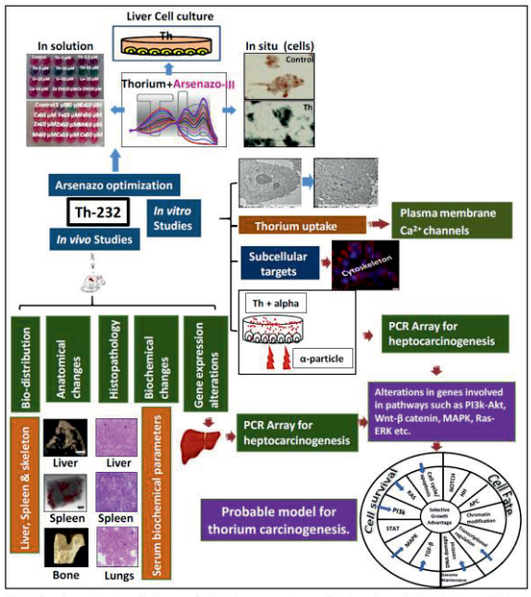

Fig: Thorium Cytotoxicity and Carcinogenesis under in-vitro & in-vivo conditions

Thorium Cytotoxicity and Carcinogenesis under in-vitro & in vivo conditions

3.2.6 Biochemical changes as tools for rapid monitoring of microbial spoilage in minimally processed fruits

Fresh cut fruits have acquired their permanent places on shelves in food industry. Microbial quality is the deterministic factor of the overall quality of such produce having short shelf life. Conventional plate count technique takes 48-72h to determine microbial quality. Thus, rapid methods for microbial quality assessment of minimally processed fruits (jackfruit, pomegranate and pineapple) were exploited using two approaches. In the first approach, instrumental techniques such as HS-SPME-GCMS and FTIR that allow rapid, reagent less and non-destructive means to analyse the microbial status of stored minimally processed fruit samples were explored. Both GCMS and FTIR aided in monitoring the metabolic profile during storage of fruit samples. It was observed that during storage, alcohols such as ethanol, 3-methyl-1-butanol, 2-methyl-butanol and esters such as methyl acetate, ethyl acetate, 2-methyl-1-butanol acetate, 3-methyl-1-butanol acetate and other ethyl ester derivatives showed correlations with microbial spoilage. Microbial activity also leads to production of organic acids from sugars. Chemometric tools such as Partial Least square regression and artificial neural networks were successfully employed to generate prediction models for microbial quality estimation using FTIR and GCMS data. In the second approach, cheap phenol based Time Temperature Indicator (TTI) was developed for application on minimally processed fruit packages. Colour development of selected TTIs for the fruit packages demonstrated good correlations with microbial growth in wide temperature range of 10-37 °C. In addition, microbial status of samples stored under temperature abusive conditions was successfully evaluated using TTIs by observing colour change

employing DSLR camera. In summary, both the approaches aided in rapid microbial quality assessment in minimally processed fruit samples.

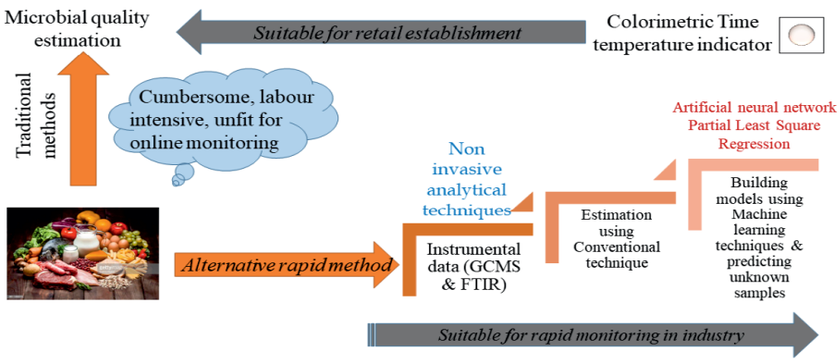

Schematic of the work carried out in thesis

3.3 Institute of Mathematical Sciences, Chennai

3.3.1 Allosteric effects in protein dynamics and their interactions with membranes

Ras superfamily of small GTPase proteins is a major player in many cellular functions like cell proliferation, cytoskeletal morphology, and cellular adhesion, etc. The effects of phosphorylation of a serine residue on the structural and dynamic properties of Ras-like protein, Rap, and its interactions with effector protein Ras binding domain (RBD) of Raf kinase, in the presence of GTP, are investigated via molecular dynamics simulations. The simulations show that phosphorylation significantly affects the dynamics of functional loops of Rap which participate in the stability of the complex with effector proteins. The effects of phosphorylation on Rap are significant and detailed conformational analysis suggests that the Rap protein, when phosphorylated and with GTP ligand, samples different conformational space as compared to non-phosphorylated protein. In addition, phosphorylation of SER11 opens up a new cavity in the Rap protein which can be further explored for possible drug interactions. Residue network analysis shows that the phosphorylation of Rap results in a community spanning both Rap and RBD and strongly suggests transmission of allosteric effects of local alterations in Rap to distal regions of RBD, potentially affecting the downstream signalling. In the figure below, the long range interaction at Raf L4 loop as a result of SER11 phosphorylationis illustrated.

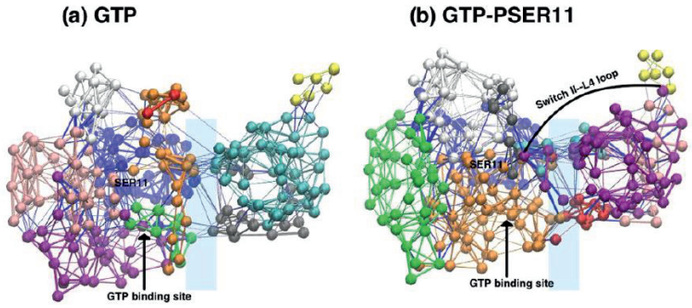

The communities detected in (a) GTP- (wild type) and (b) GTP-PSER11 (phosphorylated) cases. The yellow community represents the L4 loop.

Binding free energy calculations suggest that phosphorylation of SER11 residue increases the binding between Rap and Raf corroborating the network analysis results. The increased binding of the Rap-Raf complex can have cascading effects along the signalling pathways where availability of Raf can influence the oncogenic effects of Ras proteins. These simulations underscore the importance of post-translational modifications like phosphorylation on the functional dynamics in proteins and can be an alternative to drug-targeting, especially in notoriously undruggable oncoproteins belonging to Ras-like GTPase family.

3.4 National Institute of Scientific Education and Research, Bhubaneswar

3.4.1 The role and signaling mechanism of IQGAP2 in breast cancer tumorigenesis and angiogenesis

The thesis deciphers the role of IQGAP2 in breast cancer and its molecular mechanism. The study revealed that depletion of IQGAP2 in breast cancer cell decreases ROS and phospho-p38 level, thereby impairing p53 mediated cellular apoptosis. It was observed that the reduced IQGAP2 expression induced an increase in phospho-MEK and phospho-ERK levels. This, in turn resulted in increased expression of EMT markers such as N-cadherin, Snail, Twist and EMT promoting cytokines such as IL-6, CCL2, whereas E-cadherin, a MET marker showed a reduced expression. The possible underlying mechanism behind ERK activation might be either due to loss of direct inhibitory effect of IQGAP2 or due to increase in IQGAP1 to IQGAP2 ratio. Furthermore, the depletion of IQGAP2 in breast cancer cells increased VEGF-A secretion, which promotes angiogenesis by activating VEGFR2 receptor and phospho-AKT473 level in nearby endothelial cells. Using Pan-cancer datamining approach, it is revealed that low IQGAP2 and higher IQGAP3 expression associate with poor prognosis of patient in most cancer types. The findings suggest that IQGAP2 plays a major role in suppressing breast cancer via regulating cellular apoptosis, EMT and angiogenesis. Hence, this study highlights IQGAP2 as a potential therapeutic target for breast cancer treatment.

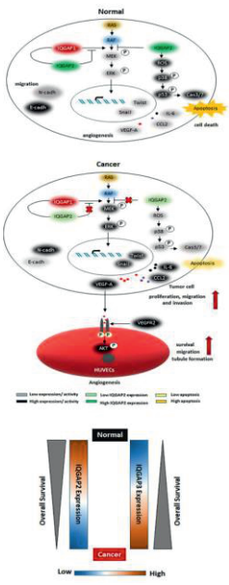

IQGAP2 depletion leads to breast cancer progression and tumor angiogenesis, differential expression of IQGAP2 and IQGAP3 associates with poor survival of cancer patients

3.4.2 Crosstalk between cytoskeleton and membrane components with thermosensitive ion channels in the context of diverse physiological functions

Transient Receptor Potential (TRP) family of non-selective cation channels are a group of ion channels that are involved in a large number of physiological processes and are polymodal in nature.
The study is primarily focused on the cross-talk between membrane cholesterol and sub-membranous microtubules with two thermosensitive TRP ion channels, namely TRPV1 and TRPA1 and possible impact of such crosstalk in the ion channel functions and also on the cells.

This work establishes that the interaction of TRPV1 with soluble tubulin and/or polymerized microtubules play an important role in the channels' open probability in response to activation stimuli, whereas subtle changes in interactions with tubulin dimers and/or polymerized microtubules or microtubule dynamics have impact on the channel properties, leading to make the channels insensitive to certain stimuli. Apart from sub-membranous cytoskeletal elements, interaction of TRPV1 with membranous cholesterol has evolutionary relationship in vertebrates and such interactions may play crucial role to prevent spontaneous opening of the channel, which may have severe impact on cell physiology. Though TRPA1 represents a highly diverged protein, it is endogenously present in sperm cells in all vertebrate phyla. TRPA1 activation does not significantly affect capacitation and acrosomal reaction, but it induces hyperactivated motility of sperm cells in mammals. TRPA1 co-localize with tyrosinated tubulin at the neck and tail regions of bovine sperm cells which indicates a possible role of TRPA1-tubulin/microtubule interaction in inducing hyperactive motility of sperm cells. *In silico* results suggest that TRPA1 may form H-bonds with cholesterol and localize to lipid rafts. The residues mediating such interaction were observed to be at Asn855 and Arg852. The mutation in these residues is known to form a constitutively open channel leading to a pathological situlation. Over all, the study elucidates the roles of membrane cholesterol and cytoskeleton on the regulatory function of two thermosenrtive ion channels, namely for TRPV1 and TRPA1.

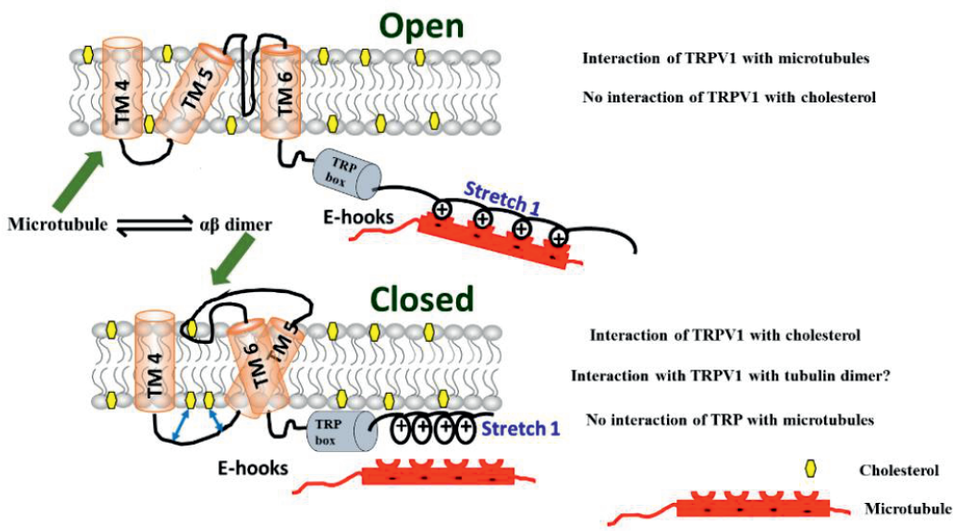

A tentative model demonstrating how TRP channel gating can be influenced by membrane cholesterol and submembranous cytoskeleton.

3.5 Saha Institue of Nuclear Physics, Kolkata

3.5.1 Understanding the roles played by receptor tyrosine kinases and non-coding RNAs in neurogeneration

Altered expressions of protein-coding genes and microRNAs have been implicated in the pathogenesis of Alzheimer's disease (AD) by the causative agents Aβ and AICD. The involvement of RTKs and other long non-coding RNAs (lncRNA) is being realized recently.

Using small RNA sequencing from an AD cell model, we observed perturbations in the levels of several miRNAs and lncRNAs. An Aβ treated cell model showed deregulation of two key RTKs- EPAH2 and ROR1. Effect of Aβ and AICD, individually and in combination, were validated with top regulated miRNA hits. Several of these miRNAs were found to target these RTKs. An additional layer of complexity revealed that two strongly deregulated lncRNAs MALAT1 and NEAT1 governed the aforesaid miRNA-RTK network. This network is functionally relevant in AD research as the miRNA-MALAT1-EPHA2 axis governs memory formation and/or impairment via the CREB pathway while the miRNA- NEAT1-ROR1 axis governs cytoskeletal degradation and rearrangement. Using a similar high throughput sequencing approach, we could identify two key lncRNAs – MEG3 and NEAT1 which regulated Tp53 expression and the phenotypic changes observed in cell and animal models of Huntington's disease (HD). Understanding the total cellular non-coding transcriptome (the network of miRNA-lncRNA-RTK- Transcription Factor in the context of neurodegenerative diseases (NDDs) is likely to open up new putative targets for the disease intervention.

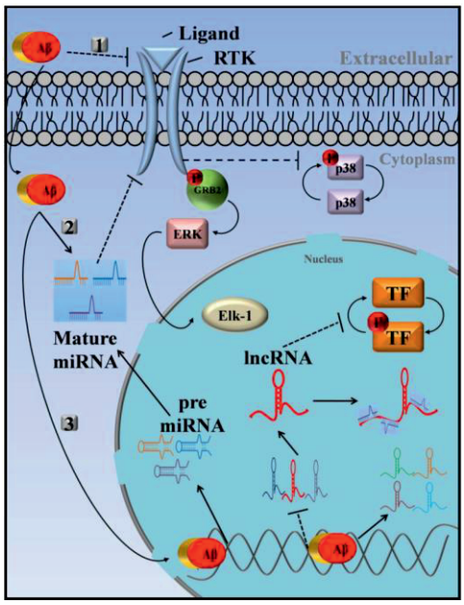

Schematic representation of molecular events in cell models of AD. Extracellular treatment of Aβ1-42 has multiple effects on cells. Extracellular Aβ1-42 seems to inhibit the basal levels of RTKs and their downstream effectors, notably CREB. Cytosolic Aβ1-42 affects the mature miRNA pool, which targets and inhibits the RTKs. Nuclear translocated Aβ1-42 differentially activates miRNAs and a subset of lncRNAs, but represses another subset of lncRNAs. Out of the repressed lncRNAs, several sponge the miRNAs and affect the TFs.

3.5.2 Non-canonical base pairs in RNA and their involvement in double helix formation.

Though RNA has almost similar structural elements as DNA, it can regulate huge number of diverse cellular processes. Apart from the regular helical regions with Watson-Crick base pairs there exists a variety of structural motifs like, pseudo helices, hairpin structural elements with variable loop region, internal loops, multi-way junctions, bulges and many more. While proteins use twenty amino acids of various properties to perform different tasks through molecular recognition, RNA possesses only four nucleotide bases. These four bases can pair in various different ways, which are commonly referred to as non-canonical base pairs, to offer various steric and electrostatics shapes for molecular recognition. The thesis presents a combined network of web-servers and database (http://hdrnas.saha.ac.in//) for RNA structural perspective. The study has also attempted to understand stability of these unusual contacts using Density Functional Theory based studies. (http://hdrnas.saha.ac.in/rnabpdb) The study indicated sufficient strengths of interactions in the non-canonical base pairs and their stacks. It was found that G: A S:HT base pair is one of the most frequent non-canonical base pair. A quantum chemical hybrid DFT-D based stacking energy analysis has been developed which enables one to find the most probable configuration of the dinucleotide step containing a non-canonical base pair (G: A S: HT: C: G W:WC). Using the above-described work as a benchmark study, the study tried to decode the promiscuous nature A: A w: wC base pair where one of the hydrogen bonds is weak C-H…N mediated. Molecular dynamics simulation coupled with quantum chemical calculation and bioinformatics study ultimately dig out the hidden truth behind the promiscuous nature A: A w: wC base pair when it is stacked on sheared G: U W: WC base pair. The research work has been extended on non-canonical base pair to find the most probable configuration SL1 helix of RNA of corona virus. In the SL1 motif, either A:C +: WC or U:C W: +C base pairs are possible. Th hybrid stacking energy analysis along with transition state calculation, hassupported on protonation of Adenine residue in A:C +: WC base pair.

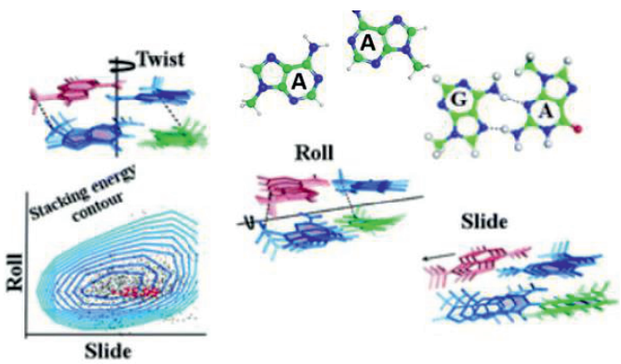

Stacking Energy scan of dinucleotide step with one non-canonical base pair in roll-slide hyperspace for different twist angle

3.5.3 Role of Epstein - Barr virus in epithelial cell cancer

Epstein Barr Virus (EBV) is a ubiquitous γ-herpesvirus, known to establish persistent life-long infection in humans. EBV infection has been classified as a Group I carcinogen (IARC monograph, 1997), indicating its carcinogenicity in blood cell and epithelial cell cancer. In most of the EBV-associated epithelial malignancies, the virus has developed number of strategies to evade host immune response in order to establish latent infection. During latency, EBV expresses viral latent

gene, Latent Membrane Protein 2A (LMP2A) along with few other genes. LMP2A plays crucial role in maintenance of latency during infection. As a result, it is reported to alter a number of cellular signaling pathways. In the thesis, the role of viral protein, LMP2A in regulation of host immune response is investigated. The previous studies report that LMP2A causes downregulation of HLA-ABC surface expression in EBV associated gastric carcinoma. Cytotoxic T Lymphocytes (CTLs) identify viral antigenic peptides displayed by Human Leukocyte Antigen (HLA) class I molecules (HLA-ABC) on the surface of the infected cell. However, the detailed mechanism that leads to this downregulation remains unclear.

Here, in the study it is shown that LMP2A exhibits hypermethylation of the HLA-ABC promoter region through increased expression of epigenetic regulators; DNMT-1, DNMT-3B, and UHRF-1 in epithelial cell cancer. Decreased HLA-ABC surface expression resulted in ablation of CTL response as the infected cells could no longer display the viral antigenic peptides to the cognate CTLs. Interestingly, according to the missing self' hypothesis, loss of HLAABC expression, should result in increased NKG2D ligands expression on the surface of infected cells to facilitate Natural Killer (NK) cell mediated cytotoxicity. Expression of NKG2D ligands (MIC-A/B) on the surface of infected cell plays important role in recognition of the infected cell by the NK cells. Interestingly, MIC-A/B surface expression in response to viral gene, LMP2A was observed to be downregulated in epithelial cell cancer. Expression of NKG2D ligands is transcriptionally regulated by several cellular stresses associated during viral infection. The stress signals that alert the host immune cells of the infection includes DNA damage response, oxidative stress, and Unfolded Protein Response (UPR). Further, UPR proteins were studied for their role in the regulation of MIC-A/B surface expression. The current study signifies the role of UPR protein, PDI in the downregulated expression of membrane-bound MIC-A/B in response to the viral gene, LMP2A. In summary, the regulation of HLA-ABC expression through epigenetic regulation resulted in ablation of CTL response along with UPR mediated regulation of MIC-A/B surface expression helps in regulating NK cell mediated cytotoxicity of the virus-infected cell.

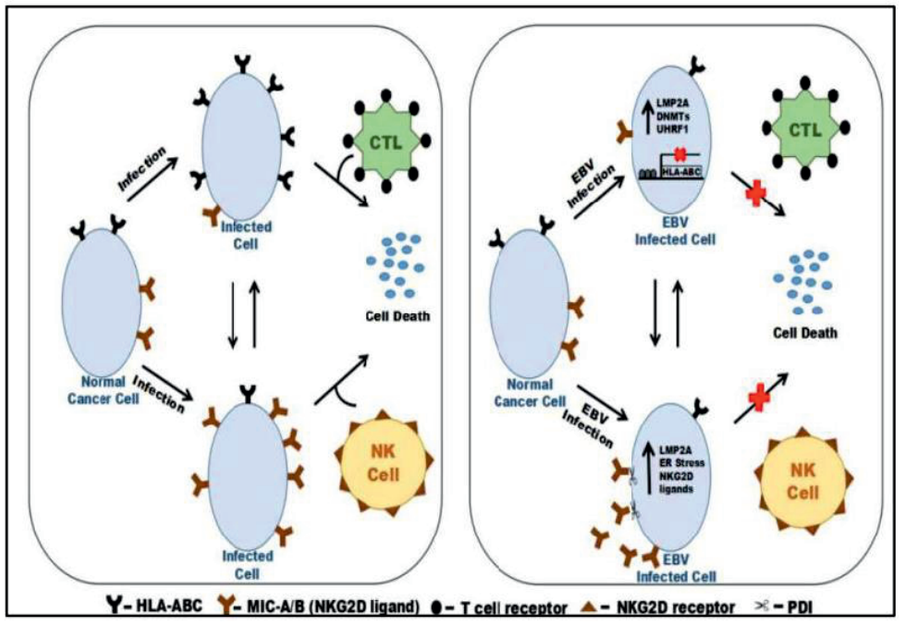

Schematic description of the current findings

4. Mathematical Sciences

During the period of report, HBNI has awarded 13 Ph.D. degrees in Mathematical Sciences. A few of the theses are summarized below.

4.1 Harish-Chandra Research Institute, Prayagraj

4.1.1 Problems in the theory of connections in algebraic geometry

The thesis is on the theory of connections in algebraic geometry and presents a *sufficient condition* for the existence of relative holomorphic connections in a holomorphic vector bundle over a family of connected compact complex manifolds. Relative Chern classes of a holomorphic vector bundle over a family of compact Kähler manifolds are shown to vanish if the bundle admits a relative holomorphic connection. The thesis shows the existence of a natural compactification of the moduli space of logarithmic connections, singular over a finite subset of a compact Riemann surface. Picard group of the moduli space of logarithmic connections with fixed determinant turns out to be isomorphic to the set of integers and does not admit any non-constant algebraic function, although it admits non-constant holomorphic functions. The algebraic functions are characterized on the moduli space of logarithmic connections with arbitrary residues over a compact Riemann surface.

4.1.2 Some topics on Dirichlet L-functions

Real-valued Hardy Z-function is defined to study the Riemann zeta function. Gonek and Ivic showed that the Lebesgue measure of the subset of the real line on which the Hardy Z-function is positive or negative, in the interval [T, $2T$] is at least cT, where c is a positive constant. The thesis shows analogous results, which hold for any real linear combination and some special type of complex linear combinations of Z-functions associated with Dirichlet L-functions for different characters. A. A. Karatsuba's lower bound for the number of odd order zeros of any real linear combination of Z-functions associated with Dirichlet L-functions for different characters is extended to any complex-linear combination of Z-functions associated with Dirichlet L-functions. The general formula for the quadratic twisted mean values of Dirichlet L-functions is an open question. The thesis establishes a connection between quadratic twisted mean values of Dirichlet L-functions at positive integers and Zagier's higher dimensional Dedekind sums. New formulae for higher dimensional Dedekind sums are used to derive explicit formulae of quadratic twisted mean values of Dirichlet L-function. Furthermore, some special cases of a question of Straub on values of trigonometric Dirichlet L-series were investigated.

4.1.3 On some problems in additive combinatorics and related areas

The thesis is about some problems on the regularity of Diophantine equation, weighted zero-sum constants attached to a finite abelian group, determination of zero-sum l-generalized Schur numbers and fractionally dense sets. The thesis provides a non-linear equation which is r-regular for every r and uses Szemeredi number to prove the result '*An equation L is said to be r-regular, if for every r-coloring*

of positive integers, there is a monochromatic solution to the equation L'. This result is important for the settlement of the famous *Rado's boundedness Conjecture*. The thesis then derived upper bounds and, in few cases, exact values of some weighted zero-sum constants attached to a finite abelian group for some particular weight sets. The thesis then focusses on computing exact values of zero-sum generalized Schur number and 2-color zero-sum *l*-generalized Schur number. Hobby and Silberger proved that the set of all prime numbers is fractionally dense in the set of all positive real numbers. The thesis gives more examples of sets which are fractionally dense. It is proved that, for any 2-partition of a non-zero ideal of an order of an imaginary quadratic field, there exists at least one part which is fractionally dense in the set of all complex numbers.

4.2 Institute of Mathematical Sciences, Chennai

4.2.1 The multismet partition algebra

The thesis introduces new diagram algebra, its representation theory and related combinatorics. An example of diagram algebra is the partition algebra based on set partitions. Partition algebra emerged from Potts model, used to understand the ferromagnets. An associative finite-dimensional "Multiset Partition Algebra (MPA)" is defined in terms of a basis indexed by certain multiset partition diagrams. MPA is **Cellular** and describes the parameters for which the algebra is **semisimple**. MPA acts on a specific tensor product of symmetric powers and commutes with a natural action of the Symmetric group algebra on the same tensor space. The thesis proves the **Schur-Weyl duality**, which relates the representation theory and combinatorics of one algebra with that of another. There are three closely related open problems in the representation theory of the symmetric group: Kronecker coefficients, Plethysm and Restriction problem. Dimensions of irreducible representations of the MPA are obtained by counting multiset tableaux. A generating function provided for multiset tableaux in terms of **the plethysm** of Schur function enables to understand the **restriction** problem.

Bijections in algebraic combinatorics are often manifestations of representation theory. Sometimes combinatorial identities can be used to prove results in representation theory. For instance, the classification of the irreducible representations of symmetric groups and Young's rule are deduced from the **Robinson–Schensted–Knuth** (RSK) correspondence. The thesis extends the **RSK** correspondence for multisets to offer a bijection between multiset partition diagrams and pairs of multiset tableaux, which correspond to Wedderburn decomposition of the MPA.

4.2.2 Pi-systems of symmetrizable Kac-Moody algebras.

The thesis presents the study on pi-systems of symmetrizable Kac-Moody (KM) algebras and regular sub-algebras of affine KM algebras. A pi-system is a finite subset of the real roots of a KM algebra with pairwise differences of elements of this subset that are not roots of the KM algebras. The notion of pi-systems was introduced for classification of regular semisimple sub-algebras of semisimple Lie algebras. The definitions of pi-systems and regular sub-algebras are generalized in the thesis and their fundamental properties are established. pi-systems, regular sub-algebras and closed sub-root systems of affine KM algebras are shown to be in one-to-one correspondence. The thesis classifies and

explicitly describes the maximal closed sub-root systems of affine KM algebras. The thesis describes a procedure to get classification of all regular sub-algebras of affine KM algebras in terms of their root systems.

The orbit of the Weyl group action on pi-systems of symmetrizable KM algebras is shown to be transitive for many pi-systems of interest in physics. The thesis explicitly describes the maximal closed subroot systems of affine root systems and addresses the Weyl group action on pi-systems. Finally, general principles formulated for constructing pi-systems and criteria for the non-existence of pi-systems of certain types to determine the set of maximal hyperbolic diagrams in ranks 3-10 relative to the partial order of admitting a pi-system.

4.2.3 Parameterized complexity of conflict-free solutions

The thesis introduces *conflict-free* variants of several classical problems in Graph Algorithms from the viewpoints of Classical and Parameterized Complexity. Feedback Vertex Set (FVS) problem is extended to hypergraphs. In the Vertex Deletion (VD) problem corresponding to Q (Q-VD), for a given graph G and a non-negative integer *k*, the goal is to delete a set S of at most k vertices such that the remaining graph G-S belongs to the family of graphs Q. In the conflict-free version of the VD problem (CF-Q-VD), a conflict graph H is given together with the graph G and an integer *k* to find a set S, which is a subset of vertices of the graph G of size at most *k*, such that S is a solution to (G,*k*) of Q-VD and S is an independent set in H.

For graph properties with finite forbidden characterization, CF-Q-VD is shown to be FPT (Fixed-Parameter Tractability) and admits a polynomial kernel. For graph properties without finite forbidden characterization, if Q is characterized by a “well-behaved” infinite family of forbidden induced subgraphs, then CF-Q-VD is W[1]-hard. In particular, the conflict-free version of FVS (CF-FVS) is W[1]-hard even when G is a disjoint union of cycles. A similar result holds for the conflict-free version of Odd Cycle Transversal (CF-OCT), Chordal Vertex Deletion (CF-CVD) and Interval Vertex Deletion (CF-IVD). *CF-VD with infinite forbidden characterizations is FPT for restricted conflict graphs*. A complete dichotomy is obtained on the Parametrized Complexity of the problem H-CF-FVS, where the conflict-free graph H belongs to graph class H (for hereditary H), in terms of the Independent Set problem. H-CF-FVS is shown to be in FPT if and only if H+Cluster Independent Set is in FPT. Conflict-free versions of Both Maximum Matching (CF-MM) and Shortest Path (CF-SP) problems are shown to be W[1]-hard, when parametrized by the solution size. A variant of CF-MM and CF-SP are studied, where instead of conflicting conditions being imposed by independent sets in a conflict graph, they are imposed by independent constraints in a matroid. Finally, FVSon hypergraphs are W[2]-hard, when parametrized by the solution size. FPT algorithms for FVS on hypergraphs are obtained, when the input hypergraph is restricted to d-hypergraphs and linear hypergraphs.

4.2.4 Advancing the algorithmic tool-kit for parameterized cut problems

The thesis presents a study of several (di)graph cut problems from the perspective of parametrized complexity and kernelization. The goal is to extend the otherwise limited understanding of

parametrized cut problems on directed graphs, present novel applications of the toolkit available for undirected cut problems and to develop tools that allow reuse of the algorithms to solve the respective problems in presence of an additional constraint. This thesis addresses some major open problems in the area such as, existence of a polynomial kernel for Directed Feedback Vertex/Arc Set, sub-exponentiality in FPT beyond tournaments, parameterized algorithms beyond the classical partitioning problems, the existence of single exponential FPT algorithm for stable versions of classical cut problems and the parametrized complexity of Stable Multicut. In particular, connections between kernelization and fault-tolerant subgraphs are established. Another result is based on a novel application of important separators in the design of polynomial kernels, which is a rare sight in kernelization. The results give an interesting and usefulcombinatorial insight about the problem at hand.

4.2.5 Some results on graph contraction problems

The thesis explores FF-Contraction for various graph classes FF from the viewpoints of parametrized complexity, lossy kernelization and exact algorithms. Heggernes et al. (Algorithmica 2014) showed that Path Contraction admits a polynomial kernel, but Tree Contraction does not. In this thesis, properties of path that separates it from trees and allow Path Contraction to have a polynomial kernel were investigated. It is shown that number of leaves/gives polynomial kernels a lower bound on the kernel under a standard complexity assumption. Similar results were obtained for Cactus Contraction and Out-Tree Contraction. By presenting a non-trivial exact exponential algorithm that breaks the 2n-barrier, the thesis addresses the question of determining the length of the largest path to which a given graph can be contracted. An α-lossy kernel was presented for the Tree Contraction problem of polynomial size. For a given graph G on *n* vertices, an integer *k* and an approximation parameter $\alpha >$ 1, it is formally proved that there is an algorithm that runs in polynomial time and outputs graph G1 and integer *k* such that for every *c* >1, a *c*-approximate solution for (G1, *k*1) can be turned into (*c* x α)-approximate solution for (G, *k*) in polynomial time. Similar results were obtained for Cactus Contraction and Out-Tree Contraction.

The thesis presents an FPT algorithm for Cactus-Contraction with running time single exponential in *k*. For a collection of graphs T(q) that can be converted into a tree by deleting at most q edges, an α-lossy kernel of polynomial size is designed for T(q)-Contraction problem. Generalization of Clique Contraction problem calleds-Club Contractionis studied and proved that forany $s \geq 2$, it does not admit a lossy kernel of polynomial size under a standard complexity assumption.

5. Medical & Health Sciences

During the period of report, HBNI has awarded Ph.D.degree to 2 students in Medical & Health Sciences on successful completion of academic programmes. The summary of the doctoral theses is given below.

5.1 Tata Memorial Centre, Mumbai

5.1.1 Dosimetric and quality assurance studies in high dose diagnostic imaging modalities to establish national radiation protection programme

The research work is focused on the overall radiation safety aspects in the field of interventional radiology. Interventional Radiology is one of the advanced modalities used for fluoroscopically guided interventional procedures. Thesis comprises of the dosimetric and quality assurance studies carried out on interventional radiology system which has direct impact in optimizing the radiation dose to patients as well as associated medical professionals. The work concludes with the salient features of proposed national radiation protection program, which is an essential part of the quality management for the catheterization laboratory. The important outcomes are the methodology for skin dose measurements in the complex interventional radiology (IR) procedures, formation of local Diagnostic Reference Levels (DRLs) for common cardiac procedures, assessment of operator doses in the cardiac catheterization laboratory, quality assurance and audit of interventional radiology facilities and proposal to regulatory body for implementation of National Radiation Protection Programme in the country for IR practice. Implementation of this requires coordinated and collaborative effort involving physicians, staff, medical physicists, and hospital administration. Interventional cardiologists are an essential part of this process and need to ensure the best possible outcomes for radiation safety of operators and for patients. The skill of the medical practitioner, knowledge about the equipment and inclination towards radiation safety are the key parameters for minimizing radiation exposure to the patient and the operators. It suggests about the future scope of large-scale studies for establishment of national DRLs involving good representation of number of facilities all over the country for data collection for different types of procedures and a national dose registry can be generated.

5.1.2 Performance of HPVDNA test in presence of co-infection with common reproductive tract infections

The objective of the research work carried out in the thesis was to study whether the presence of clinical cervicitis or co-infections with Lab diagnosed RTIs interfere with the test result of HPV DNA by HC2 method. A total of 508 women, 254 women with clinical cervicitis and 254 asymptomatic women without cervicitis were enrolled as cases and control respectively. A baseline cervicovaginal swabs for RTIs and HC2 test samples were collected for all women enrolled in the study. All women in case arm received syndromic treatment for cervicitis while women in control arm received no treatment. A repeat cervicovaginal swabs and HC2 test was collected for all women enrolled in the study after 7-14 days. The study demonstrated that the overall detection rates of HPV by HC2 test improve by 4.5% among women treated for mucopurulent cervicitis. On controlling the biological and behaviour determinants by modelling, the study demonstrated the influencing role of mucopurulent discharge associated with cervicitis on the test results of HC2 test.

6. Physical Sciences

During the period of report, HBNI has awarded 109 Ph.D. degrees in Physical Sciences with research topics from a variety of areas including accelerator physics, condensed matter physiscs, nuclear physics and material physics. Few theses are summarized below.

6.1 Condensed Matter Physics

6.1.1 Bhabha Atomic Research Centre, Mumbai

6.1.1.1 Uncertainty modeling of thermoluminescence glow curve and development of deconvolution technique to resolve TL peak

In themoluminescent materials, a small fraction of charge carriers trapped in defect centers are thermally excited into delocalized energy states. The excited charge carriers recombine with trapped carriers of opposite charge to produce luminescence. If the oppositely charged trapped carrier sites are spatially close, recombination proceeds through quantum mechanical tunnelling. This phenomenon known as afterglow follows power law decay with exponent ranging from 0.5 to 2.0. A simplistic rectangular potential barrier between trap and recombination centers could not account for whole range of exponents observed. The thesis invokes non-rectangular barrier to successfully explain exponents. Further, a realistic material has multiple trapping sites. Experimental TL signal will therefore be a convolution of thermoluminiscence signals from a set of sites. The thesis developed a mixture model and Bayes' theorem-based methodology to deconvolute the TL signal to understand the detailed mechanism of thermoluminiscence glow.

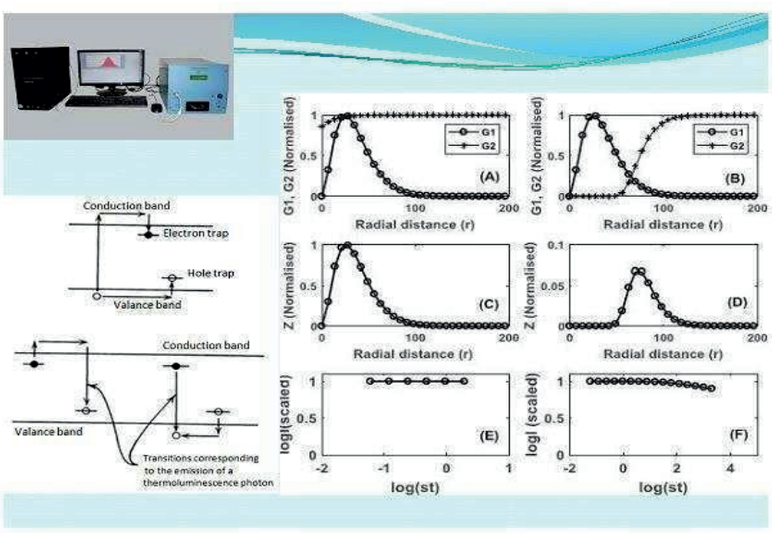

Basic TL apparatus (top left); Mechanisn of TL (bottom left); Explanation of non-linearity in afterglow (right)

6.1.1.2 Liquid metal MHD studies at high magnetic fields relevant to fusion test blankets

The Indian proposal of Lead Lithium cooled Ceramic Breeder (LLCB) Test Blanket Module (TBM) for ITER program is conceptualized with the philosophy of self cooling and tritium breeding from both the solid ceramics ($LiTiO_3$) and liquid metal Lead-Lithium (PbLi) eutectic in a single variant. The flow of PbLi in channels of LLCB is subject to high toroidal magnetic field (B_0=4T) which leads to coupled flow-field interaction through induced Lorentz force.

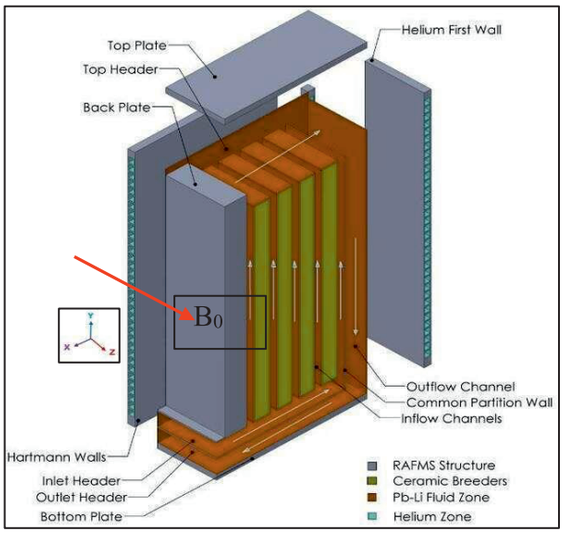

PbLi flow configuration in LLCB TBM

The electromagnetic force has dominant contribution to thermal hydraulic performance determined by magnetohydrodynamics (MHD) at high characteristic Hartmann number and Interaction parameter N. The thesis presents analytical, numerical and experimental studies performed at high magnetic fields ranging from 1 to 4 Tesla to analyse MHD phenomena of a generic liquid metal blanket. Series of liquid metal experiments in magnetic fields were performed in various complex geometries with multiple 90 degree bends, electrically coupled multichannel test sections, shielding effects of magnetic structural material, etc. 3-D simulations to understand the limitations of numerical models and its applicability to fusion relevant parameters were performed. MHD simulations were carried out in a full-scale variant integrated with complex helium cooled first wall. The velocity and flow rate distribution in different channels, pressure drop, electrical coupling of parallel flow channels, wall temperatures, the buoyancy effects and heat load sharing among helium and PbLi coolant circuits have been estimated for a realistic heat deposition based on neutronic calculation.

6.1.1.3 Structural phase transitions and phonon anomalies in alkaline niobate based functional materials.

This thesis presents a study on $(1-x)NaNbO_3$-$xBaTiO_3$: NNBTx ($0.0 < x < 0.20$) solid solutions, which are lead-free piezoelectric materials. Using dielectric and x-ray diffraction studies, it is observed that the parent antiferroelectric (AFE**)** phase of $NaNbO_3$ is destabilized with increasing x in favour of a series of ferroelectric phases accompanied by an increase in the dielectric constant. Sequence of structural

phase transitions as a function of temperature in NNBTx (x=0.03 and 0.05) was inferred from X-ray and neutron diffraction, which confirmed the stabilization of functional monoclinic phase at low temperature. Raman Spectroscopy at different compositions revealed not only the characteristic modes responsible for the phase transitions but also clearly indicated that the transition is first-order in nature, consistent with the X-ray and neutron diffraction studies.

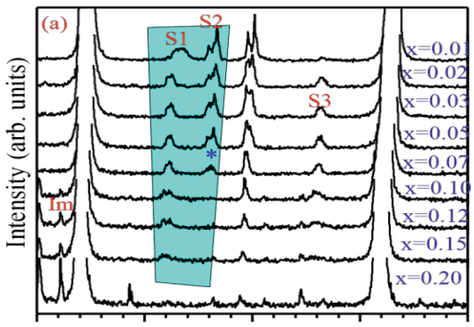

Evolution of powder X-ray diffraction patterns with increasing x

6.1.1.4 Studies on sensitivity of nano sized energetic materials

High energy materials such as TNT, RDX, PETN and composites of Resorcinol and Ammonium nitrate release enormous amounts of energy abruptly. This thesis focuses on the effect of particle size and presence of voids on the performance of these materials. TNT, RDX and PETN were prepared with particle sizes in the range of 50nm to 350 µm using solvent/non solvent precipitation, spray drying and sol-gel processing. Chemical and structural characterisation and microstructure were studied using FTIR spectroscopy, XRD, TG-DSC, Electron microscopy and SAXS measurements. Reduction in particle size to around 200 nm, resulted in a remarkable improvement in their ignition sensitivity and performance. Sensitivity to thermal and impact initiation in these materials decreased significantly with reduction in particle size. Further, the sensitivity to impact initiation increased on introduction of porosity. Reduction in particle size also improved the detonation velocity of these materials.

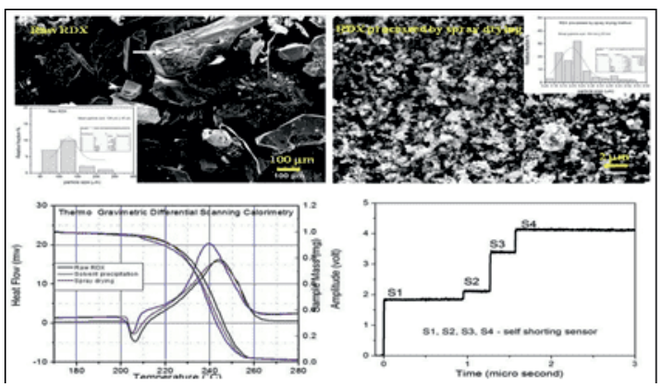

Energetic Material (RDX) with reduced particle size results in drastic decrease in ignition sensitivity at the same time with increase in detonation

6.1.1.5 Evolution of depth dependent structure and magnetic properties of multilayers on annealing

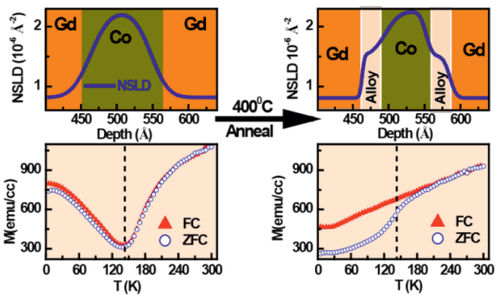

Figure 1. Nuclear scattering length density (NSLD) and corresponding temperature dependent magnetization curves of as-deposited and annealed Gd/Co multilayer

Antiferromagnetic coupling at the interfaces of Rare Earth (RE) – Transition metal (TM) heterostructures makes them potential candidates for realizing devices with higher speed and density. The thesis presents the evolution of depth-dependent structure and magnetism as a function of temperature in Gd/Co multilayers grown under different conditions. A negative exchange bias below the compensation temperature T_{comp} and antisymmetric magnetoresistance (MR) at T_{comp} were observed using magnetization and magnetotransport measurements respectively. Specular polarized neutron reflectivity showed the formation of a helical magnetic structure with planar 2π domain walls below T_{comp}, which is responsible for the observed negative exchange bias. Annealing of the multilayers increases interface roughness and alloying, which drastically modify the magnetic properties of the multilayers.

6.1.2 Indira Gandhi entre for Atomic Research Kalpakkam

6.1.2.1 Fabrication and characterization of SiO_2 microcantilevers for relative humidity sensing

SiO_2 microcantilevers (MCs) were fabricated using Direct Laser writer and wet chemical etching methods. The cantilevers are used to detect relative humidity (RH) by measuring the shift in the resonance frequency of the cantilevers using Nano Vibration Analyzer. The thesis describes a two-step process to fabricate SiO_2 MCs. As-fabricated SiO_2 MCs were found to be highly sensitive to Relative Humidity (RH) as measured by the shift in the resonance frequency. Introduction of controlled micropatterns on the surface of MCs yielded unprecedented RH sensitivity (10.45 Hz/% RH) without compromising their response/recovery times and reversibility. Functionality of the cantilevers is demonstrated by real-time monitoring of human respiration during fast and slow cycles of healthy adult.

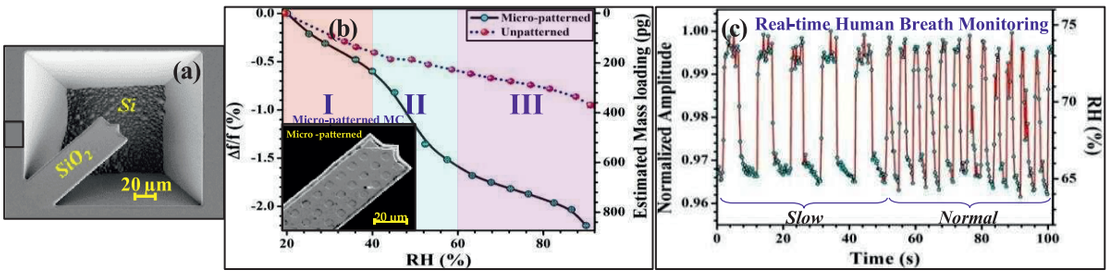

(a) FESEM image of the as-fabricated SiO_2 microcantilever. (b) Relative resonance frequency shift of micro-patterned and unpatterned microcantilever withrespect to RH. (c) Response of a micro-patterned microcantilever for slow and normal breathing inhale-exhale cycles of a healthy male adult. The right axis shows the independent RH measurement using a commercial RH sensor.

6.1.2.2 Studies on the effect of magnetic field induced aggregation on properties of ferrofluids

Exposure to magnetic field alters physical properties of ferrofluids by field induced aggregation of magnetic nanoparticles. Focus of this thesis is to understand the aggregation dynamics of the ferrofluids. The fast kinetics in ferrofluids (exposed to magnetic fields) with large particles favours formation of thick and long aggregates.

This is detrimental to heat transport, while the viscosity enhancement is very high. On the other hand, ferrofluids with narrow size distribution, without large aggregates, display high thermal conductivity in magnetic field but negligible viscosity enhancement, owing to the large number density of fine aggregates. Aggregation kinetics also affects wetting properties. Contact angle for ferrofluids without large aggregates decreases with magnetic field. Magnetic field ramp rate has a profound effect on thermal and rheological properties of ferrofluids. Faster ramps result in formation of high aggregate density, which is beneficial to heat transport. Ferrofluids exhibit aging and glassy dynamics under rapid quenches from high magnetic fields, owing to structural arrest of field induced aggregates.

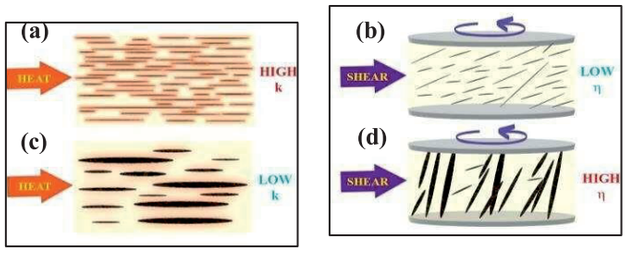

Schematic of the field induced microstructure (a) favorable and (c) detrimental to heat transport and the microstructure that is (b) detrimental and (d) favorable for viscosity enhancement.

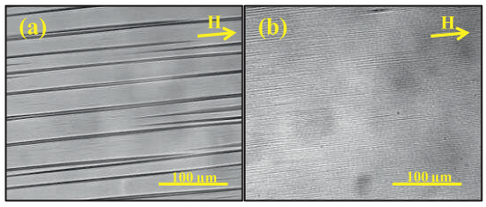

Phase contrast microscopy images of field induced microstructure of a ferrofluid subjected to (a) slow and (b) fast magnetic field ramp rate to 630 G.

6.1.2.3 Development of TDEM system with SQUID and fluxgate for geophysical and NDE applications

A Superconducting Quantum Interference Device (SQUID) based Time Domain Electromagnetic (TDEM) system is developed and tested at laboratory level using aluminum plates as conducting target. The performance of the system is compared with an induction coil sensor. Central loop sounding measurements were performed using SQUID based TDEM system in the terrain consisting of a thin conductive shale layer buried below a thick resistive layer at Tumallapalle. Dual behavior of fluxgate magnetometer was observed during TDEM measurements. Further investigation confirmed that it works as an induction coil at early time (measuring voltage directly) and as magnetometer (measuring magnetic field) at later time. A transient eddy current non-destructive evaluation (NDE) system was developed by combining fluxgate and double "D" excitation coil used to detect defects in aluminum plates at various depths ranging from 2 mm to 20 mm. A direct correlation between the diffusion time of eddy current and depth of the defect is established using this technique.

6.1.3 Raja Ramanna Centre for Advanced Technology, Indore

6.1.3.1 Study of structural and optical properties of oxides in soft X-Ray regime

Oxides of Aluminum, Magnesium and Zirconium are ideal coating materials for optical devices in the soft X-ray region. X-ray optics community relies largely on the Henke tabulated optical constants database for simulating the optical performance of a material to be used in device applications. While the values of optical constants in the database may be appropriate for elemental materials, weighted average method used to obtain the optical constants of compounds is erroneous as the effect of chemical bonding is not taken into account, which is more pronounced in the vicinity of the absorption edges of the constituent elements. This thesis reports optical constants of widely used coating materials Al2O3, MgO and ZrO2 measured in the soft X-ray region and correlated them to their structure and composition. The understanding led to the application of these materials in Fresnel's Zone plate and other optical elements in EUV/Soft X-ray region.

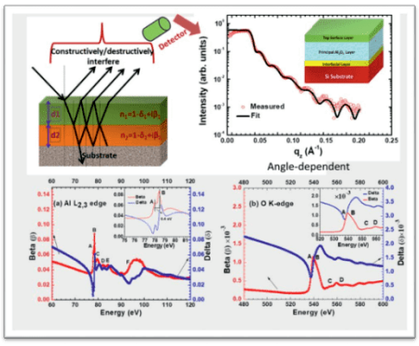

Angle and energy dependent X-ray reflectivity of layered structures

6.1.3.2 Studies on electromagnetically induced transparency in ^{87}Rb atoms.

The electromagnetically induced transparency (EIT) is a quantum interference phenomenon, where a resonant weak probe field is transmitted through an otherwise opaque medium with sub-natural line width. The thesis presents experimental and theoretical investigations on Lambda systems, N-systems and inverted-Y systems in ^{87}Rb atoms with a particular focus on control and manipulation of the EIT signal for applications such as tight frequency locking, high resolution spectroscopy and optical switching. For instance, the D_2-line of ^{87}Rb atom in two Lambda systems splits into three EIT peaks on application of magnetic field. This phenomenon finds application in multi-channel optical communications. One of the Lambda systems coupled to a standing wave field exhibits a sharply enhanced absorption signal.

N-systems, formed by introducing an additional energy level and a control field to a Lambda system, exhibit two EIT peaks around the central transmission dip. N-systems have potential applications in optical switching devices as the EIT peaks and the central transmission dip can be manipulated by control and coupling fields. Finally, spectral features of a modified inverted-Y system (IY^+) with multiple energy levels and control fields were studied theoretically. IY^+ system allows shifting, splitting and inter-conversion of the absorption and transmission peaks by manipulating the control fields. Switching off some control fields reduces IY^+-system to Lambda system.

6.1.3.3 Study on plasmonic response of metal nanoparticles of varied morphologies and their interaction with semiconductor nanostructures

This thesis addresses the growth of nanoparticles (NPs) and NP films of Noble metals and their alloys such as Au, Ag and Ag-Au alloy films using laser ablation. Noble metal NPs exhibit tunable optical response and enhanced electric near field due to localized surface plasmon resonance (LSPR) excitation. LSPR could be controlled by varying film thickness or alloy composition to obtain maximum Surface Enhanced Raman Scattering (SERS) signal. This can be used in trace detection of 500 nanomolar Rhodamine 6G dye for possible application in food safety, narcotics, explosives, etc.

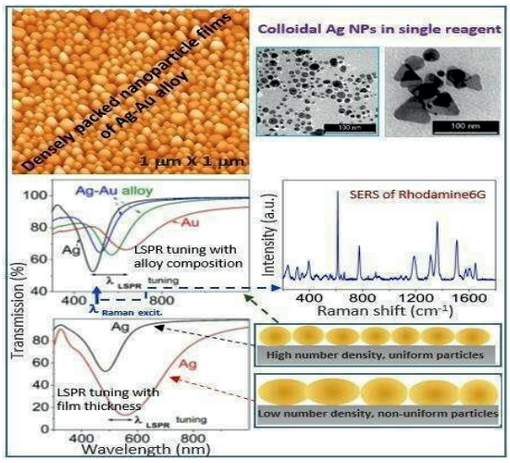

Densely packed Ag-Au NP films and Ag NPs for SERS based detection of Rh6G dye (500nM)

The thesis also reports the optimised process for large scale synthesis of environment friendly Au-ZnO core-shell and Au NP decorated ZnO nanorods, which can be used for treatment of dye effluents by photocatalytic degradation under low power UV light. The study revealed the role of hydroxyl radical in the degradation process, where high pH alters surface charge characteristics of the photocatalyst in such a way that cationic dyes degrade faster.

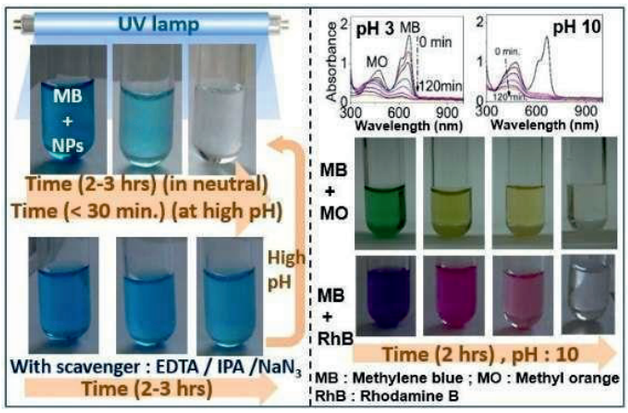

Au-ZnO NPs for photocatalytic degradation of MB dye and binary mixtures. Degradation is selective at high pH and simultaneous at low pH

6.1.3.4 Magneto-optical transport studies on ultra-low disordered semiconductor quantum wells grown by MOVPE.

The thesis demonstrates the possibility of enhanced radiative recombination of excitons in III-V semiconductor GaAs under magnetic field using magneto-optical spectroscopy. A part of the thesis addresses the development of a maskless photolithography system to fabricate semiconductor devices. It is known that the PL intensity related to disorder bound excitons decreases under a high magnetic field. A phenomenological model of magneto-excitons is proposed to estimate point defect density in QWs from the magnetic field-driven reduction in bound-exciton PL. Magneto-optical spectroscopy revealed competitive electro-optical processes in quantum structures, which are consistent with quantum Hall data. The thesis demonstrates that the electron-hole pairs can be separated by a magnetic field parallel to the QW plane, which reduce the PL intensity and develop an in-plane photo-voltage signal. Finally, it is shown that the carrier recombination and redistribution processes in semiconductor devices can be controlled by a magnetic field, which offers tunability in lasing wavelength and enhances the charge collection efficiency in photodetectors. Besides the physics of magneto-excitons, the thesis provided clear guidelines for magnetic field controlled advanced electro-optical device development.

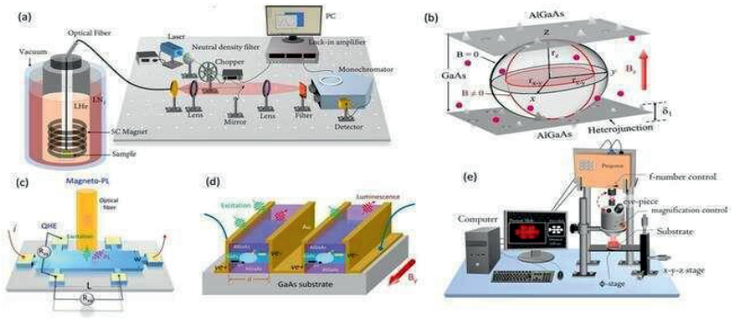

Schematic of the experimental setup for magneto-optical measurements and (b) magnetic field-driven spatial confinement of excitons in a QW. (c) Simultaneous measurement of magneto-PL and quantum Hall, (d) measurements of in-plane charge separation under a parallel magnetic field, and (e) schematic of the maskless photolithography setup.

6.1.4 Harish-Chandra Research Institute, Prayagraj

6.1.4.1 Quantum information processing in noisy environments

Various aspects of quantum information processing in open quantum systems, in presence of environmental noise and disorder were presented in this thesis. A new distance-based measure of non-Markovianity was proposed. A set of dynamical maps called "ϵ-Markovian" maps of an open quantum system were constructed. By defining "ϵ-nonmarkovianity" of any general dynamical map as the minimized distance from the map to the set of ϵ-Markovian maps, an upper bound on the ϵ-nonmarkovianity is derived. In the special case of ϵ = 0, the bound is shown to depend on the entanglement between system and environment.

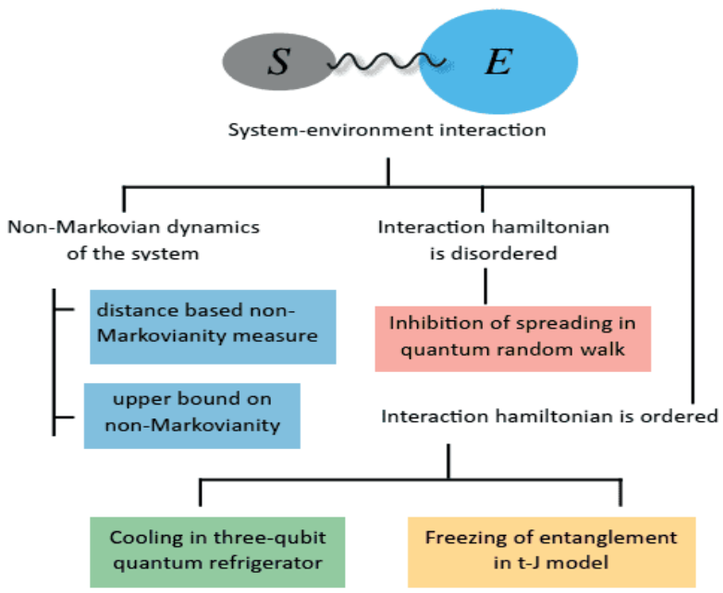

Quantum information processing in noisy environments

The thesis demonstrates that quantum states, such as qubit and qutrit states, with large initial coherence are disturbed less by a quantum measurement. Quantum coherence sets the upper limit

on the maximum information that can be extracted from a measurement process. The thesis introduces uncertainty relations based on a new measure “mean deviation uncertainty” with a wider applicability than the commonly used uncertainty. The new relations are useful in detecting Quantum Steering and Quantum Entanglement. For mean deviation-based uncertainty relations, Laplace states are shown to be as classical as the Gaussian states. This work establishes a connection between uncertainty relations and Preparation Contextuality and an upper bound on fine-grained uncertainty inequalities for arbitrary set of observables in all dimensions.

6.1.4.2 Uncertainty relations, quantum coherence and quantum measurement

A quantum measurement disturbs the system irreversibly (loss of coherence) and gives only a probabilistic distribution (uncertainty) of possible outcomes.

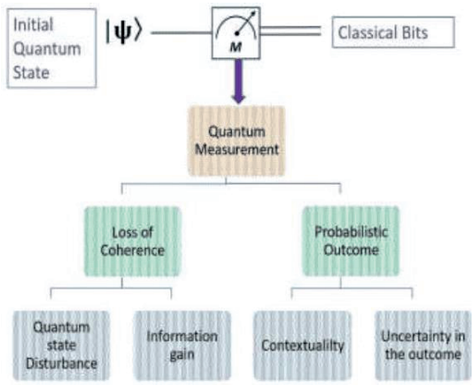

The thesis demonstrates that quantum states, such as qubit and qutrit states, with large initial coherence are disturbed less by a quantum measurement. Quantum coherence sets the upper limit on the maximum information that can be extracted from a measurement process. The thesis introduces uncertainty relations based on a new measure “mean deviation uncertainty” with a wider applicability than the commonly used uncertainty. The new relations are useful in detecting Quantum Steering and Quantum Entanglement. For mean deviation-based uncertainty relations, Laplace states are shown to be as classical as the Gaussian states. This work establishes a connection between uncertainty relations and Preparation Contextuality and an upper bound on fine-grained uncertainty inequalities for arbitrary set of observables in all dimensions.

6.1.4.3 Thermal properties of strongly correlated Bosonic and Fermionic superfluids

Ultra-cold atomic systems have emerged as a powerful tool to engineer model Hamiltonians, including correlated Bose and Fermi superfluids in the laboratory. At energies relevant to cold atom experiments, center of mass coordinate and the effective spin, which determine fermionic or bosonic character of the atom, are the only relevant dynamical variables. In optical lattice realizations of cold atoms, model Hamiltonians over a wide parameter window, avoiding uncontrollable ‘solid state’ effects like phonons and disorder, were explored. Important highlights of the thesis include the realization of a superfluid to Mott insulator transition in bosons and the BCS to BEC crossover in attractively interacting fermions. The results from these atomic studies provide insight into the role of inter-particle interactions in condensed matter systems.

6.1.5 Institute of Mathematical Sciences, Chennai

6.1.5.1 Uncovering functional correlates of structural organization in brain networks at multiple scales: From a worm to the human

The thesis addresses the structural organization of brain networks at different levels of complexity to understand (i) how the brain network is formed during development with its precise connectivity ('wiring problem'), (ii) how the structure of brain networks relates to their function ('structure-function correspondence') and (iii) how diverse is the structure of the brain network across a population?

Wiring problem is addressed by showing how the strategies for connecting the neurons arise from the developmental trajectory of the nematode *Caenorhabditiselegans*, the only organism for which the connections of the entire nervous system were mapped. An analysis of the connectivity structure, spatial organization and lineage revealed the developmental constraints that shape the nervous system.

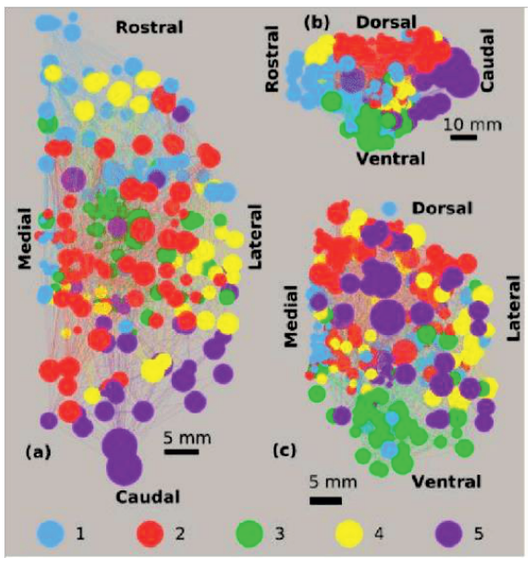

Mesoscopic organization of the Macaque brain. The network of brain regions, shown in (a) horizontal, (b) sagittal and (c) coronal projections, cleary indicates that the nodes (filled circles) are organized into five modules, each characterized by dense intraconnectivity. The modular membership of each node is represented by its color, while node sizes provide a representation of the relative volumes of the corresponding brain regions

For the Macaque brain, the modular organization of the connectome is shown to have counter-intuitive properties. Instead of information encapsulation by modules, the arrangement of inter- and intra-modular links facilitate extremely rapid dissemination of information, even faster than in random, homogenous networks. Analysis of an ensemble of human brain network shows that connection weights have a Poisson distribution. Representative network connections are identified by rescaling the link weights that correspond to functional networks.

6.1.5.2 Understanding mechanical response of bacterial cell walls and cell membranes against antimicrobial agents

Bacterial infections are treated using antibiotics, which either kill bacteria or retard its growth. However, several strains of bacteria have been developing an alarming resistance to antibiotics. It is therefore necessary to unravel the Biophysics of the bacterial cell, its design principles and the action of anti-microbial agents on the cell. Biophysical methods were employed to study the efficacy of biomimetic methacrylate polymers as antimicrobial agents. The molecular level architecture of the peptidoglycan (PG) mesh, the primary component of the cell wall, and its role in enhancing the toughness of the cell wall was explored in detail. The effect of variability in the elastic properties of the PG mesh on its bulk mechanical response was also investigated. Conformational characteristics, aggregation dynamics and interactions with model bacterial membrane of biomimetic methacrylate ternary antimicrobial polymers (AMPolys) were studied, using detailed atomistic molecular dynamics simulations.

6.1.5.3 Shock propagation in dilute inelastic and elastic media.

The radial distribution of pressure, density, temperature and flow velocity of a blast wave following an intense explosion has so far been studied by hydrodynamics (TvNS theory). This thesis presents a large-scale event-driven molecular dynamics simulations which are compared with the results of the TvNS theory. The discrepancies between the two approaches are identified to be resulting from the “local thermal equilibrium” assumption made in the TvNS theory. Simulations performed on a two-dimensional system are not at all in agreement with the TvNS theory. The problem is extended to the case where localized perturbation by a single impact is replaced by a localized but continuous perturbation. The radial growth of the disturbance created by the energy injected is determined by scaling arguments and by large-scale event-driven molecular dynamics simulations.

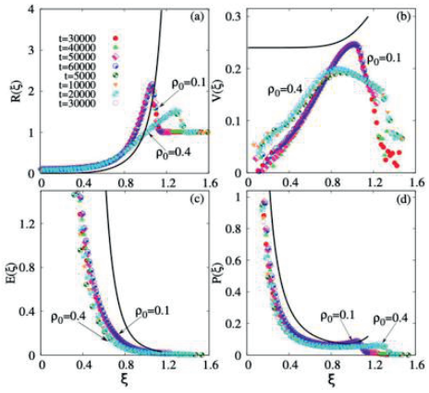

The variation of dimensionless scaling functions density R, velocity V, temperature E, and pressure P with scaled distance in three-dimensions. The data shown are for two different densities and are plotted for 4 different times. The black solid line corresponds to TvNS solution

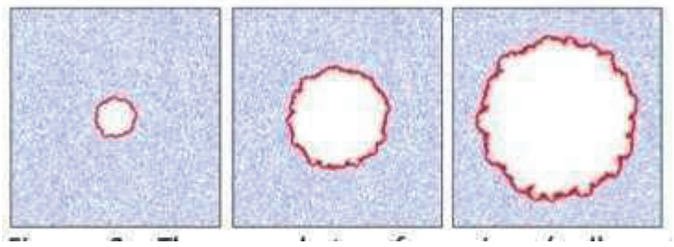

The snapshots of moving (red) and stationary (blue) particles in an inelastic system following continuous injection of particles at the center

6.1.5.4 Entropy driven phase transition in hard core lattice gas models in three dimensions

There is a class of phase transitions where the transition to the ordered state is driven by a gain in entropy. The transitions are manifested in experimental systems like freezing in hard-spheres of PMMA colloids, nematic transitions in liquid crystals, etc. The minimal models for studying the transitions are volume exclusion models, in which the constituent particles are not allowed to intersect. They serve as nice abstractions for actual experimental systems. Understanding their phase diagrams on lattice is helpful in general understanding of entropy-driven phase transitions. Simulation of the models in 3D is complicated due to the lack of efficient algorithms. Traditional evaporation-deposition algorithms fail to equilibrate at high densities or for large exclusion volumes. This thesis developed a version of grand canonical Monte Carlo algorithm with cluster moves, which enables to equilibrate systems at densities close to full-packing. The algorithm could be easily parallelised.

Detailed phase diagram was obtained to characterize the phase transitions in two problems on a cubic lattice, viz., (1) hard rods of length k and (2) hard cubes of size $2 \times 2 \times 2$. In the latter case, phases are: disordered, layered, sublattice and columnar in the increasing order of density. The disordered-layered transition is continuous, which is consistent with Heisenberg universality class with cubic anisotropy. The next phase is the sublattice phase, in which the density of cubes is periodic in all the three perpendicular directions with a period 2. The high-density phase is the columnar phase in which the system breaks up into a set of columns and the density of cubes is periodic along the two mutually perpendicular directions with a period 2. Both the layered to sublattice and the sublattice to columnar transitions were found to be first order in nature.

6.1.5.5 Beyond quantum nonlocality in continuous variable systems and thermalization of a qubit

Quantum correlations are an important area of study in quantum information theory. They can be classified into kinematic (correlations that do not change in time, e.g., measurement statistics obtained from spatially separated parties/observers) and dynamic (those evolving in time due to the system-environment interaction) correlations. The thesis studied kinematic correlations that are nonlocal and beyond quantum theory (i.e., postquantum) to understand how both nonlocality and postquantumness of multimode systems can be established. A class of continuous outcome postquantum nonlocal correlations for a generic m-mode scenario was constructed. While the nonlocality of the correlations is ensured through violation of Cavalcanti-Foster-Reid-Drummond

(CFRD) inequalities, postquantum nature is guaranteed by the violation of Robertson-Schrödinger uncertainty relation. This study helps to understand the foundational principles of quantum theory.

Dynamic correlations between a two-level quantum system and its environment are introduced through the quantum optical master equation to describe the approach to equilibrium. Using an ancillaqubit in an appropriate thermal state, the thesis simulates a two-qubit Hamiltonian with reduced system dynamics. The thesis concludes by deriving a class of Lindblad-type master equations that can describe either Markovian or non-Markovian processes to enhance our understanding of a major area in quantum thermodynamics.

6.2 Nuclear Physics

6.2.1 Bhabha Atomic Research Centre, Mumbai

6.2.1.1 Studies of reactor anti-neutrinos with ISMRAN

Indian Scintillator Matrix for Reactor Anti-Neutrino (ISMRAN) detector is intended for remote monitoring of reactor power by measuring anti-neutrinos from a reactor. The thesis highlights the development of a mini prototype ISMRAN consisting of a 4 x 4 array of plastic scintillators (PS), which was set up to carry out characterization and benchmarking studies. The response of the PS bars is linear in energy with a resolution function ~20%/ √E. Digitizers constituting the multi-digitizer DAQ are synchronized to provide a time resolution down to ~ 220 picoseconds between two PS bars to enable detection of cosmic muons. 3D position reconstruction is enabled by correlating the timestamp difference of PMTs to the Z position of event in a PS bar. Event numbers extracted by analysing four months uninterrupted mini-ISMRAN reactor data are close to theoretical predictions, albeit with large statistical and systematic uncertainties.

6.2.1.2 Understanding of fission dynamics from fragment mass distribution Studies

At energies near the Coulomb barrier, non-equilibrium fission processes, such as fast fission (FF), quasi-fission (QF) and pre-equilibrium fission compete with fully equilibrated compound nuclear fission. ^{28}Si + ^{197}Au reaction studied at BARC-TIFR Pelletron-Linac clearly indicated that the variance of the mass distribution decreases and saturates close to Coulomb barrier V_B and again decreases at sub-barrier energies. The deviation of the variance from dynamical and statistical model calculations was attributed to QF. For ^{9}Be + ^{232}Th reaction, mass distribution is asymmetric while it is symmetric in the case of ^{9}Be + ^{209}Bi reaction even at lower excitation energies in the range of 26 MeV, indicating the role of nuclear fissility in fission reaction. Fission fragment mass distribution of ^{191}Au, through the entrance channel ^{37}Cl+^{154}Sm was observed to be significantly broader (around 30%) than that of ^{16}O+^{175}Lu channel at similar excitation energies and angular momentum. Semi-empirical code GEF and the 4D Langevin dynamical model provided a conclusive evidence of the role of QF in explaining the broad mass distribution. The Di-nuclear System Model prediction of 22% QF in case of ^{37}Cl+^{154}Sm channel was also in good agreement with the observation. A systematic analysis of the experimental data indicated the role of QF whenever heavier projectiles (Z ≥ 17) were used with spherical or

deformed target nuclei around A~200. Analysis of neutron - deficient nuclear fission data in sub-lead region revealed that the light fragment proton number $Z_L \approx 36$ has a key role in deciding fragment mass distribution, in contrast to predictions where neutron shells were considered important in the fission in pre-actinide region.

6.2.1.3 A study of active experimental techniques for neutron dosimetry in positive ion accelerator

A Genetic Algorithm based Monte Carlo de-convolution code using the activation technique (GAMCD) was developed to determine neutron energy spectrum. An activation foil measurement for $^{1}H + ^{9}Be$ at 20 MeV and a proton recoil measurement for $^{12}C + ^{nat}Ag$ system at 144 MeV were unfolded to obtain the underlying neutron energy distributions. The response matrix was prepared for one of the detectors from the measured pulse height of monoenergetic neutron sources DD and DT. Neutron yield and its angular distribution measured using time of flight method for thin $^{12}C + ^{12}C$ system for projectile energy range 44 MeV – 110 MeV is compared with the predictions of statistical code PACE. The neutron yields from the intermediate projectile energies were linearly interpolated over energy bin size of 1.0 MeV. The yield from the projectile energy was integrated and compared with the thick target neutron yield, which is used in calculating secondary neutron dose in heavy or light ion therapy. Double differential cross section, neutron energy spectrum and the angular distribution were measured by time of flight for thick targets $^{12}C + ^{27}Al$ at 115.0 MeV at BARC-TIFR Pelletron-Linac facility.

Neutron dosimetry in accelerator environment using conventional rem-meters is complex due to dynamic field and energy ranges involved. Ambient neutron dose for ^{12}C + thick ^{12}C system at 116.0 MeV was measured using commercial dosimeters which were compared with those estimated from spectral distributions obtained from time-of-flight measurements and reaction codes using ICRP 74 fluence to dose conversion coefficient.

6.2.1.4 Monte-Carlo simulation studies of imaging atmospheric Cherenkov gamma Ray Telescope MACE (Major Atmospheric Cherenkov Experiment)

MACE (Major Atmospheric Chrenkov Experiment) gamma ray telescope being installed at Hanle, India is equipped with 21 m diameter reflector, for gamma ray detection in the energy range 10 GeV – 20 TeV. The telescope collects images of extensive air showers (EAS) generated by very high energy gamma rays and cosmic rays and extract gamma ray signals and their energy from the cosmic ray dominated data. This thesis presents results of experiments on various subsystems of the MACE telescope and associated simulations. The trigger rate of the MACE telescope varies from 1 kHz at zenith angle of 0° to 756 Hz at 60°. The 50 hour integral flux sensitivity of the telescope is 2.4% of Crab flux above the energy threshold of 30 GeV and 1.7% above that of 52 GeV. Angular Resolution and energy resolution over the energy range of 30 GeV – 3 TeV are 0.15^{o} and 26% respectively over the zenith angle range of 0° to 40°. Simulations indicate that MACE can significantly contribute to Very High Energy gamma ray astronomy and high energy astrophysics.

.

MACE Gamma Ray Telescope at Hanle, Ladakh, India

6.2.1.5 Radiation background studies for rare decay experiments

Neutrons constitute an important background for neutrino-less double beta decay (0νββ), dark matter search, solar neutrino experiments and other rare event searches. Interactions of neutrons with nuclei either produce nuclear recoils in the detector active volume or lead to the production of excited nuclear states, leading to additional γ-ray background. The thesis studied sources of background relevant to the TIN. Muon Induced Neutron measurement setup at TIFR (MINT) was developed to understand the neutron production from cosmic muons. In a Pb target 8.1±2.4 neutrons g^{-1} cm^{-2} day^{-1} were measured for 30 cm thick Pb target. Further, neutron production from stopping muons in Pb is 40 times that of Fe. The gamma-ray background from muon induced fast neutrons was directly measured for the first time via (n, n'γ) reactions in Ge and Cu in TiLES (TIFR Low-background Experimental Setup). The measurements are supported by Monte Carlo simulations using GEANT4.

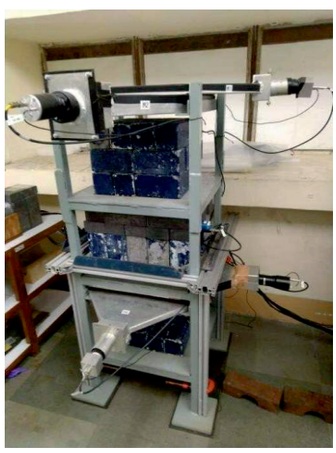

Muon induced neutron measurement setup at TIFR (MINT) has been developed for the measurement of neutrons produced from cosmic muon interactions

6.2.1.6 A study of Hadron energy estimation in ICAL@INO and feasibility of a PET Device based on multi-gap RPCs

ICAL (Iron Calorimeter) enables accurate reconstruction of muon tracks. Charged hadrons, produced in the atmospheric neutrino interactions, also produce hits in the Resistive Plate Chambers (RPC) of

the ICAL. Most often, the hits due to hadrons cannot be reconstructed into tracks because (a) the energy of a typical hadron is much smaller than the energy of the muon and (b) the hadrons can be absorbed in the detector. A significant number of baryons, which carry almost all the hadron energy, are produced in a large fraction of atmospheric neutrino events for hadron energy < 5 GeV. A correlation between the hits produced by the baryons and their energy is established.

Multigap RPCs (MRPC) are detectors made of many highly resistive plates (eg. glass) with a thin layer of gas between them. A high voltage is applied on the outermost electrode with all the inner electrodes electrically floating. Two MRPCs are horizontally mounted with a ^{22}Na source placed asymmetrically between the detectors. Positron emitted by ^{22}Na is annihilated by an electron almost at rest producing two gammas of 511 keV with opposite momenta, which are detected by the detectors in coincidence with each other.

6.2.1.7 Developments of improved methods for lattice and core physics simulations of thermal reactors

Neutron flux distribution and K-effective in nuclear reactors are routinely estimated by following a two- step process, where a representative cell (lattice) is treated first and then the full core. This thesis reports accurate and computationally efficient methods developed for both these steps, which are implemented in computer codes BOXER3 and FDPEM for analysis of LWRs. BOXER3 gives neutron flux distribution as a function of burnup in fine energy groups by 3 solution methods, viz., collision probability (CP), combination of CP & interface current (IC) and method of characteristics (MOC). Anisotropic scattering upto third order can be treated in MOC module. In the CP approach, an improved method for normalization of CPs is implemented. A more accurate neutron flux distribution is obtained at the lattice stage by introducing leakage corrected CPs, instead of the infinite medium CPs. To solve the diffusion equation at core level, a combination of finite difference (FD) along X & Y and polynomial expansion along Z are employed in the code. Treatment of transverse leakage by fourth order polynomial permits the use of long nodes along Z axis resulting in a significant savings in computer time. The code provides pin wise power distribution of the LWR core without compromising on the accuracy.

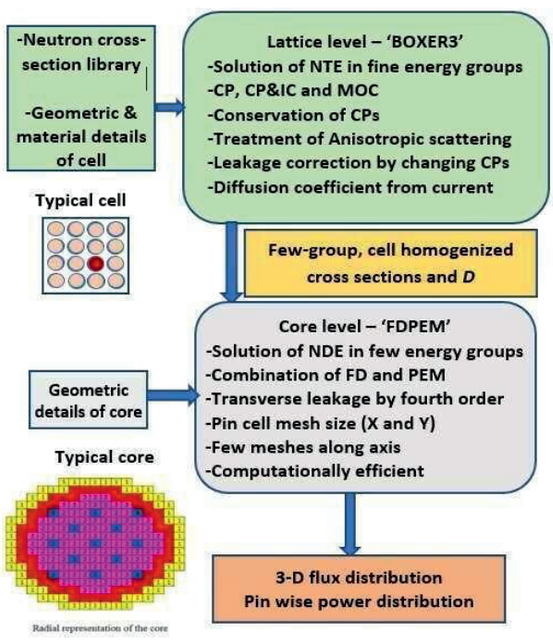

Salient features of methods and codes developed for two step process of reactor analysis

6.2.1.8 Study of effect of deformation & irradiation on the microstructure of fcc materials using X-ray diffraction

Microstructure strongly influences physical and mechanical properties of materials. It can be tuned by controlling the metal forming processes or may be altered by the in-service conditions (deformation, irradiation, etc.). Microstructural changes in face centered cubic (fcc) materials, caused by deformation and irradiation, were studied in this thesis using X-ray diffraction. The three problems addressed are defect enhanced diffusion, deformation induced phase transformation and the dependence of deformation path history and the nature of defect dynamics along different crystallographic planes during annealing. Alloy D9, SS304 and electrolytic Copper were chosen to carry out the studies.

6.2.2 Indira Gandhi Centre for Atomic Research, Kalpakkam

6.2.2.1 Studies on stability characteristics of MOX and metal fueled fast reactor cores

A nuclear reactor core is required to have neutronics stability for ensuring safe operation under various types of reactivity perturbations. Tools and methods were developed to characterise the stability behaviour of the pooltype SFRs having different power levels, core sizes and fuel types. The transfer function method using Nyquist criteria was adopted for linear stability analysis. The computer code DYNRCO capableof heat transfer and reactivity feedback calculations in the frequency domain is developed. The code is used for the stability analysis of MOX and metal fuelled FBR cores. Even though the feedback power coefficient is larger for oxide core, its stability margin is lower compared to metal cores. The smaller time constant due to better heat transferproperties of the metal core give a higher stability margin for the metal fuelled FBRs. Safety of PFBR under various reactivity perturbations such as sinusoidal type and seismic fluctuations are studied. The power evolution with time is simulated. It is demonstrated that design safety limits are respected during Safe Shutdown Earthquake (SSE) even when the reactor is not scrammed. Non-linear stability analysis is also performed for the first-time using bifurcation method and time domain analysis. It is found that these reactors are stable even with large reactivity perturbations. processes.

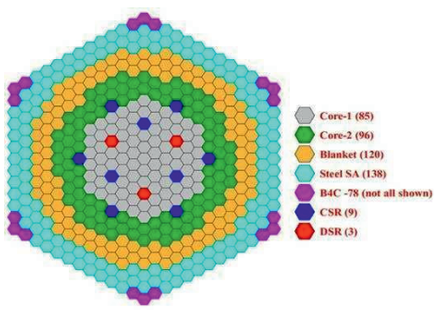

Core configuration of 500 MWe MOX core

6.2.3 Saha Institute of Nuclear Physics, Kolkata

6.2.3.1 Search for Higgs boson pair production in the HH → bbττ channel in p-p collisions using CMS data at √s = 13 TeV at the LHC

Measurement of Higgs boson self-coupling is one of the major goals of the LHC, where Higgs boson pair (HH) production cross-section is one important handle. This thesis analyses HH → bbττ reaction for the semi-leptonic and fully hadronic decay modes of the τ pair, which constitute ~80% of all τ pair decays. No excess background beyond the expected value was found and 95% CL limit on both resonant and non-resonant σ_{HH}×B(HH → bbττ) is set. The observed (expected) limit on the Standard Model HH → bbττ production cross-section is 31 (25) × the Standard Model prediction.

LHC will be upgraded for 5 - 7 times the current luminosities. To work efficiently in the extremely high radiation environment, CMS will go through the Phase-2 upgrade involving replacement of the current tracker with better radiation hardness, lower material budget and higher granularity. Phase-2 tracker will be equipped with modules, to reduce data volume for tracking at the Level1 (L1) trigger system, by selecting high-p_T tracks at the detector front-end. The performance of prototype Strip-Strip (2S) detector modules of the Phase-2 tracker was studied under realistic beam conditions. The capability of CMS at the HL-LHC to trigger on rare, low-p_T, fully hadronic 5nal states, like B^0_S → ϕ ϕ → 4 Kaons, using tracks reconstructed at the L1 trigger, has also been studied.

6.2.3.2 Study of nuclear structure near shell closure

Nuclear structure of the two doubly magic nuclei ^{100}Sn and ^{132}Sn and their neighbourhood has been studied in this thesis. Two irradiation experiments using analog (with Clover-Clover-LEPS detectors) and digital techniques (using single HPGe detector) were performed at VECC, Kolkata for decay spectroscopy of $^{117g;118m}$Sb and ^{117m}Sn and resolved some of the ambiguities present in the adopted level scheme of ^{118}Sn. The half-life of 3/2$^+$ state of ^{117}Sn was measured using VENTURE array and the half-lives of parent nuclei, $^{117g;118m}$Sb were extracted. PIN diodes procured from Bharat Electronics Limited (BEL) have shown excellent performance in detecting X-rays, conversion electrons and low energy gamma rays. Experimental findings were interpreted using large basis shell model calculations and excitation energies and transition probabilities associated with different isomeric states present in $^{117;118}$Sn were estimated.

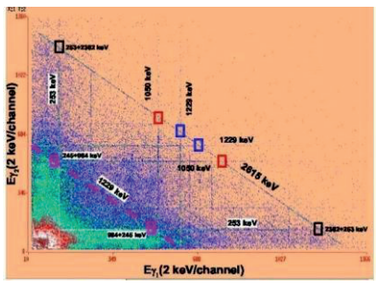

E_{γ}- E_{γ} matrix obtained from two Clover data is shown. The Compton lines ($E_{\gamma 1}$+ $E_{\gamma 2}$ = E_{γ}) corresponding to E = 1229 keV and 2615 keV are shown. This correlation data is important to resolve uncertainities present in adopted data of ^{118} Sn

6.2.3.3 Bottomonium studies at LHC energy using ALICE muon spectrometer

The bottomonium (ϒ) is a useful probe to investigate the properties of the deconfined medium, created in ultra-relativistic heavy-ion collisions. The medication of ϒ production at LHC energies in heavy-ion collisions with respect to the binary-scaled yield in pp collisions is explained in this thesis by color screening mechanisms. In the bottomonium sector, the regeneration effects are expected to be negligible due to small number of b quarks produced in relativistic heavy-ion collisions. However, the Cold Nuclear Matter (CNM) effects, which include shadowing, parton energy loss, interaction with hadronic medium may also lead to a modification of bottomonium production. In order to disentangle the CNM effects from the hot nuclear matter effects, ϒ production has been studied in p-Pb collisions in which the QGP is not expected to be formed. Bottomonium production via di-muon decay channel in pp, p-Pb and Pb-Pb collisions has been studied using the ALICE Muon Spectrometer.

6.2.3.4 Composite Higgs and physics beyond the Standard Model

A major limitation of the Standard Model (SM) of particle physics, viz., the stability of the weak scale using a composite Higgs setup, is addressed in this thesis. The composite Higgs framework, where Higgs originates as a pseudo Nambu-Goldstone boson of a spontaneously broken global symmetry in some strongly interacting sector, has two major phenomenological consequences. First, this scenario predicts the existence of non-standard spin-1 particles as well as additional colored fermions also known as top-partners, which can in principle be searched at the Large Hadron Collider (LHC). The connection between a light Higgs boson and a light top-partner resonance, which is somewhat in tension with the present LHC data, is also explored. A possible avenue to depart from such strong correlations is suggested in a next-to-minimal setup using the mechanism of level repulsion between the doublet Higgs boson and an additional scalar singlet.

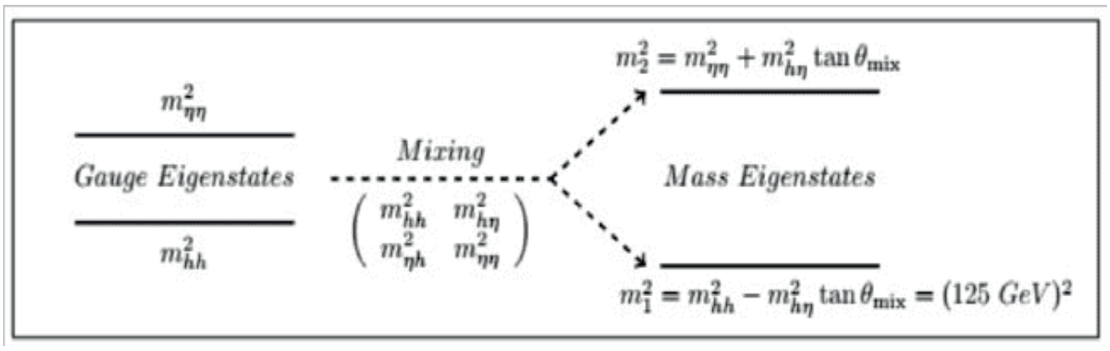

Level repulsion mechanism between a doublet Higgs boson and a singlet scalar state in the next-tominimal composite Higgs model can lift the strong connection between the light Higgs and light top-partners.

Modification of the Higgs couplings with other SM particles, from their SM reference values, were studied under various composite Higgs frameworks. Georgi-Machacek model composed of doublet and triplet Higgs bosons and its phenomenology in the presence of higher dimensional operators was studied.

6.2.3.5 Multi-wavelength long term monitoring and spectral energy distribution modeling of bright active galactic nuclei Markarian 421 (Mrk 421)

During 2015-2016, Mrk 421 was in a state of low activity in the X-ray and very-high-energy (VHE) γ-ray, the energy bands where the emitted power is the largest, and has shown correlated behavior in X-rays and VHE γ-rays. Apart from the non-zero correlation around a time-lag of ~45 days between optical (and high-energy γ-ray band) vs radio bands, the emergence of a new spectral component in the hard X-ray band was observed by the Swift-BAT telescope. For the first time, with the help of the time dependent leptonic model, all the three states during the outburst have been explained and realization of MWL radiation profiles derived in this thesis. The study revealed that as the flare evolves from a low- to a high-flux state, higher bulk kinetic energy is injected into the system with a harder particle population and a lower magnetic field strength.

6.2.3.6 Structural evolution of weakly deformed nuclei in mass ~ 140 region with increasing angular momentum

Mechanisms of angular momentum generation resulting in the evolution of nuclear structure in weakly deformed nuclear mass region of A~140, high-spin level structure of ^{141}Sm (Z = 62, N = 79), ^{142}Eu (Z = 63, N = 79) and ^{140}Eu (Z = 63, N = 77) have been investigated in this thesis using the gamma-ray spectroscopy in BARC-TIFR Pelletron-linac facility. High spin states of ^{141}Sm were populated by the reaction ^{116}Cd (^{31}P, p5n) with E_{Lab} = 148 MeV. Deexciting gamma rays were detected by the Indian National Gamma Array (INGA). This study established three dipole sequences, where magnetic dipole transition rates (B(M1) was found to decrease with increasing spin. The routhian plot showed a rapid increase in frequency with angular momentum, which indicates the onset of collectivity along the MR band. The existence of degenerate ΔI = 1 doublet bands II and III suggest that the ^{141}Sm can have triaxial deformed nuclear shape at the higher spins, indicating a smooth transition from planar (MR) to an aplanar (chiral) nuclear shape.

6.2.3.7 Search for physics beyond the Standard Model in photon + missing transverse momentum final state in proton-proton collisions using the compact muon solenoid detector at LHC

After the discovery of the Higgs boson, an important goal for the LHC include the search for Dark Matter and extra dimensions. Dark Matter as well as ADD gravitons are invisible particles which account for the missing transverse momentum and can be produced along with visible particles like a photon. Photons give a clean final state and have proved to be a very important channel both in ATLAS and CMS. A search for new physics beyond the standard model using data collected by CMS at center of mass energy 13 TeV has not resulted in any deviation from the predictions of Standard Model. For DM simplified models, the observed (expected) lower limit on the mediator mass has been set at 950 (1150) GeV for dark matter mass around 1 GeV. For ADD model of large extra dimensions, for number of extra dimensions between 3 and 6, effective Planck scale up to 2.85 to 2.90 TeV have been excluded. Collimated neutral pion decays and machine induced backgrounds like beam halo photons are very important backgrounds for the physics analysis. But the estimates using traditional techniques have limitations. A new way of estimating experimental backgrounds is shown using state of the art

machine learning techniques, which provided powerful tests for hypothesis testing than traditionally employed techniques.

6.2.3.8 Charmonium studies at forward rapidity with ALICE muon spectrometer at the LHC

The cross section of ψ(2S) production as a function of p_t and rapidity in pp collisions at 5.02 TeV are crucial for understanding the QCD processes and production of the charmonia. Comparing with the published ALICE results at 7, 8 and 13 TeV, this thesis establishes that the ratio of ψ(2S) and J/ψ does not show any significant energy dependence. ψ(2S) is well described by the NRQCD calculations except for higher p_t bins, while the NLO calculation based ICEM model overestimates at high p_t. The ratio of inclusive ψ(2S)-to-J/ψ production cross sections are well reproduced by the calculations based on NRQCD+CGC.The multi-differential and single-differential ψ(2S) cross-sections were measured and the analysis of J/ψ in Pb–Pb collisions at 5.02 TeV at forward rapidity was performed to understand the recombination scenario in heavy-ion collisions. The high statistics of 2015+2018 datasets made it possible to precisely show the effect of recombination which is visible only at low p_t in the most central collisions.

6.2.4 Institute of Physics, Bhubaneswar

6.2.4.1 Production of Higgs boson in association with another two bosons at the Hadron Colliders

The production of various bosonic multi-particle states with at least one Higgs boson was considered in the thesis. The main focus had been gluon-gluon (gg) fusion contribution to these processes, mediated by heavy quarks in the loop. At the Colliders, gluon flux increases with center-of-mass energy of the colliding protons. This gg fusion channel occurs at NNLO in QCD coupling constant, α_S, at the amplitude-squared level. gg fusion channel is the main contributor to hhh production. For pp→hhZ, the qq initiated channel is not suppressed. At the LHC, gg fusion channel's contribution is comparable to NLO QCD correction in the qq channel, and significantly more at 100 TeV collider. Various interference effects have been studied in the gg fusion channel, which facilitates better understanding of various features of the differential and inclusive cross-sections. The thesis also highlighted new physics on the gg fusion channel. The gg→hhh and gg→hhZ processes show modest dependence on the anomalous trilinear and hZZ couplings, respectively.

6.2.5 National Institute of Science Education and Research, Bhubaneswar

6.2.5.1 Angular and momentum distribution of vector mesons produced in proton-proton and heavy-ion collisions at LHC energies

A large angular momentum (O(10^7) hh) is expected to be created in ultra-relativistic heavy ion collision, when two heavy-ion nuclei collide with non-zero impact parameter. The spin-orbit interaction can polarize the quarks produced, which can be transferred to the hadrons produced. Spin alignment of vector mesons produced in heavy-ion collisions is quantified by measuring the spin density matrix element ρ_{00}, which is the probability of finding a vector meson in spin state 0 out of the

possible spin states (-1, 0, 1). In the absence of spin alignment, ρ_{00} = 1/3 as all 3 spin states are equally probable. The ρ_{00} values will deviate from 1/3 in presence of spin alignment or preferential orientation of vector meson spin. The ρ_{00} values for vector mesons can be measured experimentally by studying the angular distribution of the decay daughter of vector meson with respect to the direction of angular momentum. A significant spin alignment for vector mesons in heavy-ion collisions was observed for the first time. A deviation of ρ_{00} from 1/3 at low transverse momentum and in mid-central Pb–Pb collisions supports the presence of a large initial angular momentum in non-central heavy-ion collisions.

6.2.6 Variable Energy Cyclotron Centre, Kolkata

6.2.6.1 Development of fast timing array at VECC and its application in nuclear structure study around Z = 50 and N = 82 shell closure

Knowledge of inverse of nuclear level lifetimeprovides insight intothe interplay of single-particle and collective behaviors of nuclear structure of nuclei around double shell closure ^{132}Sn, far from the β-stability line. Electric Quadrupole Moment (EQM) is ameasure of deformation from sphericity. However, experiments on these neutron rich nuclei are rather rare due to the difficulty in accessing this region. Scintillation detectorsusing $LaBr_3$(Ce), $CeBr_3$, etc., enable exploring into the low-lying states. As most nuclear lifetimes lie in the sub-nanosecond to picosecond region, development of a γ-γ fast timing array is necessary for measurement of lifetime along with EQM. Individual 1” diameter x 1” thick $CeBr_3$ detectors coupled to Hamamatsu R9779 photomultiplier tubes were characterized and the fast-timing array, *VECC Array for Nuclear fast Timing and AngUlar CorRElation (VENTURE)* was developed at VECC. The array was used in its stand-alone mode as well as with the array of Clover HPGe detectors like VENUS or INGA. VENTURE array was tested for both off-beam and in-beam experiments for direct lifetime measurement using Generalised Centroid Difference method.

The first ofits kind facility was used for measurement of nuclear level lifetime in neutron rich nuclei ^{131}I, ^{132}Xe. The transition probabilities are consistent with double shell closure of ^{132}Sn and establish octupole correlations in ^{131}I. An angular correlation table developed using Time Differential PAC (TDPAC) technique was used for EQM measurements in ^{131}I and ^{132}I. The deformation and quadrupole moment are in conformity with shell closure at N=82.

6.3 Accelerator Physics

6.3.1 Raja Ramanna Centre for Advanced Technology, Indore

6.3.1.1 Optimization of a multi bunch train filling pattern for the suppression of beam ion instability in electron storage ring: Case study of Indus-2

Electron collisions with the residual gas molecules in an electron storage ring produce positively charged ions. Electron bunches interacting with the ions cause conventional ion trapping (CIT) and

fast beam ion instability (FBII) producing transverse electron oscillations, which are detrimental to beam current accumulation and betatron$_{600}$ tune. CIT was observed in Indus-2 with vertical tune shift and beam current saturation at around 100 mA. This thesis discusses a theoretical model to obtain an optimum bunch filling pattern which more than doubles the beam current with enhanced lifetime. When the residual gas density in the storage ring is high, FBII develops in spite of a higher clearing gap, leading to transverse dipoleoscillation of the electron bunches with amplitude increasing in time along the bunch train resulting in the deterioration of beam quality. FBII was studied numerically using FASTION code applied to Indus-2 with CO molecules 50 nTorr pressure. In practice, multiple molecular species generate spread in ion oscillation frequency and weaken the instability due to Landau damping. The instability can be reduced by replacing single long bunch train into many shorter bunch trains. An optimal multi-train bunch filling pattern, which can minimize FBII even at 50 nTorr was arrived at for Indus-2.

6.3.1.2 Studies on ion acceleration in ultrashort ultra-high intensity laser matter interaction

The thesis demonstrates proton/ion acceleration from solids, thin foils and nano structured targets using high power pulsed Ti:Sapphire lasers. Dependence of acceleration on laser and target parameters was investigated. Negative H^- ions were generated by controlling irradiation parameters of targets. Laser accelerated proton and deuteron beam is used to produce short lived positron emitting isotopes and to achieve proton-boron fusion.

While atomic number of the material is critical for proton or ion acceleration, it can be significantly enhanced by adjusting the Laser Temporal characteristics. Using 150 TW laser, proton and C^{5+} ions were accelerated to10-11 MeV and 14.5 MeVrespectively. By using transparent CH solid target, H^- ion were accelerated with a flux > 10^{10} /shot. In typical laser ion acceleration, protons are the most dominant species with a broad energy distribution. Contrary to this, quasi mono-energetic sub-MeV gold ions were produced for the first time from gold-carbon nano-composite and multilayer targets irradiated at laser intensities of 10^{18} -10^{19} W/cm^2. Flux and energy distribution of alpha particles produced in p,B fusion reaction driven by laser accelerated proton beam was studied. ^{11}B(p,n)^{11}C and ^{10}B(d,n)^{11}C reactions, which are main channels for generation of ^{11}C (positron emitter) radioisotopes were explored using Laser acceleration technique. About 5.2 kBq activity equivalent to 9×10^6 atoms of ^{11}C radio-isotope was produced in a single laser shot through ^{11}B(p, n)^{11}C reaction. Higher yields were produced with both deuteron and proton beams using CD_2target.

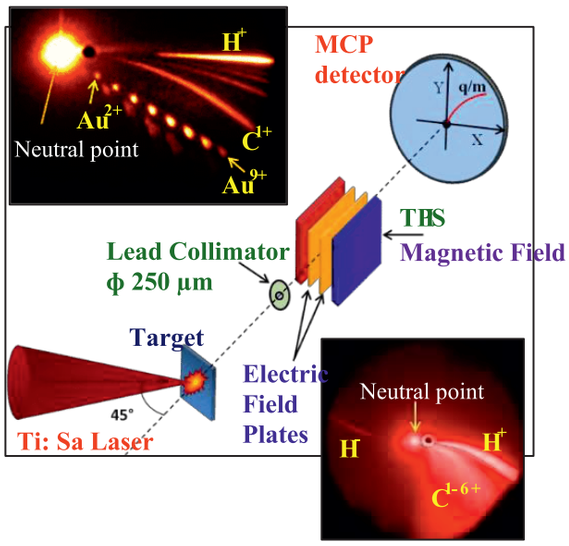

The ultrahigh intensity laser is focused on thin target and ions are accelerated at the target rear. The ions are analysed using Thomson parabola ion spectrometer (TPSI). Typical ion signal recorded from Au-C nano composite target showing quasi mono-energetic Au ions (top left) and negative ions from PMMA target (bottom right).

6.3.1.3 Studies on characterization and application of ultrashort higher harmonic radiation

The thesis studies the generation of higher harmonic radiation by interaction of ultrashort high intensity Ti: Sapphire 800 nm laser pulseswithnonlinear media and proposes its application in multicolor radiography of plasmas. Owing to their coherence, it is possible to generate ultrashort (attosecond or as) pulses of higher harmonics. Phase matching between the driver laser pulse and the harmonics generated is a key to efficient harmonic generation. Spectral analysis of harmonic radiation reveals how different electron trajectories contribute to harmonic beam divergence, spectral width and spatial coherence.

A high-resolution electron time of flight spectrograph is developed for temporal characterization of the harmonic pulses. Cross-correlation of the harmonic radiation with the laser pulse at IR (800 nm) gives temporal pulse shape. Both odd harmonics (17th to 25th order) generated from argon cell and IR laser pulse are collinearly focused on ions in a low-pressure gas sheath (N_2 at ~10^{-5}mbar) to produce photoelectrons of energy corresponding to even harmonics, called sideband energy peaks. The temporal delay scan between the harmonics and IR pulse produces oscillation in signal of sideband electron energy peaks at twice the IR frequency. The relative phase between harmonics is measured from sideband photo electron signal amplitude. The relative phase and amplitude, is used to reconstruct attosecond pulse train, which is determined to be ~ 300as and repeating at ~ 1.33 fs (half laser cycle).

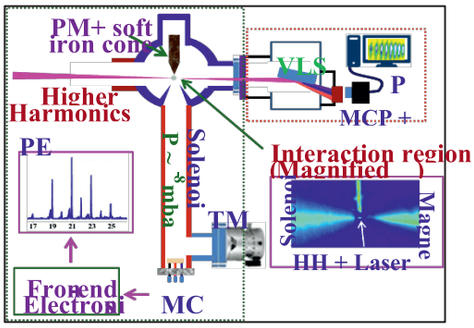

A schematic of an in-house developed magnetic bottle electron time of flight (MBETOF) spectrograph and flat field grating spectrograph (FFGS), HH-Higher harmonics, IRinfrared laser, VLSG-Variable line spaced grating, MCPmicrochannel plate, PM-permanent magnet, PE-Photoelectron

6.3.1.4 Electromagnetic design and beam dynamics studies in elliptic superconducting radiofrequency (SRF) cavities

Indian Spallation Neutron Source (ISNS) is proposed to be a linear accelerator based pulsed neutron source. While the injector linac is designed to consist of five sets of superconducting radio-frequency (SRF) cavities, two are elliptic cavities for medium and high energy range. This thesis presents optimization scheme for optimization of the cavities for maximum acceleration gradientandcalculate threshold beam current responsible for excitation of beam break-up instability. Cavity is stiffened to minimize dynamic detuning of the cavity due to Lorentz pressure during pulsed mode operation. Electromagnetic performance study of the SRF cavities using a magnetothermal analysis indicated that low purity (cost) commercial niobium to be aviable alternative high RRR Niobium.

The thesis also discusses a compact design of the 1 GeV, 1 MW H^- ion superconducting injector following the $nonequipartitioned$ design approach. Stability of mismatched envelope oscillations have been analysed for a three-dimensional beam bunch. Particle Core Model, considering the actual periodicity of the ISNS lattice, was used to estimate the maximum radial extent of the halo particle in case of a mismatch in the input beam parameter.

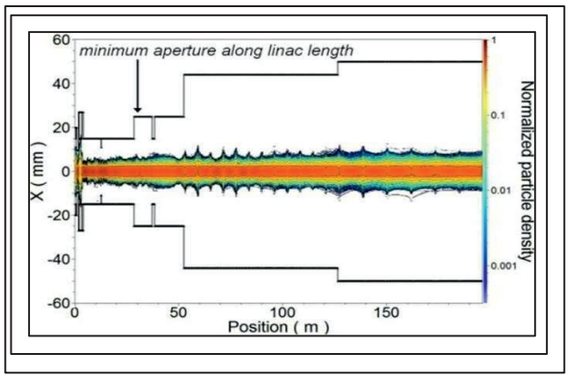

Color map shows radial distribution of normalized particle density along with the available aperture (black) along the linac

6.3.1.5 Laser driven plasma-based electron acceleration, applicable mechanisms and its applications

The thesis presents investigations on Laser Plasma Acceleration (LPA) for generation of relativistic electron beams using ultra-short, ultra-high intensity laser interaction with gas-jet plasma targets with particular emphasis on its application in electron radiography. 2D PIC simulations are used to estimate energy gain and understand dephasing effects.

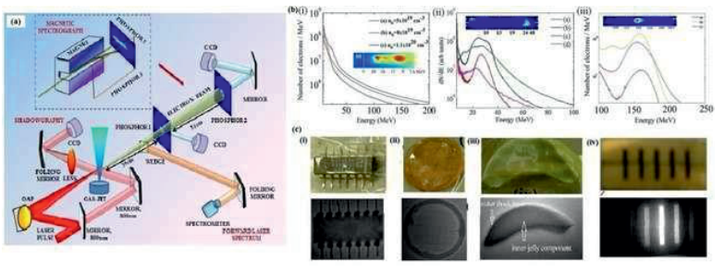

(a) Schematic of experimental set up. (b) Electron beam spectra in He gas-jet target with laser pulse duration of (i) ~200 fs through DLA (ii) ~55 fs through hybrid, (iii) in mixed gas-jet target of N_2+50%He with laser pulse duration of ~60 fs through DLA and (c) Radiographs of various samples recorded using relativistic electron beams generated from LPA.

Chirped Pulse Amplification (CPA) based 25 fs, 150 TW Ti:sapphire laser was used in Direct Laser Acceleration (DLA) and hybrid acceleration regime (DLA + wakefield) of electrons in different gas-jet targets such as He, N_2, Ar and mixed gas targets of He + N_2. Quasi-thermal and quasi-monoenergetic electron beams with peak energy of ~168 MeV were observed with 200 fs laser pulse in He gas-jet target. DLA was identified to be the acceleration mechanism in this case. In the Hybrid regime, maximum electron energy of 750 MeV was achieved. Application of relativistic electron beams for radiography and radiotherapy is being explored.

6.4 Material Physics

6.4.1 Bhabha Atomic Research Centre, Mumbai

6.4.1.1 Computational and experimental studies on the damage response of ferritic and austenitic steels under extreme conditions

Ferritic steels have mechanical properties appropriate for making nuclear reactor pressure vessels while austenitic stainless steels are used in internal structures of pressurized water reactors. The thesis studies the microstructural changes produced in these materials subjected to extreme temperature and radiation fields. Atomic Probe Tomography of the materials indicated the formation of Cu-rich precipitates (CRPs) in irradiated binary Fe-Cu alloys. A signature of morphological transformation of the CRPs from spherical to ellipsoidal shape with a significant change in aspect ratio (9R-3R structural transition) was inferred from Small Angle Neutron Scattering experiments. Attractive interactions between Cu & Cu and V &Cu predicted by the first principles density functional theory (DFT)

calculations isfound to be responsible for the formation of Cu-clusters. One of the novelties of thestudy is the analysis of the origin of the binding energy (BE) in vacancy-solute complexes by decomposing the BE into electronic and distortion energy contributions. The thesis also presents the effect of small solute atoms in both bcc- and fcc-Fe lattices on BE studied using DFT calculations. Furthermore, the evolution of crystal structure and microstructure in heavy ion (Ag and Au) irradiated SS316 is investigated. Both, the extent of damage as well as the identity of ions are found to affect the nature of radiation-induced phase transformation in this steel.

6.4.2 Indira Gandhi Centre for Atomic Research, Kalpakkam

6.4.2.1 Fabrication, selected microstructure-property correlations and applications of Si nanowalls

The thesis describes growth of Si nanowalls (Si NWs) for sensor applications. Single crystalline vertically aligned SiNWswere grown on a Si wafer by facile and CMOS compactible 2-step metal assisted chemical etching (MACE) technique. The lightly doped porous Si NWs were also grown by a MACE technique combined with anodic polarization etching process. Si NWs obtained by low etching times exhibit excellent anti-reflectivity and superhydrophobicty, the properties which can enhance the efficiency and life time of optoelectronic devices like Si solar cells. Lightly doped porous Si NWs show visible photoluminescence, which arises mostly from quantum structures present in porous Si NWs. This reveals that MACE combined with anodic polarization etching is capable of producing visible light emitting porous Si NWs. Pristine and Pt and Pd functionalized Si NWs, denoted by Si NWs, Pt-Si NWs and Pd-Si NWs respectively, show hydrogen sensing behaviour. Pt-Si NWs and Pd-Si NWs exhibit enhanced sensitivity to hydrogen at low and high temperatures. Successful fabrication and functionalization of Si NWs by CMOS compatible technique opens up an opportunity to scale-up the fabrication process.

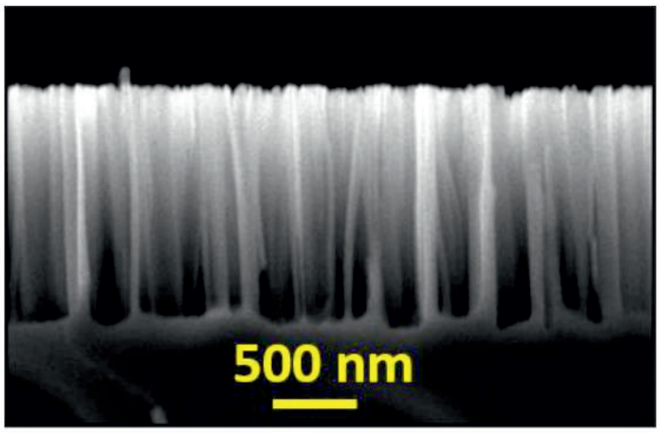

Scanning electron microscopy image of SiNWs fabricated by metal assisted chemical etching

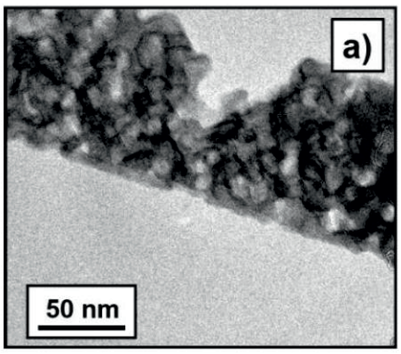

Transmission electron microscopy image porous SiNW.

6.4.2.2 First-principles studies on effect of functionalization and adsorption of various gases on two-dimensional nanostructures

Group-III two-dimensional (2D) mono-elemental systems such as borophene and aluminene have a number of allotropes with interesting electronic properties due to metallic bonding. Predictions of new allotrope ofaluminene monolayers, with interesting Dirac cones lying close to the Fermi level with Fermi velocity comparable to that of graphene and a new transition metal mono-chalcogenides with bandgaps were successful. Such systems hold promise as new members of *Dirac materials* and *2D bandgap materials* respectively, with potential applications in nanoelectronics and as energy materials. Exciting properties like emergence and tuning of magnetic moments and the charge polarities, signature of Fermi surface nesting, bandgap opening in metallic planar aluminene via formation of the van der Waals (trilayer) heterostructures of planar aluminene with BN monolayers have been observed from the studies of functionalization of 2D aluminene lattice. Besides, these pristine (2D aluminene and monochalcogenides) and functionalized systems have been employed to utilize their properties for various applications, like gas sensing behavior of these 2D materials. A comparative analysis reveals that 2D surfaces probed in this thesis may be superior tomany well-known pristine 2D systems, in terms of adsorption and sensing of gas molecules.

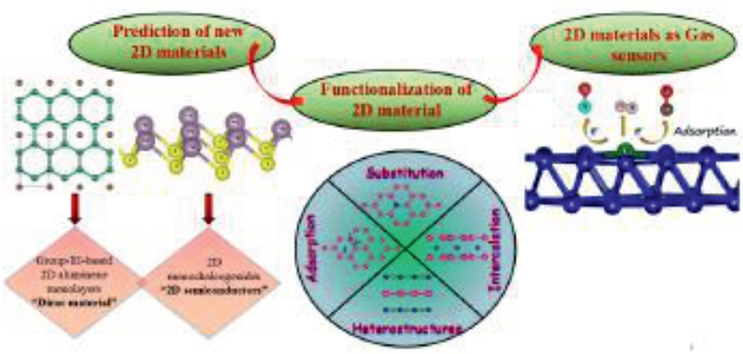

Prediction of novel 2D materials (aluminene and monochalcogenides) and functionalization of different allotropes of aluminene in pursuit of gas sensing applications.

6.4.3 Raja Ramanna Centre for Advanced Technology, Indore

6.4.3.1 Electronic transport studies on GaN epitaxial layers for the fabrication of radiation hard ultraviolet photodetectors

This thesis describes the fabrication of high performance GaN based ultraviolet (UV) photodetectors (PDs) for application in high radiation environment. Owing to a wide band gap, GaN based optoelectronic devices can operate under electric fields exceeding 1 kV and at high temperatures up to 600^0C. A Metal Organic Vapour Phase Epitaxy (MOVPE) system was developed for growing epitaxial films of GaN. Electronic transport measurements are performed on commercial samples of GaN grown using MOVPE and Hydride Vapour Phase Epitaxy (HVPE). While a highly conducting interfacial layer is present in HVPE GaNepilayers, it's absence in MOVPE GaN epilayers makes them attractive for device development. A method to enhance the detector performance is demonstrated by inserting a thin ZrO_2 layer in metal-oxide-semiconductor geometry. Thickness of ZrO_2 layer is rather critical where the specific detectivity of PDs is found to be similar or better than the state-of-the-art values reported in literature. Further, the role of dry etching in thefabrication of GaN PIN detectors in vertical geometry is discussed where a method to recover the etching induced damage is demonstrated using post etch O_2 plasma treatment. The PDs developed are also found to be radiation resistant to a high dose of ^{60}Co gamma rays. Systematic electronic transport measurements are performed to understand the fundamental mechanisms associated with current conduction in GaN epilayers and PDs under various experimental conditions. The understanding developed in this thesis is useful for the development of high-performance radiation hard GaN ultraviolet PDs.

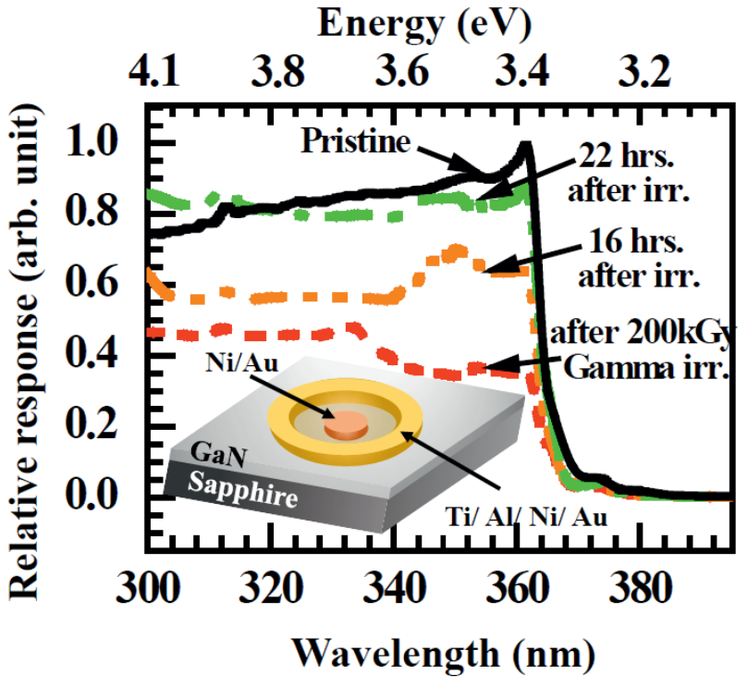

The photo response of GaN Schottky photo detector after irradiation with ^{60}Co Gamma source. Inset shows the schematic of device geometry

6.4.3.2 Static and ultrafast optical response of metal-semiconductor hybrid nanostructures

Metal-semiconductor hybrid nanostructures (HNS) is an emerging paradigm for construction of multi-functional advanced materials with synergistic interactions between metal nanoparticles (MNPs) and semiconductor quantum dots (SQDs). Appropriately designed HNS have potential applications as sensors, energy harvesters, efficient emitters and as better photocatalysts. This thesis demonstrated that in a mixed colloid of MNP and SQD, the properties of hybrid samples prepared by self-organized growth is decided by the variation in number density of hybrid vs unattached particles and not due to a continuous change in the interaction between them. This allowed structural characterization of self-organized HNS by optical measurements. These studies are crucial for the advancement in the area of colloidal self-organization. Using this method, a semiconductor quantum dot could be placed between two Ag nanospheres in the hot-spot region. This assembly technique can be extended to other noble metals and semiconductor quantum dots capped with thiols. This is an important step for the applications of hot-spot. The underlying mechanism of ultrafast response in HNS is modelled using electromagnetic theory, two-temperature model and hot-electron transport. Each of these variations plays an important role depending on the structure of Ag-CdTe hybrid. To quantify the hot-electron transport in HNSs, a method is developed that estimates the number of electrons hopping between the two constituents of the hybrid at ultrafast time scales. This provides a way to optimize the design of a metal-semiconductor hybrid system for optoelectronic and catalytic applications.

6.4.3.3 Thermal conductivity and critical current density of vanadium based alloy superconductors

Thermal conductivity κ and critical current density are the two most important properties for high magnetic field applications of superconductors. This thesis presents the studies on $V_{1-x}Ti_x$ alloys, which may emerge as an alternative to Nb based superconductors. Thermal conductivity κs of these alloys in the superconducting state increases with decreasing temperature, indicate thepredominance ofphononcontribution to heat conduction below Tc, whileit is electrons which contribute to heat conduction in the normal state. This is attibuted to electronic mean free path being in the range of interatomic distancewhile the grain size is very large. Addition of 1 at.% Gd in $V_{0.60}Ti_{0.40}$ results in twenty-fold enhancement inJc at 4K(without any complicated thermo-mechanical treatments) due to formation of Gdprecipitates along the grain boundaries. While the addition of Gdsuppresses the phonon thermal conductivity by 80%, electronic thermal conductivity reduces only by 15% and a crossover occurs from phonon dominated to electron dominated heat conduction in the superconducting state at 8 Tesla. Further, not only superconductivity persists in these alloys even in the presence of the ferromagnetic order, the superconducting transition temperature increases slightly. The very high Jc of the $V_{1-x}Zr_x$ alloys were observed to be due to the presence of huge number of grain boundaries generated during the eutectic reaction. Moreover, the presence of different metallurgical phases that remain normal down to 2 K led to the formation of normal channel of heat conduction in the $V_{1-x}Zr_x$alloys when bulk of the sample remains superconducting. In summary, this thesis provides insights into both the scientific and technological aspects of the V-based alloy superconductors

6.4.3.4 Strongly correlated band insulators and emergent superconductivity: A generalized Gutzwiller projection approach

The thesis treats strong correlations in a system where inhomogeneities and e-e interactions are equally strong using Gutzwiller projection of holes from the low energy Hilbert space at some lattice sites while excluding doublons from the low energy Hilbert space at some other lattice sites. The effective Hamiltonian has non-zero hopping terms even at half-filling, in contrast to the strongly correlated limit of the Hubbard model, which is a frozen Heisenberg model at half-filling. Unconventional superconductivity (SC) occurs when a strongly correlated antiferromagnetic (AF) Mott insulator or a moderately correlated spin density wave insulator is away from commensurate filling with charge carriers. Well known examples arecuprates, organic superconductors, pnictides, chalcogenides and more recently in magic angle twisted bilayer graphene. This thesis shows how unconventional SC is born out of a strongly correlated band insulator at half-filling. Advantage of realizing SC at half-filling is the absence of disorder that usually accompaniesa doped system. The thesis studies the ionic Hubbard model (IHM) which has in addition to onsite Coulomb repulsion U, a staggered ionic potential Δ applied to itinerant electrons. At half-filling, in the limit of U≈Δ>>t, SC appears by formation of a coherent macroscopic quantum condensate of electron pairs, provided the metal has enough low energy quasiparticles and the system has enough frustration against the magnetic order. The SC phase is surrounded by exotic metallic phases like ferrimagnetic metal, paramagnetic metal and a sliver of AF half metallic phase. The SC phase has a high $T_c$comparable to cuprates which may be further enhanced by tuning parameters in the Hamiltonian.

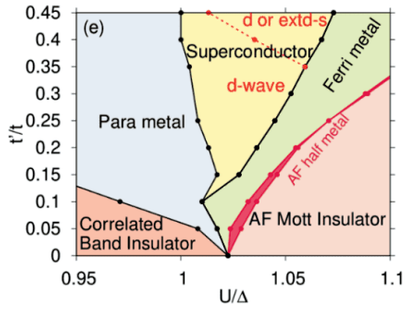

Sufficient frustration stabilizes unconventional SC in strongly correlated band insulators at half-filling

6.4.3.5 Oxide dispersion, microstructure, texture and radiation stability of high Cr ODS alloys

The thesis studies the effect of Ti & Cr on the microstructure, texture and hardness in model Oxide Dispersion Strengthened (ODS) alloys of composition Fe-0.3Y_2O_3, Fe-0.2Ti-0.3Y_2O_3 and Fe-14Cr-0.2Ti-0.3Y_2O_3. The Cr added alloy has finer microstructure with random texture whereas Fe-0.3Y_2O_3 and Fe-0.2Ti-0.3Y_2O_3 alloys have alpha texture. Texture evolution was studied in the commercial alloy 18 Cr ODS as a function of cold work and annealing temperature.

Substructure formation initiated at 1150 °C. Different Alpha and gamma texture components were excited with cold work and retained up to 1050 °C. Texture transformation was observed towards Goss or Brass orientation at higher temperatures. The mechanism of the texture transformation is aided by high energy boundaries with high mobility associated with a misorientation range of 15-45°.

TEM study showed that refinement of particle size takes place on addition of Ti and a further refinement is observed in presence of Cr. Ti forms complex oxide particles structurally consistent with orthorhombic Y_2TiO_5 orfcc $Y_2Ti_2O_7$.Cr favoursorthorhombic Y_2TiO_5. No specific correlation between composition and size of oxide particle was observed. Ni ion irradiation (5 MeV) of $Fe_{0.2}Ti_{0.3}Y_2O_3$ and Fe-14$Cr_{0.2}Ti_{0.3}Y_2O_3$ alloys was studied for a damage level of 40 dpa at 600 and 700 °C. Particle size reduces at 700 °C. In presence of Cr, the reduction is more pronounced. Possible explanations for the role of Cr in speeding up the oxide particle dissolution process are (i) dissolution of initial finer particles promptly increases the frequency of much finer ones or (ii) Cr rich shell around particles with lower displacement energy created net vacancy bias towards particles favouring dissolution/mass loss.

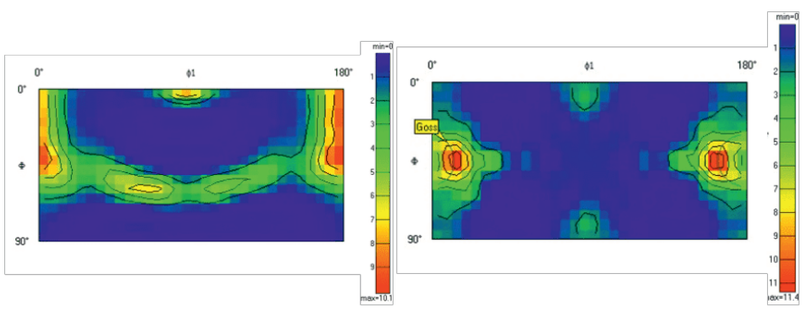

Texture-ODF in 50 % CW 18 Cr ODS –annealed at 1050 °C-Φ_2=45° (top) and 1250 °C - Φ_2=0° (bottom) section.

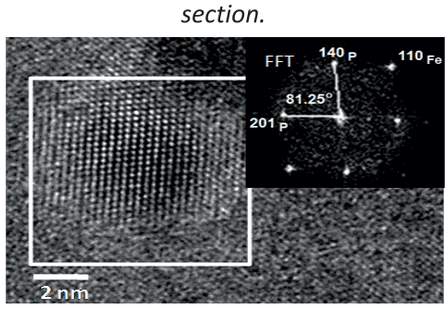

HRTEM image from a particle in Fe–14Cr–0.2Ti–0.3Y_2O_3 with the FFT taken from the highlighted region indexed as orthorhombic Y_2TiO_5

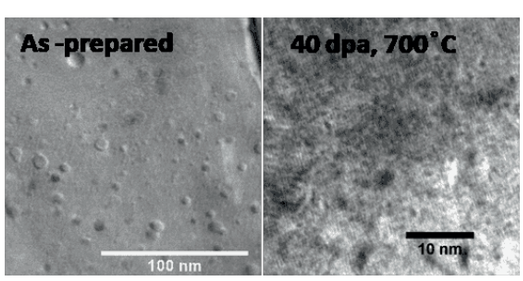

Bright field-TEM images of the Fe-14Cr-0.2Ti-0.3Y_2O_3 alloy (a) as-prepared with oxide particles; (b) 5 MeV Ni^{2+} ion irradiated at 40 dpa at 700 °C with extremely fine particles.

Section III
List of students who have completed Ph.D. during April 1, 2020-July 31, 2021

Discipline: Chemical Sciences

S. No.	Name of the Student	CI	Enrolment No.	Title of the Thesis
1	Rahul Kumar	BARC	CHEM01201404024	Theoretical Studies on Selected Organic Chalcogen Systems
2	Dipak Kumar Sahoo	NISER	CHEM11201404004	Non covalent Interactions in Ionic Liquids: Key to their Applications in Gas Absorption Solvolysis and Biomolecule Interactions
3	Abhishek Das	BARC	CHEM01201404021	Synthesis, Mechanistic Study and Interaction of Metal Nanoparticles with Biologically Important Molecules
4	Abhishek Kumar Sharma	BARC	CHEM01201204015	Radiochemical Separation and Purification of Molybdenum-99 for Medical and Industrial Applications
5	Amrita Das	BARC	CHEM01201104009	Synthesis of Novel Ligands for Extraction of Metal Ions from Aqueous Medium and Theoretical Investsigation for the Extraction Mechanism
6	Asmita Sharma	BARC	CHEM01201404007	Kinetic Studies of Gas Phase Reactions of Volatile Organic Compounds (VOCs) Relevant in Atmospheric Chemistry
7	Biranchi Muni Tripathi	BARC	CHEM01201304016	Synthesis, Characterization and Sinterability of Nanoceramics
8	Deepak Rawat	BARC	CHEM01201304001	Thermodynamic Investigations of Phosphate-based Crystalline Ceramic Matrices for HLW Immobilization
9	Dheeraj Jain	BARC	CHEM01201204014	Preparation, Characterization and Thermophysical Investigations on Thorium-based Nuclear Fuels and Related Systems
10	Diksha Pant	BARC	CHEM01201404022	Isotope and Hydrochemical Investigation on Uranium in Groundwater of South-West Punjab and Central Rajasthan
11	Lokpati Mishra	BARC	CHEM01201404006	Experimental Detection of Actinides in Human body and Computational Investigations of their Decorporation Mechanism

12	Madhusudan Ghosh	BARC	CHEM01201304020	Studies on interaction of Niobium and Protactinium with Hydrous Oxides
13	Meenakshi Joshi	BARC	CHEM01201504005	Electronic Structure and Chemical Bonding in Novel Lanthanide and Actinide Compounds: A Comprehensive Theoretical study
14	Nicy Ajith	BARC	CHEM01201404005	Studies on Uptake of Arsenic by Metal Oxides
15	Prithwish Sinharoy	BARC	CHEM01201604005	Synthesis and Evaluation of Specific Extractants for Separation Processes in Back-end of Fuel Cycle
16	Rajwardhan N. Ambade	BARC	CHEM01201304009	Studies on the Development of Technology for the Production, Separation and Purification of Iodine-131 for Formulation of Therapeutic Radiopharmaceuticals
17	Santosh Lala Gawali	BARC	CHEM01201504019	Interfacial Modification of Nanoparticles for Biomedical Applications
18	Santosh Lala Gawali	BARC	CHEM01201504019	Interfacial Modification of Nanomaterials for Biomedical Applications
19	Sriram Kumar	BARC	CHEM01201404025	Investigation of Bi-metallic Oxide Composites for Electrochemical and Photoelectrochemical Splitting of Water
20	Sumit Pahan	BARC	CHEM01201504001	Preparation and Characterization of Ligand Functionalized Solid Support for the Selective Extraction of f- Elements
21	Vidya S. Thorat	BARC	CHEM01201204018	Chemical Durability Assessment of Glasses for Immobilization of High-Level Radioactive Waste
22	Vijay M. Telmore	BARC	CHEM01201304011	Chromatography based Methods for Determination of Trace Elements in Nuclear Materials
23	Y. Sunitha	BARC	CHEM01201504016	Proton Induced Gamma-ray Emission in the Analysis of Semiconductors and Energy Materials
24	Kantamani Rama Swami	IGCAR	CHEM02201504004	Solvent Extraction of Some Trivalent Lanthanides and Actinides in Alkyldiglycolamides and the Aggregation and

				Spectroscopic Investigations on the Extracted Phase
25	G. Murali Krishna	IGCAR	CHEM02201404004	Some Studies on the Electrochemical Behavior of Actinides and Fission Products in Room Temperature Ionic Liquids for Nuclear Fuel Cycle Applications
26	Sitakanta Panda	IGCAR	CHEM02201504006	Lanthanide and Transition Metal Ions Activated Phosphors for Optical and Radiation Dosimetry Applications
27	Shubhra Sarkar	IGCAR	CHEM02201504010	N-H···X (X=O, N, p) Hydrogen-bonded Interactions of Pyrrole: Matrix Isolation Infrared and Computational Studies
28	T. V. Beatriceveena	IGCAR	CHEM02201504003	Investigations on $AgInO_2$ and PbS: Preparation, Characterization and Gas Sensing Behaviour of Thick and Thin Films
29	Srinivasarao Kintali	RRCAT	CHEM03201204001	Second Harmonic (SH) Spectroscopic Studies on the Effect of Amphiphilic Molecules- induced Adsorption and Transport Characteristics of an Organic Cation across a POPG Lipid Bilayer.
30	Sandip Kumar De	SINP	CHEM05201504003	Crystal Engineering to Fabricate Au, Ag and Au-Ag Alloy Nanoparticles: Application in Technology, Pathology and Theranostics
31	Khokan Chowdhuri	NISER	CHEM11201504003	Sustainable Strategies for Carbon-Sulfur Bond Formation Reactions in Organic Synthesis
32	Ramu V. Ranga Naidu Chinta	NISER	CHEM11201504005	Naphthalimide, Naphthaldehyde and Benzaldehyde based Fluorescent Materials: Synthesis of 1,2-Disubstituted Ferrocenes from Ferrocenyl *p*-tolylSulphoxide
33	S. Thiyagarajan	NISER	CHEM11201504016	Catalysis Based on Ruthenium Pincer Complexes
34	Sangya Chitranshi	NISER	CHEM11201504006	Contracted and Expanded Carbaporphyrinoids: Syntheses, Conformation and Coordination Chemistry
35	Suhas Shahaji Gawali	NISER	CHEM11201504008	Catalysis by Iron and Manganese Pincer Complexes

36	Syamasrit Dash	NISER	CHEM11201604031	Expanded Porphyrins: Ideal Models to Probe Conformational Topology, Möbius and Hückel Aromaticity

Discipline: Engineering Sciences

S. No.	Name of the Student	CI	Enrolment No.	Title of the thesis
1	Sree Ranjini K. S.	IGCAR	ENGG02201404011	Design Development and Optimization of High Temperature Motors for In Service Inspection devices
2	Mayank Rajput	IPR	ENGG06201504004	Study of Transmutation Gas Production and Displacement Damage in Iron, Tungsten and Chromium for D-T Neutron Irradiation
3	Jay Kirtikumar Joshi	IPR	ENGG06201504005	Inferring the Magnetization Effect in High Density CCRF Discharges- An Electrical Approach
4	Amit Sur	BARC	ENGG01201204004	Phase Extraction of Optical Interferometric Signals based on Improved Time-frequency Method with Application to High Strain Rate Measurement
5	Amol Wakankar	BARC	ENGG01201204009	Theories, Techniques and Tools for High Integrity Heterogeneous Embedded Systems
6	Shivam Mishra	BARC	ENGG01201204012	Design Analysis and Performance Evaluation of Fiberoptic Pressure Sensors based on Fabry-Perot Interferometer
7	Rupesh Kumar Choudhary	BARC	ENGG01201204015	Formation of Alumina Coatings by Thermal and Anodic Oxidation Processes and their Characterization
8	Bhuvaneshwar Gera	BARC	ENGG01201204022	Studies on Buoyancy Driven Flows through Large Openings
9	Paridhi Goel	BARC	ENGG01201304009	Design of an Efficient Venturi-Scrubber for Retention of Radionuclides during Severe Accident of a Nuclear Reactor
10	Sujay Bhattacharya	BARC	ENGG01201304027	Surface Characterization and Optimization of Wire Electric

				Discharge Machining Process of P91 Steel
11	Joti Nath Sharma	BARC	ENGG01201304031	Development of Macrocyclic Extractants for Selective Separation of Cesium, Strontium and Technetium from Radioactive Waste Solutions
12	Vakil Nafees Ahmed	BARC	ENGG01201304032	Evaluation of Bunsen Reaction and Phase Separation in Continuous Reactor
13	Mihir Chatterjee	BARC	ENGG01201304034	Investigation of Gas Species and Thermal Separation in Ranque-Hilsch Vortex Tube
14	Uttam Jain	BARC	ENGG01201304035	Development of Vanadium Alloys for Advanced Energy Systems
15	K. Sairam	BARC	ENGG01201304036	Processing and Properties of Boron Carbide based Composite with Rare Earth Metal Oxide as Sinter Additive
16	Darekar Mayur Ramesh	BARC	ENGG01201404004	Liquid-liquid Two-Phase Flow and Mass Transfer in Microchannels
17	Vikram Shukla	BARC	ENGG01201404010	Characterization of the Catalyst used in Passive Autocatalytic Recombiners for Hydrogen Mitigation in a Nuclear Reactor and Formulation of a Method for Containment Analysis
18	Abhishek Kaushik	BARC	ENGG01201404017	Robot-based Autonomous Neuroregistration and Neuro-navigation for Neurosurgery
19	Patel Shrenik Babulal	BARC	ENGG01201404022	State Estimation and Multivariate Process Monit-oring in Multiscale Framework
20	Dond Shantaram Kisan	BARC	ENGG01201404024	Parametric Influence on Electromagnetic Forming Processes
21	Anita Gupta	BARC	ENGG01201504003	Multipass Optical Cavity Based Technique for Trace Level Detection of Heavy Water
22	Amita Bedar	BARC	ENGG01201504008	Development and Characterization of Radiation Resistant Nanocomposite Polymeric Membranes

23	Ravi Kiran Akella	BARC	ENGG01201504016	Risk-based Seismic Performance Assessment of Pressurized Piping Systems Considering Ratcheting
24	Hrishekesh Mishra	BARC	ENGG01201718002	Design and Optimization of Microwave System for Energy Efficient Remediation of Nuclear and E-Waste
25	Padmanabhan G.	IGCAR	ENGG02201104028	Studies on Deep Excavation Behaviour in Engineered Backfilling Adjacent to Nuclear Safety Related Structures
26	Chandan Kumar Bhagat	IGCAR	ENGG02201204005	Design and Development of Wireless Acoustic Emission Sensor System for Structural Health Monitoring Applications
27	P. A. Manojkumar	IGCAR	ENGG02201204016	Synthesis and Modification of Graphene Nanowalls using Plasma Immersion Ion Implantation and Deposition Facility
28	G. Suneel	IGCAR	ENGG02201204018	Numerical Modelling of Joule Heated Ceramic Melter
29	Vinita Daiya	IGCAR	ENGG02201204019	Wirelessly Powered Secured Backscatter Communication for Wireless Sensor Network
30	Pradyumna Kumar Parida	IGCAR	ENGG02201304005	Study of Nano-dispersoid Characteristics in Oxide Dispersoid Strengthened Alloys
31	M. Divya	IGCAR	ENGG02201304006	Weldability of Borated Stainless Steel-(SS 304B4)
32	Saju T. Abraham	IGCAR	ENGG02201304007	Characterization of Polycrystalline Microstructure using Ultrasonic Nonlinearity Parameter
33	T. Sakthivel	IGCAR	ENGG02201304008	Effect of Geometry, Composition and Thermo-mechanical Treatment on the Type IV Cracking during Creep in Advanced 9Cr Ferritic Steels Weld Joint
34	K. Natesan	IGCAR	ENGG02201304010	Development of Mathematical Models and Investigation of FBR Plant Behaviour During Transients by a Coupled Single and Multi-dimensional Approach

35	Nidhin T.	IGCAR	ENGG02201304014	Study of Radiation Effects in SRAM-Based FPGAs for NPP I&C System Design
36	Kanhu Charan Sahoo	IGCAR	ENGG02201405008	Prediction of Creep Deformation and Rupture Behavior of 304HCu Austenitic Stainless Steel under Uniaxial and Multiaxial State of Stress at Different Temperatures
37	P. Rohith	IGCAR	ENGG02201405016	A Study on Deformation Mechanisms in Perfect and Twinned Cu Nanowires by Atomistic Simulations
38	Matcha Nani Babu	IGCAR	ENGG02201504004	Fatigue Crack Growth Behaviour of Nitrogen Bearing Austenitic Stainless Steel and its Weld: Analysis using Unified Approach
39	Athimoola S. Krishnan	IGCAR	ENGG02201504008	Investigation on Ductile Fracture of Structural Steels and Welds: Numerical Analysis and Experimental Assessment
40	Jinoop A. N.	RRCAT	ENGG03201604001	Experimental Studies and Parametric Investigation on Laser Directed Energy Deposition based Additive Manufacturing of Hastelloy-X Thin Walls and Bulk Structures
41	Zubairuddin Naimuddin Mohammed	IPR	ENGG06201104002	Thermo-mechanical Analysis of GTA Welding of Modified 9Cr-1Mo Steel considering the Effects of Phase Transformation, Pre heating and Post heating
42	Jain Yogesh Mithalalji	IPR	ENGG06201504001	Design, Development and Characterisation of a Passive Active Multijunction RF Launcher Compatible with Aditya -Upgrade Tokamak
43	Bhuva Montu Prafulbhai	IPR	ENGG06201504002	Magnetic Field Effects on Cold Hollow Cathode DC Discharge: An Experimental and Modeling Study
44	Zala Arunsinh Bakulsinh	IPR	ENGG06201504007	Investigations on Weldability of Aluminide Coated 9Cr Steel

45	Priti Kanth	IPR	ENGG06201504009	Nuclear Activation Studies in Fusion Systems: New Methods and Algorithms

Discipline: Life Sciences

S. No.	Name of the Student	CI	Enrolment No.	Title of the thesis
1	Parasani Neha Rajkumar	BARC	LIFE01201304003	Molecular Processes of Adaptive Response in Human Peripheral Mononuclear Cells in Response of Ionizing Radiation
2	Shridhar Suresh Paranjape	BARC	LIFE01201404007	Starvation Induced Physiological Changes in Vibrio Cholerae
3	Saran Chattopadhyaya	SINP	LIFE05201404002	DNA Replication-Repair in Megakaryopoiesis
4	Saujanya Acharya	TMC	LIFE09201204002	Characterization of High Temperature Requirement Serine Protease and its Binding Partners
5	K Raghupathi	TMC	LIFE09201304015	Deciphering the Mode of Regulation and Understanding Protein-Protein Interactions of Human HtrA Serine Proteases
6	Bibekananda Sahoo	NISER	LIFE11201304002	Regulation Mechanism of Chikungunya Virus Cell Entry Proteins
7	Md Khurshidul Hassan	NISER	LIFE11201304003	Understanding the Role of EEF1A2 in Tumor Angiogenesis and Progression
8	Omprakash Singh	NISER	LIFE11201304004	TRH-containing System and its Regulatory Circuitry in the Brain: Organization, Evolution and Role in Regulation of Food Intake and Energy Balance
9	Bushra Hayat	NISER	LIFE11201404001	Dissecting the Role of Genes Involved in Proteostasis Maintenance and Wnt Signaling in the Pseudoexfoliation Pathogenesis
10	Rakhee Yadav	BARC	LIFE01201304007	Cellular and Molecular Basis of Thorium-induced Cytotoxicity and Carcinogenesis

11	Ravi Prakash Sanyal	BARC	LIFE01201404001	Molecular and Biochemical Characterization of Cu/Zn Superoxide Dismutase Splice Variants of Rice (Oryzasativa)
12	Neena Girish Shetake	BARC	LIFE01201404004	Biological Evaluation and Mechanistic Insights of Targeted Nano-formulation for Combinatorial Cancer Therapy
13	Shikha Pachauri	BARC	LIFE01201404005	Structural and Functional Analysis of a Trichoderma virens GAPDH Associated with a Secondary Metabolism Related Gene Cluster
14	Avi Raizada	BARC	LIFE01201404006	Development of Genic-markers for Yellow Mosaic Virus and Bruchid Resistance Traits in Black Gram (*Vigna mungo* (L.) Hepper)
15	Ravindra Bansal	BARC	LIFE01201504001	Functional Analysis of Three Genes Downregulated in a Non-conidiating Mutant of *Trichoderma virens*
16	Vanshika Adiani	BARC	LIFE01201504004	Biochemical Markers as a Tool for Rapid Detection of Microbial Spoilage in Minimally Processed Fruits
17	Dhiman Chakravarty	BARC	LIFE01201504005	Physiological and Structural Characterization of a Manganese Catalase (KatB) from the Filamentous, Heterocystous, N_2-fixing Cyanobacterium *Anabaena* PCC 7120
18	Manish Pandey	BARC	LIFE01201504006	Studies on Redox Associated Molecular Changes under Salt Stress in Rice (Oryza Sativa L.)
19	Deepti Singh	BARC	LIFE01201504014	Investigation of Molecular Mechanisms Underlying Antibacterial Potential of Allylarene and Stilbene Class of Phytochemicals
20	G. Kiran Kumar Reddy	BARC	LIFE01201604005	Antibiofilm and Antimacro-fouling Potential of Alkylimidazolium Ionic liquids

21	Satyabrata Maiti	SINP	LIFE05201504004	Non-Canonical Base Pairs in RNA and their Involvement in Double Helix Formation
22	Kaushik Chanda	SINP	LIFE05201504005	Understanding the Roles Played by Receptor Tyrosine Kinase(s) and Non-Coding RNA(s) in Neurodegeneration
23	Shweta Singh	SINP	LIFE05201504007	Role of Epstein-Barr Virus in Epithelial Cell Cancer
24	Shalini Dimri	TMC	LIFE09201304001	Molecular Imaging of STAT3 Signaling In Vivo
25	Asmita Sharda	TMC	LIFE09201304002	Histone H3 Modifications and their Role in DNA Damage Response
26	Marathe Pravin Vitthal	TMC	LIFE09201304003	Creation of Novel Photochangable Fluorescent Protein through Directed Evolution
27	Amnekar Ramchandra Vijay	TMC	LIFE09201304005	Phosphoacetylation of Histones during Cellular Transformation in Mammalian Cells
28	Kadam Chittarnjan Rajashree	TMC	LIFE09201304006	Elucidating the Role of Clusterin in Human Oral Cancers
29	Dhanashree Chandrakant Mundhe	TMC	LIFE09201304008	Assessing the Role of Activins /Inhibins in Human Oral Cancers
30	Raikamal Paul	TMC	LIFE09201304012	Role of miR-592 and miR-204 in Medulloblastoma Patho-genesis
31	Raghava Reddy Sunkara	TMC	LIFE09201304013	Defining the Molecular Signaling Mechanism in Epidermal Stem Cell Regulation and Cancer
32	Mahalakshmi Ramachandran Harish	TMC	LIFE09201304014	Fine Specificity of Domain-motif Interaction and the Role of Structure: A Case Study with Proteasomal Chaperones
33	Mythreyi Narasimhan	TMC	LIFE09201304016	Proteomic Profiling of Leukemic Cells in Philadelphia Chromosome Positive Leukemia
34	Togar Trupti Ajay	TMC	LIFE09201404002	Genome-wide Approaches to Characterize Novel Genetic Elements Causing Cancer

35	Rathod Maitreyi Amit	TMC	LIFE09201404007	Identifying Mechanisms that Regulate Human Sodium Iodide Symporter gene (hNIS) in breast cancer
36	Harish Shrikrishna Bharambe	TMC	LIFE09201404008	Molecular Mechanism Underlying the Effect of miRNA Expression on Medulloblastoma Cell Behavior
37	Dhadve Ajit Chandrakant Shobha	TMC	LIFE09201404011	Investigating the Role of IGF-1R Signalling in Development and Maintenance of Chemoresistance in Ovarian Carcinoma
38	Abhilash Nitin Deo	TMC	LIFE09201504017	Role of IGF1R in Ovarian Cancer Metastasis
39	Devanand T.	IMSc	LIFE10201404002	Allosteric Effects in Protein Dynamics and their Interactions with Membranes
40	Dinesh Kumar	NISER	LIFE11201404002	The Role and Signaling Mechanism of IQGAP2 in Breast Cancer Tumorigenesis and Angiogenesis
41	Sanjai Kumar P.	NISER	LIFE11201404006	Role of TRP Channels in Experimental Cell Mediated Immunity
42	Pratikshya Ray	NISER	LIFE11201404008	Effects of Perturbation of Gut Microbiota on host Physiology: In C57BL/6 BALB/c Mice Models
43	Somdatta Saha	NISER	LIFE11201404011	Crosstalk between Cyto-skeleton and Membrane Components with Thermo-sensitive Ion Channels in the Context of Diverse Physio-logical Functions

Discipline: Mathematical Sciences

S. No.	Name of the Student	CI	Enrolment No.	Title of the thesis
1	Bhuwanesh Rao Patil	HRI	MATH08201204001	Additive and Multiplicative Patterns in the Natural Numbers
2	Pradeep Das	HRI	MATH08201304002	Topics in the Symplectic and Kahler Geometry of Moduli Spaces of Representations of Quivers

3	Bidisha Roy	HRI	MATH08201504001	Some Problems in Algebraic and Combinatorial Number Theory Connected with Finite Abelian Groups
4	Jaitra Chattopadhyay	HRI	MATH08201504003	Some Problems in Ideal Class Groups and Related Topics
5	Mithun Kumar Das	HRI	MATH08201304005	Some Topics on Dirichlet L-Functions
6	Anoop Singh	HRI	MATH08201404001	Problems in the Theory of Connections in Algebraic Geometry
7	Subha Sarkar	HRI	MATH08201504005	On Some Problems in Additive Combinatorics and Related Areas
8	Narayanan P. A.	IMSc	MATH10201304004	Eigenvalue Statistics of Higher Rank Anderson Tight Binding Model over the Canopy Tree
9	Tale Prafullkumar Prabhakar	IMSc	MATH10201305002	Some Results on Graph Contraction Problems
10	Krishanu Roy	IMSc	MATH10201305003	Pi-systems of Symmetrizable Kac-Moody Algebras.
11	Digjoy Paul	IMSc	MATH10201504005	The Multiset Partition Algebra
12	Lawqueen Kanesh	IMSc	MATH10201504008	Parameterized Complexity of Conflict-free Solutions
13	Sanjukta Roy	IMSc	MATH10201504009	Select, Allocate, and Manipulate via Multivariate Analysis
14	Roohani Sharma	IMSc	MATH10201504012	Advancing the Algorithmic Tool-kit for Parameterized Cut Problems
15	Oorna Mitra	IMSc	MATH10201504013	Qusai-isometries of Zn and Twisted Conjugacy in Certain Linear Groups
16	Amit Kumar	NISER	MATH11201504001	Comparison of Order Projections in Absolute Matrix Order Unit Spaces
17	Sujeet Kumar Singh	NISER	MATH11201504002	Certain Congruences among Hermitian Jacobi Forms and Hermitian Modular Forms

Discipline: Medical & Health Sciences

S. No.	Name of the Student	CI	Enrolment No.	Title of the thesis
1.	Arti R. Kulkarni	TMC	HLTH09201204001	Dosimetric and Quality Assurance Studies in High Dose Diagnostic Imaging Modalities to Establish National Radiation Protection Programme
2.	Kavita V. Anand	TMC	HLTH09201304007	Performance of HPVDNA Test in Presence of Co-infection With Common Reproductive Tract Infections

Discipline: Physical Sciences

S. No.	Name of the Student	CI	Enrolment No.	Title of the thesis
1	Sherley Joseph Ray	BARC	PHYS01201304034	Development of Improved Methods for Lattice and Core Physics Simulations of Thermal Reactors
2	Madhusmita Panda	IGCAR	PHYS02201304007	Synthesis and Characterization of Diamond Like Carbon (DLC) based Nano-composite Thin Films Grown by PLD
3	Sithara Vinod	IGCAR	PHYS02201404001	Studies on the Effect of Magnetic Field Induced Aggregation on Physical Properties of Ferrofluids
4	Mukund Kumar	RRCAT	PHYS03201404004	Studies on Characterization and Application of Ultrashort Higher Harmonic Radiation
5	Subhomoy Haldar	RRCAT	PHYS03201404012	Magneto-Optical Transport Studies on Ultra Low Disordered Semiconductor Quantum Wells Grown by MOVPE
6	Soumik Bhattacharya	VECC	PHYS04201404003	Yrast And Near-Yrast Structure of Nuclei In A ~ 200 Region Involving High-J Orbitals
7	Sajad Ahmad Bhat	SINP	PHYS05201504018	Some Studies on Novel Phases of Neutron Stars and their Observational Consequences
8	Sonu Yadav	IPR	PHYS06201204012	Effect of Inhomogeneous Magnetic Field on Helicon Antenna Produced Expanding Plasma
9	Harshita Raj	IPR	PHYS06201304012	Study Of Generation and Transport of Runaway Electrons in Aditya and Aditya-U Tokamak
10	Ashis Kumar Manna	IOP	PHYS07201304006	Growth of TiO_2, ZnO Nano-structured Films for Investigation of

				Resistive Switching Photo Absorbance Properties, Glucose Sensing and Structural Phase Transition
11	Debashis Saha	IOP	PHYS07201304008	Production Of Higgs Boson in Association with another Two Bosons at the Hadron Colliders
12	Dheeraj Kumar Mishra	IMSc	PHYS10201304006	Thermodynamic Corrections Due to an Invariant Ultraviolet Scale and its Implications
13	Shilpa Kastha	IMSc	PHYS10201404001	Gravitational Waves from Compact Binary Coalescences: Tests of General Relativity and Astrophysics
14	R Prashanth	IMSc	PHYS10201404003	Positive Geometry of Scalar Theories
15	Atanu Bhatta	IMSc	PHYS10201204005	Holographic Conformal Partial Waves
16	Prafulla Oak	IMSc	PHYS10201304007	Holographic and Exact RG Beta Function Computations of the Sine-Gordon Model
17	Debadeepti Mishra	NISER	PHYS11201304011	Particle Production Studies in Au+Au and U+U Collisions using the Star Detector at RHIC and Understanding the Freeze-out Dynamics
18	Sushree Subhadarshinee Sahoo	NISER	PHYS11201304013	Applications of FWM and XPM Induced by Ground State Coherence in Thermal Atomic Vapor
19	Anil Kumar Singh	BARC	PHYS01201304014	Pulsed Laser Surface Treatment of Metals for Enhanced Field Emission Studies
20	Argala Srivastava	BARC	PHYS01201304017	Neutronic Studies for the Development of a Time Dependent Monte Carlo Code
21	Naveen Kumar Sudama Prasad Gupta	BARC	PHYS01201304023	Surface Enhanced Vibrational Spectroscopy and High-Pressure Studies of Biomolecules
22	Ingale Sanjay Vishwasrao	BARC	PHYS01201304025	Studies on Sensitivity of Nanosized Energetic Materials
23	Nishant Kumar	BARC	PHYS01201304027	Understanding of Fission Dynamics from Fragment Mass Distribution Studies
24	Gyan Chandra Chauthwani	BARC	PHYS01201304036	Analysis of Radioisotope Depletion and Generation using Klopfenstein-Shampine Family of Numerical Differentiation Formula
25	Vitisha Suman Dagre	BARC	PHYS01201304038	A Study of Active Experimental Techniques for Neutron Dosimetry in Positive Ion Accelerator
26	Mohammad Nizam	BARC	PHYS01201404006	A Study of Hadron Energy Estimation in ICAL@INO and Feasibility of a PET Device Based on Multi-gap RPCs

27	Chinmay Raghunath Borwankar	BARC	PHYS01201404012	Monte Carlo Simulation Studies of Imaging Atmospheric Cherenkov γ Ray Telescope MACE (Major Atmospheric Cherenkov Experiment)
28	Paramjit Rana	BARC	PHYS01201404017	Study of Spectral Beam Combination Techniques for High Power, Pulsed Dye Laser Applications
29	Shilpi Gupta	BARC	PHYS01201404018	Shell Effects in Fission Fragment Mass Distribution of Neutron Deficient Nuclei around A~200
30	Harisree K.	BARC	PHYS01201404019	Radiation Background Studies for Rare Decay Experiments
31	Pravat Kumar Swain	BARC	PHYS01201404021	Liquid Metal MHD Studies at High Magnetic Fields Relevant to Fusion Test Blankets
32	Pethuraj S.	BARC	PHYS01201404022	Studies of Atmospheric Fluxes at the Prototype Iron Calorimeter Detector
33	Dhurv Dinesh Mulmule	BARC	PHYS01201504023	Studies of Reactor Anti-neutrinos with ISMRAN
34	Mrinal Jauhari	BARC	PHYS01201504026	Structural Phase Transitions and Phonon Anomalies in Alkaline Niobate Based Functional Materials
35	Sarita	BARC	PHYS01201604002	Computational and Experimental Studies on the Damage Response of Ferritic and Austenitic Steels under Extreme Conditions
36	Manish Kumar Sahai	BARC	PHYS01201604010	Uncertainty Modeling of Thermoluminescence Glow Curve and Development of Deconvolution Technique to Resolve TL peak
37	Nirmal Kumar Ray	BARC	PHYS01201604021	Reactivity Measurement Using Deterministic and Noise Methods in Brahmma Subcritical System
38	Pralay Paul	BARC	PHYS01201604026	Structural and Magnetization Studies on Selected Multiferroic Oxides
39	Mulla Ahmad Basha	BARC	PHYS01201604027	Evolution of Depth Dependent Structure and Magnetic Properties of Multilayers on Annealing
40	Sumita Santra	IGCAR	PHYS02201104012	Oxide Dispersion, Microstructure, Texture and Radiation Stability of High Cr ODS Alloys
41	Narayanan M. M.	IGCAR	PHYS02201204012	Development of Non-contact Ultrasonic Guided Wave-based Methodology for Inspection of Steam Generator Tubes of PFBR
42	Anuraj V. L.	IGCAR	PHYS02201204018	Studies on Stability Characteristics of MOX and Metal Fueled Fast Reactor Cores

43	M. Mohideen Abdul Razak	IGCAR	PHYS02201204019	Studies on PHWR Transients using Modified Exponential Time Differencing Method with Improved Quasi Static (IQS) Model and Associated Dynamic Sensitivity Analysis
44	Alaka Panda	IGCAR	PHYS02201404003	Mössbauer Studies on Some Fe-based Multiferroic Materials
45	P. Balasaritha	IGCAR	PHYS02201404004	Inert Gas Ion Irradiation Effects on Microstructural and Optical Properties of Monoclinic Zirconia
46	Anil Kumar Behera	IGCAR	PHYS02201404008	Fabrication, Selected Micro-structure- Property Correlations and Applications of Si Nanowalls
47	Harimohan V.	IGCAR	PHYS02201404010	Magneto-transport Studies on the Single Crystals of $TaAs_2$ and $NbAs_2$ Semimetals
48	Rakesh P. T.	IGCAR	PHYS02201404011	Observational Analysis and Numerical Simulation of Meteorological Phenomena Leading to Severe Radiological Impact
49	Bijay Kumar Das	IGCAR	PHYS02201504008	Infrared Spectroscopic Studies on Pristine and Doped Bismuth Ferrite Ceramics
50	Thirukkumaran K.	IGCAR	PHYS02201504015	Acoustic Emission Signal Characterization and Infrared Thermography Studies during Drilling of Metal Matrix Composites
51	Ijee Mohanty	IGCAR	PHYS02201504016	Development of TDEM System with SQUID and Fluxgate for Geophysical and NDE Applications.
52	Balasubramanian S.	IGCAR	PHYS02201504018	Fabrication and Characterization of SiO_2 Microcantilevers for Relative Humidity Sensing
53	Binaya Kumar Sahu	IGCAR	PHYS02201504020	Growth and Applications of Low Dimensional SnO_2
54	Gopinath Sahoo	IGCAR	PHYS02201504023	Surface Modification and Polymer-Free Transfer of Vertical Graphene Nanosheets for Electrochemical Capacitor Applications
55	Reshmi Mohan P.	IGCAR	PHYS02201504027	Numerical Modelling Studies on the Impact of Horizontal Resolution, Explicit Convection and SST Boundary Forcing on the Prediction of Tropical Cyclones over North Indian Ocean
56	Revati Rani	IGCAR	PHYS02201604002	Tribological Properties of Ultrananocrystalline Diamond Films at High Temperature and Controlled Atmosphere

57	Arup Ratan Jana	RRCAT	PHYS03201304004	Electromagnetic Design and Beam Dynamics Studies in Elliptic Superconducting Radiofrequency (SRF) Cavities
58	Vinod Kumar Saini	RRCAT	PHYS03201304005	Laser Based Isotope-Selective Photoionization Studies on Lithium
59	Dipanjana Hazra	RRCAT	PHYS03201304009	Laser Driven Plasma Based Electron Acceleration, Applicable Mechanisms and its Applications
60	Saroj Kumar Jena	RRCAT	PHYS03201404001	Optimization of a Multi Bunch Train Filling Pattern for the Suppression of Beam Ion Instability in Electron Storage Ring: Case Study of Indus-2
61	Praveen Kumar Yadav	RRCAT	PHYS03201404002	Studies on Synchrotron Radiation Induced Contaminations and Development of Optics Refurbishing Techniques
62	Mohammad Tayyab	RRCAT	PHYS03201404003	Studies on Ion Acceleration in Ultrashort Ultra-high Intensity Laser Matter Interaction
63	Arindam Majhi	RRCAT	PHYS03201404006	Surface/Interface Studies of Thin Films and Development of Ultra-Short Period W/B_4C Multilayer Mirrors with Large Layer Pairs
64	Charu Mishra	RRCAT	PHYS03201404009	Studies on Electromagnetically Induced Transparency in ^{87}Rb Atoms
65	Mangalika Sinha	RRCAT	PHYS03201404011	Study of Structural and Optical Properties of Oxides in Soft X-ray Regime
66	Dhanshree Pandey	RRCAT	PHYS03201504002	First- Principles Studies on Effect of functionalization and Adsorption of Various Gases on Two-Dimensional Nanostructures
67	Sabina Gurung	RRCAT	PHYS03201504003	Static and Ultrafast Optical Response of Metal-Semiconductor Hybrid nanostructures
68	Abyay Ghosh	RRCAT	PHYS03201504005	Lifshitz Transition in Some Recently Discovered Iron based Superconductors
69	Sabyasachi Paul	RRCAT	PHYS03201504009	Thermal Conductivity and Critical Current Density of Vanadium based Alloy Superconductors
70	Abhishek Chatterjee	RRCAT	PHYS03201504011	Electronic Transport Studies on GaN Epitaxial Layers for the Fabrication of Radiation Hard Ultraviolet Photodetectors
71	Shweta Verma	RRCAT	PHYS03201504012	Studies on Plasmonic Responses of Metal Nanoparticles of Varied Morphologies and their Interaction with Semiconductor Nanostructures

72	Santu Dey	VECC	PHYS04201304011	Study of Effect of Deformation & Irradiation on the Microstructure of FCC Materials using X-ray Diffraction
73	Shaikh Safikul Alam	VECC	PHYS04201404007	Development of Fast Timing Array at VECC and its Application in Nuclear Structure Study around Z = 50 and N = 82 Shell Closure
74	Shabnam Mohsina	VECC	PHYS04201404010	Systematic Study of Entrance Channel Effect using Langevin Dynamics in Heavy-ion Induced Reaction
75	Ranabir Banik	VECC	PHYS04201404012	Single Particle and Collective Excitations near Z=50
76	Nachiketa Sarkar	VECC	PHYS04201404013	A Study of Hadronic Phase of Strongly Interacting Matter with Finite Size Effects
77	Soumen Nandi	VECC	PHYS04201504014	Experimental Study of Shape Evolution in Nuclei near Z=82
78	Biswajit Banerjee	SINP	PHYS05201304005	Multiwavelength Long Term Monitoring and Spectral Energy Distribution Modeling of Bright Active Galactic Nuclei Markarian 421
79	Shamik Ghosh	SINP	PHYS05201304015	Search For Physics Beyond the Standard Model in Photon + Missing Transverse Momentum Final State in Proton-Proton Collisions Using the Compact Muon Solenoid Detector at The Large Hadron Collider
80	Rajarshi Bhattacharya	SINP	PHYS05201304017	Search for Higgs Boson Pair Production in the $HH\,bb_{TT}$ Channel in p-p collisions using CMS data at $\sqrt{s}$ = 13 TeV at the LHC
81	Anway Pradhan	SINP	PHYS05201404003	Study of MOCVD Grown AlGaAs/GaAs (100) Spontaneous Superlattice and its Application for Optoelectronic Devices
82	Gourab Bhattacharjee	SINP	PHYS05201404007	Noble Metal Core-Shell Nanoparticles with High-Energy Facets for Application in Surface Enhanced Raman Scattering and Biosensing
83	Suman Mukherjee	SINP	PHYS05201404008	Growth and Characterization of Semiconductor Quantum Dots for Optoelectronic Device Applications
84	Arghya Mukherjee	SINP	PHYS05201404010	Hadronic Properties in Presence of Magnetic Field
85	Abhijit Roy	SINP	PHYS05201504002	Structural Study of Metal Nanostructure on Semiconductor Surface and their Multifunctional Applications

86	Mantu Nirmal Modak	SINP	PHYS05201504003	Fundamental and Functional Properties Associated to Exotic Phase Transitions in Novel Rare Earth based Intermetallic Compounds and Heusler Alloys
87	Sangeeta Das	SINP	PHYS05201504004	Study of Nuclear Structure Near Shell Closure
88	Jhuma Ghosh	SINP	PHYS05201504005	Charmonium Studies at Forward Rapidity with ALICE Muon Spectrometer at the LHC
89	Moumita Das	SINP	PHYS05201504008	Study of Magnetic, Thermal and Dielectric Properties of some Rare-Earth based Oxides
90	Sajad Ali	SINP	PHYS05201504010	Structural Evolution of Weakly Deformed Nuclei in Mass ~140 Region with Increasing Angular Momentum
91	Wadut Shaikh	SINP	PHYS05201504011	Bottomonium Studies at LHC Energy using Alice Muon Spectrometer
92	Abhishek Rakshit	SINP	PHYS05201504012	Transition Metal Oxide-based Devices for Memory Applications
93	Arpita Das	SINP	PHYS05201504017	Study of Laser Induced Coherent Phenomena in the Rubidium Atomic Medium
94	Avik Banerjee	SINP	PHYS05201504020	Composite Higgs and Physics Beyond the Standard Model
95	Augniva Ray	SINP	PHYS05201504021	Aspects of Supersymmetric Localization and Exact Results in N=2 Supersymmetric Theories
96	Anwesha Chattopadhyay	SINP	PHYS05201604002	Strongly Correlated Band Insulators and Emergent Superconductivity: A Generalized Gutzwiller Projection Approach
97	Aranya Bhattacharya	SINP	PHYS05201604004	On Holographic Entanglement Entropy and Sub-region Complexity of Various Black Solutions in AdS/CFT
98	Sathi Sharma	SINP	PHYS05201604008	Study of Low Energy Resonances and β -Decay relevant for Nuclear Astrophysics
99	Rajkumar Santra	SINP	PHYS05201604018	Indirect Experimental Techniques For Nuclear Astrophysics
100	Meenakshee Sharma	IPR	PHYS06201304002	Perturbation Studies in a Plasma Confined by Multi-Pole Line-Cusp Magnetic Field
101	Lachhvani Lavkesh Tekchand	IPR	PHYS06201404001	Long-time Confinement of Toroidal Electron Plasma in SMARTEX-C
102	Garima Arora	IPR	PHYS06201504004	Laboratory Studies of Stationary and Non-stationary Structures in Flowing Complex Plasmas

103	Amit Kumar	IoP	PHYS07201404012	Polymeric Models for Chromosome Organization: Impact of Cross-Linkers, Crowders and Confinement
104	Ganesh Chandra Paul	IoP	PHYS07201404014	Transport And Magnetic Exchange Properties of Spin-Orbit Coupled, Anisotropic Dirac Materials and Majorana Nanowires
105	Vijigiri Vikas	IoP	PHYS07201404018	Some Aspects of Proton Dynamics in Squaric Acid Crystal using Pseudo-spin Formalism
106	Abhishek Joshi	HRI	PHYS08201005001	Thermal Properties of Strongly Correlated Bosonic and Fermionic Superfluids
107	Arijit Dutta	HRI	PHYS08201105001	Nonequilibrium Response and Dynamics in the Mott Insulator
108	Sauri Bhattacharyya	HRI	PHYS08201105005	Finite Temperature Dynamics in Strongly Correlated Systems
109	Samiran Roy	HRI	PHYS08201304002	New Physics with Neutral and Charged Current Measurements at Long-Baseline Neutrino Experiments
110	Gautam Sharma	HRI	PHYS08201305003	Uncertainty Relations, Quantum Coherence and Quantum Measurement
111	Sreetama Das	HRI	PHYS08201305005	Quantum Information Processing in Noisy Environments
112	Biswajit Sahoo	HRI	PHYS08201405004	Classical and Quantum Subleading Soft Theorem in Four Spacetime Dimensions
113	Somdeb Ghose	IMSc	PHYS10200605010	Population Fluctuations, Nonequilibrium Flows and Instabilities in Some Model Systems
114	Prathik Cherian Jangid	IMSc	PHYS10201205003	Beyond Quantum Nonlocality in Continuous Variable Systems and Thermalization of a Qubit
115	Abinash Kumar Nayak	IMSc	PHYS10201205009	Right-Handed Currents and Electroweak Penguins in *B* decays.
116	Anand Pathak	IMSc	PHYS10201205010	Uncovering Functional Correlates of Structural Organization in Brain Networks at Multiple Scales: From the worm to the human
117	Jilmy P Joy	IMSc	PHYS10201205012	Shock Propagation in Dilute Inelastic and Elastic Media
118	Vigneshwar N	IMSc	PHYS10201404002	Entropy Driven Phase Transition in Hard Core Lattice Gas Models in Three Dimensions
119	Sourav Ballav	IMSc	PHYS10201404004	Surface Operators, Seiberg-Dual Quivers and Contours
120	Garima Rani	IMSc	PHYS10201504003	Understanding the Mechanical Response of Bacterial Cell Walls and Cell Membranes against Antimicrobial Agents

121	Protick Mohanta	NISER	PHYS11201204013	Heavy Hadron Spectrum on Lattice with NRQCD Bottom and HISQ Lighter Quarks
122	Ashutosh Dash	NISER	PHYS11201305001	Influence of Hadronic Interactions and Magnetic Field on the Bulk Properties of Matter Produced in Heavy-Ion Collision
123	Deepali Mishra	NISER	PHYS11201404001	Black Hole Microstates and Solution Generating Techniques
124	Dushmanta Kara	NISER	PHYS11201404002	Study of Rydberg Blockade and Anti-Blockade in Rubidium Atomic Vapor
125	Ekta Bhatia	NISER	PHYS11201404003	Natural and Synthetic Domain Wall Induced Spin Triplet Correlations in Superconducting Multilayers and Josephson Junctions
126	Sagarika Nayak	NISER	PHYS11201404008	Static and Dynamic Magnetic Properties of Soft/Hard Ferro-magnetic and Ferromagnetic /Antiferromagnetic Bilayers
127	Sourav Kundu	NISER	PHYS11201504005	Angular and Momentum Distribution of Vector Mesons Produced in Proton-Proton and Heavy-Ion Collisions at LHC Energies

Section IV
List of students who have completed M.Tech. and M.Sc. (Engg.) during April 1, 2020-July 31, 2021

M.Tech.

S. No.	Name of the Student	CI	Discipline	Enrolment No.	Thesis Title
1	Sougata Bag	BARC	Chemical	ENGG01201701008	Characterization of Glass Fiber Reinforced Polymer Exposed to Seawater
2	Ranjeet Singh	BARC	Civil	ENGG01201701017	Kinematic Interaction Effect on the Beahaviour of Piles under Senmic Loading
3	Vineet Tiwari	BARC	Civil	ENGG01201701019	Performance Evaluation of RC frame under Elevated Temprature
4	Gagan Deep Singh	BARC	Mechanical	ENGG01201701050	Effect of PWHT on Mechanical & Corrosion Behaviour of Carbon Steel (SA106 GB) weld with Low Alloy Steel (SA335 P22)
5	Kanha Chaturvedi	IGCAR	Chemical	ENGG02201701001	CFD Modeling of Natural Convection in Cover Gas of FBTR
6	Rishabh Kumar Mishra	BARC	Chemical	ENGG01201701001	Studies on Magnesio-thermic Reduction of Zirconium Tetrachloride
7	Ayisha Shaikh	BARC	Chemical	ENGG01201701003	Removal of Radioactive Ar-41 From Exhaust Air of Dhruva Reactor Using Various Zeolites
8	Ajay Singh Chouhan	BARC	Computer	ENGG01201801059	Extracting Model for Application Behaviour Fingerprinting
9	Anagha Athavale	BARC	Computer	ENGG01201801060	Scalable Formal Verification Techniques for Model-Based Design Frameworks
10	Bhabani Shankar Dash	BARC	Metallurgical	ENGG01201701009	Quantitative Measure-ment of Porosity by Image Analysis of Micrographs of Irradiated MC and MOX fuel
11	Jay Madan Vivarekar	BARC	Electronics	ENGG01201801035	Study, Design and Simulation of Wireless

					routing Protocol for Mobile Ad-hoc Networks
12	Mekala Venkatesh Yadav	BARC	Electronics	ENGG01201801036	Study, Parameter-ization and Validation of Path Loss Model for VHF/UHF Wireless Communication System for Mumbai Terrain and Climatic Conditions
13	Jagath Saran J	BARC	Electrical	ENGG01201701026	Sensing Applications of Short-range Frequency Modulated Continuous Wave Radar
14	Sampada D. Bhujbal	BARC	Instrumentation	ENGG01201801008	Study, Design and Simulation of Time Triggered Protocol for Distributed Sensor Network
15	Yadav Rahul Babaso	BARC	Mechanical	ENGG01201701039	Study of Seismic Response of Multiple Supported Ventilation Ducts Considering Seismic Anchor Movements
16	Apratim Gupta	BARC	Mechanical	ENGG01201701043	Parametric Analysis of Leak Rate in Slip-on Type Pipeto Pipe Connections for Developing Design Criteria
17	Anuj Palat	BARC	Mechanical	ENGG01201801040	Characterization of Surface Flaws Using Rayleigh Waves
18	Dixit Velraj	BARC	Mechanical	ENGG01201801042	On the Limit, Characterization and Transformation Ten-dency of Delta-ferrite in Stainless Steel 304L Forging
19	Vivek Shiv kumar	BARC	Mechanical	ENGG01201801056	Optimized Strategies for In-service Inspection of Reactor Components
20	Tirumala Sudheer K. Vuddanti	IGCAR	Mechanical	ENGG02201701003	Effect of Flaw geometry and Orientation in Alloy-800 Steam Gene-rator Tubes on Signal in

					array Probe Eddy Current Testing
21	Niramay Joshi	IGCAR	Mechanical	ENGG02201701007	Validation of the Numerical Methods in Computing Asymptotic Crack Size and Its Comparison with Design Code Under Cyclic Loading
22	Shekhar Kumar	BARCTS (NFC) Hyderabad	Mechanical	ENGG1A201801012	Numerical Investigations on the Tool Wear of Single Crystal Diamond Tool While Modulation Assisted Machining of Hardened Steel
23	P Lalit Naidu	BARC	Metallurgical	ENGG01201801006	Sponge Formation Mechanism in Kroll Process for Titanium
24	Abhishek Ashok Sawkar	BARC	Radiological	ENGG01201801058	Design and Development of a Detector System for Workplace Monitoring of Lower Energy Neutrons (< 500 kev) in Reactor Environment
25	Omkar Nath Sahu	BARC	Radiological	ENGG01201701054	Size Segregated Composition & Dosimetric Implications of Particulate Radionuclide during Uranium Processing in a Reprocessing Plant
26	Soumitra Panda	BARC	Radiological	ENGG01201801063	A Rapid Sequential Separation Methodology for Estimation of Pu & Am in Physical Samples using Extractive Liquid Scintillation Spectrometry
27	Sonali Khurana	BARC	Radiological	ENGG01201801064	Study on Leaching Characteristics of Cs-137 and Tc-99 from Cement Matrix

28	Rahul Roy	BARC	Radiological	ENGG01201801067	Impact of Dietary Intake of Stable Iodine on Bioassay Functions of ^{131}I using Latest Biokinetic and Dosimetric Models
29	Kirti	BARC	Radiological	ENGG01201801068	Criticality Safety Evaluation of a Typical Fuel Fabrication Facility using an Open-Source Monte Carlo Code
30	Jagriti Sharma	BARC	Radiological	ENGG01201801069	Temperature and Wavelength Dependence of OSL in Al_2O_3:C, $LiCaAlF_6$:Eu,Y and $LiMgPO_4$:Tb,B Dosimetric Phosphors

M.Sc. (Engg.)

Sr. No.	Name of the student	CI	Programme	Enrolment No
1	Tejas Jagdishbhai Parekh	IPR	M.Sc. (Engg)	ENGG06201603001
2	Rohit Agarwal	IPR	M.Sc. (Engg)	ENGG06201603005
3	D Prasadrao Palaparti	IGCAR	Int.Ph.D.(Dual Degree)	ENGG02201505017
4	Shaik Abdul Rahman	IGCAR	Int.Ph.D.(Dual Degree)	ENGG02201605004
5	Mahesh Mahadeo Ghate	IPR	M.Sc (Engg.)	ENGG06201603002
6	Venkata Nagaraju M	IPR	M.Sc (Engg.)	ENGG06201603007
7	Ravi Pandey	IPR	M.Sc (Engg.)	ENGG06201603008
8	Dheeraj Kumar Sharma	IPR	M.Sc (Engg.)	ENGG06201603009
9	Manoahstephen Manuelraj	IPR	M.Sc (Engg.)	ENGG06201603011
10	Sumit Kumar Kochar	BARC	M.Sc. (Engg.)	ENGG01201605004

Section V
List of students who completed D.M., M.Ch. and M.D. degrees during April 1, 2020-July 31, 2021

D.M. Degree

S. No.	Name of the Student	CI	Programme	Enrolment No.
1	Dr. Nishanth Baliga	TMC	D.M.-Critical Care Medicine	HLTH09201710044
2	Dr. (Ms.) A Srilekha	TMC	D.M.-Critical Care Medicine	HLTH09201710045
3	Dr. Nirmalyo Lodh	TMC	D.M.-Critical Care Medicine	HLTH09201810043
4	Dr. Utkarsh Pradeep Chhanuchure	TMC	D.M.-Gastroenterology	HLTH09201810045
5	Dr. Vishalkumar Ratnakar Seth	TMC	D.M.-Gastroenterology	HLTH09201810046
6	Dr. Sahil Sheikh	TMC	D.M.-Gastroenterology	HLTH09201710046
7	Dr. Raosaheb Taru Rathod	TMC	D.M.-Gastroenterology	HLTH09201710047
8	Dr. (Ms.) Amrita Narang	TMC	D.M.-Interventional Radiology	HLTH09201710048
9	Dr. Mohd Shariq	TMC	D.M.-Interventional Radiology	HLTH09201710049
10	Dr. Saket Ramnarayan Rao	TMC	D.M.-Interventional Radiology	HLTH09201810047
11	Dr. David Narayan Rameswarapu	TMC	D.M.-Interventional Radiology	HLTH09201810048
12	Dr. Sativ Khaddar	TMC	D.M.-Medical Oncology	HLTH09201710025
13	Dr. Ventrapati Pradeep	TMC	D.M. -Medical Onlology	HLTH09201710026
14	Dr. Ramnath Shenoy K	TMC	D.M.-Medical Oncology	HLTH09201710027
15	Dr. Amit Kumar	TMC	D.M.-Medical Oncology	HLTH09201710028
16	Dr. Shikhar Kumar	TMC	D.M.-Medical Oncology	HLTH09201710029
17	Dr. Gurvinder Singh	TMC	D.M.-Medical Oncology	HLTH09201710030
18	Dr. (Ms.) Kripa Bajaj	TMC	D.M.-Medical Oncology	HLTH09201710032
19	Dr. Ravindra Nandhana	TMC	D.M.-Medical Oncology	HLTH09201710033
20	Dr. (Ms.) Narmadha R	TMC	D.M.-Medical Oncology	HLTH09201710034
21	Dr. George Abraham	TMC	D.M.-Medical Oncology	HLTH09201710035
22	Dr. Anoop Rajkumar Mantri	TMC	D.M.-Medical Oncology	HLTH09201710036
23	Dr. Suresh Kumar B	TMC	D.M.-Medical Oncology	HLTH09201710037
24	Dr. (Ms.) Annu Rajpurohit	TMC	D.M.-Medical Oncology	HLTH09201710039
25	Dr. Abhinav Bhagwan Zawar	TMC	D.M.-Medical Oncology	HLTH09201710040
26	Dr. Gunjesh Kumar Singh	TMC	D.M.-Medical Oncology	HLTH09201710038
27	Dr. Lakhan Kashyap	TMC	D.M.-Medical Oncology	HLTH09201810025
28	Dr. Goutam Santosh Panda	TMC	D.M.-Medical Oncology	HLTH09201810026
29	Dr. Vasu BabuGoli	TMC	D.M.-Medical Oncology	HLTH09201810027
30	Dr. Amit Kumar Choudhary	TMC	D.M.-Medical Oncology	HLTH09201810028
31	Dr. Prahalad Elamarthi	TMC	D.M.-Medical Oncology	HLTH09201810029
32	Dr. Kishore Kumar Kote	TMC	D.M.-Medical Oncology	HLTH09201810031

33	Dr. Akhil R	TMC	D.M.-Medical Oncology	HLTH09201810033
34	Dr. Shasanka Sekhar Das	TMC	D.M.-Medical Oncology	HLTH09201810034
35	Dr. (Ms.) Anne Srikanth	TMC	D.M.-Medical Oncology	HLTH09201810035
36	Dr. Aditya Pavan Kumar Kanteti	TMC	D.M.-Medical Oncology	HLTH09201810036
37	Dr. Rahul Ravind	TMC	D.M.-Medical Oncology	HLTH09201810038
38	Dr. Singh Ajaykumar Chandrabhan	TMC	D.M.-Medical Oncology	HLTH09201810039
39	Dr. (Ms.) Apurva K. Mundada	TMC	D.M.-Oncopathology	HLTH09201810049
40	Dr. (Ms.) Ann Thomas	TMC	D.M.-Oncopathology	HLTH09201810050
41	Dr. (Ms.) Arshi Beg	TMC	D.M.-Oncopathology	HLTH09201810051
42	Dr. Shyam Srinivasan	TMC	D.M.-Pediatric Oncology	HLTH09201710041
43	Dr. Venkata Rama Mohan Gollamudi	TMC	D.M.-Pediatric Oncology	HLTH09201710042
44	Mande Radnyi Uday	TMC	D.M.-Pediatric Oncology	HLTH09201710043
45	Anuj Singh	TMC	D.M.-Pediatric Oncology	HLTH09201810040
46	Dr. (Ms.) Juhi Jhaverchand Shah	TMC	D.M.-Pediatric Oncology	HLTH09201810041
47	Dr. (Ms.) Nidhi Dhariwal	TMC	D.M.-Pediatric Oncology	HLTH09201810042

M.Ch. Degree

S. No.	Name of the Student	CI	Programme	Enrolment No.
1	Dr. Ravi Shankar	TMC	M.Ch.- Head & Neck Surgery	HLTH09201710017
2	Dr. Shikhar Sawhney	TMC	M.Ch. Head & Neck Surgery -	HLTH09201710018
3	Dr. Krishnan Kartik Vasudev	TMC	M.Ch.- Head & Neck Surgery -	HLTH09201710019
4	Dr. (Ms.) Komal Lamba	TMC	M.Ch.-Head & Neck Oncology	HLTH09201710020
5	Dr. Sasi Krishna Kavutarapu	TMC	M.Ch.-Head & Neck Oncology	HLTH09201810017
6	Dr. Nityanand C	TMC	M.Ch.-Head & Neck Surgery	HLTH09201810018
7	Dr. Natarajan R	TMC	M.Ch.-Head & Neck Surgery	HLTH09201810019
8	Dr. (Ms.) Pavithra S	TMC	M.Ch.-Head & Neck Surgery	HLTH09201810020
9	Dr. (Ms.) Stuti Gupta	TMC	M.Ch.- Gynecological Oncology	HLTH09201710023
10	Dr. (ms.) Pooja Singh	TMC	M.Ch.- Gynecological Oncology	HLTH09201710024
11	Dr. (Ms.) Vaishali Paliwal	TMC	M.Ch.- Gynecological Oncology	HLTH09201810023
12	Dr. (Ms.) Ushashree Das	TMC	M.Ch.- Gynecological Oncology	HLTH09201810024
13	Dr. Firoz Rajiv Borle	TMC	M.Ch.- Plastic & Reconstructive Surgery	HLTH09201710022

14	Dr. Rounak Kalwani	TMC	M.Ch.- Plastic & Reconstructive Surgery	HLTH09201810021
15	Dr. Himanshu Gupta	TMC	M.Ch.- Plastic & Reconstructive Surgery	HLTH09201810022
16	Dr. (Ms.) Saneya Abdulwahab Pandrowala	TMC	M.Ch.- Surgical Oncology	HLTH09201710001
17	Dr. Rajkumar Prakash	TMC	M.Ch.- Surgical Oncology	HLTH09201710002
18	Dr. Sreedhran M	TMC	M.Ch.- Surgical Oncology	HLTH09201710003
19	Dr. Voppuru Saiesh Reddy	TMC	M.Ch.- Surgical Oncology	HLTH09201710004
20	Dr. Jajoo Bhushan Rahul	TMC	M.Ch.- Surgical Oncology	HLTH09201710006
21	Dr. Anuj Singh	TMC	M.Ch.- Surgical Oncology	HLTH09201710007
22	Dr. Abhijit Kotabagi	TMC	M.Ch.- Surgical Oncology	HLTH09201710008
23	Dr. Deepak Ramraj	TMC	M.Ch.- Surgical Oncology	HLTH09201710009
24	Dr. Hemant Singh Niranjan	TMC	M.Ch.- Surgical Oncology	HLTH09201710010
25	Dr. Shravan Nadkarni	TMC	M.Ch.- Surgical Oncology	HLTH09201710011
26	Dr. Arvind Guru	TMC	M.Ch.- Surgical Oncology	HLTH09201710012
27	Dr. Anand Mohan	TMC	M.Ch.- Surgical Oncology	HLTH09201710013
28	Dr. Jaganmurgan R	TMC	M.Ch.- Surgical Oncology	HLTH09201710014
29	Dr. Tej Pratap Singh	TMC	M.Ch.- Surgical Oncology	HLTH09201710016
30	Dr. (Ms.) Suvarna B. Prashant	TMC	M.Ch.- Surgical Oncology	HLTH09201710005
31	Dr. (Ms.) Chandana Vemuri	TMC	M.Ch.- Surgical Oncology	HLTH09201710015
32	Dr. (Ms.) Preeti V	TMC	M.Ch.- Surgical Oncology	HLTH09201810001
33	Dr. Srivishnu S	TMC	M.Ch.- Surgical Oncology	HLTH09201810002
34	Dr. Janesh M	TMC	M.Ch.- Surgical Oncology	HLTH09201810003
35	Dr. Suresh M	TMC	M.Ch.- Surgical Oncology	HLTH09201810004
36	Dr. Rigved Nittala	TMC	M.Ch.- Surgical Oncology	HLTH09201810005
37	Dr. (Ms.) Jasmine Agarwal	TMC	M.Ch.- Surgical Oncology	HLTH09201810006
38	Dr. Nischal N	TMC	M.Ch.- Surgical Oncology	HLTH09201810007
39	Dr. Kaival Ketan Gundavda	TMC	M.Ch.- Surgical Oncology	HLTH09201810008
40	Dr. Sahil Mittal	TMC	M.Ch.- Surgical Oncology	HLTH09201810009
41	Dr. Nishit Shrivastava	TMC	M.Ch.- Surgical Oncology	HLTH09201810011
42	Dr. Tejas Prakash Vispute	TMC	M.Ch.- Surgical Oncology	HLTH09201810012
43	Dr. Prudvi Raj S	TMC	M.Ch.- Surgical Oncology	HLTH09201810013

44	Dr. Rajat Lohia	TMC	M.Ch.- Surgical Oncology	HLTH09201810014
45	Dr. Sri Siddhartha Nekkanti	TMC	M.Ch.- Surgical Oncology	HLTH09201810015

M.D. Degree

S. No.	Name of the Student	CI	Programme	Enrolment No.
1	Dr. (Ms.) Prathiba Thiagarajan	TMC	M.D.-Anaesthesiology	HLTH09201709001
2	Dr. (Ms.) Priyadarshini R	TMC	M.D.-Anaesthesiology	HLTH09201709002
3	Dr. Girish Kanna	TMC	M.D.-Anaesthesiology	HLTH09201709003
4	Dr. (Ms.) Neha Sharma	TMC	M.D.-Anaesthesiology	HLTH09201709004
5	Dr. (Ms.) Mehta Niyati Kamlesh	TMC	M.D.-Anaesthesiology	HLTH09201709006
6	Dr. (Ms.) Divya Rajendra Choudhari	TMC	M.D.-Anaesthesiology	HLTH09201709007
7	Dr. (Ms.) Nimisha George	TMC	M.D.-Anaesthesiology	HLTH09201709010
8	Dr. (Ms.) Sayali Sukhadeo Khandekar	TMC	M.D.-Anaesthesiology	HLTH09201709012
9	Dr. (Ms.) Rekha Bhanudas Bhosale	TMC	M.D.-Anaesthesiology	HLTH09201709013
10	Dr. (Ms.) Unnathi Purushotham Manampadi	TMC	M.D.-Anaesthesiology	HLTH09201709014
11	Dr. (Ms.) Gayatri Ashok Chaudhari	TMC	M.D.-Anaesthesiology	HLTH09201709017
12	Dr. (Ms.) Shilpa Kamalakarrao Awaskar	TMC	M.D.-Anaesthesiology	HLTH09201709018
13	Dr. Suhas Sadashiv Dhole	TMC	M.D.-Anaesthesiology	HLTH09201709019
14	Dr. (Ms.) Rutuja Chandrakant Pathak	TMC	M.D.-Anaesthesiology	HLTH09201709020
15	Dr. (Ms.) Karkhanis Dhanashri Ramesh	TMC	M.D.-Anaesthesiology	HLTH09201809001
16	Dr. (Ms) Gargi Amol Deshpande	TMC	M.D.-Anaesthesiology	HLTH09201809007
17	Dr. (Ms.) Priyal U. Ramteke	TMC	M.D.-Anaesthesiology	HLTH09201609067
18	Dr. (Ms.) Sonal Ganesh Kadam	TMC	M.D.-Anaesthesiology	HLTH09201709008
19	Dr. (Ms.) Minal Chatrapati Mali	TMC	M.D.-Anaesthesiology	HLTH09201709009
20	Dr. Amit Namadev Pinjari	TMC	M.D.-Anaesthesiology	HLTH09201709011
21	Dr. Vidyasagar D. Nagargoje	TMC	M.D.-Anaesthesiology	HLTH09201709015
22	Dr. Jayant Krushna Pandhare	TMC	M.D.-Anaesthesiology	HLTH09201709016
23	Dr. Deshmukh Bhakti Yashvant	TMC	M.D.-Anaesthesiology	HLTH09201809002
24	Dr. Agrawal Mayur Ashokkumar	TMC	M.D.-Anaesthesiology	HLTH09201809003
25	Dr. (Ms.) Roshni Ravichandran	TMC	M.D.-Anaesthesiology	HLTH09201809005
26	Dr. (Ms.) B Meenakshi Unnithan	TMC	M.D.-Anaesthesiology	HLTH09201809006
27	Dr. Vignesh B	TMC	M.D.-Anaesthesiology	HLTH09201809008

28	Dr. (Ms.) Bhargavi Vallabhaneni	TMC	M.D.-Anaesthesiology	HLTH09201809009
29	Dr. Nidhin K. Alex	TMC	M.D.-Anaesthesiology	HLTH09201809010
30	Dr. (Ms.) Rathod Resham Rajesh	TMC	M.D.-Anaesthesiology	HLTH09201809011
31	Dr. Maji Manoj Anup	TMC	M.D.-Anaesthesiology	HLTH09201809012
32	Dr. (Ms.) Chandankhede Sneha Madhorao	TMC	M.D.-Anaesthesiology	HLTH09201809013
33	Dr. (Ms.) Gholap Supriya Bhausaheb	TMC	M.D.-Anaesthesiology	HLTH09201809014
34	Dr. (Ms.) Medha Lipika Ramganesh	TMC	M.D.-Anaesthesiology	HLTH09201809015
35	Dr. Saratchandra Satyanarayanbabaji	TMC	M.D.-Anaesthesiology	HLTH09201809016
36	Dr. Vinay Khare	TMC	M.D.-Anaesthesiology	HLTH09201809017
37	Dr. (Ms.) Hatwar Mrunalini Bhagwat	TMC	M.D.-Anaesthesiology	HLTH09201809018
38	Dr. Agawane Nitesh Subhash	TMC	M.D.-Anaesthesiology	HLTH09201809019
39	Dr. Sagar Dinesh Pargunde	TMC	M.D.-Anaesthesiology	HLTH09201909012
40	Dr. Gourav Gopal Bain	TMC	M.D.-Immuno-Haematology & Blood Transfusion Medicine	HLTH09201709072
41	Dr. (Ms.) Kotadiya Aafreen Nasser	TMC	M.D.-Immuno-Haematology & Blood Transfusion Medicine	HLTH09201709071
42	Dr. (Ms.) Najnin Ladkhan Bangi	TMC	M.D.-Immuno-Haematology & Blood Transfusion Medicine	HLTH09201709073
43	Dr. Madkaiker Deep	TMC	M.D.-Immuno-Haematology & Blood Transfusion Medicine	HLTH09201809074
44	Dr. (Ms.) Charmode Juilee Shalik	TMC	M.D.-Immuno-Haematology & Blood Transfusion Medicine	HLTH09201809075
45	Dr. (Ms.) Gaikwad Pallavi Pradip	TMC	M.D.-Immuno-Haematology & Blood Transfusion Medicine	HLTH09201809076
46	Dr. (Ms.) Jahagirdar Sabina Mustupha	TMC	M.D.-Microbiology	HLTH09201709074
47	Dr. (Ms.) Keerti Sitani	BARC	M.D.-Nuclear Medicine	HLTH01201709001
48	Dr. (Ms.) Sreya Ghosh	TMC	M.D.-Nuclear Medicine	HLTH09201709021
49	Dr. Manikandan M V	TMC	M.D.-Nuclear Medicine	HLTH09201709022
50	Dr. Atul Yashwant Gosavi	TMC	M.D.-Nuclear Medicine	HLTH09201709023
51	Dr. Varun Shukla	TMC	M.D.-Nuclear Medicine	HLTH09201709024
52	Dr. (Ms.) Suchismita Ghosh	TMC	M.D.-Nuclear Medicine	HLTH09201709025
53	Dr. (Ms.) Dev Indraja Devidas	TMC	M.D.-Nuclear Medicine	HLTH09201709026
54	Dr. (Ms.) Sonali Sanjay Jadhav	BARC	M.D.-Nuclear Medicine	HLTH01201709002

55	Dr. Loharkar Sarvesh Vijay	TMC	M.D.-Nuclear Medicine	HLTH01201809002
56	Dr. Arvind Suresh	TMC	M.D.-Nuclear Medicine	HLTH09201809021
57	Dr. (Ms.) Anjali Prakash	TMC	M.D.-Nuclear Medicine	HLTH09201809022
58	Dr. Yash Hemant Jain	TMC	M.D.-Nuclear Medicine	HLTH09201809023
59	Dr. Suthar Ritesh Ramesh	TMC	M.D.-Nuclear Medicine	HLTH09201809024
60	Dr. Kale Shubham Anil	TMC	M.D.-Nuclear Medicine	HLTH09201809025
61	Dr. Mohite Ashish Anil	TMC	M.D.-Nuclear Medicine	HLTH09201809026
62	Dr. (Ms.) Rutula N. Sonawane	TMC	M.D.-Palliative Medicine	HLTH09201709039
63	Dr. (Ms.) Pallavi Singh	TMC	M.D.-Palliative Medicine	HLTH09201709040
64	Dr. (Ms.) Shamali Srinivas Poojary	TMC	M.D.-Palliative Medicine	HLTH09201709041
65	Dr. Avinash Kumar Tiwari	TMC	M.D.-Palliative Medicine	HLTH09201709042
66	Dr. (Ms.) Jyothsna Kuriakose	TMC	M.D.-Palliative Medicine	HLTH09201809038
67	Dr. Prasun P	TMC	M.D.-Palliative Medicine	HLTH09201809039
68	Dr. (Ms.) Prarthana Jayaseelan	TMC	M.D.-Palliative Medicine	HLTH09201809040
69	Dr. (Ms.) Duhita Rajesh Kodare	TMC	M.D.-Pathology	HLTH09201609017
70	Dr. Vividh Vishwas Raje	TMC	M.D.-Pathology	HLTH09201709027
71	Dr. (Ms.) Tanaya Chaba	TMC	M.D.-Pathology	HLTH09201709028
72	Dr. (Ms.) Shah Priyanka Jatin	TMC	M.D.-Pathology	HLTH09201709030
73	Dr. (Ms.) Nair Tara Thulasidharan	TMC	M.D.-Pathology	HLTH09201709031
74	Dr. (Ms.) Khushboo Mukesh Sahetia	TMC	M.D.-Pathology	HLTH09201709032
75	Dr. (Ms.) Akshaya Suren Jadhav	TMC	M.D.-Pathology	HLTH09201709033
76	Dr. (Ms.) Sampada Subhash Ghate	TMC	M.D.-Pathology	HLTH09201709034
77	Dr. (M.) Bhagyashri R. Rathod	TMC	M.D.-Pathology	HLTH09201709035
78	Dr. (Ms.) Arathi Suresh Kumar	TMC	M.D.-Pathology	HLTH09201709036
79	Dr. (Ms.) Radhika Vinodkumar Agrawal	TMC	M.D.-Pathology	HLTH09201709037
80	Dr. More Balaji Govindrao	TMC	M.D.-Pathology	HLTH09201709038
81	Dr. (Ms.) Arya K	TMC	M.D.-Pathology	HLTH09201809004
82	Dr. (Ms.) Shah Prarthna Sunil	TMC	M.D.-Pathology	HLTH09201809027
83	Dr. (Ms.) Lakshmi Ramabadran	TMC	M.D.-Pathology	HLTH09201809028
84	Dr. Sagar Ranjan Tripathy	TMC	M.D.-Pathology	HLTH09201809030
85	Dr. (Ms.) Janani Amudha kumar	TMC	M.D.-Pathology	HLTH09201809031
86	Dr. Shah Ashish Vivek	TMC	M.D.-Pathology	HLTH09201809032
87	Dr. (Ms.) A. Vishesha Vipul	TMC	M.D.-Pathology	HLTH09201809033
88	Dr. (Ms.) Kharat Reshma H.	TMC	M.D.-Pathology	HLTH09201809036
89	Dr. (Ms.) Bharati Sitaram Hubale	TMC	M.D.-Pathology	HLTH09201909033
90	Dr. (Ms.) Shreya Shankar Kunder	TMC	M.D.-Radiation Oncology	HLTH09201609024
91	Dr. (Ms.) Harshita K	TMC	M.D.-Radiation Oncology	HLTH09201709043

92	Dr. (Ms.) Sachita Pal	TMC	M.D.-Radiation Oncology	HLTH09201709044
93	Dr. (Ms.) Debanjali Datta	TMC	M.D.-Radiation Oncology	HLTH09201709045
94	Dr. (Ms.) Preethi S	TMC	M.D.-Radiation Oncology	HLTH09201709046
95	Dr. Vedanta Ray	TMC	M.D.-Radiation Oncology	HLTH09201709047
96	Dr. (Ms.) Disha Kharbanda	TMC	M.D.-Radiation Oncology	HLTH09201709048
97	Dr. Khurud Pallavi Udayrao	TMC	M.D.-Radiation Oncology	HLTH09201709049
98	Dr. (Ms.) Baviskar Yamini Padmakar	TMC	M.D.-Radiation Oncology	HLTH09201709050
99	Dr. Atul Nanarao Raut	TMC	M.D.-Radiation Oncology	HLTH09201709051
100	Dr. (Ms.) Adsul Ketaki Kantilal	TMC	M.D.-Radiation Oncology	HLTH09201709052
101	Dr. (Ms.) Swati Chugh	TMC	M.D.-Radiation Oncology	HLTH09201709053
102	Dr. (Ms.) Nishtha Sehra	TMC	M.D.-Radiation Oncology	HLTH09201709054
103	Dr. (Ms.) Seerat Puri	TMC	M.D.-Radiation Oncology	HLTH09201709055
104	Dr. (Ms.) Akanksha Anup	TMC	M.D.-Radiation Oncology	HLTH09201709056
105	Dr. (Ms.) Khan Asfiya Akram Khan	TMC	M.D.-Radiation Oncology	HLTH09201709058
106	Dr. (Ms.) Alvina Vadassery	TMC	M.D.-Radiation Oncology	HLTH09201809041
107	Dr. Nilesh Ranjan	TMC	M.D.-Radiation Oncology	HLTH09201809042
108	Dr. (Ms.) Ann Christy Saju	TMC	M.D.-Radiation Oncology	HLTH09201809043
109	Dr. (Ms.) Tahseena Tahmeed	TMC	M.D.-Radiation Oncology	HLTH09201809044
110	Dr. (Ms.) Jince Mary Mathew	TMC	M.D.-Radiation Oncology	HLTH09201809045
111	Dr. Prarabdh Singh	TMC	M.D.-Radiation Oncology	HLTH09201809046
112	Dr. Rabi Shankar Das	TMC	M.D.-Radiation Oncology	HLTH09201809047
113	Dr. Prithwijit Moitra	TMC	M.D.-Radiation Oncology	HLTH09201809048
114	Dr. Amrendra Kumar	TMC	M.D.-Radiation Oncology	HLTH09201809049
115	Dr. (Ms.) Kashid Sheetal Raju	TMC	M.D.-Radiation Oncology	HLTH09201809050
116	Dr. (Ms.) Mehta Prachi Sanjay	TMC	M.D.-Radiation Oncology	HLTH09201809051
117	Dr. P. Abhinav Chandrakant	TMC	M.D.-Radiation Oncology	HLTH09201809052
118	Dr. (Ms.) Chopade Pradnya S.	TMC	M.D.-Radiation Oncology	HLTH09201809053
119	Dr. (Ms.) Siddiqui Aasma Kalim	TMC	M.D.-Radiation Oncology	HLTH09201809056
120	Dr. Ronny John Mathew Abraham	TMC	M.D.-Radiation Oncology	HLTH09201809058
121	Dr. Anurag Gupta	TMC	M.D.-Radio-diagnosis	HLTH09201709059
122	Dr. (Ms.) Pavithra Devi A	TMC	M.D.-Radio-diagnosis	HLTH09201709060
123	Dr. (Ms.) Sweta Bothra	TMC	M.D.-Radio-diagnosis	HLTH09201709061
124	Dr. Vatsal Prakash Kania	TMC	M.D.-Radio-diagnosis	HLTH09201709062
125	Dr. (Ms.) Madhuri Ramkishan Waghmare	TMC	M.D.-Radio-diagnosis	HLTH09201709063
126	Dr. (Ms.) Asawari Sunil Lautre	TMC	M.D.-Radio-diagnosis	HLTH09201709064
127	Dr. Kalpesh Shyamlal Jain	TMC	M.D.-Radio-diagnosis	HLTH09201709065
128	Dr. Mayuresh Sandeep Akolkar	TMC	M.D.-Radio-diagnosis	HLTH09201709066
129	Dr. Ankur Chand	TMC	M.D.-Radio-diagnosis	HLTH09201709067
130	Dr. G Venkatesh M Gopal M Swami	TMC	M.D.-Radio-diagnosis	HLTH09201709068
131	Dr. Raghavendra Gulabrao Mali	TMC	M.D.-Radio-diagnosis	HLTH09201709069

132	Dr. Tanksale Viram Rajiv	TMC	M.D.-Radio-Diagnosis	HLTH09201709070
133	Dr. (Ms.) Palsetia Delnaz Rustom	TMC	M.D.-Radio-Diagnosis	HLTH09201709075
134	Dr. Thakkar Jay Bhartkumar	TMC	M.D.-Radio-Diagnosis	HLTH09201709076
135	Dr. Shubhankar Vivek Deshpande	TMC	M.D.-Radio-diagnosis	HLTH09201709077
136	Dr. Kanhaiya Kumar	TMC	M.D.-Radio-diagnosis	HLTH09201709078
137	Dr. (Ms.) Kembhavi Pooja Ravindra	TMC	M.D.-Radio-diagnosis	HLTH09201709079
138	Dr. (Ms.) Kamaxi H. Teivedi	TMC	M.D.-Radio-Diagnosis	HLTH09201809057
139	Dr. (Ms.) Jeba Nazneen	TMC	M.D.- Radio-Diagnosis	HLTH09201809059
140	Dr. Gurukrishna B	TMC	M.D.- Radio-Diagnosis	HLTH09201809060
141	Dr. (Ms.) Anuradha Shukla	TMC	M.D.- Radio-Diagnosis	HLTH09201809061
142	Dr. Vineeth K M	TMC	M.D.- Radio-Diagnosis	HLTH09201809062
143	Dr. Mahesh Kumar	TMC	M.D.- Radio-Diagnosis	HLTH09201809063
144	Dr. Nandakumar P G	TMC	M.D.- Radio-Diagnosis	HLTH09201809064
145	Dr. Ujjwal Agarwal	TMC	M.D.- Radio-Diagnosis	HLTH09201809065
146	Dr. Sardar Gurtejsingh Harvindersingh	TMC	M.D.- Radio-Diagnosis	HLTH09201809066
147	Dr. Patwardhan Saket Sanjeev	TMC	M.D.- Radio-Diagnosis	HLTH09201809067
148	Dr. (Ms.) Pande Pooja Vishnu	TMC	M.D.- Radio-Diagnosis	HLTH09201809068
149	Dr. (Ms.) Kulkarni Tanaya Gopinath	TMC	M.D.- Radio-Diagnosis	HLTH09201809069
150	Dr. Burrewar Mayur Dayanand	TMC	M.D.- Radio-Diagnosis	HLTH09201809070
151	Dr. Chavhan Arvind Devsingh	TMC	M.D.- Radio-Diagnosis	HLTH09201809071
152	Dr. Meshram Swapnil Sanjay	TMC	M.D.- Radio-Diagnosis	HLTH09201809072
153	Dr. (Ms.) Khandode Nanda Ramji	TMC	M.D.- Radio-Diagnosis	HLTH09201809073
154	Dr. (Ms.) Himangi M. Unde	TMC	M.D.- Radio-Diagnosis	HLTH09201909050
155	Dr. Vedprakash K. Maknikar	TMC	M.D.-Radiotherapy	HLTH09201609021
156	Dr. (Ms.) Ashwini S. Nagargoje	TMC	M.D.-Radiotherapy	HLTH09201609023
157	Dr. Bhadane Manish Umakant	TMC	M.D.-Radiotherapy	HLTH09201709057

राष्ट्रीय मूल्यांकन एवं प्रत्यायन परिषद

विश्वविद्यालय अनुदान आयोग का स्वायत्त संस्थान

NATIONAL ASSESSMENT AND ACCREDITATION COUNCIL

An Autonomous Institution of the University Grants Commission

Certificate of Accreditation

The Executive Committee of the
National Assessment and Accreditation Council
is pleased to declare the
Homi Bhabha National Institute
(Deemed to be University u/s 3 of the UGC Act, 1956)
Anushaktinagar, Mumbai, Maharashtra as
Accredited
with CGPA of 3.40 on four point scale
at A+ grade
valid up to March 15, 2026

Date : March 16, 2021

S. C. Sharma
Director

EC(SC)/61/2nd Cycle/MHUNGN11171

Contact Details

VICE-CHANCELLOR

Prof. P. R. Vasudeva Rao	022-25597638	vasudeva@hbni.ac.in

DEAN

Prof. P. D. Naik	022-25595358	deanhbni@hbni.ac.in

REGISTRAR

Dr. B. Chandrasekar	022-25597627	registrar@hbni.ac.in

INSTITUTE CHAIR PROFESSORS

Prof. B. K. Dutta	022-25597640	bkdutta@barc.gov.in
Prof. B. S. Tomar	022-25597628	tomarbs@hbni.ac.in

ASSOCIATE DEANS

Prof. D. K. Maity	022-25597623	asso_dean@hbni.ac.in
Prof. A. K. Dureja	022-25597629	dureja@hbni.ac.in
Prof. G. Ravikumar	022-25597624	ravig@hbni.ac.in

DEPUTY REGISTRAR

Shri. B. V. Balaji	022-25597637	bvbalaji@hbni.ac.in

ADMINISTRATIVE OFFICER(III)

Shri J. N. Makwana	022-25597554	ao3hbni@hbni.ac. in

HOMI BHABHA NATIONAL INSTITUTE

(A Deemed to be University u/s 3 of UGC Act 1956 and a Grant-in-Aid Institute of the Department of Atomic Energy, Govt. of India)

2nd Floor, Training School Complex,
Anushaktinagar, Mumbai 400 094
Ph: 022 25597554, 022 25597626
www.hbni.ac.in